

See discussions, stats, and author profiles for this publication at: <https://www.researchgate.net/publication/346029727>

ARCTIC RIFT COPPER Part of world's newest metallogenic province: Kiffaanngissuseq

Technical Report · November 2020

DOI: 10.13140/RG.2.2.18610.84161

CITATIONS

0

2 authors, including:



Jonathan Bell

Curtin University

17 PUBLICATIONS 13 CITATIONS

SEE PROFILE

Some of the authors of this publication are also working on these related projects:



Greenland View project

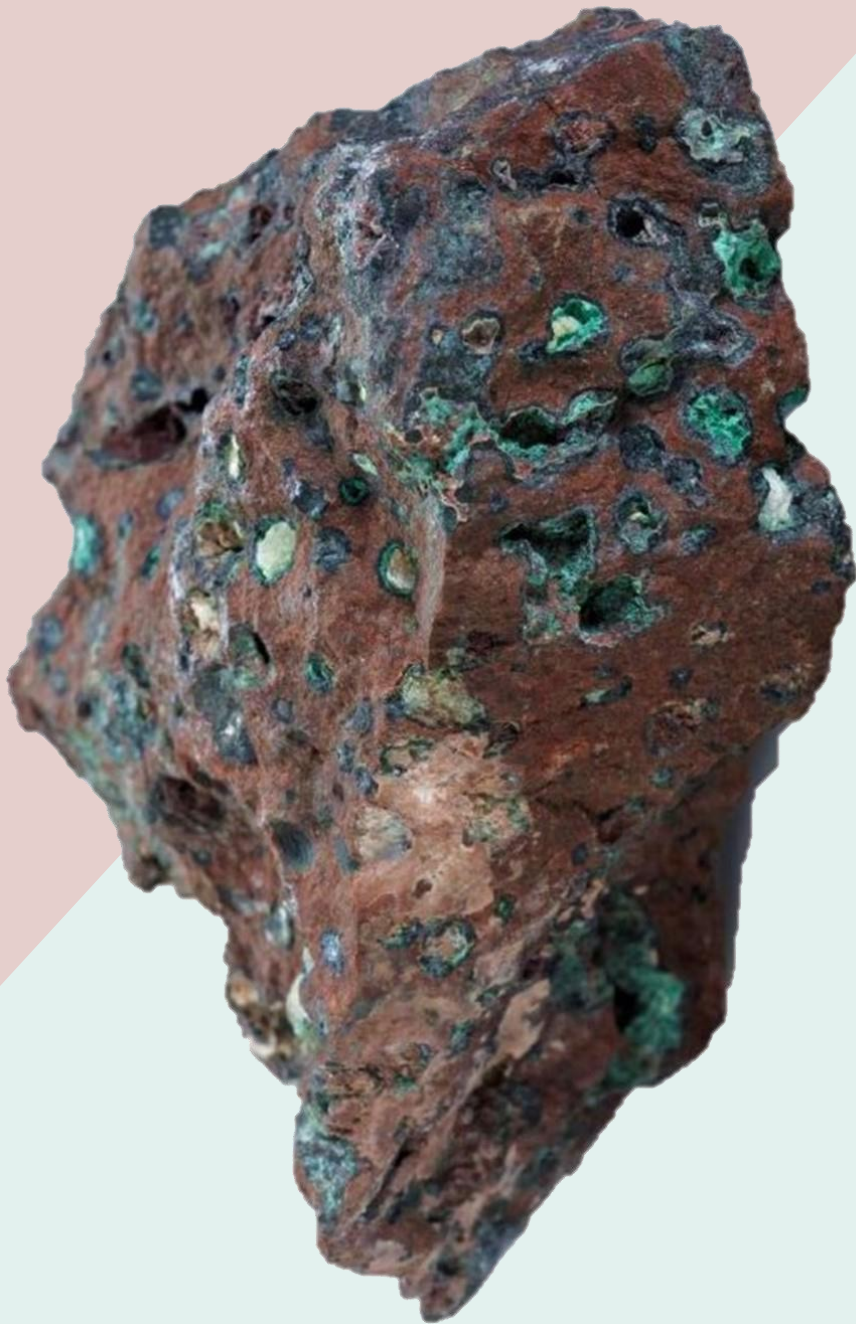


Mineral asset valuation and pricing View project

ARCTIC RIFT COPPER

*Part of world's newest metallogenic province:
Kiffaanngissuseq*

Technical Assessment Report



Greenfields Exploration Ltd
November 2020

This report presents a holistic view of north eastern Greenland's geology. The empirical evidence of mineralisation and geological record are tied in with mineral system components from global through to prospect scales. The source rocks, geodynamic triggers, pathways, and deposition sites are all identified within a preserved terrane. This work defines the Kiffaangissuseq metallogenic province, a **previously undescribed mineral system**.

For the first time, we identify a c. 1,250 Ma orogenic event in the basement as the geodynamic trigger related to the basalt-hosted **native copper** within the Arctic Rift Copper project. A c. 385 Ma fluid migration is identified as the trigger for a second **copper-sulphide** mineralising event expressed within the project, that also emplaced a distal zinc deposit within Kiffaangissuseq. This multi-episodal mineral system is supported by a regional geochemical and hydrodynamic framework that is not articulated elsewhere. The large scale of the mineral system, widespread copper anomalism, combined with dual mineralising events are analogous to Earth's great copper systems. The Company considers that Kiffaangissuseq has the **potential to be a world-class mineral province**.

A coincident magnetic-gravity-conductivity and high-grade geochemical copper anomaly occurs within the project. The anomalism is located at an oxidation boundary and is proposed to be the expression of a hydrothermal outlet. This site of focussed fluid flow forms the basis of a **high-priority, near-term target**, known as the 'Minik Singularity'.

Authors:

Dr Jonathan Bell (lead author), Greenfields Executive Director (Technical)

PhD Mineral Economics, MSc Mineral Economics, BSc Applied Geology, Member of the Australian Institute of Geoscientists¹ (MAIG, #3116), Graduate of the Australian Institute of Company Directors² (GAICD), Associate of the Resources and Energy Law Association, Affiliate of the Stockbrokers Association of Australia (AfSAFAA), RG146 Accredited³.

Joel Burkin (contributor), Greenfields Geologist

BSc (Hons) Geology, Graduate of the Australian Institute of Geoscientists (GAIG, #7724), Fellow of the Geological Society of London (FGS, #0001040164).

Lindsay Dick (contributor), Greenfields Executive Director (Corporate)

BSc Chemistry, LLB (Dist), Young Professional of the Resources and Energy Law Association.

Reviewers:

Mathew Longworth (internal review), Greenfields Chairperson

BSc Geology, Member of the Australasian Institute of Mining and Metallurgy (MAusIMM, #110783).

Dr Mark Hutchison (external, paid review), Consultant Director of Trigon Geoservices Ltd

PhD Geology, BSc (Hons) Geology, Member & Registered Professional Geologist of the Australian Institute of Geoscientists (MAIG RPGeo, #10080).

Consent & Disclaimer:

Greenfields prepared this Report and gives its consent to use this document for Public Reporting purposes. This Report meets the minimum requirements of the VALMIN Code (2015), which is the industry standard designed to fit with the Australian regulatory frameworks. All beliefs expressed in this Report by the Company are expressed in good faith and are believed to have a reasonable basis on the knowledge available to The Company. However, to the extent permitted by law the Company and the authors of this Report disclaim any liability for any expenses, losses, damages or costs incurred from any reliance on the content of this Report. The Company advises that this Report may contain forward-looking statements which may be subject to significant uncertainties outside of The Company's control. Actual future events may vary from these forward-looking statements and you are cautioned not to place undue reliance on any forward-looking statement.

© Greenfields Exploration Ltd, ABN 50 619 328 442, 17/11/2020

Contact details & registered address

Level 14, 197 St Georges Terrace
Perth WA 6000
P: 08 6270 6318
E: basecamp@gexpl.com

Online

gexpl.com
[linkedin.com/company/Greenfields-exploration-ltd/](https://www.linkedin.com/company/greenfields-exploration-ltd/)
[facebook.com/gexpl/](https://www.facebook.com/gexpl/)
Twitter: GreenfieldsExpl

Document information:

Reporting standards
Report date:
Effective date
Status:

JORC Code 2012, VALMIN Code 2015
18 November 2020
17 November 2020
Draft for client review

¹ <https://www.aig.org.au/>

² <http://aicd.companydirectors.com.au/>

³ <http://asic.gov.au/regulatory-resources/find-a-document/regulatory-guides/rg-146-licensing-training-of-financial-product-advisers/>

CONTENTS

Contents	4
1 Summary	10
2 Introduction	12
2.1 Scope of Work	12
2.2 Effective Date	12
2.3 Reporting Standards	12
2.4 Reliance on Other Experts	12
2.5 Information Sources	13
2.6 Site Visit	13
2.7 Report costs and Relationships	13
2.8 Qualifications and Experience	13
3 Project Description and Location	14
3.1 Location and Tenure	14
3.2 Accessibility, Climate, Local Resources, Infrastructure and Physiography	20
3.3 Mining Industry	25
4 History	28
5 Geological Setting	29
5.1 Regional Geology	29
5.2 Local Geology	47
6 Exploration	65
6.1 Prospecting	65
6.2 Geochemistry	65
6.3 Geophysics	67
6.4 Singularity	68
6.5 Drilling	70
6.6 Prospectivity and Endowment Study	70
7 Mineralisation	71
7.1 Known Prospects	73
7.2 Deposit Type	79
7.3 Mineral System	85
8 Data Integrity	103
8.1 Sample Preparation, Analyses and Security	103
8.2 Data Verification	103
9 Mineral Resource Estimates	103
10 Modifying Factors	103
10.1 Environmental Studies Permitting, and Social/Community Impact	103
10.2 Project Infrastructure	105
10.3 Mining Methods	106
10.4 Mineral Processing and Metallurgical Testing	107
10.5 Recovery Methods	107

10.6	Capital and Operating Costs	108
10.7	Market Studies and Contracts	108
10.8	Economic Evaluations	110
11	Ore Reserve Estimates	110
12	Other Relevant Data and Information	110
13	Interpretations and Conclusions	111
13.1	New insights	111
13.2	Significance	112
13.3	Knowledge Gaps	113
14	Recommendations	114
15	References	117
16	Consent and Compliance Statement: Dr Bell	143
17	Appendix 1: JORC Table 1	144
18	Appendix 2: Licence Details	148
19	Appendix 3: Supporting figures	149

Tables

Table 1:	Licence details and estimated holding costs	14
Table 2:	Geochronological dating summary	64
Table 3:	North Greenland mineral system hierarchy	86
Table 4:	Empirical evidence of a mineral system	87
Table 5:	Mineral system certainty estimates c. 1,250 Ma	101
Table 6:	Mineral system certainty estimates c. 385 Ma	102
Table 7:	Proposed budget	116
Table 8:	ARC licence co-ordinates	148

Figures

Figure 1:	Historical results	11
Figure 2:	ARC's location	14
Figure 3:	Greenland's bureaucratic structure	16
Figure 4:	Licence map	19
Figure 5:	Daylight statistics for Station Nord	20
Figure 6:	Weather statistics for Station Nord	21
Figure 7:	Physiography of Neergaard Dal/Elv	21
Figure 8:	Buildings in Jørgen Brønlund Fjord	22
Figure 9:	Arctic sea ice extent	23
Figure 10:	Satellite image of J.C. Christensen Land	24
Figure 11:	Miners at the historical Blyklippen lead-zinc mine in eastern Greenland	26
Figure 12:	Photo from the portal of the Black Angel in western Greenland	26
Figure 13:	Adjacent projects and deposits	26
Figure 14:	Airplanes used to explore North Greenland 1933-1938	28
Figure 15:	Geology of Greenland	30
Figure 16:	Timeline of geological events in North Greenland	31



Figure 17: Reconstruction of Columbia at c. 1,600 Ma	32
Figure 18 Neoproterozoic-aged sedimentary basins of the Laurentian margin	32
Figure 19: Arctic plates and volcanic provinces	33
Figure 20: Basins of North Greenland	34
Figure 21: LIPs in the time interval relevant to Columbia Supercontinent reconstruction	35
Figure 22: LIP plumbing framework	36
Figure 23: HALIP evidence	37
Figure 24: Hotspot trace	38
Figure 25: Grenville and Elzevirian orogens at the time of Rodinia	39
Figure 26: Caledonian and stylised Elzevirian orogens	39
Figure 27: Caledonian Orogeny front and its fluid front	40
Figure 28: Tectonic map of Ellesmerian deformation	41
Figure 29: Map of areas affected by Eurekan deformation	41
Figure 30: Fault zones and lineaments	42
Figure 31: Major faults and topographic lineaments in North Greenland	44
Figure 32: Folding in North Greenland	45
Figure 33: Geological timeline of North Greenland and J.C. Christensen Land	46
Figure 34: Geological map of J.C. Christensen Land	47
Figure 35: Lithostratigraphy of the Independence Fjord Group	48
Figure 36: Halite pseudomorphs from an Independence Fjord Group siltstone	49
Figure 37: Intrusions in the Independence Fjord Group	49
Figure 38: East-west time-space cross-section of North Greenland	50
Figure 39: Synoptic correlation diagram across the Zig-Zag Fm	50
Figure 40: Zig-Zag Fm trace element variation	52
Figure 41: Rheopsammite emplacement mechanism	53
Figure 42: Total Alkali Silica diagram of Midsommersø Intrusions	54
Figure 43: Conceptual diagram of Neoproterozoic depositional environment on Laurentian margin	55
Figure 44: Type locality of Hagen Fjord Group in Hagen Fjord	56
Figure 45: Franklinian Basin with a shelf-trough transition	57
Figure 46 Hydrocarbons within Portfjeld Fm	57
Figure 47: Schematic cross-section of Franklinian Basin sediments at Nordenskiöld Fjord	58
Figure 48: Faults and topographic lineaments of J.C. Christensen Land	59
Figure 49: Mineralisation fluids in pH-pO ₂ space	61
Figure 50: Metamorphic alteration of basalt	63
Figure 51: Geochemical data points	66
Figure 52: 1978 ground-based gravity map	67
Figure 53: AWI airborne total magnetic intensity	67
Figure 54: AEM1998 total magnetic intensity	68
Figure 55: AEM1998 apparent conductance	68
Figure 56: CAMP gravity map	68
Figure 57: Minik Singularity	69
Figure 58: Time-space plot of the known mineralisation in North Greenland	71
Figure 59: Schematic of main mineralisation processes	72

Figure 60: Large native copper specimens from ARC	73
Figure 61: Location of the Discovery Zone	74
Figure 62: Mineralisation types of the Discovery Zone	75
Figure 63: Breccia bound copper mineralisation	75
Figure 64: 'Black Earth' copper mineralisation	76
Figure 65: Stratiform mineralisation in the Jyske Ås Fm	76
Figure 66: Stratiform copper mineralisation (pervasive) in the poorly consolidated Jyske Ås layer	76
Figure 67: Reduced and oxidised beds of the Campanuladal Fm	77
Figure 68: Galena in a Campanuladal Fm sample	77
Figure 69: Ni:MgO plot	78
Figure 70: Astrup Dal pentlandite	78
Figure 71: Hybrid metamorphic-meteoritic brine model of native copper deposition	82
Figure 72: Depiction of ancient mining activity at Lake Superior	83
Figure 73: Native copper boulder from Quincy 2 Shaft	83
Figure 74: Massive native copper protrusion, Quincy 2 Shaft, Michigan	83
Figure 75: Massive native copper in the Calumet mine, Michigan	83
Figure 76: Massive native copper from an unspecified mine, Michigan	83
Figure 77: Copper vs grade by deposit types	84
Figure 78: Sediment-hosted copper deposit endowments	85
Figure 79: Non-hierarchical mineral system framework	87
Figure 80: Redbeds in Neergaard Valley	88
Figure 81: Deposits and lithospheric thickness	89
Figure 82: Potassic-altered tuff	90
Figure 83: Sediment-hosted mineral system	91
Figure 84: Kiffaangissuseq metal belt	92
Figure 85: Portjeld Fm hydrocarbons	94
Figure 86: Fluid flow staining within the Campanuladal Fm	94
Figure 87: Malachite breccia within redbeds	94
Figure 88: Native copper from the Zig-Zag Fm	95
Figure 89: Schematic of the shelf, slope and trough sequences	96
Figure 90: Low pressure intersections	97
Figure 91: Designated sites from the Government portal	105
Figure 92: Arctic sea routes	106
Figure 93: Macro trends withing the mining industry	107
Figure 94: Copper prices	109
Figure 95: Silver prices	109
Figure 96: AUD-DKK exchange rate	110
Figure 97: AUD-USD exchange rate	110
Figure 98: Chalcocite filled vesicles of the Zig-Zag Fm	116
Figure 99: Neergaard average temperatures and precipitation	149
Figure 100: Neergaard cloudy, sunny and precipitation days	149
Figure 101: Neergaard maximum temperatures	150
Figure 102: Neergaard average temperatures and precipitation	150



Figure 103: Neergaard wind speed	151
Figure 104: Neergaard wind direction	151
Figure 105: Copper-silver correlation from the Discovery Zone	152

Common terms and abbreviations

ARC	Arctic Rift Copper project
Archean	Archean Eon: 4,000 to 2,500 Ma.
ASIC	Australian Securities and Investments Commission.
ASX	Australian Securities Exchange.
c.	Circa, a Latin term commonly used in English, meaning 'approximately'.
Codes of practice	JORC - Australasian Code for Reporting of Exploration Results, Mineral Resources and Ore Reserves – The JORC Code – 2012 Edition. VALMIN - Australasian Code for Public Reporting of Technical Assessments and Valuations of Mineral Assets – The VALMIN Code – 2015 Edition.
Currency	AUD – Australian dollar, USD – United States dollar, DKK – Danish Krone.
Craton	A relatively intact piece of Earth's crust that has been stable since 541 Ma.
Cretaceous	Cretaceous Period, 145 to 66 Ma.
eH	A scale used to denote the electrical potential of a solution.
Elements	Cu – copper, Ni – nickel, Co – cobalt, Zn – zinc, Pb – lead, Ag – silver, Au – gold, K – potassium, Ca – calcium, Na – sodium, O – oxygen, Rb – rubidium, Sr – strontium, U – uranium, Ge – germanium.
Eocene	Eocene Eon: 56 to 33.9 Ma.
Eon	The largest division of geologic time.
Era	A subdivision of an Eon on the geological time scale.
Greenfields	Greenfields Exploration Ltd.
Feasibility Study	Means a "comprehensive technical and economic study of the selected development option for a mineral project that includes appropriately detailed assessments of applicable Modifying Factors together with any other relevant operational factors and detailed financial analysis that are necessary to demonstrate at the time of reporting that extraction is reasonably justified (economically mineable). The results of the study may reasonably serve as the basis for a final decision by a proponent or financial institution to proceed with, or finance, the development of the project. The confidence level of the study will be higher than that of a Pre-Feasibility Study" (JORC, 2012).
Fm	Formation.
Kiffaangissuseq	A West Greenlandic term for independence, used by Greenfields as a provisional name for a previously undescribed metallogenic province.
LIP	Large Igneous Province, an extremely large accumulation of igneous intrusive and extrusive rocks.
Ltd	Limited.
Ma	<u>Million years before present.</u>
Neoproterozoic	Neoproterozoic Era, 1,000 to 541 Ma.
northern Greenland	For the purpose of this report, areas higher than 80°N.
North Greenland	For the purpose of this report, the areas between Danmark Fjord, and Victoria Fjord. Note, that in the literature North Greenland is often a reference to the area between Hagen Fjord and Victoria Fjord.
Measurement units	t – tonne, Mt – million tonnes, m – metre, km – kilometre, ppm – parts per million, g/t – grams per tonne (same as ppm).
Mesoproterozoic	Mesoproterozoic Era, 1,600 Ma to 1,000 Ma.
Mesozoic	Mesozoic Era, 251.9 Ma to 65 Ma.
Metallogenic province	A geographical domain of mineral deposits that formed which are characterised by a common reason for emplacement, related mineral composition, form of the deposits, or intensity of mineralisation. For convenience, Greenfields uses 'metal belt' interchangeably with 'metallogenic province'.
MgO	Magnesium oxide, volumetrically important mineral component often associated with mafic/ultramafic rock types.
Mineral species and chemical formulae	Bornite: Cu_5FeS_4 containing 63.31% Cu, brochantite: $Cu_4(SO_4)(OH)_6$ containing 56.2% Cu by weight, chalcocite: Cu_2S containing 79.85% Cu, chalcopyrite: $CuFeS_2$ containing 34.63% Cu, galena: PbS containing 86.6% Pb, malachite: $Cu_2(CO_3)(OH)_2$ containing 57.48% Cu, pentlandite: $(Fe,Ni)_9S_8$ containing 34.21% Ni. Silica dioxide: SiO_2 , a major component in many minerals.
Palaeoproterozoic	Palaeoproterozoic Era, 2,500 Ma to 1,500 Ma.
Palaeozoic	Palaeozoic Era, 541 Ma to 251.9 Ma.
Period	A subdivision of an Era on the geological time scale.
PGE	Platinum group elements – platinum, palladium, rhodium, ruthenium, iridium, osmium. Metals associated with PGEs include copper, silver, gold mercury, and rhenium.
pH	A logarithmic scale used to denote the acidity or basicity of a liquid.
Phanerozoic	Phanerozoic Eon, less than 541 Ma.
Proterozoic	Proterozoic Eon, 2,500 Ma to 541 Ma.
Redbed	A term used for group oxidised sedimentary rocks that primarily comprise sandstone, siltstone or shale. These sedimentary rocks usually form in terrestrial settings.
Redox	Reduction-oxidation, a term typically used in relation to a change in chemical oxidation state.
Singularity	An unexplained departure from the predicted values in a given measurement. In a geological context, Greenfields defines a singularity as having meaningful, contextually discrete, and coincident anomalies that have unrelated physical properties (e.g. magnetic, gravity, electrical, chemical, structural). Greenfields uses a minimum of four coincident anomalies to designate a singularity.
Symbols	° degrees, % percent
Tertiary	Tertiary Period, 66 Ma to 2.6 Ma.
XRD	X-ray diffraction, an analytical technique used for phase identification of crystalline material.
XRF	X-ray fluorescence, a non-destructive analytical technique used to determine the elemental composition of material.



1 SUMMARY

Greenfields Exploration Ltd ('Greenfields, or the 'Company') prepared a Technical Assessment on its 100% owned Arctic Rift Copper Project ('ARC', or 'Project'). Greenfields is an unlisted public company domiciled in Western Australia. This Technical Assessment ('Report') has an Effective Date of 17 November 2020. The Company has been active in Greenland for three years and considers it a highly desirable destination for exploration investment. The Company believes that the single most important consideration is choosing which country to operate in, as it can make the difference between massive wealth creation, and utter destruction of value – irrespective of geological considerations. Greenland has many favourable attributes, such as being stable, pro-mining, with little corruption, simple laws and regulations, low royalties, favourable tax treatment for mineral projects, and good access to markets.

The centre of ARC⁴ is located at approximately 180 km west of Station Nord, and 130 km south of the Citronen deposit⁵ in North Greenland. The Project is in an Arctic desert that, aside from a military outpost and research station, is unpopulated. Big fjords surround the 5,774 km² Project and provide deep-water access throughout the ARC licence. An airstrip capable of handling heavy-lift aeroplanes is adjacent to the Project, and sites suitable for smaller airstrips are located within it.

Greenfields applied for the ARC licence on the basis that it has:

- **Direct evidence.** Copper and silver occur in the source rocks, faults, and in 'classic' deposition sites. The previous sampling found that 80% of stream sediment samples contain native copper. Native copper is frequently found in the moraines with individual clasts of native copper weighing 1 kg or more. Furthermore, very high-grade copper sulphides, up to 2.15% Cu and 35.5 g/t Ag over 4.5 m true width, are known from trench sampling of faults within sedimentary rocks. Individual assay grades from large samples are much higher (e.g. 53.8% Cu) and demonstrate the intensity of the mineralisation process. The fault hosted mineralisation was subject to much of the prior, albeit limited, exploration work. The extensions to the known stratiform targets in the sediments⁶ and basalts are subject to little, to no, dedicated work.

HIGH
GRADE

- **Indirect evidence.** The known areas of in situ high-grade copper are located at a coincident gravity, conductivity, and magnetic anomaly. Greenfields interprets the anomaly to be the signature of oxidation and depressurisation of a copper bearing hydrothermal conduit. This area is considered a high-priority target with near-term discovery potential, and is called the 'Minik Singularity'.

OBVIOUS
FOOTPRINT

THE RIGHT
ADDRESS

- **Ideal location.** ARC is close to a lithospheric-asthenospheric boundary that is intersected by a large oceanic transform fault. Such geological locations account for much of the world's sediment-hosted copper, and all the giant deposits within that grouping. Given the favourable setting, there is potential for the known copper to be part of an extensive system.
- **Complete mineral systems.** The sources of energy, fluids, salts, metals, permeable architecture, focus and precipitation mechanisms are all identified in a large sedimentary succession in an area with high levels of preservation. The timing of two orogenic events are well constrained and shown to be copper mineralising events. These orogenies

⁴ ARC is pronounced like the word 'ark', as in electric arc (i.e. "ahrk").

⁵ Owned 100% by a subsidiary of Ironbark Zinc Limited, a corporation that is unaffiliated with Greenfields.

⁶ In reference to the stratiform mineralisation exposed in faults that cut the Jyske Ås Formation.

mobilised copper-bearing brines that were focused into low-pressure zones near the junction of intersecting faults and topographic lineaments, where copper⁷ is present. With mechanical erosion being the only form of weathering in largely undeformed rocks of low-metamorphic grade, the preservation potential is high. This mineral system defines the boundaries of the 'Kiffaangissuseq metallogenic province'.

A VERY
BIG SYSTEM

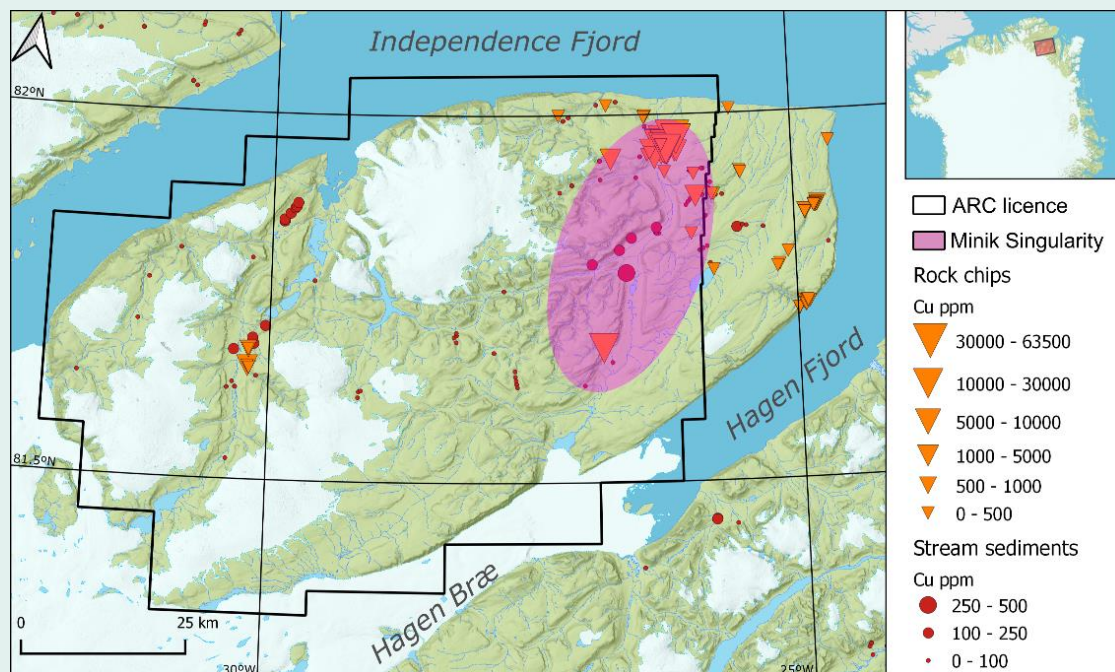
MORE THAN ONE DEPOSIT

- **Mineral camp.** The significant Citronen zinc deposit was formed in the same system as ARC. The presence of a substantial deposit nearby is important as deposits tend to cluster. The presence of a large well-defined deposit is a favourable indicator for a major ARC deposit.

Greenfields interprets the points above to be indicative of an extensive mineral system capable of hosting world-class copper deposits, thereby giving it the potential to be **economically important**. Furthermore, this Report makes a substantial contribution to science by defining a **new, 50,000 km² metallogenic province** that is oriented perpendicular to historical interpretations. The identification of the Kiffaangissuseq metallogenic province is a paradigm shift that fundamentally affects future work programs in North Greenland.

Despite ARC being subject to minimal exploration, the strong empirical evidence combined with the Company's application of the mineral system approach has resulted in a remarkably well constrained, and high-probability copper target. With the presence of world-class deposits often being said to be obvious in retrospect, **Greenfields considers that ARC's mineral potential is already obvious.**

Figure 1: Historical results



Source: Greenfields with stream sediment data from GEUS (2020) (1); rock chip data from Haugaard (2011) and Rehnström (2012) (2; 3); and magnetic data from Rasmussen (1999) (4).

⁷ In the sedimentary rocks, significant amounts of silver is known to have formed with copper sulphides.



2 INTRODUCTION

2.1 SCOPE OF WORK

Greenfields has prepared a Technical Assessment of the Arctic Rift Copper project. This Report summarises the previous work carried out in the Project area, the Company's interpretation of the mineral system, and proposes a work program. The Report does not constitute investment advice. This Report's intended audience consists of mining and exploration professionals, with an emphasis on geoscientists.

2.2 EFFECTIVE DATE

The Effective Date of this Report is 17 November 2020. The outcomes of this Report reflect the prevailing conditions and circumstances that are relevant as at the Effective Date. Greenfields cautions the reader that new technical information could result in a change in ARC's merit. The Company advises the reader to investigate whether there are any systematic (e.g. macroeconomic) or non-systematic (i.e. project-specific) changes after the Effective Date that may materially affect the project's risk and value.

2.3 REPORTING STANDARDS

This Report aligns with the criteria set out in the:

- The Australasian Code for Reporting of Exploration Results, Mineral Resources and Ore Reserves – the 'JORC Code' (5);
- The Australasian Code for Public Reporting of Technical Assessments and Valuations of Mineral Assets – the 'VALMIN Code' (6); and
- Australian Securities and Investment Commission's ('ASIC') regulatory guidelines RG111, RG112 and RG170 (7; 8; 9).

PEERLESS
REPORTING

The Report is written in the context of the Australian reporting requirements for listed⁸ public companies; the format largely⁹ aligns with those outlined in the Canadian National Instrument 43-101 ('NI43-101') (10); and it includes the requirements of Chapter 5 of the Listing Rules of the Australian Securities Exchange ('ASX') (11). Finally, the Report has a level of thoroughness and transparency that is akin to that of a doctoral thesis. **Due to the Report's extensive detail and use of the NI43-101 layout, it may be more effective for some readers to skip to the more commercially relevant section 7 on page 71 before reading the more contextual background information.**

2.4 RELIANCE ON OTHER EXPERTS

Greenfields has not relied on third parties in preparing this Report. However, the Technical Assessment uses third-party reports and data, much of which is available in the public domain. Where there are no attributions, the authors take responsibility for the statements to the extent set out in the Consent & Disclaimer.

⁸ Greenfields is not a listed company. However, the Company conducts best practice reporting.

⁹ To help with the readability of this Report, the NI43-101 heading 'Geological Setting and Mineralisation' was split into two standalone sections. In turn, the 'Deposit Types' heading was demoted to a sub-heading under 'Mineralisation'. This modification was necessary to reflect that deposit types are no longer considered good practice and are replaced by mineral systems.

2.5 INFORMATION SOURCES

In preparing this Report, Greenfields undertook a review of information available in the public domain. The Company confirms that:

- full, accurate, and true disclosure of all material information in its possession has been made available in this Report;
- the availability of information does not compromise the integrity, accuracy, conclusion and recommendation; and
- the Report does not contain commercially sensitive or confidential information.

TRANSPARENT
AND
AUTHORITATIVE

The end of this Report contains a list of 411 citations. These citations are mostly from peer-reviewed academic sources and documents from government institutions.

2.6 SITE VISIT

There has been no site visit to ARC by Greenfields. The licence document was approved in November 2020, which is when there is no daylight and little nautical twilight, and temperatures are well below freezing¹⁰. The Company deemed it impractical and unproductive to undertake a site visit to the Project during this time. However, given ARC's early-stage of exploration, and that Greenfields has relied on reputable and often peer-reviewed sources, the Company has no concerns about the integrity of the information it relied upon. Greenfields intends to visit ARC during the field season between late May and early September in either 2021 or 2022.

2.7 REPORT COSTS AND RELATIONSHIPS

The cost of this Report is not contingent on its conclusions or success of ARC as it was internally generated and paid for by Greenfields and its preparation was not subject to a third-party commercial contract. The principal author of this Report is Dr Jonathan Bell (founder and Managing Director of Greenfields). The secondary contributors to this Report are Mr Joel Burkin and Mr Lindsay Dick. Internal peer review was performed by Mr Mathew Longworth. A remunerated external peer reviewed was conducted by Dr Mark Hutchison, who has extensive experience in Greenland. Dr Bell, Mr Dick, Mr Burkin and Mr Longworth are Company insiders and shareholders. Dr Hutchison has no financial interest in Greenfields or its assets.

2.8 QUALIFICATIONS AND EXPERIENCE

The person responsible for preparing and taking responsibility for this Technical Assessment is Dr Jonathan A. Bell, who:

- holds a PhD in Mineral Economics, a Master's degree in Mineral Economics, and a Bachelor of Science in Applied Geology. Dr Bell is a Graduate of the Australian Institute of Company Directors, a member of the Resources and Energy Law Association, and an Affiliate of the Stockbrokers Association of Australia;
- meets the JORC Code and VALMIN Code criteria to be considered as a Competent Person, and Specialist, respectively;

¹⁰ Daily high of -14°C and a low of -19°C (52).



- has over 20 years of continuous experience in the mining industry across a wide range of commodities, and more than a decade of experience as a consultant specialising in mineral asset evaluation, valuation, and market pricing;
- is a Member of the Australian Institute of Geoscientists ('AIG') (membership number 3116); and
- agrees to take responsibility for this Report. Dr Bell's consent and sign-off are in Section 16 on page 143.

Mr Joel Burkin made contributions to this report (primarily in the Geological Setting and Deposit Model sections). Mr Burkin has three years of continuous experience and is a Graduate of the Australian Institute of Geoscientists (membership number 7724). Mr Lindsay Dick contributed to the Location and Tenure sections. Dr Bell provided oversight and guidance to Mr Burkin, and Dr Bell takes responsibility for Mr Burkin and Mr Dick's contributions.

3 PROJECT DESCRIPTION AND LOCATION

3.1 LOCATION AND TENURE

ARC is located inside the high-North of Greenland in J.C. Christensen Land, with a centre at approximately 81.7°N and 28.2°W. Independence and Hagen Fjords flank the Project (Figure 2). ARC comprises a single Special Exploration Licence with an officially recorded area of 5,774 km² (Table 1, Appendix 1). The licence is held directly by Greenfields without the use of a subsidiary entity.

Figure 2: ARC's location



Source: Greenfields.

Table 1: Licence details and estimated holding costs

Licence name	ID	Expires	Area (km ²)	Holding cost (DKK)	Holding cost (AUD)
Misissuiffik J. C. Christensen Land	2021-07	31-Dec-23	5,774	DKK 4,924,308	\$1,082,265

Source: Greenfields. Note: Costs use CPI factors estimated for January 2021. Any difference from the actual obligation is likely to be immaterial. The name Misissuiffik J. C. Christensen Land is what is recorded on the licence, and translates to Central J.C. Christensen Land.

GREENLAND AT A GLANCE

Area: 2.17 million km²

Capital: Nuuk

Population: 57,616

Languages: Greenlandic (official), Danish and English (recognised)

GDP: \$3.051 billion USD
(369)

As the area is uninhabited, there are few official names for geographic features in this part of northern Greenland (12). The nearest Greenlandic townships are Qaanaaq¹¹ about 925 km to the west-southwest, and Ittoqqortoormiit¹² about 1,260 km south-southeast of ARC's centroid. The most immediate settlement is in Longyearbyen on Spitsbergen Island in Norway's Svalbard archipelago, some 910 km to the east (13). The nearest permanently inhabited¹³ location is the Station Nord military facility¹⁴, approximately 200 km to the east. There are two uninhabited research stations within 30 km of ARC, the Kap Harald Moltke Station¹⁵ and Brønlundhus Station¹⁶.

Greenland, known as 'Kalaallit Nunaat' (14) in Greenlandic, is the largest island on Earth and covers 2.17 million ('M') km² (15), of which 81% is permanently under ice (15). For comparison, Western Australia covers 2.65 M km² 17% larger than Greenland. The country has a population of 57,616 inhabitants of which around a quarter live in the capital city Nuuk. Approximately 88% of Greenlanders identify as Greenlandic (15), and native title issues similar to those in Australia and Canada do not arise. The median age of a Greenlander is 34.3 years (15), which is slightly younger than the typical 37-year-old Australian (16).

Greenland is a semi-autonomous, overseas country within the Kingdom of Denmark (17). Greenland gained home-rule in 1979 (17), and in 2009 Denmark passed the *Act on Greenland Self-Government* (Act 473) which gave Greenland greater autonomy (18). Act 473 gave Greenland the right to self elect a government and parliament (19), although Denmark retains control over items like defence, currency, policing and the courts (17). The *Self-Government Act* gives unique nation-building opportunity to indigenous people within the framework of Western institutionalism (14). In addition to indigenous empowerment, Greenland¹⁷ has other favourable metrics (through Denmark) such as being the world's least corrupt country (20), 11th on the Human Development Index (21), and 6th on the Human Freedom Index (22).

¹¹ Qaanaaq was previously known as Thule, or New Thule.

¹² Ittoqqortoormiit was previously known as Scoresbysund.

¹³ Approximately five persons year-round (361), although numbers increase in the summer (13). Accommodation is also available for over twenty scientists and other personnel during the summer months (403; 13). The station has about 35 buildings (13). It is not accessible by ship (403).

¹⁴ Station Nord, 81.60° N, 16.68° W (13).

¹⁵ Kap Harald Moltke Station, ~82.15° N, 29.917° W (362).

¹⁶ Brønlundhus Station, ~82.17° N, 30.67° W.

¹⁷ Not all data sources separate Denmark and Greenland.



All minerals and hydrocarbons belong to Greenland ('Government of Greenland', or 'the Government') (15). The Government issues licenses to explore for and exploit minerals, enacted through the:

- Mineral Resources Act (23); and
- regulations concerning application procedures and standard terms for mineral exploration and prospecting (24).

The Mineral Licensing and Safety Authority¹⁸ ('MLSA') administers the licences (Figure 3) (25).

Figure 3: Greenland's bureaucratic structure



Source: Government of Greenland.

The pertinent details of all Greenlandic licences and many applications are regularly updated and published on the Government website (26). The graticular mineral licences convey rights over all mineral resources, except for radionuclides, hydrocarbons and hydropower (24). Mineral licences are categorised into those that permit exploration activity, and those that allow mining¹⁹. The exploration licences are divided into four classifications:

- **Exclusive and Non-exclusive Small-scale Licences.** These licences are only available to Greenlandic residents meeting specific criteria. An Exclusive Small-Scale Licence covers only 1 km² and allows prospecting and exploitation, valid for three years although renewal is possible. A Non-Exclusive Licence allows for prospecting across an entire municipality, except those areas under exclusive licence. These are valid for three years without extension. These Small-scale licences cannot convert to a Mining Licence (27);
- **Prospecting Licences.** These licences are valid for up to five years. Prospecting Licences are suited to reconnaissance work and have no exploration commitment. The Prospecting Licences apply to broad areas of Greenland – North, East, and West. The licences are

¹⁸ The MLSA is the one-door administrative authority for licences, mineral resource activities, and licence-related safety matters including supervision and inspections. Licensees and other parties covered by the Mineral Resources Act communicate with the MLSA and receive all notifications, documents and decisions from the MLSA. The Ministry of Mineral Resources ('MMR') is responsible for strategy and policy making, and legal aspects of mineral resources in Greenland. It is also the authority responsible for all socio-economic aspects of mineral resources, including social impact assessment ('SIA) and Impact Benefit Agreements ('IBA'). The Department of Geology within the Ministry provides geological advice related to licence applications and guidelines, delivers new geoscience data, and promotes Greenland's mineral resources internationally. The Environmental Agency for Mineral Resource Activities ('EAMRA'), under the Ministry of Labour, Research and Environment, is the administrative authority for environmental matters relating to mineral and hydrocarbon resource activities, including protection of the environment and nature, environmental liability and environmental impact assessments.

¹⁹ Officially, extraction rights are referred to as 'exploitation' but for ease of language, this Report uses the term 'Mining' to describe such rights.

non-exclusive, and third parties may lodge overlapping and exclusive Exploration Licences (28);

- **Exploration Licences.** These licences are initially valid for five years, but may be renewed for an additional five years, and then three-year renewal periods after that. Exploration Licences may be converted to an Exploitation ('Mining') License subject to approvals. Exploration Licences are exclusive and may not overlap. There is no mandatory area reduction requirement; however voluntary reductions are encouraged through annual increases in the minimum expenditure requirements (24); and
- **Special Exploration Licences ('SEL').** These are valid for three years with lower expenditure requirements compared to a conventional Exploration Licence. After a three-year term, a SEL may convert in part or whole, into a conventional Exploration License. SELs can also convert to Mining Licences (29). SELs must cover more than 1,000 km² and are only available in remote northern and eastern Greenland²⁰ (24).

Mining Licences convey exclusive extraction rights for 30 years and can be renewed for a further 20 years. For comparison, a Western Australian Mining Lease is valid for 21 years and is renewable after that (30). The area in which the Project was formerly located is in what was an 'open-door' licence area with longer-term block licences available, and some documents still reference this²¹. However, the area is now under the same licence regime as the rest of Northern and Eastern Greenland. There are no additional permitting requirements for Mining Licence applications in the Northeast Greenland National Park (the 'Park') (31).²²

A Mining Licence is available to any Greenland-domiciled limited liability corporation. Such company or its related entities must have identified and delimited mineral deposits that it intends to exploit. If a corporation holds a valid exploration licence, it must be in good standing (32). A holder of a Mining Licence may be a thinly capitalised member of an international group, but some restrictions apply (32).

As of 1 January 2020, it is not necessary for an applicant to demonstrate that a mineral deposit is commercially viable to receive a Mining Licence, and a Feasibility Study is not needed (33). However, the Mineral Resource Authority (the entity under which the MLSA falls) may impose deadlines and requirements on matters it deems to be of 'material importance'. Specifically, applicants for a Mining Licence are required to complete an environmental impact assessment ('EIA') and social sustainability assessment ('SIA') process. These processes proceed as follows (34):

- Terms of Reference are published on the respective government portals for 35 days for public comment;
- The licensee submits draft EIA/SIAs in English, Danish, and Greenlandic;
- The drafts are published and open for public comment for at least eight weeks, during which there are public hearings, and all public comments must be addressed;

AN EXPLORATION
LICENCE MAY BE
HELD DIRECTLY BY
A FOREIGN
COMPANY

²⁰ Areas in West Greenland north of 78°N and all areas in East Greenland east of 44°W (24).

²¹ Such as the announcement at http://eng.geus.dk/media/13262/qo_fs30.pdf which remains online.

²² The status of the Park is discussed in section 3.1.



- The EIA and SIA are revised based on the outcomes of the hearings;
- The licensee and government agree to an Impact Benefit Agreement based on the content of the SIA, which details arrangements around the social impacts of the licence (local labour, etc.);
- The Mining Licence is drafted and agreed – each agreement is bespoke. Most agreements are publicly available, though some are redacted (35).

Before the commencement of mining activity, a licensee must submit a development and closure plan to the MRA for approval, which is a negotiated process (24).

ARC is within the boundaries of the Park, which covers about 972,000 km² (36) (~45% of Greenland) and has an Arctic Desert climate and ice-cap (36). In 2019, the Park was withdrawn from the UNESCO Biosphere Reserve list (37). The Park is still listed on the IUCN²³ list of Class II National Parks. However the Park does not meet all the IUCN guidelines to justify this classification as the Government of Greenland permits exploration and mining within this area (36). There is recent precedent, in the form of the permitted Citronen project, demonstrating the support for this mining policy (38). Furthermore, the Government is actively investing its own money into exploring within its bounds (39), highlighting the Government's focus on modern nation-building within the framework of Western institutionalism as a unique means of indigenous self-government (14).

The requirement of granted SELs and ELs is that exploration meets a minimum expenditure amount. The Standard Terms (24) describe no rents, rates or other non-value generating financial requirements for exploration related licences. The Standard Terms state that the minimum annual expenditure for an SEL is 500 Danish Krone ('DKK') per square kilometre. For comparison, ELs have an escalating holding cost of DKK1,000/km² in years 1-2, DKK5,000/km² in years 3-5, and DKK10,000/km² in years 6-10, in addition to a fixed annual expenditure of DKK100,000, DKK200,000 and DKK400,000 respectively (24). These holding costs must be inflated against the Danish consumer price index as measured at January 1992 (i.e. 63.7, (40)). For example, if costs were incurred in 2020 (Index reading is 103.0), the inflator would be 1.62 (i.e. $\frac{103.0}{63.7}$). For ELs older than ten years, the index measures against the index at January 2012 (24).

In its experience, the Company notes that the applicable exchange rate is only known mid-year, by which point most fieldwork expenditure is already committed. There are also some minor discrepancies between the translated legislation and government practice (e.g. a fixed expenditure requirement is also levied against SELs as well as ELs). Such variation can introduce some difficulty in calculating the precise expenditure obligation ahead of time. Greenfields considers that the commitments are low enough that inconsistencies are not a significant concern.

Following the COVID-19 crisis of 2020, the Ministry of Mineral Resources ('MMR') waived all expenditure obligations for the 2020 calendar year for ELs and SELs (41), along with other allowances (42). Expenditure requirements are assessed based on licence holdings on 31 December of the relevant year (24), and area reduction can be at any point during the year. Therefore, no expenditure obligation in respect to ARC crystallises until after 31 December 2021.

The MMR has also postponed all transferred outstanding exploration obligations by one year, and extended the term of all ELs and SELs by one year (43). When combined with the expenditure waiver described above, this effectively means that the year 2020 was 'paused' for all licence holders and that the ARC SEL will expire in

**GREENLAND HAS A
COMMENDABLE
HISTORY OF
SUPPORTING THE
MINING INDUSTRY
DURING CRISES**

²³ International Union for Conservation of Nature.

late 2023. The Company is unaware of any other jurisdiction which has taken such a comprehensive approach to assist licence holders following COVID-19.

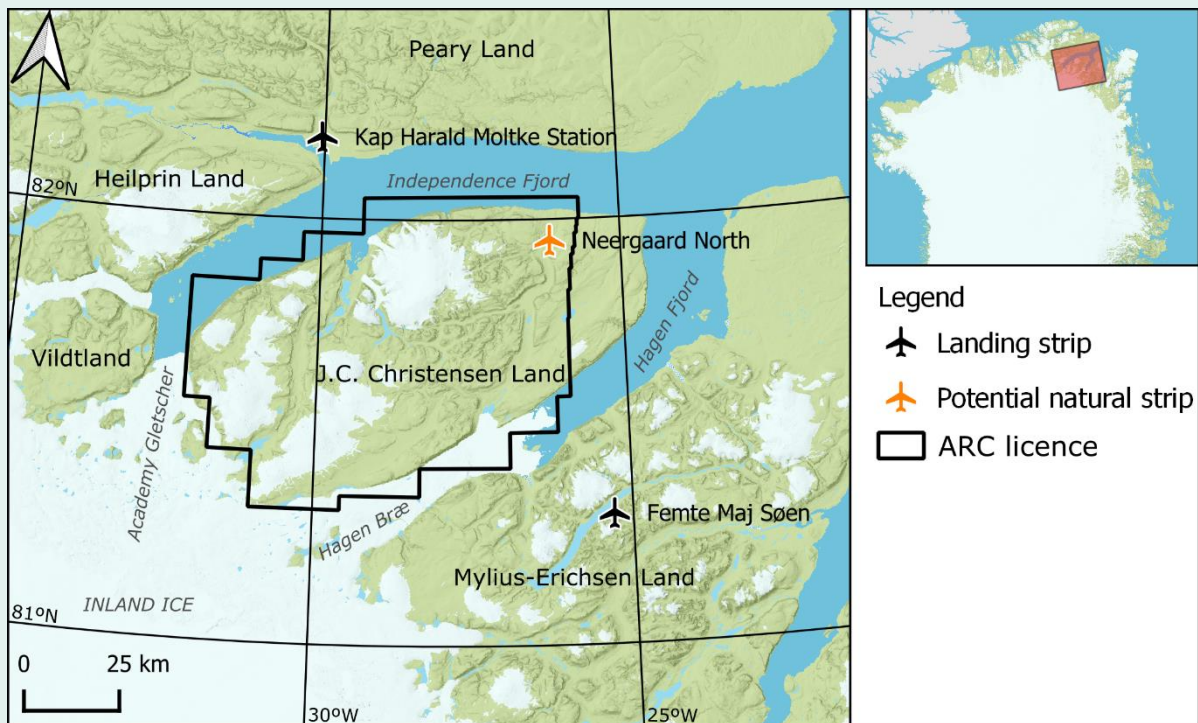
Greenfields estimates an annual expenditure requirement for ARC in 2021 will be ~AUD1.08 M. This calculation uses estimated rates for 2021 and a DKK to Australian Dollar ('AUD') exchange rate of 4.55 (44). By comparison, the Company calculates that the expense for a similarly sized project in Western Australia (30) would be in the order of AUD2.4 M, more than twice that of ARC²⁴. The ARC expenditure requirement can be reduced by relinquishing parts of the licence area.

SCALABLE
EXPENDITURE
COMMITMENT

An amendment has recently passed to the Mineral Resources Act to implement changes and clarifications concerning the granting of licences for the exploitation of minerals (45). Most importantly, this Act simplifies the process of obtaining an Exploitation Licence. This amendment brings Greenland's regulatory environment closer to those of advanced mining nations (46). The Greenland Government has flagged that the Mineral Resources Act will be further amended in the future, and these amendments should be released shortly. Any changes will not come into effect until July 2021 (47).

As ARC was established through a Government application process, it is free of third-party royalties, back-in provisions or any other rights that may affect the ownership or technical value of the Project. Similarly, there are currently no environmental or social liabilities in connection with the Project.

Figure 4: Licence map



Source: Greenfields.

²⁴ In any event such a large single exploration licence would not be permitted in Western Australia.



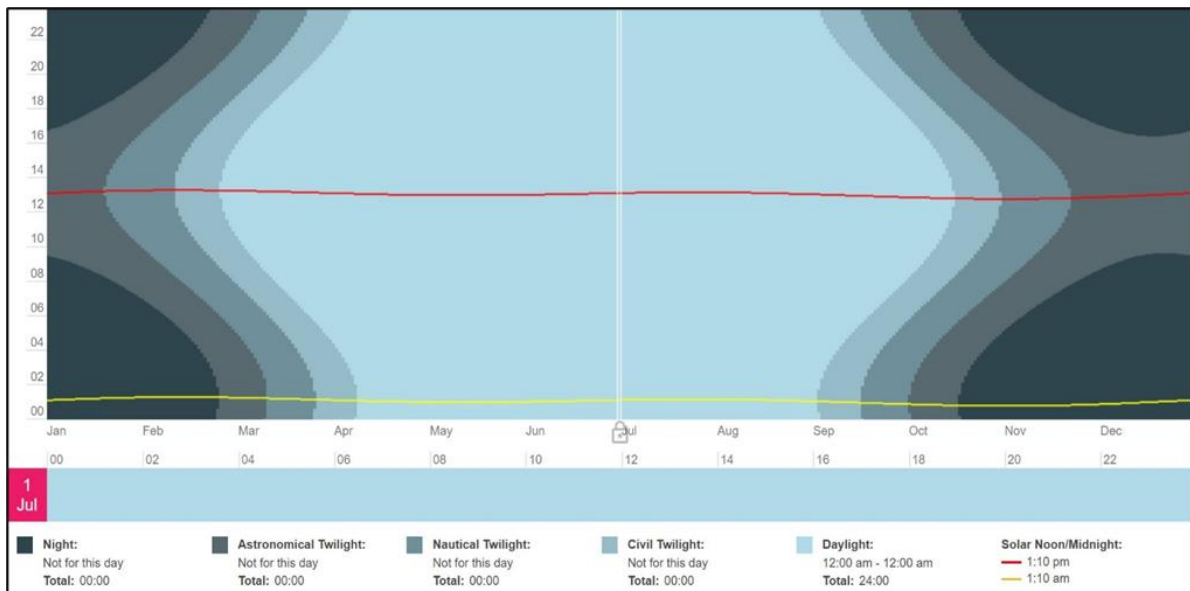
3.2 ACCESSIBILITY, CLIMATE, LOCAL RESOURCES, INFRASTRUCTURE AND PHYSIOGRAPHY

ARC is in an inner-fjord system in uninhabited North Greenland. ARC covers most of J.C. Christensen Land, a promontory that is flanked to the north and northwest by Independence Fjord, and to the southeast by Hagen Fjord (Figure 4). The region experiences seasons highlighted by months of 24-hour light or dark (Figure 5) (48). The region is an Arctic desert with climate averages for the wetter and more exposed Station Nord shown in Figure 6. Additional climate statistics are presented in Figure 99 to Figure 104 in the Supporting Figures section at the end of the Report. In mid-summer²⁵, temperatures can exceed 16°C (3). However, past climate statistics are unsuited to forecasting as models of Arctic temperatures are rising faster than models have predicted (49), at more than 1°C per decade (50; 51).

Based on Greenfields’ experience working in inner fjord systems in northeastern Greenland, J.C. Christensen Land is likely to be warmer, drier and more stable than a coastal location such as Station Nord. Flat, low elevations are typical northeast J.C. Christensen Land. The rest of the area consists of high plateaus with elevations around 1,000 m above sea level, with incised ‘U’ shaped valleys (3). Extensive glacial moraines and boulder fields result in much less exposure than suggested by type sections observed in cliff faces (2). Figure 7 shows some of ARC’s landscape. Vegetation and wildlife are minimal, and there are no designated sensitive areas within ARC (3).

TEMPERATURES
OF +16°C
REPORTED!

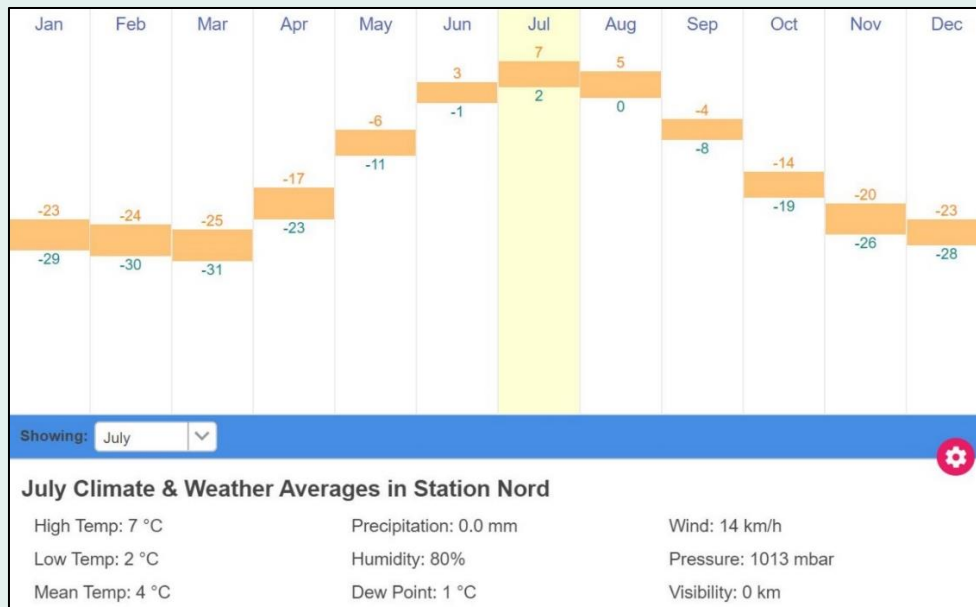
Figure 5: Daylight statistics for Station Nord



Source: TimeAndDate (52).

²⁵ Reports from a field program between 20 June and 16 August 1979 in the ARC region record temperatures ranging between +1°C and +10°C (267).

Figure 6: Weather statistics for Station Nord



Source: TimeAndDate (48)

Figure 7: Physiography of Neergaard Dal/Elv



Source: Haugaard (2011) (2) Note: Orange tents for scale in the middle of the image.

Access to North Greenland is generally via charter flights from Svalbard to Station Nord (13). A 1,800 m long unsealed runway at Station Nord can accommodate heavy-lift aircraft such as Lockheed C-130 Hercules ('C130') (53). The Danish Military resupplies Station Nord and the adjacent Villum Research facility using Lockheed C-130 Hercules, although aircraft as large as the Boeing C-17 Globemaster III have landed there (54). The Danish Military may on special request provide logistical support to other parties (55). De Havilland DHC-6 Twin Otter charter flights are also possible from Iceland via Nerlerit Inaat airport in eastern Greenland (56; 2). Locally there is



a 1,200 m long unsealed airstrip near Kap Harald Moltke Station, which may provide Project access for heavy lift aeroplanes such as C130s (57 pp. 13,17).

Access to Kap Harald Moltke Station is possible via a 200 km flight from Station Nord, or 110 km flight from the third-party airstrip located in Citronen Fjord²⁶. While the area at Kap Harald Moltke Station naturally lends itself to being an airstrip, it is at risk of flooding during wet summers (58). However, the Kap Harald Moltke airstrip suits to conversion to an all-weather strip (58). Within the licence, an area potentially suitable for landings using Twin Otters is located at the northern terminus of Neergaard Dal (2).

The uninhabited Kap Harald Moltke Station²⁷ and abandoned Brønlundhus²⁸ (Figure 8) are located to the northeast of ARC's centroid, across Independence Fjord and within Jørgen Brønlund Fjord. The buildings²⁹ were used for research purposes (60; 61). An inspection and restoration project in 2001 determined that the facilities were in good condition, although Brønlundhus is more of a museum piece (59). In early 2020, the Danish Military unit known as the Sirius Dog Sled Patrol conducted exercises near Kap Harald Moltke Station (62). Presumably, there was inspection and use of the buildings. Aside from this special-forces unit, the Company is unaware of other entities or persons recently active within or in the vicinity of ARC.

Access to ARC from the airstrip at Kap Harald Moltke Station may be via helicopter (2), or depending on the season, all-terrain vehicles³⁰ across a frozen Independence Fjord. Due to its inner fjord location, J.C. Christensen Land is dry relative to more coastal areas, and snow cover at low altitudes is reliably melted by July each year³¹. Fjord ice breaks up in August and remains open through September³². Sea ice conditions outside the fjord system are less predictable due to several external factors; however Ironbark Zinc Ltd ('Ironbark') conducted extensive research for its Feasibility Study (63) on the Citronen deposit and determined the passage to be commercially viable. Furthermore, in 2018 Ironbark successfully commissioned a polar-class cargo ship which sailed to Citronen (64). Given ARC's proximity to Citronen, Greenfields assumes that the findings of that study apply to the Project. The vessel that Ironbark commissioned frequently moves concentrate from a third-party mine in the Canadian Arctic (65). With the extent and thickness of the sea ice being in inexorable and accelerating decline (66), seaborne access is likely to improve. The minimum Arctic sea ice extent record in

Figure 8: Buildings in Jørgen Brønlund Fjord



Source: NANOK (2001) (59). Note: Brønlundhus on the top, Kap Harald Moltke Station on the bottom.

²⁶ The Citronen Fjord airstrip sits within the mining licence held by Ironbark Zinc Ltd, and in practical terms, is only of use if there are shared logistics with that entity. At the time of writing, no logistical co-operation agreement was in place between Greenfields and Ironbark.

²⁷ Constructed in 1972.

²⁸ Constructed in 1948.

²⁹ Amongst the most northerly permanent human structures on Earth (363).

³⁰ Permission must be sought and granted from the Greenland Government to operate all-terrain vehicles within the bounds of the Park (395).

³¹ Based on Greenfields inspection of Sentinel satellite imagery taken between 2016 and 2019.

³² Based on Greenfields inspection of Sentinel satellite imagery taken between 2016 and 2019.

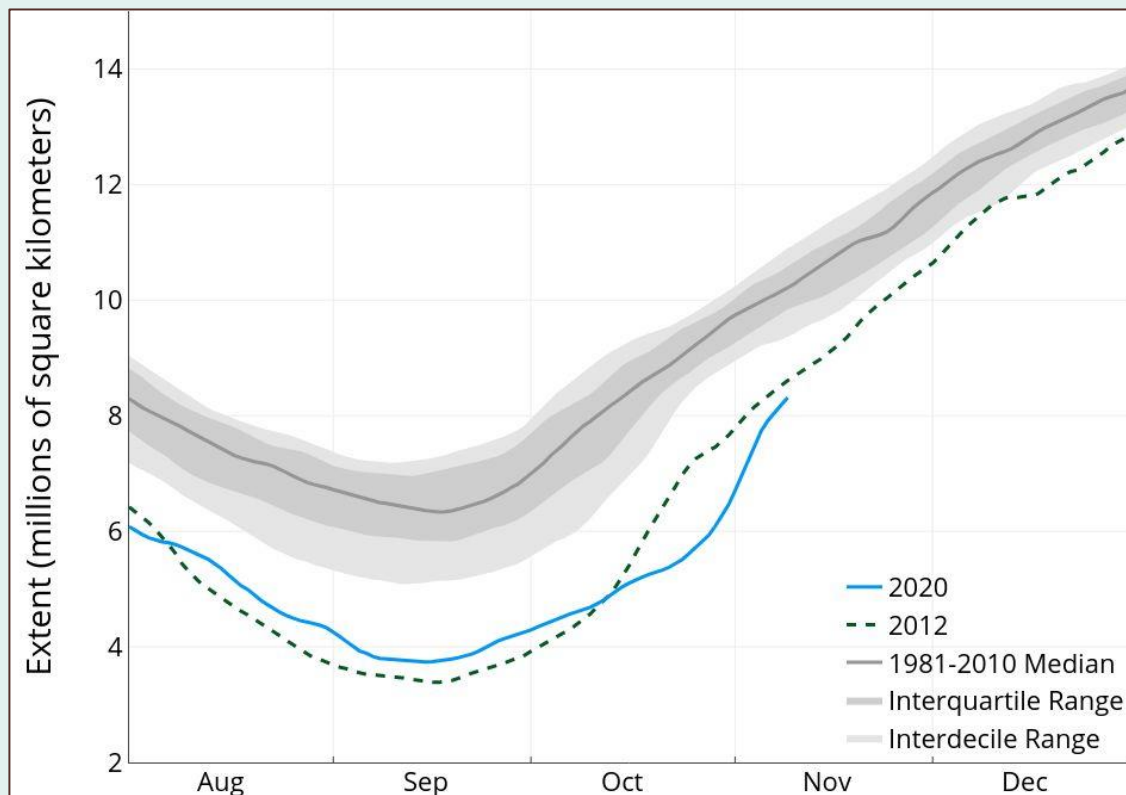
2020 was the second smallest on record (Figure 9) (67). This figure also shows that the refreezing is the slowest on record, and Greenfields thinks that this may have a substantial impact on the extent and thickness of the sea-ice in 2021. Figure 10 shows how low to medium altitudes are snow-free, and the extent of the ice in the fjords in 2019.

At a higher level, a recent study has shown that Greenland's ice sheet will likely continue to lose mass even if global warming halts overnight and the rate of surface melt decreases (68). On the surface, areas currently covered in ice are melting faster than the ice renewal. Glaciers which flow into the ocean are retreating. The study found that both trends will continue each year unless there is exceptional deposition (i.e. snowfall).³³ There is no indication that this will occur, so the ice sheet is 'likely in a long-term state of persistent loss'. The study did not focus on ARC, but Greenfields notes that ice cover is already spatially limited and precipitation is low relative to more coastal areas.

A separate study applied an updated sea ice model to historical ice trends, and the model was found to "provide independent support for predictions of ice-free [ocean] conditions by summer 2035" (49). Half of the models used in the study predict sea-ice-free conditions between 2030-2040, within a range of 2029-2066 (49).

AN ICE-FREE
ARCTIC OCEAN
WITHIN 15
YEARS.

Figure 9: Arctic sea ice extent

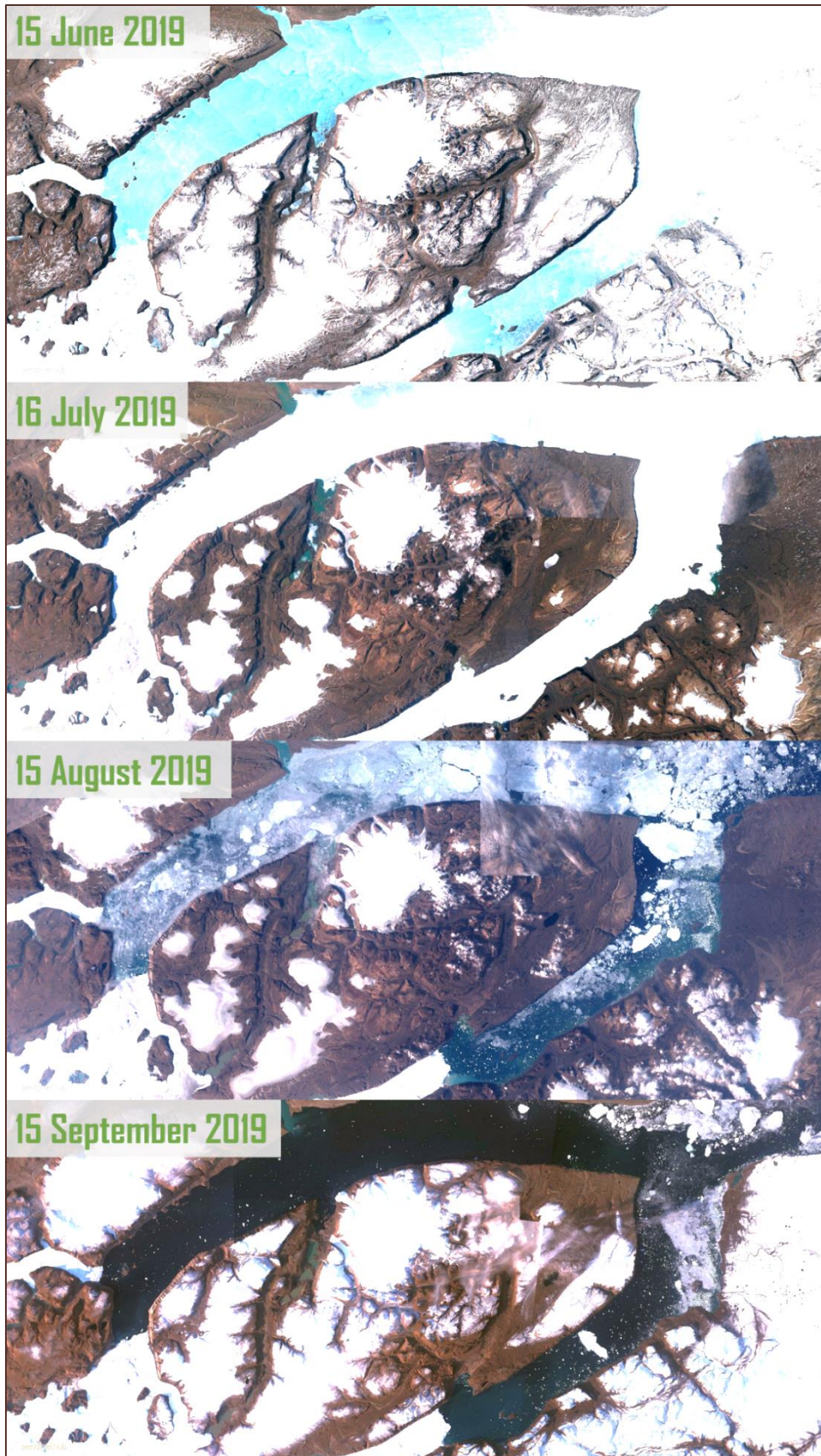


Source: National Snow & Ice Centre Data Center (67). Note: Extent is defined as an area of ocean with at least 15% sea ice, a figure which is navigable.

³³ Defined in the study as surface mass balance increase greater than two standard deviations above the 2000-2018 mean.



Figure 10: Satellite image of J.C. Christensen Land



Source: Collated by Greenfields using Sentinel Hub (2020) (69), with a 20% cloud filter. No imagery was identified after September 2019.

3.3 MINING INDUSTRY

3.3.1 Prior and current activity

Greenland has a history of mining, since 1780 (70), but overall activity is limited. Greenland's nascent mining industry is in an emergent phase. Historical mining has occurred for gold ('Au'), zinc-lead ('Zn-Pb') (Figure 11), copper, aluminium ('Al'), coal, graphite, and olivine (71; 72; 73; 74; 75; 76; 17). The most significant base-metal mine was the Black Angel deposit which produced 13.6 million tonnes ('Mt') of material with a grade of 12.3% Zn, 4.0% Pb and 29 grams per tonne ('g/t') silver over seventeen years (77; 78). The Black Angel mine is notable for its location in the side of a mountain (Figure 12). Historically, there have been economic evaluations carried out on deposits of molybdenum, tungsten, and copper (79; 80; 81; 82).

INTEREST IN
GREENLAND IS
GROWING RAPIDLY

There are two active commercial mining operations in Greenland; one mines rubies and sapphires (83); and the other anorthosite (84). There are also pre-mining projects that are either in advanced stages of evaluation or being brought into production and include:

- **Zinc-lead in North Greenland.** The Citronen Fjord ('Citronen') project is one of the largest and highest-grade undeveloped zinc-lead deposits in the world. Citronen is in a construction financing stage (85; 86). Ironbark reports that Citronen has a net present value ('NPV') of USD909 M using an 8% discount rate, and an internal rate of return ('IRR') of 35%³⁴ (87). Optimisation work is ongoing (88).
- **Rare-earth/uranium in south-western Greenland.** The Kvanefjeld project is at an advanced permitting (89) stage, is located in one of the "most unique geological environments on the planet" and when in production, may be among the world's largest rare-earth mines. Kvanefjeld has an NPV of USD1,500 M³⁵ and an IRR of 43% (90).
- **Titanium in north-western Greenland.** The Dundas project contains one of the highest-grade ilmenite mineral sands deposits in the world (91). The project has 117 Mt of material containing a grade of 6.1% ilmenite, and an Exploration Target of 300 Mt to 530 Mt grading between 0.4% and 4.8% ilmenite (92). The project was estimated to have an NPV_{5%} of US\$83.1 M, and a 34.5% IRR on a post-tax basis (92).
- **Anorthosite in south-western Greenland.** The Majorqap Qâva project is subject to a Preliminary Economic Evaluation, with the results due in February 2020 (93). Greenfields has not identified any study results or project updates.
- **Zinc-lead in west Greenland.** The historical Black Angel mine is being evaluated for renewed commercial production (78).
- **Iron in west Greenland.** The Isua magnetite deposit was subject to a Feasibility Study and is still under licence, pending financing (94).

In addition to the deposits above, the world-famous Skaergaard deposit - owned by Major Precious Metals Corp - is one of the world's largest undeveloped gold deposits, and the largest palladium deposit outside of Africa and Russia (95).

³⁴ After tax and discounted at a rate of 8% per annum, in nominal terms

³⁵ After tax and discounted at a rate of 10% per annum, in real terms Greenfields notes that since this announcement the capital cost has been reduced from US\$832 M to \$505M (360), although no corresponding NPV or IRR were identified.



There is also increasing interest in Greenlandic exploration by large mining companies. Anglo American Plc, Rio Tinto Plc, Orano and IGO Ltd are all active in the country (96; 97; 98; 99).

Figure 11: Miners at the historical Blyklippen lead-zinc mine in eastern Greenland



Source: GEUS (2005) (100).

Figure 12: Photo from the portal of the Black Angel in western Greenland



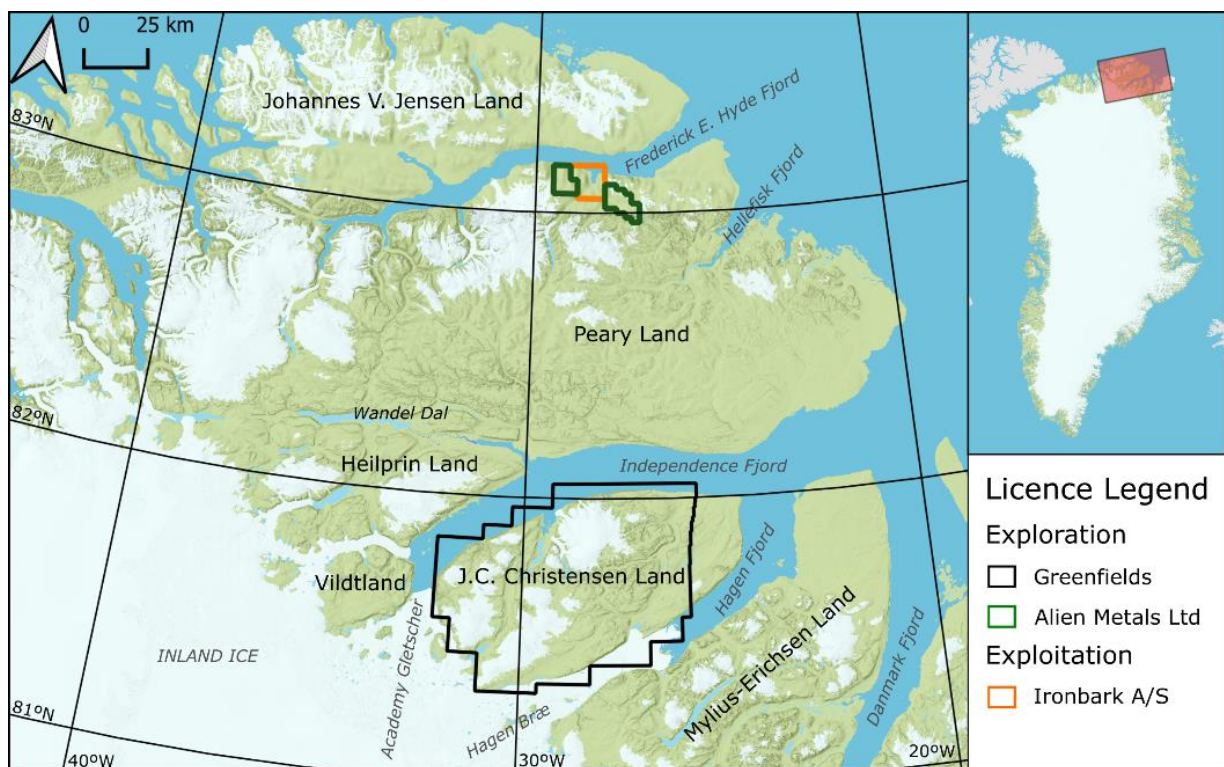
Source: GEUS (2003) (77).

3.3.2 Adjacent projects

Ironbark’s Citronen zinc-lead deposit is located approximately 130 km north of ARC. This deposit is within a granted Mining Licence (MIN 2016-30) (101). Alien Metals Ltd (‘Alien’) was granted a 208 km² EL (2020-44) contiguous to Ironbark’s in October, 2020 (102). Alien’s licence is comprised of two discrete areas on the eastern and western flanks of Ironbark’s licence (Figure 13).

Aside from the Mining Licence and EL in Fredrick E. Hyde Ford (Citronen etc.), the nearest exploration licences are over 600 km to the west in Washington Land and 900 km to the south (Greenfields’ Frontier project).

Figure 13: Adjacent projects and deposits



Source: Greenfields.

3.3.3 Importance to Greenland

Greenland considers mineral and petroleum extraction as a means of achieving financial independence from Denmark, and a means to ultimately become a country in its own right (17). Presently, the Greenland economy is highly dependent on support from Denmark to the tune of US\$613 M/year, or about one-third of the gross domestic product (103). Greenland's economy is trending to be steadily more unbalanced in the coming decades with annual budget deficits of more than 5% of gross domestic product (99). The Government is vigorously promoting and implementing favourable policies designed to entice investment in its mineral and petroleum potential (19). Government agencies make regular visits to industry trade shows and conferences in the major mining investment communities (104). To reduce administrative expense and complexity, Greenland allows foreign companies to hold exploration licences without the need to establish a local subsidiary entity (105). However, foreign companies are still required to have an address in Greenland and be listed on the 'Central Business Register (known as CVR number) (28). The Government publishes and accepts most business-related forms in English (106). While many countries claim to be pro-business, the Government of Greenland has backed it up with actions such as:

MINING IS A
MEANS TO
INDEPENDENCE

- negating all exploration licence expenditure obligations for the year 2020 in response to the macroeconomic fallout of the Coronavirus (107). Furthermore, the Government allowed mining licence holders to withdraw funds from the environmental bond to help with liquidity during this time, and 'paused' all licences so that 2020 does not count as a year towards the expiry of these licences (107). Greenfields is unaware of another jurisdiction which acted as fast, or as positively as Greenland;
- waiving all expenditure commitments for licences in years 6-11, for the year 2017 during a period when many exploration companies were unable to secure funds (108);
- increasing the number of public geologists from one to ten over a decade (109);
- overturning a uranium mining ban to enable the development of a single deposit (110);
- permitting a mine in the Park (38; 111);
- running a national mineral hunt, known as Ujarassiorit³⁶, which incentivises residents of Greenland to discover and report new and interesting mineral occurrences (112);
- committing its funds to pre-competitive, publicly available data in northeastern Greenland (113; 39); and
- starting a mining school (114).

Given the tangible steps that the Government has taken to attract and establish a mining industry, Greenfields considers Greenland a safe investment destination for exploration and mining activity.

3.3.4 Taxation and mineral royalties

Greenland's corporate tax rate for exploration and mining companies is 25%³⁷ (115; 116), which is less than Australia's headline corporate tax rate (117). Tax losses incurred by exploration

³⁶ Greenfields sponsored Ujarassiorit in 2018 and 2019. Due to the ARC licence application, the Government declined the Company's 2020 offer of sponsorship. The Company considers this action to be further evidence of the perception, and reality of rule-of-law.

³⁷ Natural resource companies are exempt from a 65% surcharge (115).



companies can carry forward indefinitely (118). Personal tax in Greenland is relatively simple and applies a flat-rate tax on labour, and certain capital income (119). The flat individual tax incurred by a non-resident working on exploration or mining projects is 35%, as opposed to the 42% on individuals working outside of the mineral sector. This lower tax rate for individuals working in mining and exploration is an incentive to grow the mining industry in Greenland (120; 116).

For copper concentrate, mineral royalties in Greenland are better than those imposed in Western Australia. The Greenland mineral royalty rate (excluding hydrocarbons, radionuclides and gemstones) is 2.5% on the value of the mine product ('*ad valorem*'), less corporate income and dividend taxes (121). In comparison, Western Australia imposes an *ad valorem* royalty on copper concentrates of 5.0% (122), from which there are no deductible items. While the effective rates of tax will be dependent on individual mine circumstances, in simple terms Greenland's mineral royalties are less than half of those in Western Australia. On this basis along with the positive actions described in section 3.3.3, **Greenfields considers that the financial attractiveness of exploring and mining in Greenland is substantially better than what is commonly perceived (123), and a suitable incentive for it to explore in this jurisdiction.**

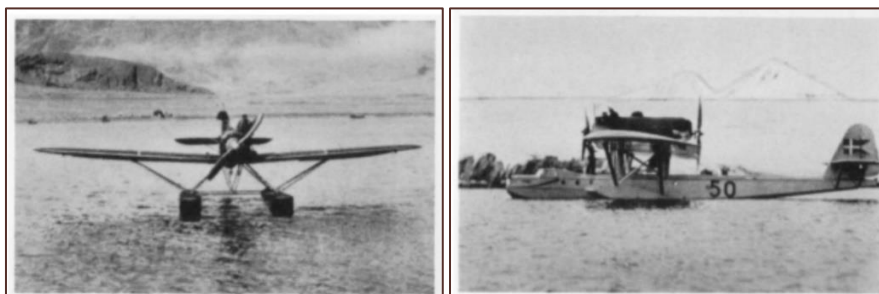
ROYALTIES LESS
THAN HALF OF THAT
IMPOSED BY
WESTERN
AUSTRALIA

4 HISTORY

North Greenland has been subject to scant exploration in every sense of the word. In the 50 years since the first description of native copper, there has been only a total of 3 years of follow up commercial exploration.

Three ancient cultures are known to have been active in the region, Independence I (2,460 to 1,860 years BC), Independence II (900 to 400 BC) and Thule (1,400 to 1,500AD) (61). Since that time there was no recorded activity until 1892 when Robert Edwin Peary³⁸ trekked across the inland ice to determine if Greenland was a Peninsula of the North Pole, and to map geology (124). In 1912, the famous Arctic explorers Knud Rasmussen, Peter Freuchen and their Inuit companions set out from what is now Thule to Independence Fjord to determine whether Peary Land was an island or an extension of Greenland (125; 126). Another big name in Arctic exploration and particularly notable in Greenlandic geology (127), Lauge Koch, conducted an expedition to the area in 1921. Lauge Koch's expeditions were the first to make dedicated geological observations of the region (128), and the pioneer of airborne exploration in the Arctic (127). Other geological expeditions occurred between 1947 to 1950, and 1966 to 1968 (128; 129; 127).

Figure 14: Airplanes used to explore North Greenland 1933-1938



Source: Dawes (1991) (127).

³⁸ Admiral Peary claimed to be the first to discover the North Pole (372).

The first commercial investigation of the geology in northern Greenland was conducted between 1969 and 1972 by the Greenarctic Consortium ('Greenarctic') (130; 58). The Greenarctic work involved a first pass evaluation of a 40,000 km² area extending from Thule to Independence Fjord (130; 58). Greenarctic reported native copper in Mylius-Erichsen Land (130). In 1972 Greenarctic explored ~5,000 km² in Heilprin Land, to the west of ARC (58). For the next forty years, only Government Surveys were active in the region. The 1973 field program identified low-grade copper, barite and made a recommendation to explore the region for zinc (58).

For the next forty years, only government surveys were active in the region. Between 1978 and 1980, the Greenland Geological Survey conducted a 20-geologist survey of the area north of 81° N and east of 40° W (131). The 1978 to 1980 program successfully identified sediment-hosted copper sulphides and oxides. The regional mapping campaign included stream sediment sampling for geochemistry, microscopy and heavy mineral analysis of stream sediment samples (128). Between 1993 and 1995, the Greenland Geological Survey conducted a 1:500,000 scale geological mapping exercise (132), with mapping and stream sediment surveys identifying sediment-hosted copper sulphides and additional native copper bearing basalts (128; 2).

The second commercial exploration activity was conducted between 2010 and 2011 by Avannaa Resources Ltd ('Avannaa'). In 2010, three Avannaa geologists conducted a twenty-day mapping and sampling program focussed in a small area at the northern terminus of Neergaard Dal³⁹ (2). In the subsequent year, Avannaa increased its Exploration Licence area and conducted a three-week, nine geologist, heli-supported reconnaissance program in a licence area expanded from 405 km on J.C. Christensen Land, to an additional 4,096 km² that extended to the southeast onto Mylius-Erichsen Land (3).

No work, commercial or Government, has occurred within ARC and its surrounds since 2011.

5 GEOLOGICAL SETTING

5.1 REGIONAL GEOLOGY

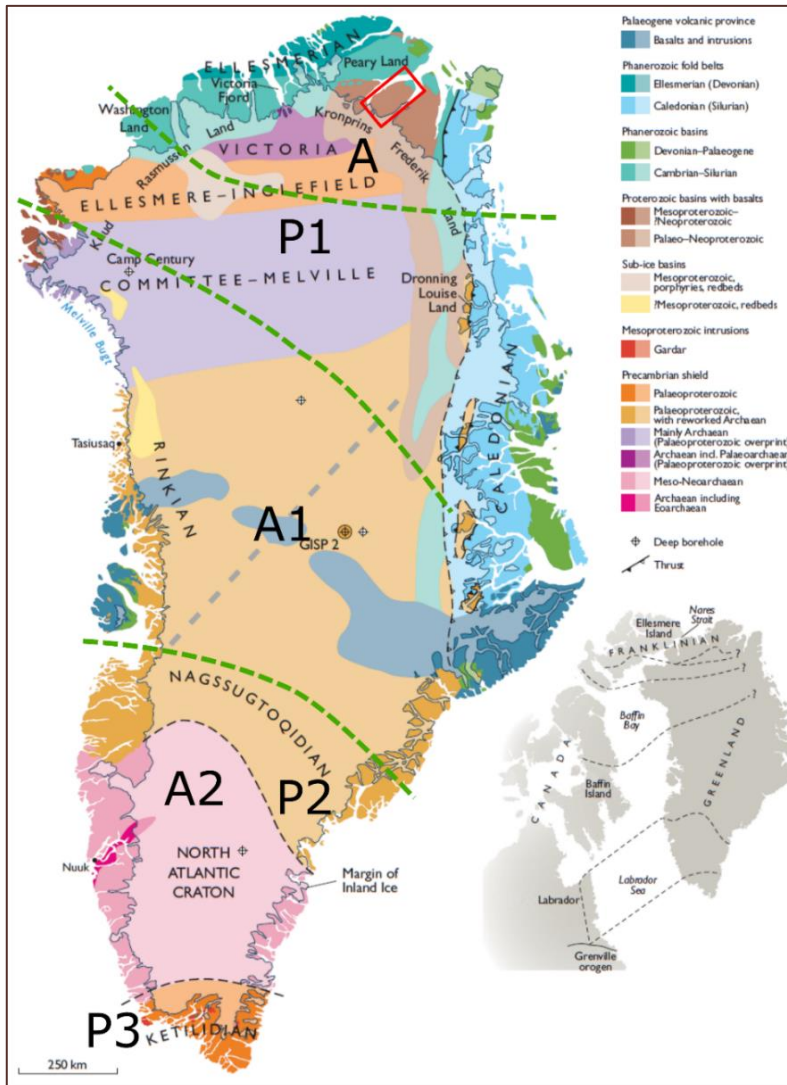
Greenland has a diverse, complex geological history which is poorly understood relative to North America, Europe and Australia. While there is adequate exposure on the coast, about 1.7 M km² (133) (~78%) of the island's interior is covered by an ice-sheet up to 3 km thick (134). The icesheet formed between 35 and 40 million years ago (135). The ice-free ~410,000 km² along Greenland's coast is of comparable size (136) to all of Sweden at 410,335 km² (137) or a 640 km x 640 km square. The first graphic interpretation of the geology underneath the ice was published in 2009 (138). Less than half the coastal exposure has ever been subject to publicly funded airborne geophysical surveys (139).

³⁹ Dal is valley in Danish and appears in many of the English publications.



Greenland contains some of the oldest rocks on Earth (141; 142), and possibly some of the oldest traces of life in the fossil record are near the capital city of Nuuk (143). The basement of Greenland comprises the Archean-aged⁴⁰ North Atlantic Craton (144) in the south; and the Rae Craton that accounts for much of central-western, and possibly central eastern-Greenland (Figure 15) (145; 136). The boundaries of the Rae craton are not well understood. Palaeoproterozoic-aged⁴¹ mobile belts separate the Archean-aged cratons (140; 146; 138). Younger sedimentary basins cover approximately 40% of Greenland’s ice-free area (147), predominantly in the east and north of the country. Mesoproterozoic⁴²-, Neoproterozoic⁴³- and Phanerozoic⁴⁴-aged sediments respectively account for 30%, 50%, and 20% of these basins (147).

Figure 15: Geology of Greenland



Source: GEUS (138).

Note the green dashed lines are superimposed by Greenfields based on geochronological interpretation by Nutman (2016) (140). ‘A’ stands for Archean-aged crust, P for Proterozoic emplaced or affected, with A1 being the Rae craton, A2 the North Atlantic craton, P1 being the Inglefield mobile belt, P2 the Nagssugtoqidian mobile belt, and P3 the Ketilidian belt. The red rectangle encapsulates J.C. Christensen Land.

⁴⁰ 4,000 to 2,500 Ma
⁴¹ 2,500 Ma to 1,500 Ma
⁴² 1,600 million years ago (‘Ma’) to 1,000 Ma
⁴³ 1,000 Ma to 541 Ma
⁴⁴ 541 Ma to 0 Ma

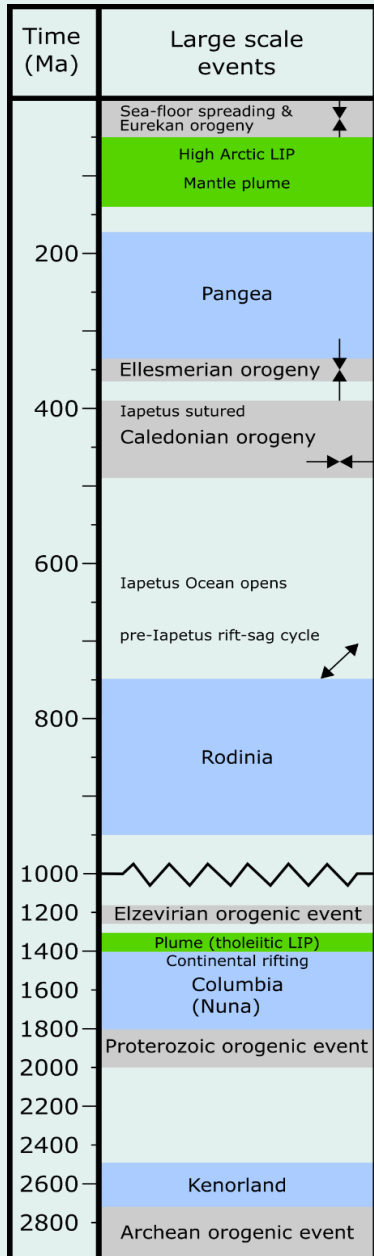


Figure 16: Timeline of geological events in North Greenland

Northern Greenland was the focus of large-scale successive geological events over time (Figure 16)^{45,46}. The area hosts examples of Archean⁴⁷ to Quaternary⁴⁸ aged rocks (148). The supracrustal rocks in North Greenland comprise Proterozoic-aged sediments and volcanics; Palaeozoic-aged⁴⁹ sediments; and Cenozoic⁵⁰-aged sediments and volcanics. These sedimentary packages deposited on a variety of tectonic settings (149). The Precambrian-aged⁵¹ rocks record Archean- and Proterozoic-aged orogenies⁵², continental flood basalts with accompanying intrusives, and two episodes of rifting (150). The breakup of supercontinents Columbia and Rodinia was the cause of the rifting (150). The Palaeozoic history includes the accumulation of more sediments and two orogenic events. These orogenies comprise the Caledonian (490 to 390 Ma) and Ellesmerian (c. 360 Ma) events (151). The Mesozoic⁵³ Era hosts sediments of a Cretaceous-aged⁵⁴ basin and plume-related volcanics that link to a large igneous province ('LIP') (152). During the Cenozoic Era, igneous activity continued as seafloor spreading initiated at the Gakkel Ridge to the north of Greenland, and the Eurekan Orogeny deformed parts of northern Greenland and Canada (153).

5.1.1 Tectonic settings

5.1.1.1 Columbia Supercontinent

During the early to middle Proterozoic Eon, Earth's proto-cratons assembled into a supercontinent named 'Columbia' (also called 'Nuna') (154). By approximately ~1,800 Ma, the supercontinent had formed by orogenesis (Figure 17). Columbia remained intact for approximately 300 million years before fragmenting around 1,500 Ma (155; 156). The oldest sedimentary rocks in northern Greenland deposited during this intracratonic extension (157). The associated crustal thinning continued, leading to 1,382 Ma plume-related flood basalts and intrusive dolerites (158; 159).

Source: Greenfields.

Note: Inward pointing arrows indicate maximum principal component direction and outward point arrows indicate minimum predominant component direction. Directions are generalised with the north being towards the top of the page.

⁴⁵ The Archean and Proterozoic orogenic events are recognised in reworked Archean gneiss in the basement present in a small area exposed at the head of Victoria Fjord (81.7°N, 46°W) (169). The basement is otherwise not exposed in North Greenland (148).

⁴⁶ Kenorland was a supercontinent comprised of Laurentia, Baltica, Western Australia, and Kalahari cratons that assembled from c. 2,700 Ma until 2,500 Ma (394; 364).

⁴⁷ 4,000 Ma to 2,500 Ma

⁴⁸ 2.58 Ma to present

⁴⁹ 541 Ma to 251.9 Ma

⁵⁰ 66 Ma to present

⁵¹ Older than 541 Ma

⁵² Orogenesis: the collision of two or more tectonic plates at convergent boundaries.

⁵³ 251.9 Ma to 65 Ma

⁵⁴ 145 Ma to 66 Ma



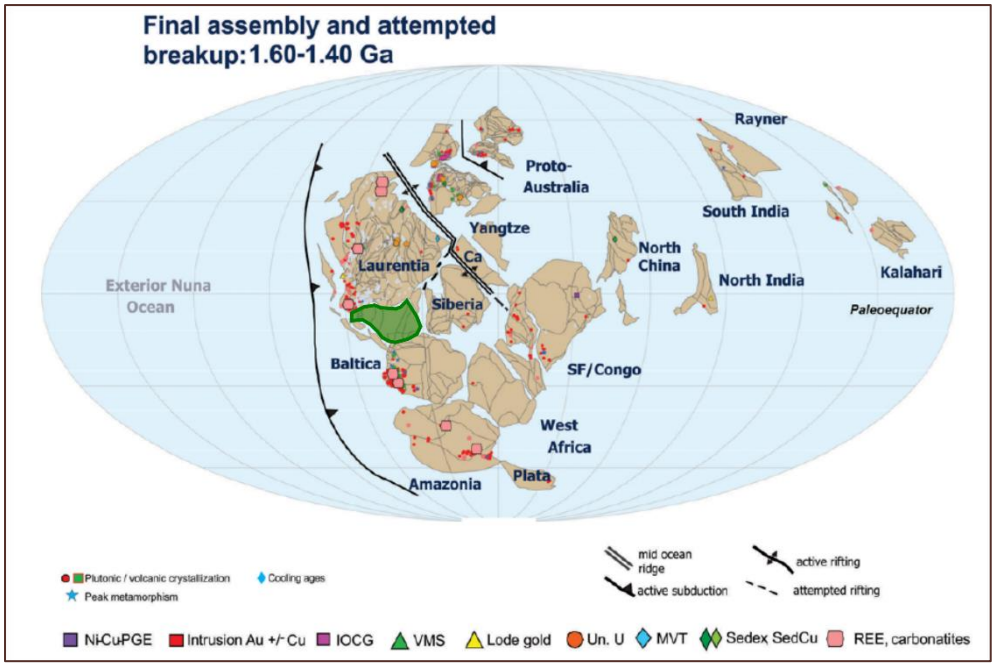


Figure 17: Reconstruction of Columbia at c. 1,600 Ma

Source: Pehrsson et al. (2015) (160)

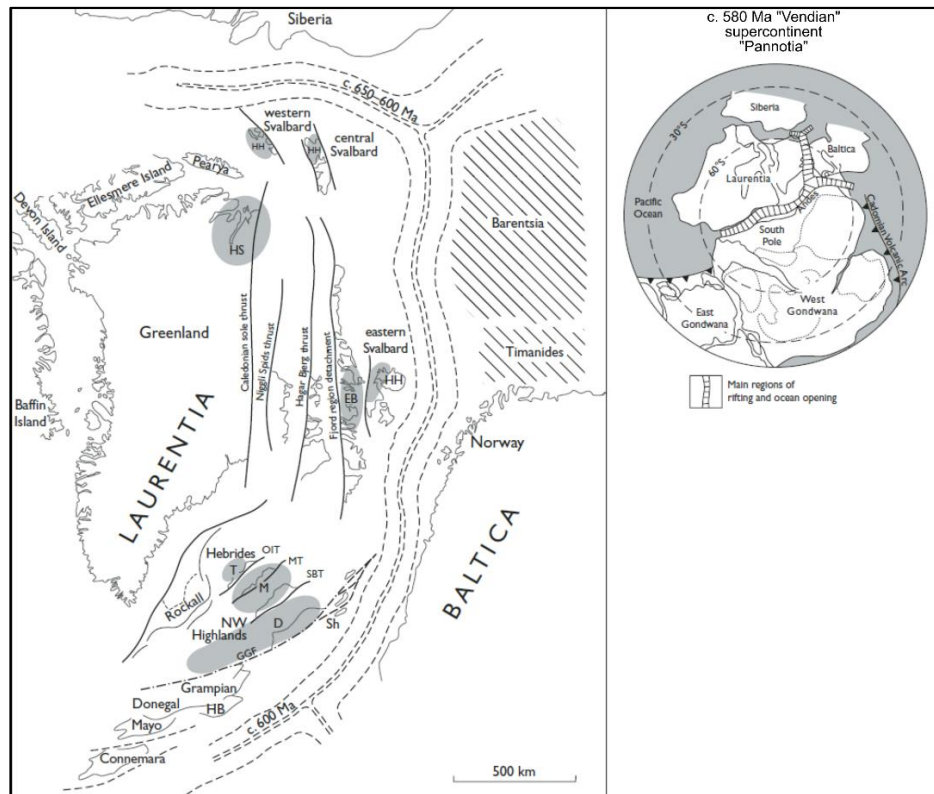
Note: Greenland's location is highlighted in green by the Company.

5.1.1.2 Rodinia Supercontinent

After the breakup of Columbia, the next supercontinent to form was the Neoproterozoic-aged Rodinia (150). Continents began to assemble again around 1,300 Ma and by c. 1000 Ma, Rodinia reached stability as a supercontinent (150). Rodinia was stable for 150 million years and began to fragment at c. 850 Ma (150). A triple junction facilitated rifting between the Laurentian, Baltic, and Siberian plates leading to the development of the Iapetus Ocean (Figure 18) (157). In northern Greenland, the Hagen Fjord Group contains sediments from this period as the Laurentian margin transitioned from early rift-sag cycles to a passive margin (157).

Figure 18 Neoproterozoic-aged sedimentary basins of the Laurentian margin

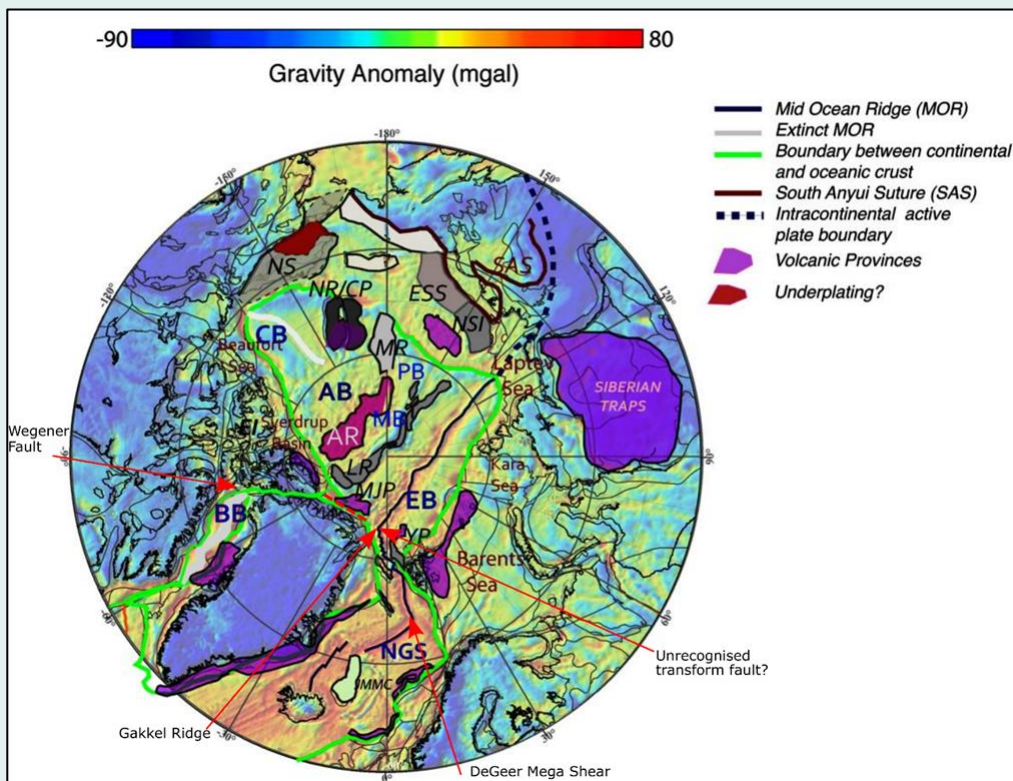
Source: S nderholm et al. (2008) (157). Note: D: Dalradian Supergroup basin; EB: Eleonore Bay Basin; GGF: Great Glen fault; HB: Highland Border; HH: Hekla Hoek succession basins; HS: Hekla Sund Basin; M: Moine Supergroup basin; MT: Moine thrust; OIT: Outer Isles thrust; SBT: Sgurr Beag thrust; Sh: Shetland Islands; T: Torridonian basin.



5.1.1.3 Plate margins

Plate boundaries surround Greenland and are affected by their relative movements (Figure 19) (161). Between Greenland and Canada in the Narres Strait, the Wegener Transform fault represents the failed arm of a triple junction (162). To the north, Greenland's continental crusts meet fresh (c. 55 Ma to present) oceanic crust born out the Gakkel Ridge mid-ocean spreading centre (163). The Gakkel Ridge is a 1,800 km long divergent plate boundary dividing the North American Plate and the Eurasian Plate between Greenland and Siberia (164). While the mid-ocean ridge initiated along the Lomonosov Ridge⁵⁵, there is uncertainty surrounding the movements of plates in the Arctic (165). The Gakkel Ridge's current position implies that it has faulted past the north coast of Greenland from c. 55 Ma to present (166; 153). The reviewed literature does not attribute any large-scale transform fault system to explain the contact between continental Greenland and the spreading Arctic Ocean sea-floor (166; 153). Irrespective of the uncertainty, the result is large-scale mantle-tapping boundaries with sympathetic fault zones cutting through North Greenland (162; 149).

Figure 19: Arctic plates and volcanic provinces



Source: Modified from Gaina et al. (2014) Fig 2 (166). Note: Microcontinents: JMMC: Jan Mayen, LR: Lomonosov Ridge, MS: Marvin Spur, MR: Mendeleev Ridge, NR/CP: Northwind Ridge/Chucki Plateau, NSI: North Siberian Islands, WI: Wrangel Islands, NS: North Slope, CT: Chukotka Terrane, ESS: East Siberian Shelf; Oceanic Basins: NGS: Norwegian Greenland Sea, EB: Eurasia Basin, MB: Makarov Basin, PB: Podvodnikov Basin, AB: Ameriasia Basin, CB: Canada Basin.

⁵⁵ The Lomonosov Ridge is an underwater sliver of continental crust in the Arctic Ocean (399). It runs from the Siberian Islands, Russia to Ellesmere Island, Canada, making it 1,700 km long (398). It divides the Amerasian and Eurasian Basins and is parallel to the Gakkel Ridge (166).



5.1.2 Sedimentation

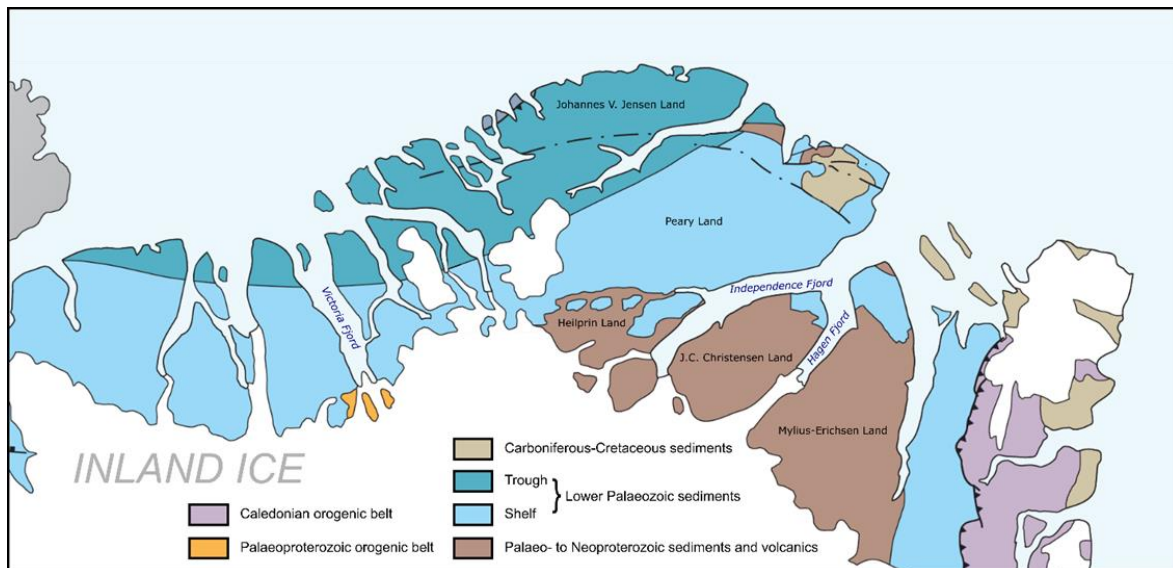
Sedimentary rocks dominate the lithology of North Greenland. The region was subject to five major events which influenced or closed and deformed basins (149). The five major events are a mid-Proterozoic-aged interior sag; mid-Proterozoic rifting and volcanism, the Elzevirian Orogeny; late-Proterozoic rifting and opening of the Iapetus Ocean; and late-Proterozoic/early-Cambrian rifting and early-Palaeozoic passive margin. These events result in the:

- **Independence Fjord Group:** Palaeo- to Mesoproterozoic-aged terrestrial sediments deposited within 30° of the equator;
- **Hagen Fjord Group:** Neoproterozoic-aged shelf sediments and turbidites, also within 30° of the equator;
- **Franklinian Basin:** Palaeozoic-aged carbonate shelf and deep-water siliclastics; and
- **Wandel Sea Basin:** Carboniferous- to Tertiary-aged, fluvial and interbedded shelf carbonates, siliclastics, and volcanics (149; 167; 150; 148).

These sediments sit above a crystalline basement that comprises gneiss, amphibolite and granitic rock (148; 168). The crystalline basement is seen approximately 250 km east of J.C. Christensen Land at the head of Victoria Fjord (169). Here, Franklinian Basin sediments unconformably overlie the basement, and are compressed into south-facing tight folds by either the Caledonian or Ellesmerian Orogeny (refer to sections 5.1.4.2 and 5.1.4.3) (148).

There is no outcropping basement contact of the Independence Fjord Group in J.C. Christensen Land (170). Approximately 200 km to the southeast around Hekla Sund, an interbedded c. 1,740 Ma mafic and intermediate extrusives overlie the basement (171). It is not known if the c. 1,740 Ma volcanics exist at depth in J.C. Christensen Land.

Figure 20: Basins of North Greenland



Source: Modified by Greenfields from Henriksen et al. (2009) (148).

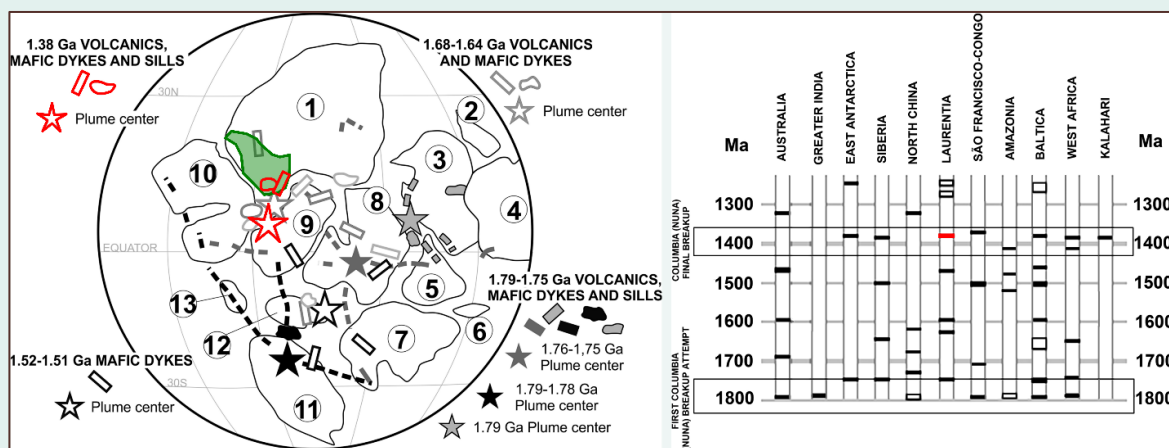
5.1.3 Volcanism

5.1.3.1 Ancient Plume

The breakup of supercontinents coincides with the timing of mantle plumes and Large Igneous Provinces⁵⁶ ('LIPs') (172). LIPs are capable of bringing large amounts of mantle-derived magma to the crust in the form of flood basalts, sills, and dykes (173).

In North Greenland, the evidence for an ancient plume is in the form of expansive continental flood basalts and mafic intrusions (159). These mafic outflows tie in with a c. 1,382 Ma⁵⁷ plume that was located at the junction between Laurentia, West Africa, and Baltica at the time of Columbia's breakup (Figure 21) (174). Volcanic evidence for this 1,382 Ma plume is preserved today in West Africa (e.g. Morocco (175)) and Baltica (e.g. Southern Urals (176)). Within North Greenland, the flow-direction of the basalts is from the northeast, which is consistent with where Chaves & Rezende (2019) place the plume centre in Figure 21 (174; 177).

Figure 21: LIPs in the time interval relevant to Columbia Supercontinent reconstruction



Source: Modified from Chaves & Rezende (2019) (174). Note: Red highlights are LIP activity relevant to North Greenland. The green shaded area is the approximate position of Greenland; added to the figure by Greenfields. A bar indicates a single pulse. A box encloses multiple pulses. (1) Laurentia; (2) Kalahari; (3) Australia; (4) Mawson East Antarctica; (5) India; (6) Tarim; (7) São Francisco-Congo; (8) Siberia; (9) West Africa; (10) Baltica; (11) Amazonia; (12) North China; (13) Rio de la Plata.

The emplacement of intrusives and extrusives within LIPs tends to follow an established pattern (Figure 22) (173). Within this framework, the flood basalts preserve the palaeo-surface and intrusions form an underlying sill province. The flood basalts⁵⁸ have a surface exposure greater than 10,000 km²⁵⁹ (159). Greenfields considers that North Greenland contains distal expressions of an ancient mantle plume based on palaeotectonic reconstructions (174), 'saucer-shaped' intrusions, lack of basalt cutting dykes, and overall low levels of metamorphic alteration (grey box in Figure 22) (173).

⁵⁶ LIPs are huge volumes of erupted and intruded magma and are exceptional volcanic event in Earth history (374). The volume emplaced material is often in the order of 10,000km³, but may range up to 100,000km³ (374).

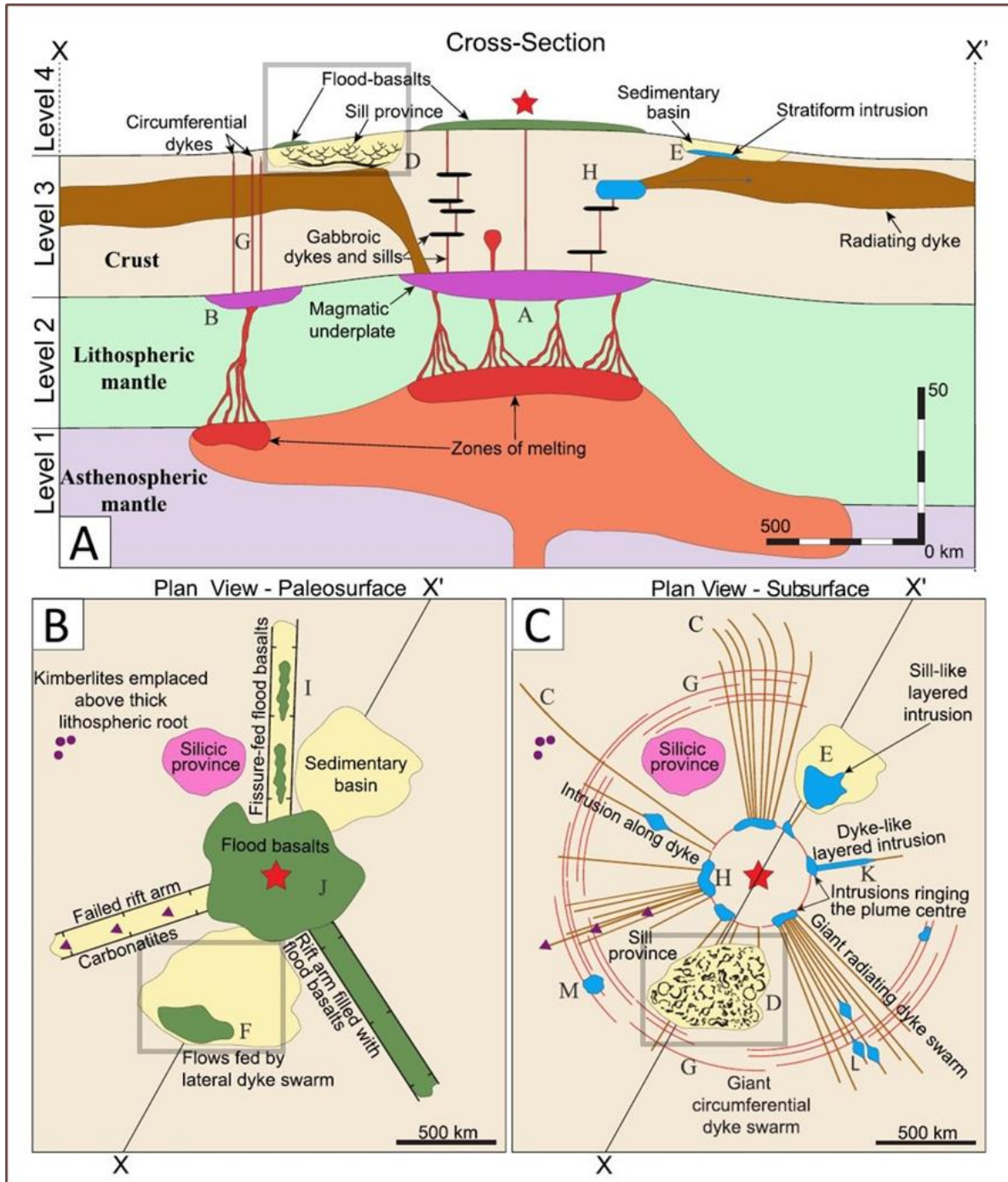
⁵⁷ Zhang et al. (2020) estimate that the Earth's core solidified between 1,300 Ma and 1,000 Ma (388). Allowing for margins of error this places the ancient mantle plume at a similar time when the flow dynamics of Earth were changing in response to a solidifying/solidified core.

⁵⁸ The Zig-Zag Fm basalts.

⁵⁹ The original extent of the Zig-Zag Fm flood basalt is not known (148). Based on the distribution of the Midsommersø Dolerites, it is thought that the basalts were eroded away to the east and west of the present exposure (159). The research by Ernst et al (2019) indicate that this may not be the case as the dolerites can be spatially independent of the basalts (173). Similarly, there are outcrops of Zig-Zag Fm basalts at Wyckoff Land some 130 km to the north, with the area between the surface exposures being covered by younger sediments (221).



Figure 22: LIP plumbing framework

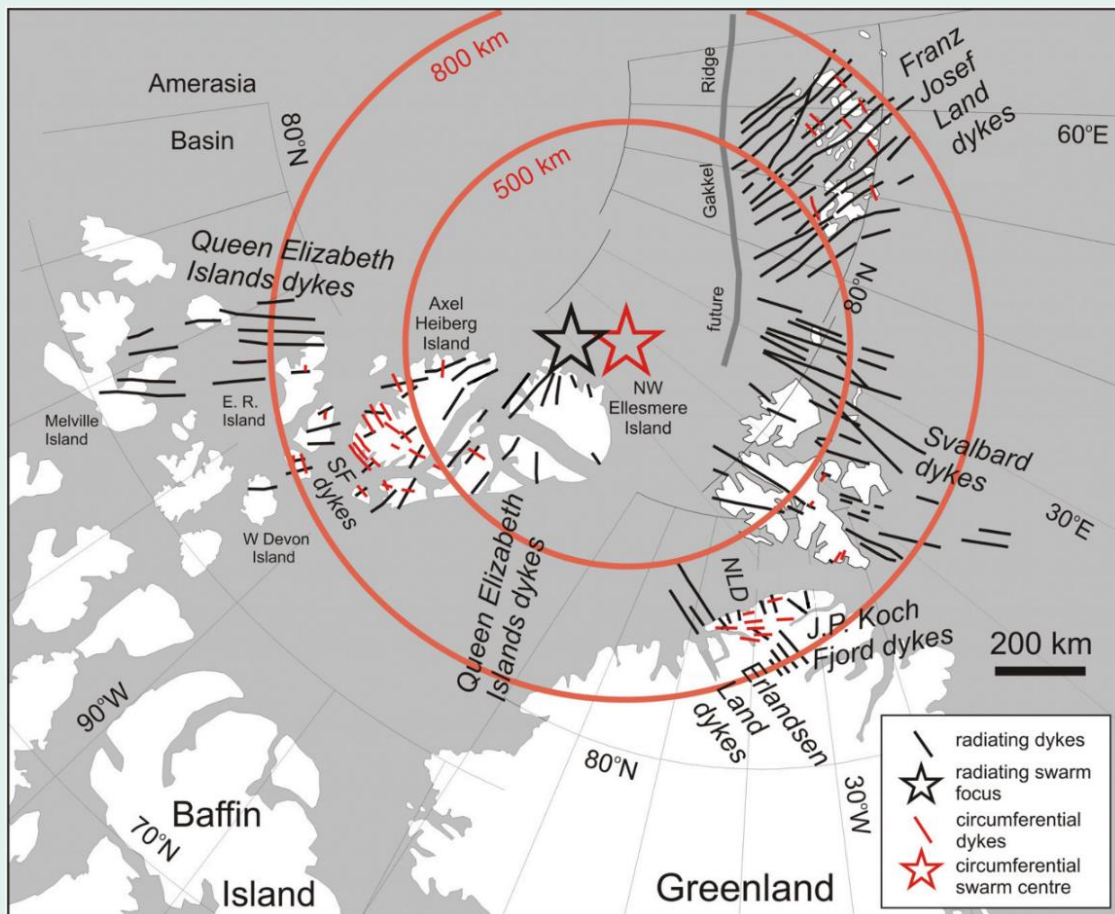


Source: Ernst et al. (2019) (173), modified by Greenfields. Note: A) cross-section, B) palaeo-surface plan view. C) subsurface plan view. The transparent grey box on each picture shows Greenfields interpreted equivalent location for the North Greenland flood basalts and intrusions

5.1.3.2 High Arctic Large Igneous Province

Another LIP was active in North Greenland during the Cretaceous⁶⁰, the High Arctic Large Igneous Province ('HALIP') (152). Volcanic evidence for HALIP was once contiguous but has since separated by plate movements (152). The evidence of HALIP magmatism extends from North Greenland, the Canadian high Arctic islands, Svalbard, and Franz Josef Land in the form of giant dyke swarms (152). Together, these dykes have ages between c. 140 to 80 Ma and represent three generations of volcanic pulses from a mantle plume (152). Although vastly separated today, reconstruction of tectonic plates to the time of emplacement can be used to identify the central point of the mantle plume (178; 173). Pieced together, these Arctic dykes are components of circumferential and radiating dyke swarms (Figure 23) (152). The reconstructed swarm centre indicates a source location close to Ellesmere Island, Canada (152). In North Greenland, three major pulses of magmatism are expressed by three sets of dykes collectively known as the Peary Land Dyke Swarm (152). As well as the dykes, HALIP magmatism is linked to North Greenland through the c. 64 Ma Kap Washington Group basaltic to rhyolitic lavas (179). The initiation of seafloor spreading adjacent to Ellesmere Island c. 56 Ma caused the emplacement of these lavas (180; 181).

Figure 23: HALIP evidence



Source: Buchan & Ernst (2018) (152).

Note: Circumferential (red) and radiating (black) dyke swarms of the HALIP with reconstructed plates c. 80 Ma. The red star is the focus of circumferential dykes, and the black star is the focus of the radiating dykes.

⁶⁰ 145 Ma to 66 Ma.



5.1.3.3 Icelandic hotspot

The Icelandic hotspot⁶¹ is one of seven⁶² hotspots with its plume originating from the deep mantle (183). From its present-day location, it can be traced back through Greenland to the Arctic 80 million years ago (182). The evidence is in the form of heat left behind from its transit (Figure 24) and a trail of progressively older mafic intrusions and flood basalts up the east and west coast of Greenland (182). In its back-tracked location offshore from Ellesmere Island, the Icelandic hotspot was at the centre of the HALIP (152). Greenfields concludes that this creates a direct link between the deep-rooted Icelandic hotspot and the mantle plume responsible for HALIP magmatism in the Arctic c. 64 to 140 Ma.

5.1.4 Orogenesis

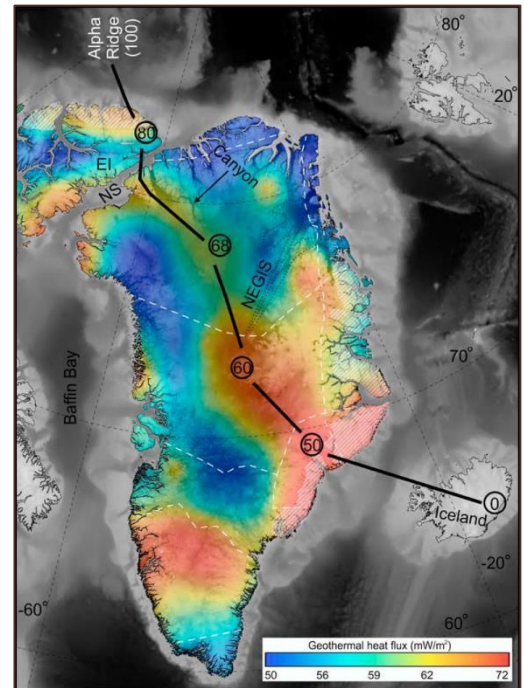
5.1.4.1 Elzevirian

The Elzevirian Orogeny⁶³ took place between 1,300 to 1,200 Ma when two blocks within Laurentia sutured together (184). The Elzevirian is an early phase of the Grenville Orogeny in North America⁶⁴, associated with the assembly of Rodinia (185). In North Greenland, Proterozoic-aged sediments are sourced mainly from the southwest and originated from topography created by the Grenville Orogen (186). The sediment provenance indicates a substantial 1,250 Ma source which coincides with the Elzevirian Orogeny (186). There are two⁶⁵ explanations for how sediments from this distal event can be in North Greenland:

1. Sediments transported across the Greenland Shield from the known exposure of the Grenville Orogen in North America to North Greenland (Figure 25a); or
2. The Elzevirian Orogeny was proximal to North Greenland and extended along the spine of East Greenland (Figure 25b) (186).

The inclusion of sediments with cobble-sized clasts and a 1,250 Ma age signature suggests that the orogenic event was proximal to North Greenland rather than distal (186). Zircon dating from eastern Greenland indicates an Elzevirian event occurred there⁶⁶ (187), and supports the proximal (Figure 25b) interpretation.

Figure 24: Hotspot trace



Source: Martos et al. (2018) (182). Note: The trace is from 80 Ma to present. El: Ellesmere Island; NS: Nares Strait NEGIS: northeast Greenland ice stream.

⁶¹ A hotspot is the surface expression of a mantle plume.

⁶² Of 49 hotspots (183).

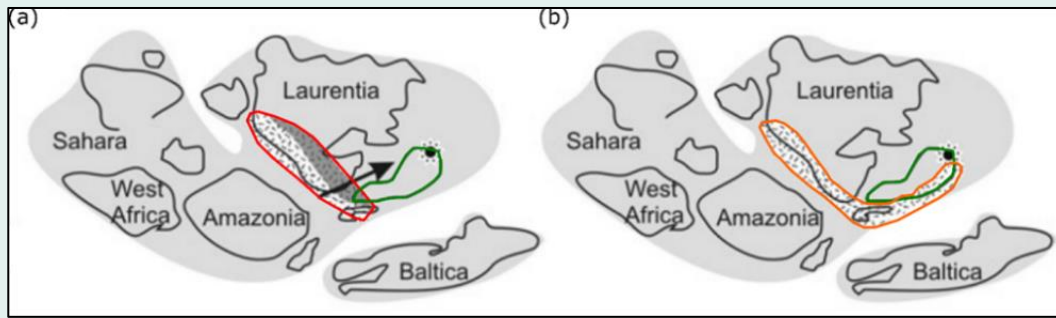
⁶³ Orogenesis are geodynamic collisional events known to affect regional fluid flow beyond their direct areas of influence (404; 402). Although the Caledonian orogeny did not fold rocks in east of Danmark Fjord, (e.g. J.C. Christensen Land) some structures further afield may still related to it (223; 151).

⁶⁴ 1,300 Ma to 900 Ma (185).

⁶⁵ Kirkland et al (2008) provide four explanations but ultimately state their preference for two (186).

⁶⁶ Sediment transport is shown to be from south to north along the east coast of Greenland (187).

Figure 25: Grenville and Elzevirian orogens at the time of Rodinia



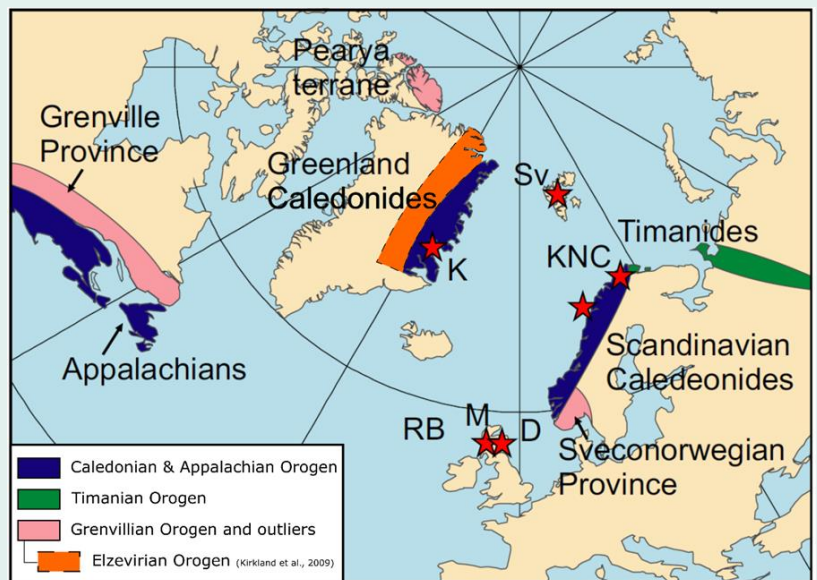
Source: Modified from Kirkland et al. (2009) (186). Note: Green outline depicts Greenland. The black dot shows the location of North Greenland. (a) Red outline depicts combined Grenville and Elzevirian orogens. (b) Orange outline depicts Grenville orogeny with a proposed extension to the Elzevirian orogeny up the spine of East Greenland.

5.1.4.2 Caledonian

The Iapetus Ocean closed during the collision between Laurentia⁶⁷, Baltica (Scandinavia) and the Avalonia microcontinent⁶⁸ between 490 to 390 Ma (189; 190). The rocks deformed by this prolonged event are collectively called the ‘Caledonides’ (191; 192). In North America, Scotland, and Ireland, the Caledonides have accreted onto the Grenville Orogen (Figure 26) (193; 186). The proposed extension of the Elzevirian Orogen up the east coast of Greenland gives the Elzevirian and Caledonian Orogens the same adjacent relationship already observed in North America, and the British Isles (193; 188; 186).

In Greenland, the Caledonides extend for 1,500 km down the eastern seaboard (191). In North Greenland, the main fold and thrust belt of the Caledonian Orogen is to the east of Danmark Fjord^{69, 70}, although it had far-reaching effects further to the west (157; 149). These effects include a westward shallowing fluid and heat migration associated with the emplacement of a granitic mid-crustal layer (194; 195). The orogeny driven fluid flow extends ~150 km to the west of the J.C. Christensen Land (Figure 26) (196).

Figure 26: Caledonian and stylised Elzevirian orogens



Source: Slagstad et al. (2019) (188). Note: Greenfields added the orange shading to indicate the extension of the Elzevirian Orogeny. Pink blocks correspond to late Meso- to early Neoproterozoic orogens, green to the late Neoproterozoic Timanian orogen, and dark blue to the Palaeozoic Caledonian–Appalachian orogen. Red stars indicate areas where late Meso- through late Neoproterozoic deposition, deformation, and magmatism, interpreted to be related to active-margin processes in a long-lived Rodinia-exterior orogen, have been found in Caledonian allochthonous nappes. D, Dalradian succession; K, Krummedal succession; KNC, Kalak Nappe Complex; M, Moine succession; RB, Rockall Bank; Sv, Svalbard terranes.

⁶⁷ North American and Greenland (397).

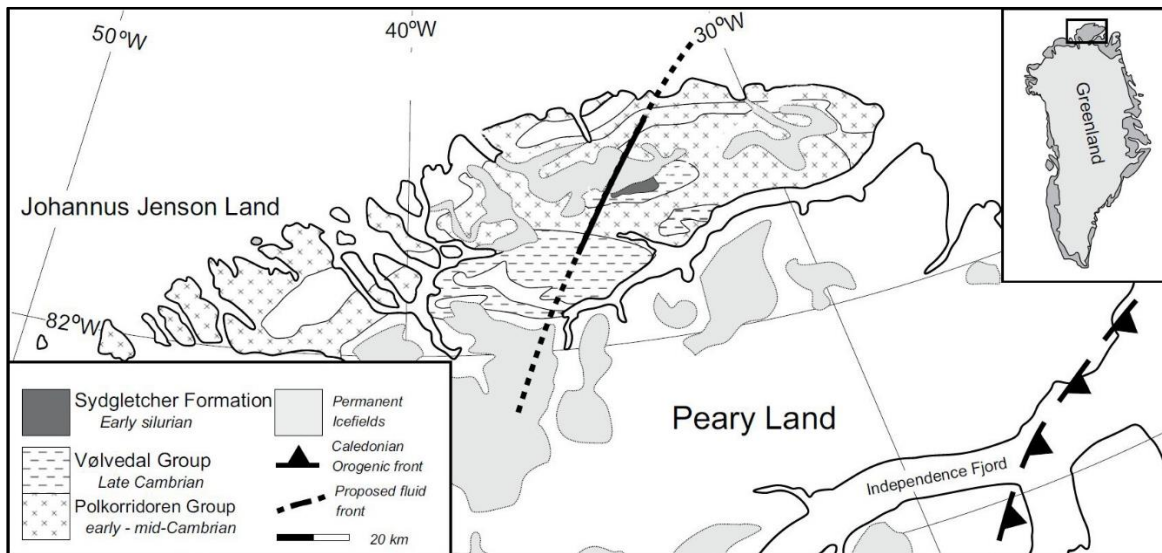
⁶⁸ Parts of Great Britain and North America (189).

⁶⁹ While the Caledonian Orogen is expressly bound by the Danmark Fjord, it has distal impacts to the west (149 pp. 38, 41).

⁷⁰ Danmark Fjord is around 120 km east of J.C. Christensen Land.



Figure 27: Caledonian Orogeny front and its fluid front

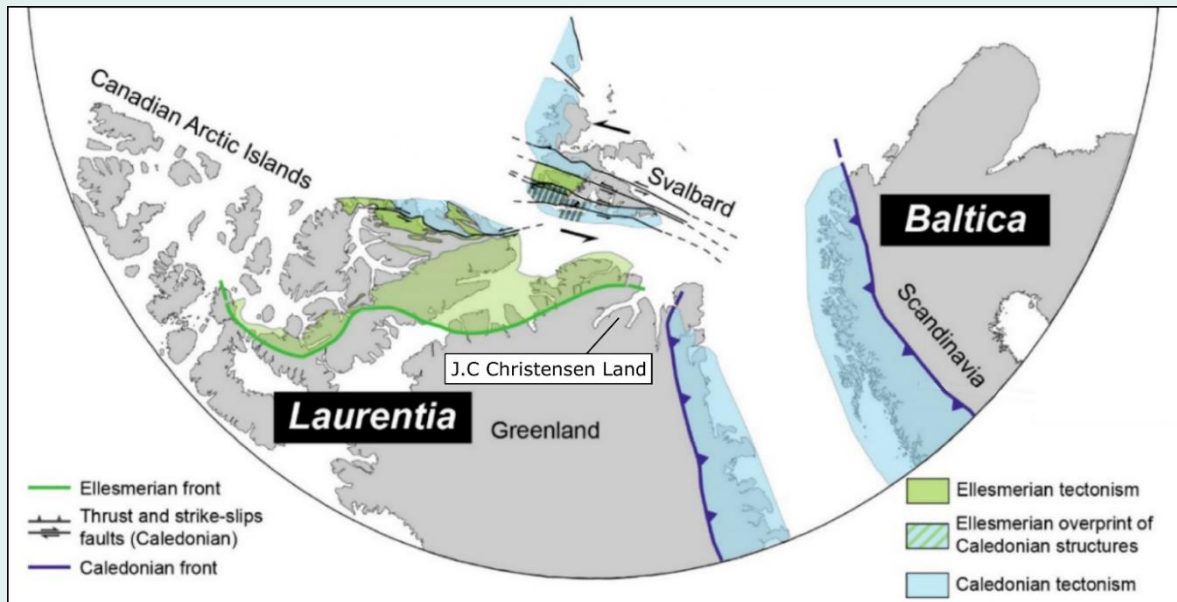


Source: Morris et al. (2015) (196). Note: Greenfields removed non-relevant sample locations from the source image.

5.1.4.3 Ellesmerian

In North Greenland, there is uncertainty surrounding the existence of the late Devonian to early Carboniferous-aged (c. 359 Ma) Ellesmerian orogeny (197). Contractual deformation is recognisable in North Greenland (198), the Yukon (199), the Canadian Arctic (200), and Svalbard (201). There is no consensus on the extent and geodynamic cause of the contraction (Figure 28) (197). In North Greenland, deformation attributed to Ellesmerian tectonism is not constrained by younger strata and lacks cross-cutting relationships to pin its timing (197). It is possible that the deformation can be attributed to the Late Caledonian Orogeny and that the Ellesmerian does not occur in North Greenland (197). The Ellesmerian also largely overlaps the younger Eurekan deformation in North Greenland (161). It is unclear if the observed pan-Arctic deformation applies to the Ellesmerian event or multiple events (197).

Figure 28: Tectonic map of Ellesmerian deformation

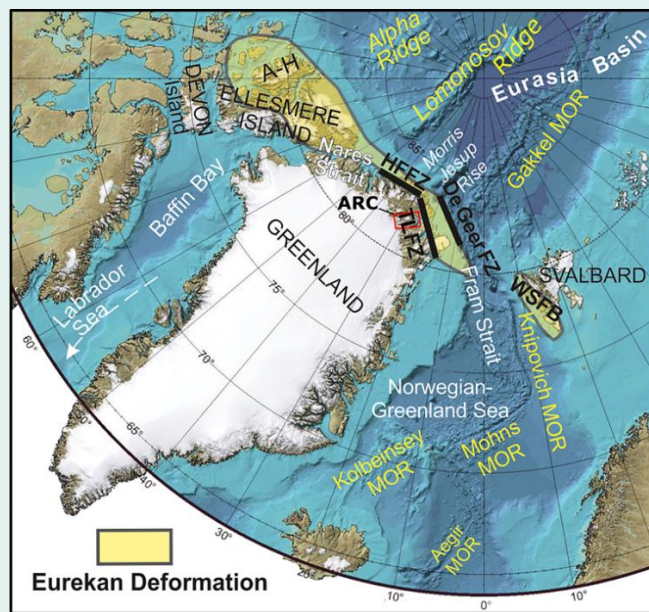


Source: Modified by Greenfields from Barnes et al. (2020) (202).

5.1.4.4 Eureka

The Eureka Orogeny is a pan-Arctic deformation belt stretching from the high-Arctic Canadian islands through parts of North Greenland to Svalbard (Figure 29) (153). The northward movement of Greenland relative to North America is the main driver of deformation (203), although seafloor spreading is recognised to play a role (153; 204). Deformation was episodal but initiated in the Early Cenozoic (c. 66 Ma) at the same time as new plate boundaries were forming in the Arctic (204). In North Greenland, the Harder Fjord Fault Zone and the Trolle Land Fault Zone accommodated Eureka deformation (205).

Figure 29: Map of areas affected by Eureka deformation



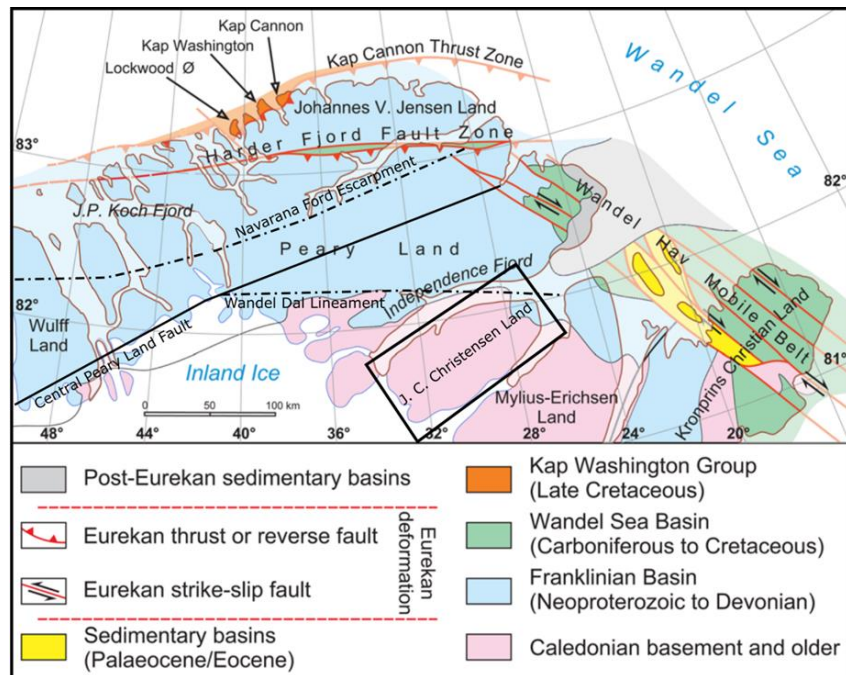
Source: Modified from Vamvaka et al. (2019) (153). Note: The location of ARC is shown with the red box. HFFZ: Harder Fjord Fault Zone; TLFZ: Trolle Land Fault Zone; WSFB: West Spitsbergen Fold Belt; MOR: Mid-ocean Ridge; A-H: Axel-Heiberg Island.



5.1.5 Structures

The structures in North Greenland developed in response to the tectonic events the region has experienced throughout its geological history. Many of the events expressed as faults that parallel major regional structures and lineaments⁷¹ (149). The oldest structures in the region may be syn-rift, while others are related to deformation events (149).

Figure 30: Fault zones and lineaments



Source: Based on Piepjohn et al. (2016) (204).

5.1.5.1 Faults

5.1.5.1.1 Northwest-southeast

The Trolle Land Fault Zone is the onshore boundary of the Wandel Hav Mobile Belt (206) (Figure 29). The mobile belt developed in response to dextral (right-lateral) strike-slip movements between the Eurasian and Greenland plates at the De Geer Shear Zone during the Cenozoic (207). The Trolle Land Fault Zone developed as a splay of the Harder Fjord Fault Zone (208). However, the fault zone may have older origins with the over-arching Wandel Hav Mobile Belt exploiting a “fossil” Mesozoic-aged plate boundary between Laurentia and Eurasia (206). Greenfields recognises secondary structures sympathetic to the Wandel Hav Mobile Belt across North Greenland, which indicates that deformation is not only confined within the belt.

5.1.5.1.2 East-west

The Harder Fjord Fault Zone is a 250 km long near-vertical east-west trending fault system (205). The fault zone has 1 to 2 km of uplift and c. 20 km of dextral strike-slip movement recognised (205). The fault zone records two distinct phases of deformation (203). The first phase developed in response to the northward movement of Greenland relative to North America and the second resulted from seafloor spreading in the Arctic (153; 203). Greenfields also recognises sympathetic orientation to the Harder Fjord Fault Zone across North Greenland.

5.1.5.1.3 Northeast-southwest

Navarana Fjord Escarpment is a palaeo-topographic feature approximately 500 km long and juxtaposes shallow and deep-marine sediments (209; 12). A deep-seated structure controlled the Navarana Escarpment and was active from the Proterozoic⁷² to the Silurian (149; 12). In North Greenland, the Navarana Fjord Escarpment has a northeast-southwest strike⁷³ (149).

⁷¹ A lineament is a linear topographical feature that is often the result of an underlying geological structure such as a fault. Some of the events responsible for these structures are better understood than others (197; 148; 204). Furthermore, the mapping within North Greenland is not 100% accurate and largely at 1:500,000 scale (210; 3).

⁷² Surlyk (1991) contends that The Navarana Fjord Escarpment is later-Proterozoic in age (149).

⁷³ In Northwest Greenland, the Navarana Fjord Escarpment has an east-west orientation.

The Central Peary Land Fault is a zone of faulting that is oriented northeast-southwest, which is notably parallel⁷⁴ to the Navarana fjord Escarpment. The Central Peary Land Fault has a mapped strike extent of approximately 350 km (149). The fault zone extends through Peary Land from G.B. Schley Fjord⁷⁵ in the northeast to the head of Victoria Fjord⁷⁶ in central North Greenland (149).

5.1.5.2 Topographic lineaments

5.1.5.2.1 Northeast-southwest

The northeast-southwest orientation of the Independence⁷⁷ and Hagen fjords is parallel to the Navarana Fjord Escarpment and Central Peary Land Fault. On opposite sides of Independence Fjord, the two Mesoproterozoic-aged formations of Independence Fjord Group (Inuiteq Sø Fm and Norsemandal Fm) do not correlate (210; 170). This sharp lithological difference implies to Greenfields that a large-scale feature has disjoined the two formations⁷⁸. Geological features influence fjords (211), and Greenfields considers that they are part of a regionally significant northeast-southwest fault system that was already established by the Mesoproterozoic. However, as geological mapping shows that sympathetic faulting occurs in Ordovician-aged sediments (212), these structures appear to have reactivated over time. Greenfields considers it likely that the Navarana Escarpment, Central Peary Land Fault and the main fjord orientations are genetically related.

5.1.5.2.2 East-west

The Wandel Dal Lineament is a 250 km long east-west lineament that expresses itself in Wandel Dal (valley) through Jørgen Brønlund Fjord to Mylius-Erichsen Land (149). At its western terminus, the lineament abuts the Central Peary Land Fault (149). It is near this western terminus that the Navarana Fjord Escarpment changes orientation. To the east, the Wandel Dal Lineament appears to influence the orientation of central Independence Fjord. The structural relationship indicates to Greenfields that the east-west lineament predates the northeast-southwest fault system.

5.1.5.2.3 North-south

In North Greenland, prominent north-south orientated fjords and valleys are common. Examples of these north-south oriented lineaments are Valdemar Glückstadt Land⁷⁹, the start of Hagen Fjord, the terminus of Independence Fjord/J.C. Christensen Land, G.B. Schley Fjord, and Citronen Fjord (Figure 31). However, while there are localised expressions in the fjords, the north-south orientations have an apparent discontinuous distribution at a larger scale.

HYDROGEOLOGIC
PLUMBING IS IN
PLACE

⁷⁴ West of Victoria Fjord, the Navarana Escarpment takes on a more east-west orientation to the Peary Land Fault.

⁷⁵ G.B. Schley Fjord, 82.866° N, 24.707° W.

⁷⁶ Victoria Fjord, 81.825° N, 46.438° W.

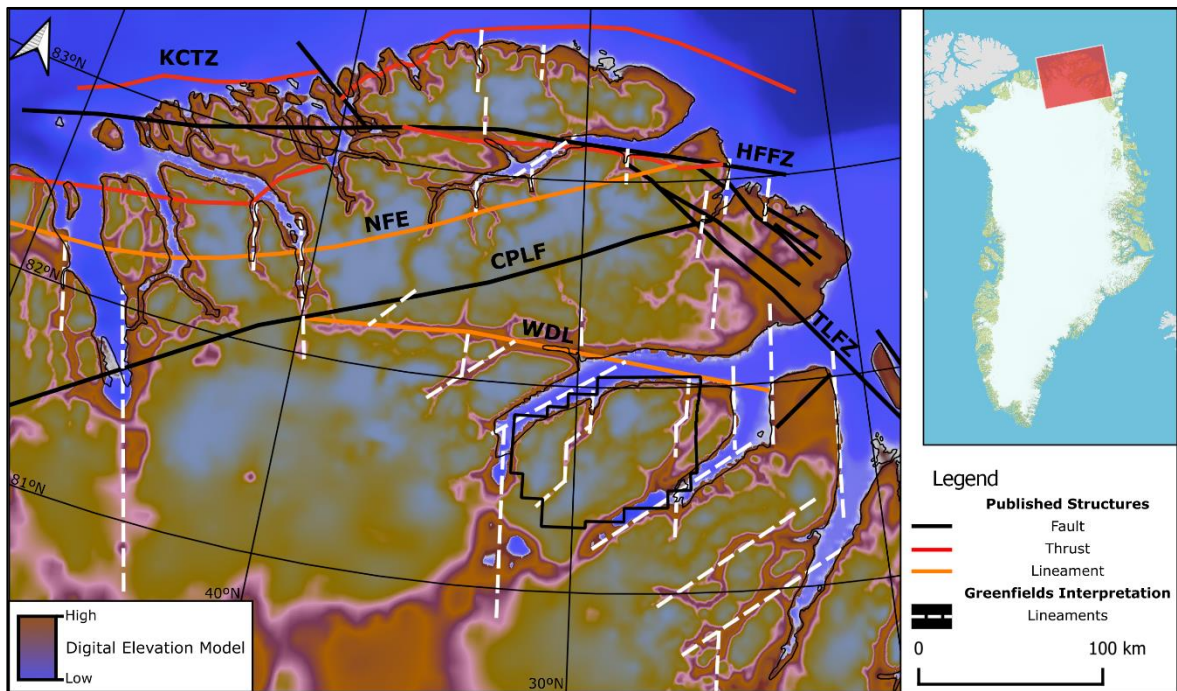
⁷⁷ At 200 km long, Independence Fjord is the fourth longest fjord in the world after Scoresby Sund, Greenland (350 km), Greely Fjord, Canada (230 km), and Sognefjord, Norway (204 km) (365).

⁷⁸ No major fault movement is identified by Greenfields, nor is there any correspondingly large lithological change between J.C. Christensen Land and Mylius-Erichsen Land. Consequently, Greenfields notes that major lateral or vertical movement along a fault is likely necessary to explain the lithological differences across Independence Fjord.

⁷⁹ The east coast of Valdemar Glückstadt Land, ~81.908° N, 21.061° W.



Figure 31: Major faults and topographic lineaments in North Greenland



Source: Greenfields using 'Published Structures' from Surlyk (1991) (149). Note: KCTZ: Kap Cannon Thrust Zone; HFFZ: Harder Fjord Fault Zone; TLFZ: Trolle Land Fault Zone; NFE: Navarana Fjord Escarpment; CPLF: Central Peary Land Fault; and WDL: Wandel Dal Lineament.

5.1.5.3 Fault-lineament relationships

Greenfields postulates that there are relationships between the:

- Trolle Land Fault Zone and the Hagen Fjord Fault Zone, which form a $\sim 145^\circ$ intersection, with the former terminating in the latter.
- Wandel Dal Lineament and the Central Peary Land Fault group, which form a $\sim 165^\circ$ angle of intersection, with the former terminating in the latter.

The similarity in age and angular relationships within these sets indicate to Greenfields that similarly oriented forces formed them.

The apparent but discontinuous north-south lineaments, which are mainly expressed in fjords and surface elevation, are not well understood. Greenfields postulates that the lineaments may partially represent tension release features⁸⁰. Tension may explain why the lineaments are discontinuous and it is consistent with a low-pressure outlet zone needed in a hydrodynamic system to form the Citronen deposit.

5.1.5.4 Folding

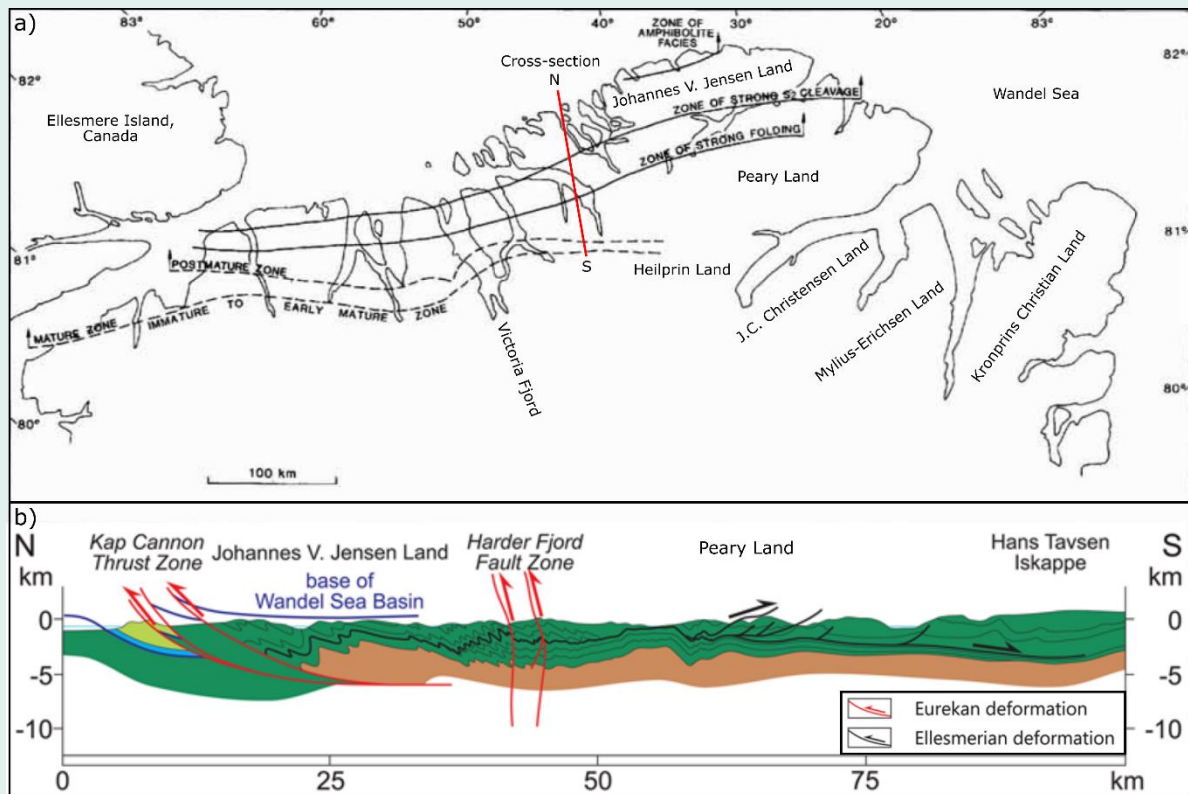
Folding in North Greenland is most pronounced in the west and north⁸¹ and generally reduces in intensity southwards across Peary Land (Figure 32) (149). South of Peary Land/Independence Fjord, folding is mostly absent. The Ellesmerian and the Eurekan orogenic events are responsible

⁸⁰ For example, the release of tension associated conjugate/sets Riedel shears (Independence and Hagen Ford oriented); the east-west opening of the Iapetus Ocean; or the Elzevirian Orogeny. Greenfields has not identified sufficient information to be more certain of what mechanism may have caused the north-south lineaments.

⁸¹ Johannes V. Jensen Land, 83.370°N, 33.479°W.

for folding and thrusting these rocks, which explains the fold distribution lessening to the south (204). However, the Ellesmerian deformation may be attributed to the Late Caledonian Orogeny (197).

Figure 32: Folding in North Greenland



Source: a) Modified from Surlyk (1991) Fig 9A (149) and b) Piepjohn et al. (2016) Fig 2B (204).

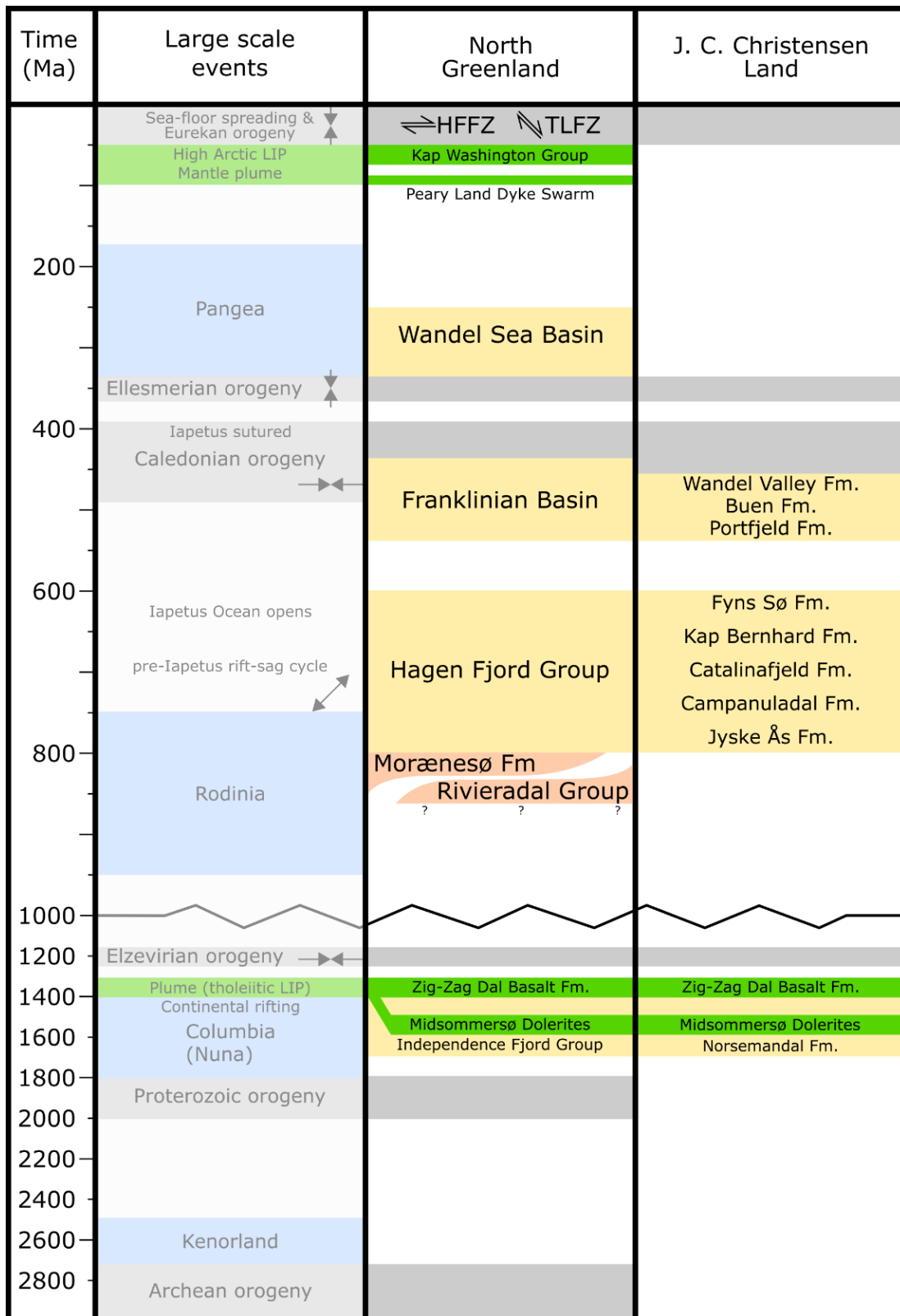
5.1.6 Metamorphism

Metamorphosed rocks across North Greenland do not form a continuous spectrum, and faulting juxtaposes different metamorphic facies. Greenland's northern tip contains a polyphase fold belt with north-verging structures, and amphibolite facies metasediments (149). Moving southwards through Peary Land, the deformation and metamorphism both dissipate 150 km from J.C. Christensen Land (149). Metamorphism in the north is ascribed to the Ellesmerian and Eurekan orogenies (161; 204). The same cannot be said for J.C. Christensen Land, where much older Zeolite Facies (125°C to 200°C) metamorphism is expressed in igneous extrusives and extensive lateral alkali hydrothermal alteration is evident (158; 213). At Hellefiskefjord 100 km to the north of J.C. Christensen Land, upfaulted and isolated extrusives covering 200 km² have altered to Greenschist Facies due to burial metamorphism (214; 159). At Citronen, the mineralising fluids had temperatures of 80° to 160°C (215).

The basement rocks of North Greenland record metamorphic events. Blocks of gneiss, amphibolite, and granite thought to be the basement are found as ice-transported blocks and as xenoliths in sills (216). The last metamorphic event the basement is linked to the Elzevirian Orogen which expresses itself as a c. 1,260 to 1,250 Ma overprint (186).



Figure 33: Geological timeline of North Greenland and J.C. Christensen Land

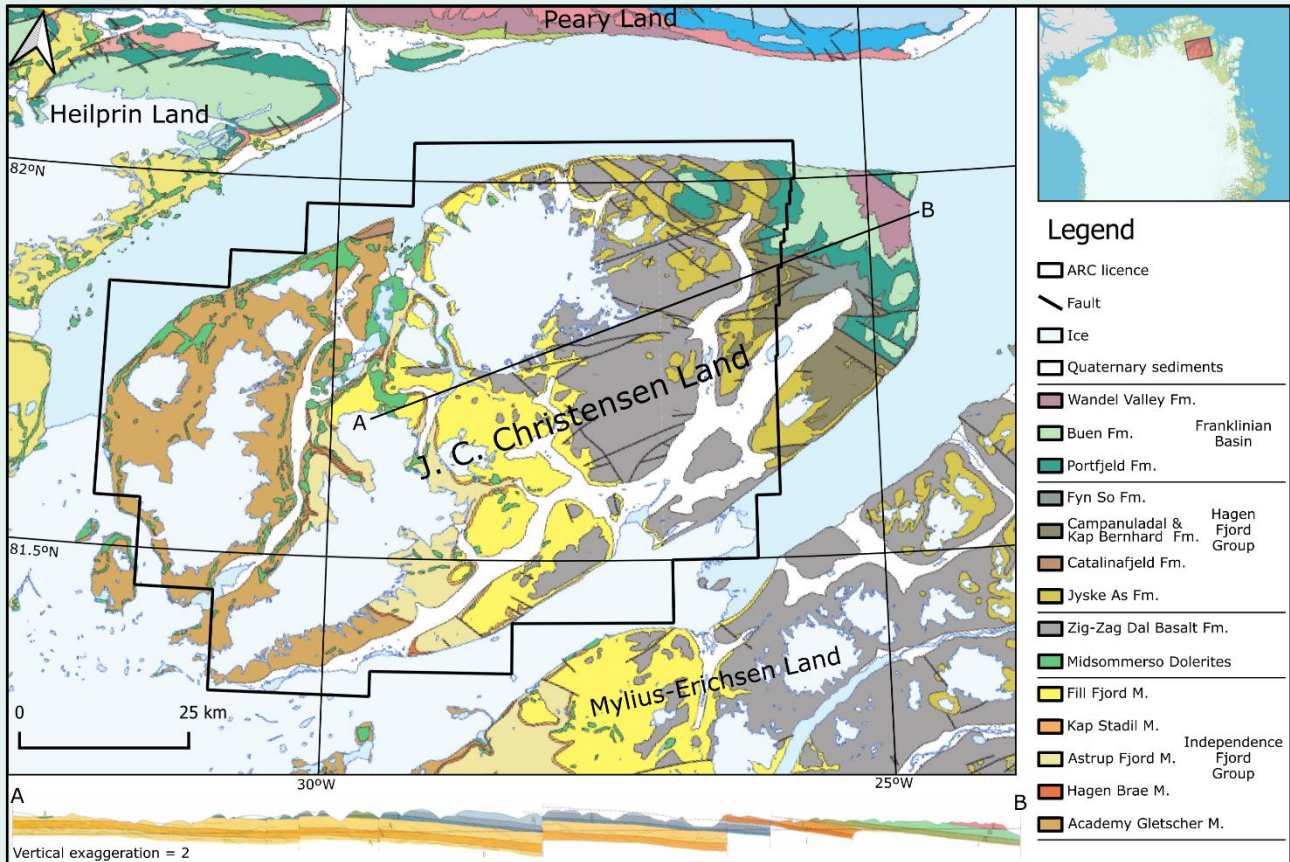


Source: Greenfields. Note: Fm: Formation. Inward pointing arrows indicate maximum principal component direction. Outward point arrows indicate minimum principle component direction.

5.2 LOCAL GEOLOGY

J.C. Christensen Land contains a sequence Proterozoic alluvial sediments and volcanic rocks capped by Palaeozoic marine sequences (Figure 33) (149). The strata dips sub-horizontally (1-3°) to the northeast and hosts fault orientations parallel to major regional structures (Figure 33, Figure 34) (151). In J.C. Christensen Land, folding is almost non-existent (149).

Figure 34: Geological map of J.C. Christensen Land



Source: Greenfields modified from the Geological Map of Greenland (1985) 1:100 000, J.C. Christensen Land (217).

5.2.1 Proterozoic-aged sediments

The oldest sedimentary rocks within ARC belong to the Palaeoproterozoic- to Mesoproterozoic aged Independence Fjord Group (c. 1,750 to 1,380 Ma) (218; 186). Greenfields notes that the Group appears to have formed after a Palaeoproterozoic-aged orogenic event, and during much of the time of the Columbia Supercontinent (169). The Independence Fjord Group is located in a virtually undeformed cratonic setting inboard from the Caledonian and Ellesmerian⁸² deformation events (219). The Group sits unconformably on the crystalline Greenland Shield, but this contact is inferred from float from near the inland ice (151).

The exposed position of the Independence Fjord Group covers 80 by 300 km. The original extent is not known and was likely much more extensive (148). The lithospheric sagging associated with fragmentation of Columbia initiated the basin's formation (155). The Group contains at least 2 km of alluvial sandstones, occasional lacustrine siltstones, and mafic intrusions (170). The Group

⁸² It is uncertain if the Ellesmerian Orogeny occurred in North Greenland (197), but for completeness, it is presented in this Report's discussion.

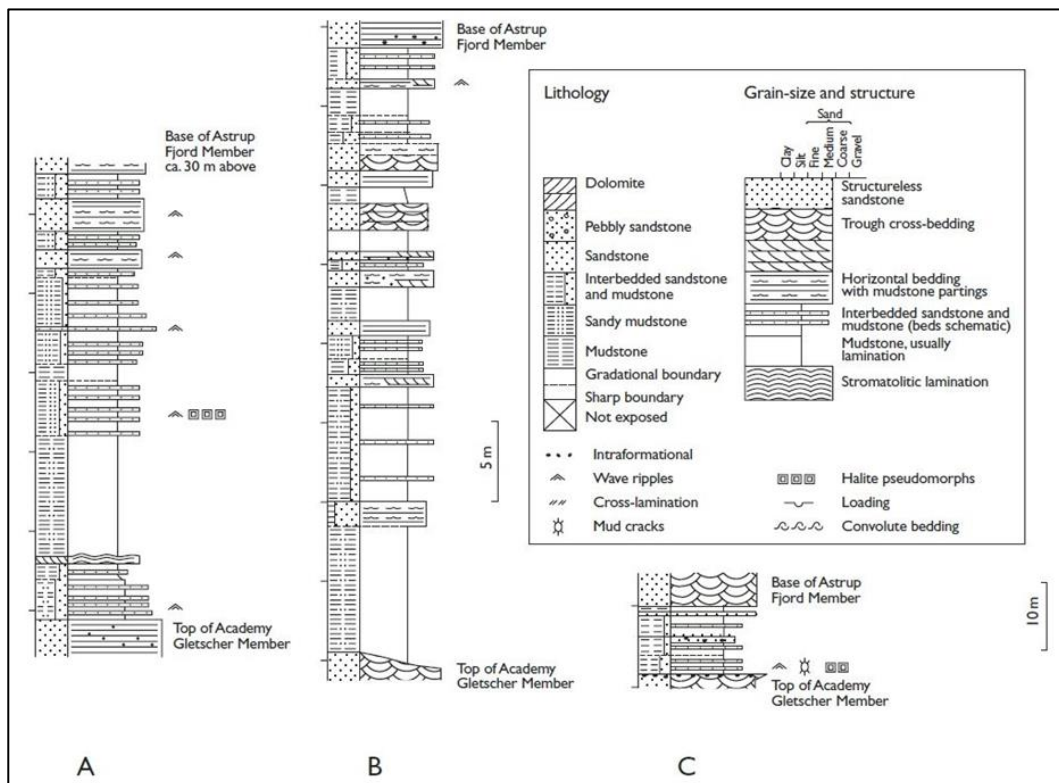


divides into two uncorrelated formations ('Fm') which are separated geographically by Independence Fjord (Figure 35):

1. **'Norsemandal Fm'** in J.C. Christensen Land and eastern North Greenland south of Independence Fjord; and
2. **'Inuiteq Sø Fm'** north of the Independence Fjord (170).

The Norsemandal Fm comprises three sandstone members separated by two redbed members (210). The Academy Gletscher Member is a 900 m thick sequence of medium- to coarse-grained feldspathic to quartzitic cross-bedded sandstones that sits at the base of the Norsemandal Fm (170). The Hagen Bræ Member overlies the Academy Gletscher Member. The Hagen Bræ Member is a 90 m thick redbed, comprised of siltstone with halite pseudomorphs, desiccation cracks, and interbedded sandstones (218). The Astrup Fjord Member sits between the Norsemandal Fm's two redbeds and is a 300 m thick sequence of medium- to coarse-grained feldspathic cross-bedded sandstone (218). The second redbed in the Formation is the Kap Stadil Member, a 90 m thick, siltstone with halite pseudomorphs, desiccation cracks, and interbedded sandstones (Figure 36) (218). The Kap Stadil Member is practically identical to the Hagen Bræ Member redbed below it (218). The two redbed members reflect an extensive ephemeral saline lake and playa systems (149; 158). Halite pseudomorphs record the thick sequence of evaporites within these redbeds. An angular discordance within the strata is the result of the evaporites removal⁸³ (149). Capping the Norsemandal Fm is the Fill Fjord Member, a 600 m thick monotonous sequence of medium to coarse-grained cross-bedded quartzite (170).

Figure 35: Lithostratigraphy of the Independence Fjord Group

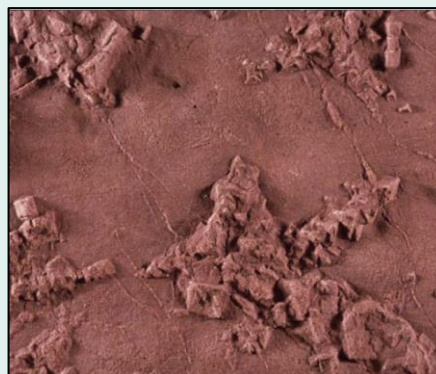


Source: Collinson et al. (2008) (219). Note: A) represents the south side of Hagen Bræ, B) the north side of Hagen Bræ and C) is from central J.C. Christensen Land.

⁸³ The mobilisation of salts provides a source of brine capable of scavenging metals (373). Both redbed members show evidence for mass brine mobilisation (149).

The Inuiteq Sø Fm may represent the stratigraphy below the Norsemandal Fm (220), but this correlation is uncertain (218). Independence Fjord geographically separates the two formations with Inuiteq Sø Fm cropping to the north, throughout Heilprin Land (218). If Inuiteq Sø Fm is lower in the sequence compared to Norsemandal Fm, their current stratigraphic positions indicate to Greenfields that Independence Fjord is concealing a large-scale normal fault. Inuiteq Sø Fm's lithology is similar to the Norsemandal Fm and comprises cross-bedded sandstone and redbed siltstone members (218). Mafic and silicic intrusions cross-cut Inuiteq Sø Fm (218; 159). Unlike in J.C. Christensen Land, where flood basalts conformably overlie the Norsemandal Fm; the Inuiteq Sø Fm is unconformably overlain by the Neoproterozoic-aged Morænesø Fm and Palaeozoic-aged Franklinian Basin sediments (Figure 33) (218).

Figure 36: Halite pseudomorphs from an Independence Fjord Group siltstone

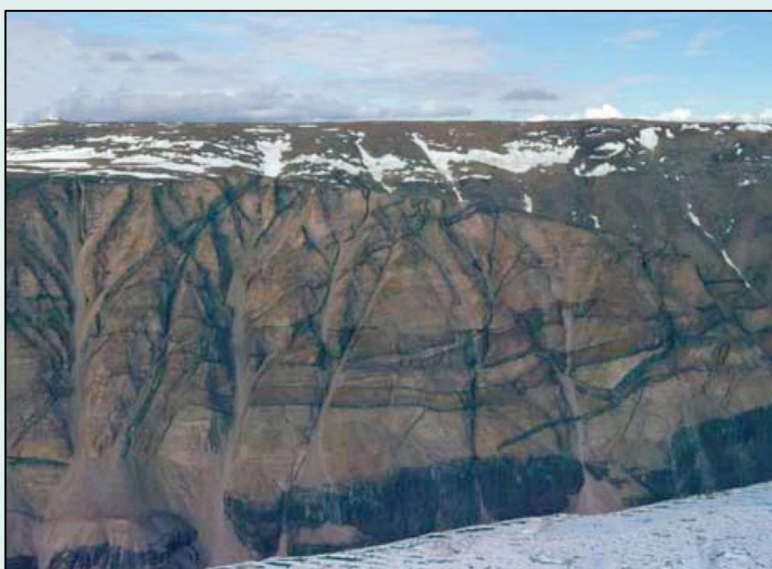


Source: Collinson et al. (2008) (219).

5.2.2 Mesoproterozoic-aged intrusives and extrusives

The lavas of the Zig-Zag Dal Basalt Formation ('Zig-Zag Fm') flooded the palaeo-surface at c. 1,382 Ma in response to a mantle plume at the triple junction between Laurentia, Baltica, and West Africa (Figure 21) (159; 174). The distal mantle plume brought tholeiitic lavas to the surface, but also intruded the Independence Fjord Group creating the Midsommersø Dolerites ('Midsommersø Intrusions') (Figure 37) (159). This volcanism interrupted sedimentation and resulted in a basaltic pile up to 800 m thick in J.C. Christensen Land⁸⁴ (221). During and after emplacement, the continued sedimentation suggests ongoing continental sagging which is expressed by the present-day morphology of the basalts (186; 222).

Figure 37: Intrusions in the Independence Fjord Group



Source: Collinson et al. (2008) (219). Note: Dolerite intrusions at the base of the fjord, with rheopsammites in the higher altitudes. The cliff is 400m high, and the dolerite margins of the rheopsammite are evident at this scale.

Greenland was near the equator at the time of magmatic emplacement (177). Palaeomagnetism shows that the flow direction of both the basalts and dolerites is from the northeast to southwest (177). This flow direction is consistent with the presence of a mantle plume located to the

⁸⁴ The Zig-Zag Fm reaches up to 1,300 m in thickness in Mylius-Erichsen Land, 600 to 800 m in central J.C. Christensen Land, and 100 to 200 m in the cliffs of Independence Fjord (218). The Zig-Zag Basalt Fm is thickest in Mylius-Erichsen Land and thins towards the northwest and southeast (Figure 38) (148; 221).



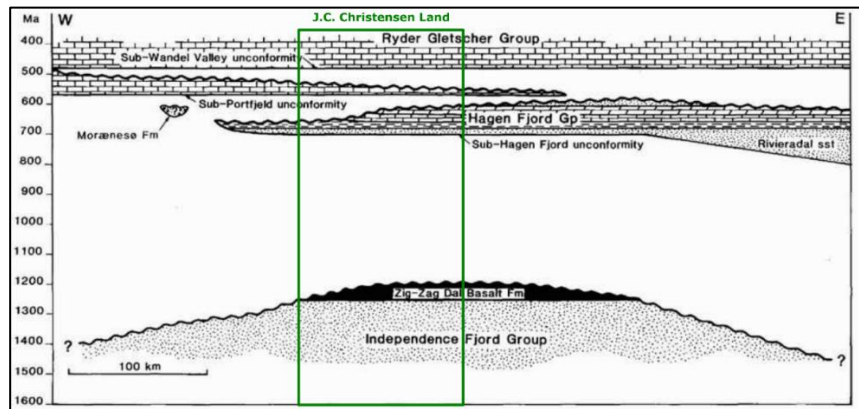
northeast of Greenland (174). Greenfields also notes that the southwest flow direction aligns with the fjords bounding J.C. Christensen Land which may have structural origins.

The original extent of the basalts is unknown due to erosion, although distant outcrops occur around northeast Greenland (221). In Hellefiskefjord 100 km to the north of J.C. Christensen Land, upfaulted blocks reveal 200 km² of Zig-Zag Fm metamorphosed to greenschist facies (214). In J.C. Christensen Land, Neoproterozoic-aged shallow marine sediments of the Hagen Fjord Group disconformably overlie the basalts (Figure 38) (222; 223). The sagging that accommodated the Independence Fjord Group sediments likely continued throughout the eruptive activity before the onset of a midocean ridge spreading centre (159; 149). The discontinuous volcanism took place over approximately 1 M years (159). Intrabasaltic sandstone, conglomerate and dolomite beds are present between flows and indicate continued sagging through pauses in volcanic activity (222).

The boundary between the Inuiteq Sø Fm and Norsemandal Fm is marked by Independence Fjord (170) which Greenfields hypothesises to represent a potential large-scale normal fault. At least two scenarios exist for the timing of this hypothesised feature. If this boundary existed during emplacement, it might have affected the lateral extent of the flood basalts, limiting their flow north-westwards. If the boundary developed after the volcanic activity, J.C. Christensen Land is the downfaulted block along Independence Fjord and was thus preserved compared to the northern side which would have been a palaeo-topography high.

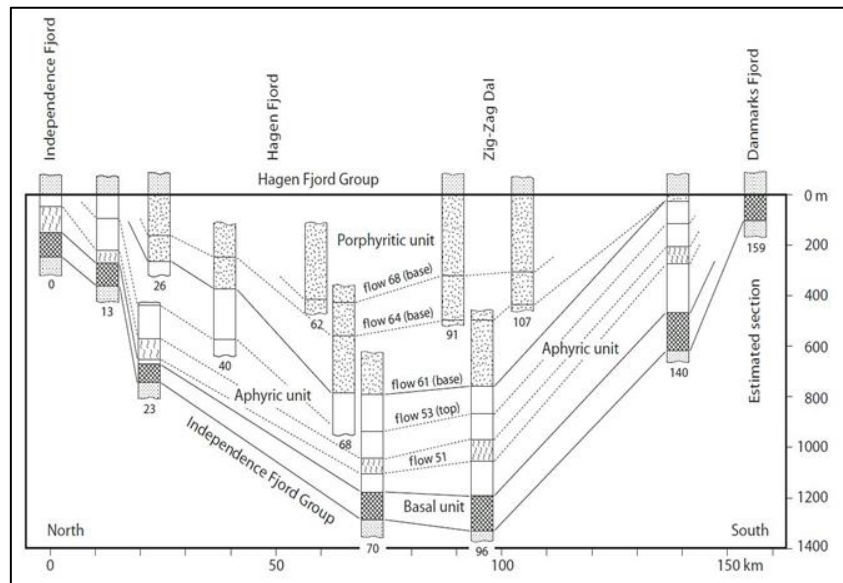
The Zig-Zag Fm is comprised of more than forty⁸⁵ individual flows that differ temporally and geochemically (Figure

Figure 38: East-west time-space cross-section of North Greenland



Source: Henriksen et al. (2009) (148), modified by Greenfields. Note: Red box indicates geology present within J.C. Christensen Land.

Figure 39: Synoptic correlation diagram across the Zig-Zag Fm



Source: Collinson et al. (2008) (219).

⁸⁵ The numbering convention for naming the flows is largely arbitrary (221). Around 40 flows are documented in the Zig-Zag Valley type locality (225).

39 and Figure 40) (159; 224). The flows are divided into three major units; 'Basal'; 'Aphyric'; and 'Porphyritic' Units (222).

The Basal Unit is between 100 to 200 m thick and is a sequence of relatively thin (1 to 10 m thick) pillow lavas and basalt flows (225; 221). The pillow lavas indicate a subaqueous setting and show spilitic alteration caused by seawater alteration (221). The Basal Unit is locally⁸⁶ separated from the overlying Aphyric Unit by a 10 to 40 m horizon of sandstone and dolomite (159). The sediment horizon marks a break in volcanic activity (159). The relative uniformity of the Basal Unit indicates that there was little erosion before sediment deposition (159).

Very fine-grained, subaerial flows dominate the 400 m thick Aphyric Unit. The Aphyric basalt flows have thicknesses generally between 10 to 120 m (221). There are abnormal flows in the Aphyric Unit (221). Near the base of the Unit, the 'Brown Marker' flow has basaltic andesite⁸⁷ composition with intense potassic and sodic alteration (159; 225). Near the top of the Aphyric Unit are red rhyolitic flows exclusive to J.C. Christensen Land (221). These rhyolitic flows add up to 100 m thick and compositionally, are a departure from the primitive basalts flows typical of the Zig-Zag Fm (221). On the east side of Hagen Fjord in Mylius-Erichsen Land the composition of the abnormal flow is trachyandesitic instead of rhyolitic (224). The reviewed literature does not elaborate on the possible mechanism for generating localised magmatic variances. An erosional surface and intrabasaltic sediments mark the top of the Aphyric Unit (221). In some locations, the erosional surface cuts into the Aphyric Unit and has accumulated up to 50 m of conglomerates, sandstones, and dolomites (221). These intrabasaltic sediments are evidence of a pause in volcanic activity before the deposition of the Porphyritic Unit (221).

**50 M THICK
PERMEABLE,
CONGLOMERITIC,
INTRABASALTIC
SEDIMENTS**

The subaerial Porphyritic Unit consists of 750 m of fine-grained basalts with millimetre-scale plagioclase phenocrysts and amygdales⁸⁸ (221). The flows in the Porphyritic Unit are generally between 10 to 120 m in thickness, but thinner flows also occur (221). Towards the top of the unit, pauses in the volcanic activity become increasingly prevalent (221). There are accumulations of conglomerates, sandstones, and dolomites between flows (221). Near the top of the Porphyritic Unit, tuffs up to 50 m thick occur with interbedded thin layers of subaqueous pillow lavas (221). The slowing in volcanic activity also permitted localised erosion (221). Erosional surfaces cut the underlying flows by up to 50 m in some localities (221). In J.C. Christensen Land, the Hagen Fjord Group sediments disconformably overlie the Porphyritic Unit (148).

The three units within the Zig-Zag Fm show geochemical variations moving up the stratigraphy (Figure 40) (159). This variation broadly tracks crystal fractionation patterns of an increasingly depleted mantle source except for the brown marker flow at 300 m (stratigraphic height) in the Aphyric Unit (221). The Brown Marker flow is basaltic andesite, a relatively mature magma compared to its neighbouring flows (159). The development of a relatively felsic magma at this time indicates that a pause in activity allowed segregation to take place in the sub-volcanic

⁸⁶ This description is from Mylius-Erichsen Land, adjacent to J.C. Christensen Land.

⁸⁷ 54.5 wt.% SiO₂ and 4.42 wt.% MgO (159).

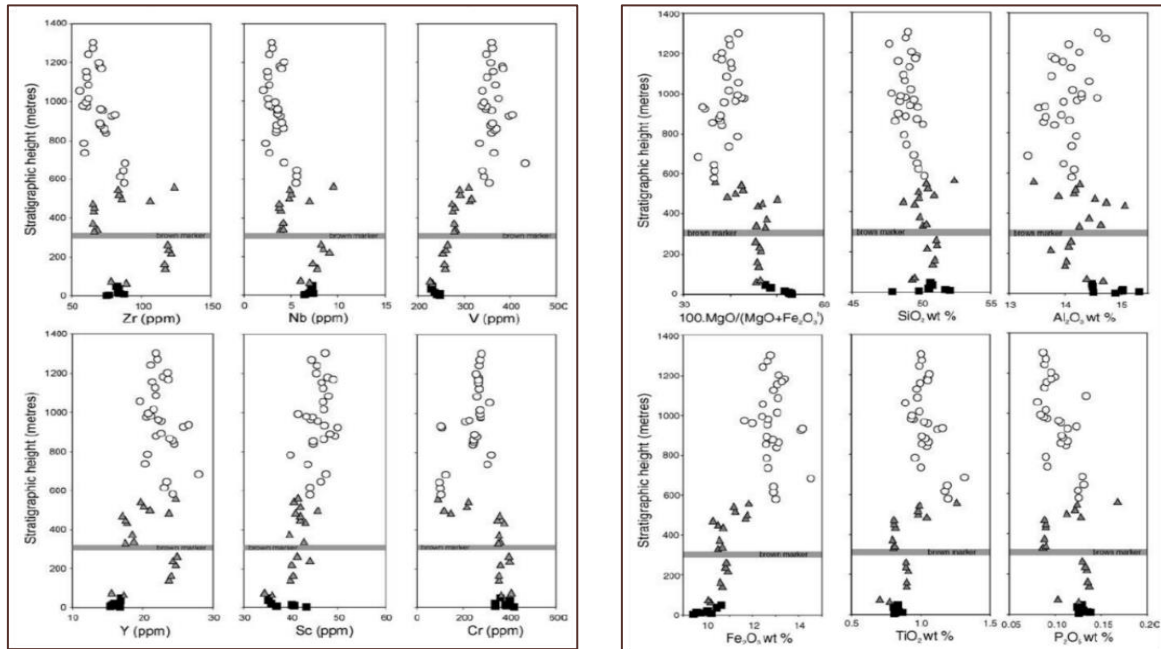
⁸⁸ Amygdales are voids in the rock created by gas bubbles within lava at the time of eruption and emplacement.



plumbing⁸⁹ (159). An initially deep but progressively shallowing⁹⁰ mantle source explains the changes in the magma chemistry (159).

After the Zig-Zag Fm's emplacement at c. 1,382 Ma, there is a 580-million-year gap in the stratigraphy (148). The current-day exposure of the flows with intrabasaltic sediments suggests that the accommodating sagging continued (186; 222). Before the deposition of Hagen Fjord Group sediments 580 million years later, erosion peneplaned the sagged lava flow succession. The erosion explains the symmetrical exposure seen today, with the Basal Unit being the most expansive and the Porphyritic Unit being the least.

Figure 40: Zig-Zag Fm trace element variation



Source: Upton et al. (2005) (159). Note: Basal Unit: solid squares; Aphyrical Unit: grey triangles; Porphyritic Unit: open circles. Shaded horizontal line represent the stratigraphic height of the Brown Marker unit.

As the Zig-Zag Fm flood basalts were erupting at the surface, the Midsommersø Intrusions were emplaced into the underlying Independence Fjord Group as sills and dykes (Figure 37) (158). The intrusions have the same geochemistry and palaeomagnetic qualities as the Zig-Zag Fm (148; 226). The Midsommersø Intrusions do not extend into the uppermost 200 m of sediments beneath the Zig-Zag Fm basalts, which indicates that the conduit is distal to the current-day exposure (158; 226). The intrusions are commonly several hundred metres thick and in some locations account for more than 75% of the stratigraphy (227). Some of the large sills show crude layering possibly related to crystal settling (158; 227). The intrusions, which cross-cut one another (227), subdivide into three main groups:

1. Grey to black, unaltered dolerites;
2. Red-brown to brick-red, and greenish altered dolerites; and
3. Red silicon-rich 'rhepsammites'⁹¹ and 'granophyres'⁹² (158; 228).

⁸⁹ The concept of a magma chamber is superseded by sub-volcanic plumbing that is dominated by large zones of hot, liquid-poor mush zones (382).

⁹⁰ The Basal Unit matches a primitive mantle source at garnet lherzolite facies (i.e. pressures of >2 GPa); the Aphyrical Unit matches depleted garnet lherzolite and depleted spinel lherzolite facies (i.e. 2 GPa); and the Porphyritic Unit matches depleted spinel lherzolite facies (i.e. 1 to 2 GPa) (159).

⁹¹ Rhepsammites are rare Si-rich (80-90 wt.% SiO₂) intrusives originating from liquified sandstone (228; 158).

⁹² Granophyres is the name used in North Greenland to describe Si-rich intrusives originating from liquified basement rock (228).

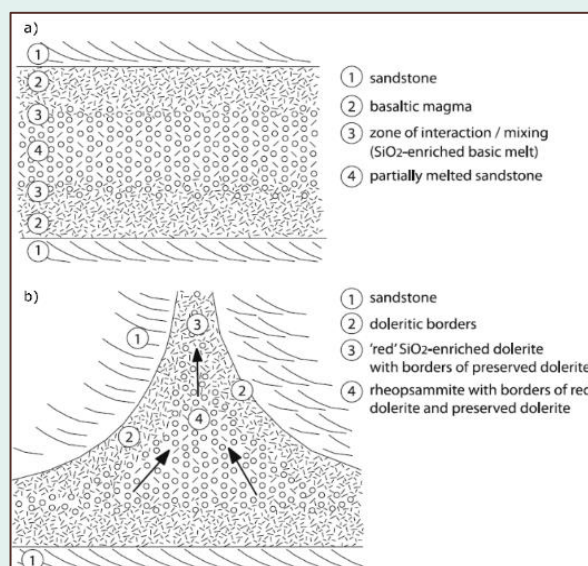
The hydrothermally unaltered dolerites are typically dark coloured with columnar jointing and chilled margins (227). The dolerites are the most common and form sheets several hundreds of metres in thickness (158). These well-preserved dolerites contain augite, plagioclase, pigeonite, and occasional olivine pseudomorphs (228). Biotite and apatite occur in minor proportions (228). There is strong zonation within the plagioclase, ranging from 80% to 40% anorthite⁹³ (158). Contact metamorphism with Independence Fjord Group sediments extends only a few centimetres (158).

The altered 'brick-red' dolerites are heavily altered when viewed in thin section (158). Despite the alteration, these sills typically feature preserved textures in the margins up to a few meters thick (158). The chilled dolerite margins are fine-grained and are typically totally altered (158). The chilled margins show evidence of extensive metasomatism by hydrothermal systems in the sandstones (158). For example, the margins are enriched in lead to 240 ppm compared to 1 to 12 ppm in fresh dolerites, and 10 to 25 ppm in the sandstones (158; 228). Augite is the only mineral within these rocks to escape complete alteration (158). The plagioclase is completely altered to sericite, and fine-grained secondary minerals make up the groundmass (matrix)⁹⁴ (158). The breakdown of plagioclase resulted in potassium ('K') replacing calcium ('Ca') and sodium ('Na') in the crystals (158). This potassic alteration enriched the groundmass in the order of 3.78% to 6.74% K₂O, compared to 0.31% to 1.64% K₂O in the fresh dolerites (158). Isotope ratios from the red dolerites indicate a 1,230 ± 20 Ma alteration event which corresponds with a c. 1,250 Ma Elzevirian orogeny (186; 158).

The 'green' altered Midsommersø Intrusives do not appear to have been the focus of any publication. Prehnite, a green mineral, is observed in the Zig-Zag Fm above and is associated with zeolite facies metamorphism (225). It is conceivable that the underlying intrusives also experienced these conditions and resulted in a similar alteration mineral assemblage.

Amongst the Midsommersø Intrusions, red silicon ('Si')-rich intrusive sheets frequently occur adjacent to the thickest dolerite intrusives (228). These intrusives are the product of remobilised country rock and are up to 65 m thick (228). Two types of Si-rich intrusives are identified and are separated based on their original protolith (228). These intrusions are amongst the most Si-rich intrusions in Earth (158). 'Rheopsammites' are remobilised sandstone, whereas 'granophyres' are remobilised granitoid basement (228). These intrusions contain up to 90 wt.% Si but invariably have dolerite chilled margins (158). These Si-rich intrusions included considerable amounts of water from the sandstones, and were gas-rich (158). The Si-rich magmas had very high viscosity, and without large amounts of dissolved gas would not have been able to

Figure 41: Rheopsammite emplacement mechanism



Source: Kalsbeek & Frie (2006) (228).

⁹³ Anorthite is the Ca-rich endmember of plagioclase feldspar (392).

⁹⁴ The brick-red colour is assumed to be due to the presence of finely disseminated haematite in the matrix (228). Greenfields notes that brick-red colouration can be contributed iron-bearing microcline (273), a mineral that is consistent with the potassium enrichment of the rock.



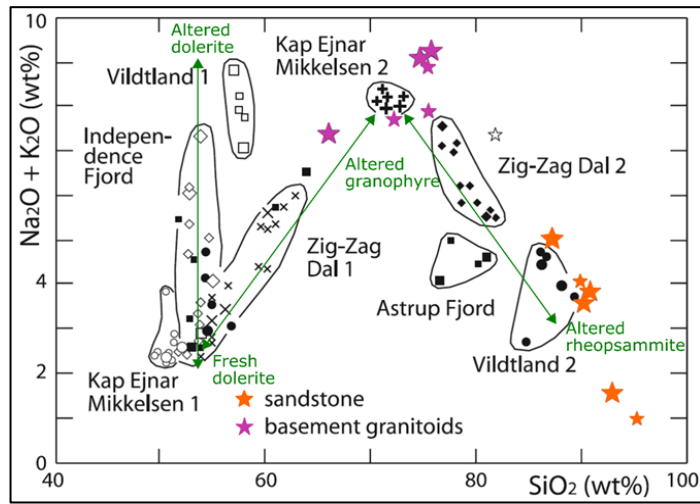
intrude (158). Consequently, the intruding Si-rich magmas needed protection from degassing when entering the sedimentary succession (158). When degassing occurred, the intrusions abruptly solidified, which resulted in undercooling textures such as ‘hollow crystal growth. A model envisages magma enveloping sheets of country-rock resulting in a poorly mixed, zoned intrusion (Figure 41a). The outer dolerite margins stem from the upper portion of a zonation while the inner Si-rich zones come from central portions of the xenolithic mush (Figure 41b) (228).

The rheopsammites are very fine-grained, altered, and contain inclusions of sandstone (158). Rheopsammites carry a Total Alkali Silica geochemical signature that matches the Independence Fjord Group sediments (e.g. ‘Astrup Fjord’ and ‘Vildtland 2’ intrusions; Figure 42) (228). The dominant mineral is quartz with common pseudomorphs of tridymite⁹⁵, which indicates rapid crystallisation (158).

The granophyres are completely altered but retain fine-grained quartz grains (228). Albite⁹⁶ feldspar alteration is complete but shows the original hollow crystal habit that is characteristic of rapid magma cooling (228). The groundmass is comprised of secondary minerals such as chlorite and devitrified glass⁹⁷ (228; 158). The geochemical signature of the granophyre intrusions plots near rocks originating from the granitoid basement (e.g. ‘Kap Ejnar Mikkelsen 2’ intrusion; Figure 42) (228).

The rheopsammites, granophyres and dolerites may result from more than one magmatic event (159). While some dolerites correlate with the emplacement of basalt, the data do not discount the potential for intrusions of variable ages (159).

Figure 42: Total Alkali Silica diagram of Midsommersø Intrusions



Source: Modified from Kalsbeek & Frie (2006) (228).

⁹⁵ Tridymite is a high-temperature polymorph of SiO₂ (391).

⁹⁶ Albite is the Na-rich endmember of plagioclase feldspar (214).

⁹⁷ Devitrification: the process by which glassy substances changes their structure into crystalline solids (mineral) (390).

5.2.3 Neoproterozoic-aged sediments

On the northeastern shelf of the Greenland Shield, the Hagen Fjord Group was deposited from c. 850 to 650 Ma into the newly-forming Iapetus Ocean as supercontinent Rodinia fragmented (Figure 18) (223). Within Greenland, the Hagen Fjord Group is similar to the Eleonore Bay Supergroup in East Greenland (229), the Thule Supergroup in North-West Greenland (230). The Hagen Fjord Group is also similar to the sedimentary successions across northern Canada (e.g. Borden Basin, Amundsen Embayment, and the Pearya Terrane (151). These Neoproterozoic-aged successions formed on the northern margin of Laurentia and comprise fine- to medium-grained sandstones, mudstones, and stromatolitic dolostones (Figure 43) (151). The Hagen Fjord Group sediments deposited in shallow marine settings (223). The Group is typical for a continental shelf margin (223). Within J.C. Christensen Land, the Hagen Fjord Group reaches up to 1 km thick and hosts five of the group's six formations:

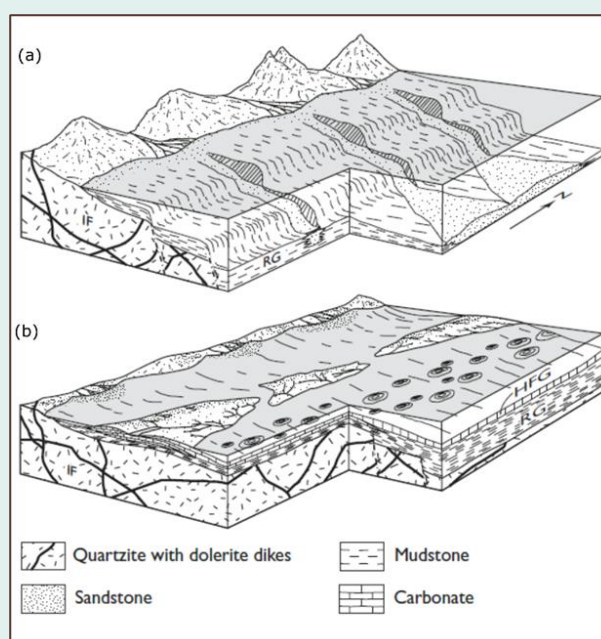
1. Jyske Ås;
2. Campanuladal;
3. Catalinafjeld;
4. Kap Bernhard; and
5. Fyns Sø Fm (Figure 44) (148).

Jyske Ås Fm is the basal unit of the group and reaches up to 500 m thick (231). This formation comprises medium-grained sandstones with interbedded mudstone units towards the top (223). The formation is coloured from red at the base to yellow at the top, with the intercalated mudstone units appearing grey-green (223). The colour may indicate the oxidation state of the units, where red/yellow represent oxidised, and grey/green represent reduced beds (232). Primary sedimentary features are present throughout the formation, with foresets, cross-bedding, cross-laminations, and mud crack features commonly occurring (223). The Jyske Ås Fm includes some fluvial sediments but mostly formed in beach and shallow shelf settings (223).

Campanuladal Fm is characterised by green and red fine-grained sandstones, siltstones, and heteroliths⁹⁸ (233). The sequence is informally divided into five units based on colour:

1. Green sandstone and siltstone;
2. Red sandstone and siltstone;
3. Green sandstone and siltstone;
4. Yellow stromatolite and dolostone; and
5. Green sandstone and siltstone (223).

Figure 43: Conceptual diagram of Neoproterozoic depositional environment on Laurentian margin



Source: Sønderholm et al. (2008) (157).

Note: (a) Conceptual diagram of sediments sourced from rivers draining highland areas composed of Independence Fjord Group sandstones cut by dolerites of the Midsommersø Dolerite Fm. (b) Late Hagen Fjord time with restricted marine circulation. IF: Independence Fjord Group; RG: Rivieradal Group; HFG: Hagen Fjord Group

⁹⁸ Heteroliths are high-frequency interbedded sandstones and siltstones (400).

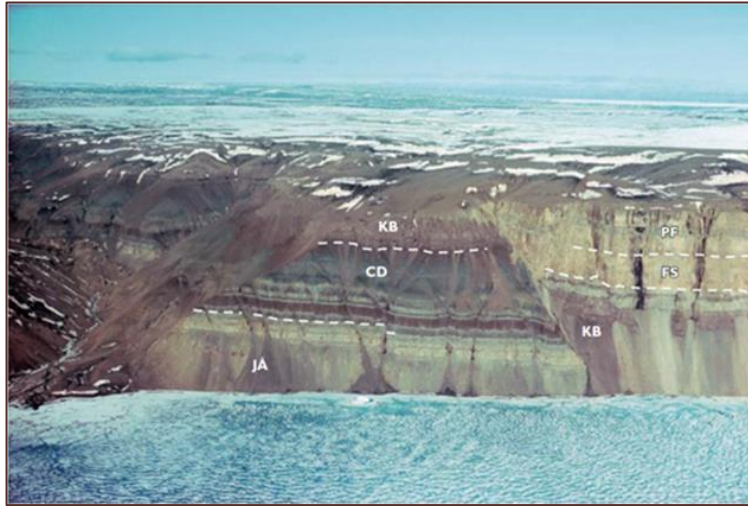


The Campanuladal Fm probably formed in shoreline and shallow marine settings interspersed with periods of subaerial exposure (231). The alternating red and green beds of the Campanuladal Fm are significant because the colours indicate the oxidation state of the rocks⁹⁹ (232).

Catalinafjeld Fm is a 260 to 350 m thick laminated grey mudstone sequence interspersed with thin graded sandstones with minimal lateral extent (234). Within J.C. Christensen Land, the Catalinafjeld Fm is present at the mouth of Astrup Fjord¹⁰⁰ for a total area c. 8 km² (223). Outside of J.C. Christensen Land, the Catalinafjeld Fm only occurs along the northern shores of Independence Fjord (opposite from Astrup Fjord) (223). The relationship of this formation within the Hagen Fjord Group is poorly understood (223).

Clemmensen & Jepsen (1992) suggest that the Catalinafjeld Fm is the deeper water equivalent to the Campanuladal Fm (223). This formation shows a general coarsening upward trend with the sandstone interbeds become coarser, thicker, and more dominant towards the top of the sequence (223). The mud-rich portion was deposited in a low-energy muddy shelf environment, with the sandstones arising from storm events (223).

Figure 44: Type locality of Hagen Fjord Group in Hagen Fjord



Source: Sønnerholm et al. (2008) (157). Note: The Fyns Sø Fm is unconformably overlain by Cambrian deposits of the Portfeld (PF) and Buen Fms. JÅ: Jyske Ås Fm; CD: Campanuladal Fm; KB: Kap Bernhard Fm; FS: Fyns Sø Fm. The cliff height is approximately 600 m.

Kap Bernhard Fm is a 215 m thick silty limestone sequence interbedded with minor siltstones (233). The change from Catalinafjeld Fm siliciclastic, to Kap Bernhard Fm carbonate sediments reflects a change in depositional environment and switch to an arid climate (223). The basal 40 m of the Kap Bernhard Fm includes soft-sediment deformation, faulting, and intraformational breccias (233). Syn-sedimentary deformation decreases moving up the stratigraphy of the Kap Bernhard Fm (234). The formation deposited in a subtidal lagoon of a carbonate platform (223).

Fyns Sø Fm is an enigmatic dolostone sequence possibly present in J.C. Christensen Land, but otherwise known from its type locality at the southern end of Danmark Fjord¹⁰¹ (233). The Fyns Sø formation contains well-developed stromatolites, slump structures, intraformational breccia, and ripple marks (235). Towards the top of the formation, terrigenous red and green siltstone units interbed the dolostones (235), and together represent deposition onto a carbonate platform (223).

⁹⁹ Redbeds is a term used for sedimentary rocks that primarily comprise sandstone, siltstone or shale (375). Redbeds are thought to have formed with abundant oxygen available leading to oxidised iron (Fe³⁺) and creating 'rusty red' staining while reduced beds were more anaemic (restricted oxygen) inhibiting the oxidation of iron (375). Typically, redbeds are associated with terrestrial deposition in oxygenated atmospheres (405). However, Cretaceous-aged marine redbeds are also known to occur on a global extent (405). The oxidation state of rocks and fluids is critical in the process of scavenging, mobilising, and depositing copper. In oxidised fluid, copper is mobile, but when metal-bearing fluids encounter a reductant, such as reduced rocks, copper is precipitated from the fluids (401). For this reason, the Campanuladal Fm is the classic-style target and has been the focus of previous exploration attempts (3; 2).

¹⁰⁰ Catalinafjeld Fm exposure at Astrup Fjord: 81.93742°N, 29.60727°W.

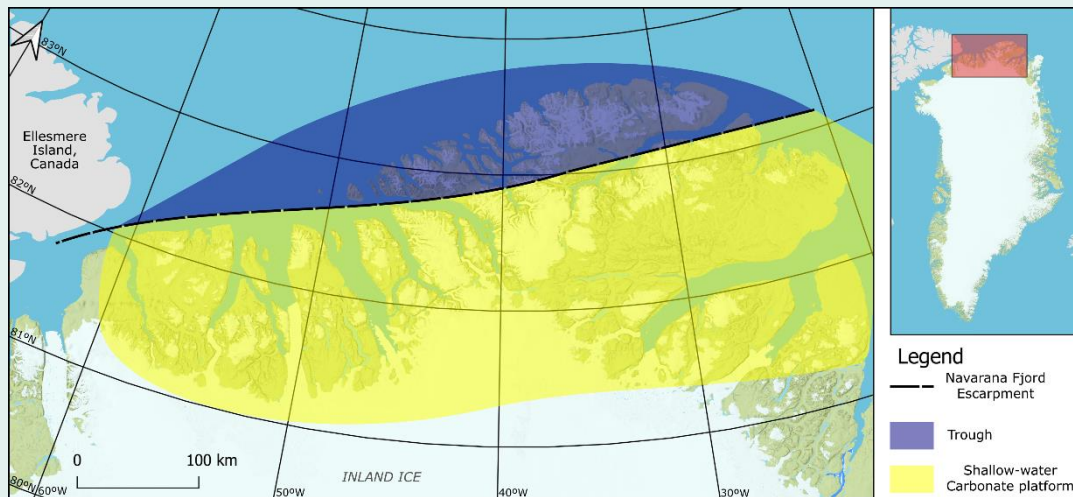
¹⁰¹ Danmark Fjord locates about 150 km to the southeast of J.C. Christensen Land.

5.2.4 Palaeozoic-aged sediments

The Early Palaeozoic-aged Franklinian Basin developed on a passive margin running from North Greenland to the Canadian Arctic Islands (236). This passive margin developed in seven defined stages with shelf sediments developing south of the Navarana Fjord lineament and deep-water correlatives north of it (Figure 45) (237). Within J.C. Christensen Land, three of the seven stages of the shelf's development dominate (149). The three formations present on J.C. Christensen Land are:

1. Portfjeld;
2. Buen; and
3. Wandel Valley Fm (149).

Figure 45: Franklinian Basin with a shelf-trough transition



Source: Reproduced from Ineson & Peel (1997) Fig 7 (238).

Portfjeld Fm is a 200 to 290 m thick¹⁰² composite sequence, comprising a lower carbonate succession capped by a mature karst profile and an upper carbonate-siliciclastic succession (149; 186). Re-investigation of this formation suggests that it also contains evidence of a Neoproterozoic in age and therefore can equally belong to the Hagen Fjord Group (186; 239; 240), but this is not officially recognised (3). The Portfjeld Fm has cross-bedded oolitic and intraclastic dolomites with abundant primary sedimentary features¹⁰³ and intraformational conglomerates (237; 241). A 10 to 15m thick chert marker bed is consistent across the formation (241). Stromatolites covered in bituminous material suggests the passage hydrocarbons in J.C. Christensen Land (Figure 46) (3; 241).

Figure 46 Hydrocarbons within Portfjeld Fm



Source: Rehnström (2012) (3). Note: Portfjeld Fm stromatolites with bituminous material.

¹⁰² At Hagen Fjord, the Portfjeld Fm is only 30 m thick (241).

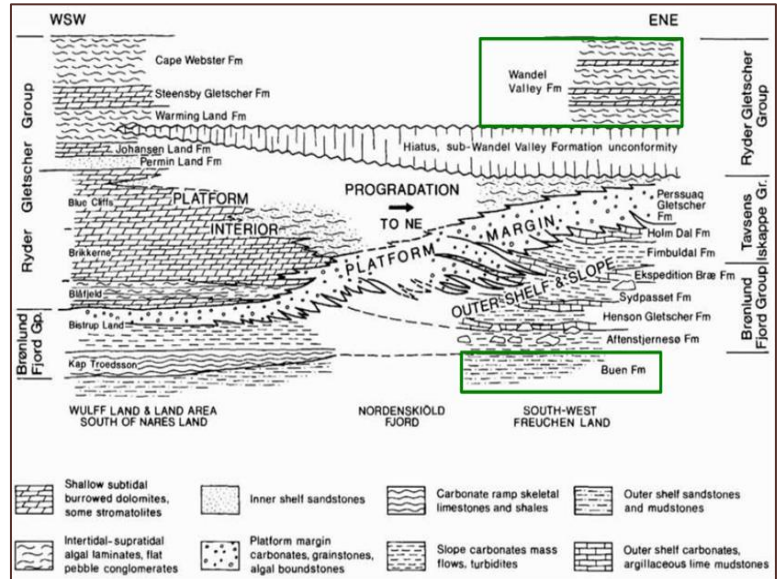
¹⁰³ Ripples, laminations, and stromatolites (237).



Buen Fm is a siliciclastic sequence which is up to 500 m thick and is characterised by sandstone with silty mudstone interbeds (238). The Buen Fm sits unconformably over the karstified Portfeld Fm (237). The units preserve primary sedimentary features¹⁰⁴ (242). The sediments of the Buen Fm represent a siliciclastic marine shelf with tidal influence and a history of storm events (237).

Wandel Valley Fm comprises well-bedded dolomites and sits unconformably over the Buen Fm (Figure 47) (238). A northwest-southeast fault bounds the formation at the northeastern tip of J.C. Christensen Land (Figure 33). The unconformity beneath the Wandel Valley Fm varies throughout North Greenland, but within J.C. Christensen Land it oversteps two groups, the Brønlund Fjord and Tavsens Iskappe Group (238). The formation is the uppermost unit of the Ryder Gletscher Group, a Cambrian-Ordovician-aged (540 to 444 Ma) sequence of shallow-water restricted platform carbonates with subordinate siliciclastic and evaporites¹⁰⁵ (243). The Ryder Gletscher Group records two upward shallowing- cycles, with each beginning with shallow, subtidal carbonates passing up into peritidal facies and evaporitic deposits (237).

Figure 47: Schematic cross-section of Franklinian Basin sediments at Nordenskiöld Fjord



Source: Modified from Higgins et al. (1991) (237). Note: Nordenskiöld Fjord is located 250km to the east-northwest of J.C. Christensen Land. The Wandel Valley Fm sit unconformably on top of the Buen Fm.

5.2.5 Structures

The North Greenland faults and lineaments developed in response to different geological events. The oldest faults in the region may be syn-rift, while others relate to deformation events (149). Within J.C. Christensen Land, many of these events are expressed as structures that parallel major regional fault zones and lineaments (Figure 31) (149).

Around J.C. Christensen Land, four sets of faults orientations are on the 1:100,000 geological map (217). These faults appear to relate to more extensive, regional-scale fault zones and lineaments, they are:

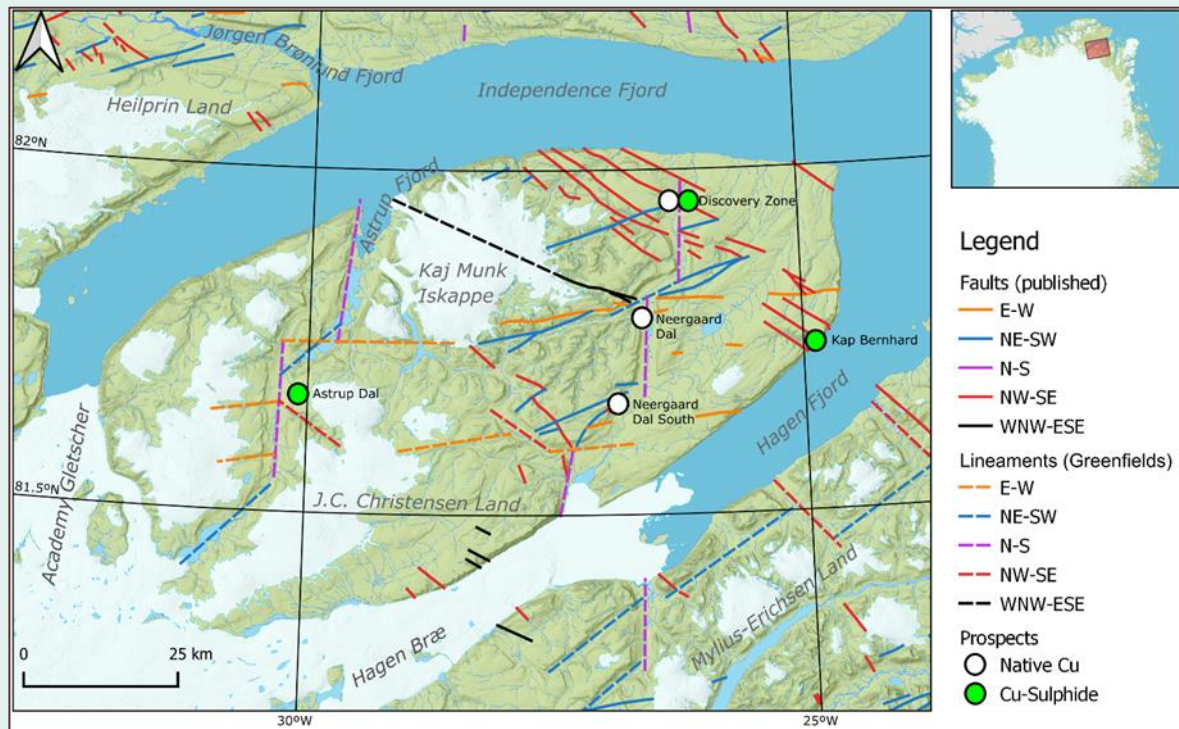
- Northwest-southeast trending faults parallel the Trolle Land Fault Zone;
- Northeast-southwest faults parallel the Central Peary Land Fault Zone, Navarana Fjord Escarpment, and conspicuous lineaments such as Independence Fjord;
- East-west trending faults parallel to the Wandel Dal Lineament; and
- North-south lineaments that do not appear to align with the identified regional structures. These features are discontinuous and appear to show offsets by other, younger, fault sets.

¹⁰⁴ Cross-bedding, hummocky cross-stratification, and mud drapes as well as bioturbation in the form of skololithos (vertical burrows) (242).

¹⁰⁵ In Washington Land to the west where the Ryder Gletscher Group is better preserved, evaporites dominate the 125 m thick Poulsen Cliff Fm and the 40 m thick Nygaard Bay Fm (237).

The published faults and the topographic lineaments identified by Greenfields are in Figure 48.

Figure 48: Faults and topographic lineaments of J.C. Christensen Land



Source: Greenfields with faults from GEUS Geological map of Greenland (217) 1:100 000, J.C. Christensen Land & native copper showings from Tukiainen & Lind (2011) (128). Note: The two symbols shown at the Discovery Zone is for clarity only, the prospect is one location and contains both native Cu and Cu-sulphide mineralisation.

Northwest-southeast faults (red) are the densest in the north of J.C. Christensen Land (Figure 48). Faults with this orientation offset the Independence Fjord Group, Zig-Zag Fm, Hagen Fjord Group, and Franklinian Basin sediments. Northwest-southeast topographic features range from near Astrup Fjord¹⁰⁶ on J.C. Christensen Land, through to Kap Næstved¹⁰⁷ on Mylius-Erichsen Land.

Northeast-southwest faults (blue) and lineaments are also evident in (Figure 48) and broadly parallel to the main orientation of the Independence and Hagen fjords. The northeast-southwest faults show a large stratigraphic offset of the Zig-Zag Fm and Norseman Dal on Mylius-Erichsen Land. Based on the published mapping, it is unclear what the relationships are with other faults in the area.

East-west faults (orange) in J.C. Christensen Land are least common. In addition to the published faults, lineaments visually identified by Greenfields are mostly in the centre of the area. Towards the west, there are large east-west trending valley/lineaments. Near Kap Bernhard¹⁰⁸ in the east, the official mapping suggests that the northwest-southeast faults terminate against an east-west fault, although this requires field validation¹⁰⁹.

¹⁰⁶ Glacier terminating at Astrup Fjord, 81.859°N, 29.259°W.

¹⁰⁷ Kap Næstved, ~80.741°N, 23.486°W.

¹⁰⁸ Kap Bernhard, ~ 81.78°N, 24.73°W.

¹⁰⁹ The fault intersection is outside the licence area and special permission is required to make such a site visit.



North-south oriented lineaments (purple) show frequent offsets and terminations against 'orange' east-west and 'blue' northeast-southwest faults. It is unknown if these lineaments are true faults, or result from extensional forces associated with other fault movements in the area.

One major published fault does not easily fit into the fault sets (black) defined above. The 12 km long west-northwest trending fault offsets basaltic stratigraphy and runs into Kaj Munk Iskappe. If it is extrapolated (black dashed line) under this icecap to Hugh Lee Bræ glacier at the mouth of Astrup Fjord, its length is 42 km. This fault-lineament may be aligned with the Jørgen Brønlund Fjord.

Fault offsets of various magnitudes are apparent in J.C. Christensen Land's geological map. The offsets created by faulting is challenging to quantify from geological maps alone. The northwest-southeast and east-west faults appear to cause the most displacement. The apparent vertical offsets range from 100's of metres (3), up to approximately 1 km. Lateral faulting is more challenging to determine, but stratigraphic offsets suggest the movement of up to nearly 5 km. If Independence Fjord is a normal-fault such that Norsemandal Fm sits above Inuiteq Sø Fm, approximately 2 km of displacement is required to level these two formations on either side of the fjord/fault.

**FAULTS CAPABLE OF
PROVIDING
FOCUSSED, VERTICAL
FLUID PASSAGE**

Around J.C. Christensen Land, the north-south lineaments are weakly expressed in the topography at Astrup Dal, Neergaard Dal and its extension into Mylius-Erichsen Land.

5.2.6 Alteration

Within J.C. Christensen Land, much of the prior research on metamorphism and alteration focusses on the basalts and intrusions. The relationship between the metamorphism, hydrothermal alteration and geochronological events is not well described. This uncertainty may be due to similar metamorphic mineral assemblages and seemingly conflicting results of age determination studies.

The Zig-Zag Fm basalts underwent spilitic metasomatism in response to the interaction of lava with seawater (221). Spilitisation is mainly characterised by enrichment in Na₂O, which can make it difficult to distinguish from subsequent metamorphic and hydrothermal events. However, the basaltic lavas of J.C. Christensen Land are metamorphosed to zeolite facies (225). These lavas show considerable signs of lateral alteration, which includes prehnite-pumpellyite bearing veins and pipes cross-cutting the flows (221; 225). Alternating red and green flows are present, but only haematite is used to explain the redness¹¹⁰ of the thin 1 to 10 m thick flows (225). Volcanic ash layers up to 60 m thick, and sedimentary horizons are also present throughout the lavas and provide additional lateral permeability for hydrothermal fluids (227). Exclusively within J.C. Christensen Land are red rhyolitic flows, which have been heavily altered and now consists of slender albite laths set in a turbid quartzo-feldspathic matrix (221). The intensity of the alkali alteration of the rhyolitic flows suggests that it was also a preferential path for lateral fluid flow. The thicker flows (>10 m) are relatively fresh, sometimes have a green colour, and commonly exhibit columnar and entabular (columnar) jointing¹¹¹, which do not show significant signs of alteration (221). However, vertical fluid flow did occur as evidenced by the veins and pipes that cross-cut the altered lavas, most commonly in the lower basalt flows (225). Notably, faults with

¹¹⁰ Potassic feldspars, such as microcline, can also impart red colouration (273).

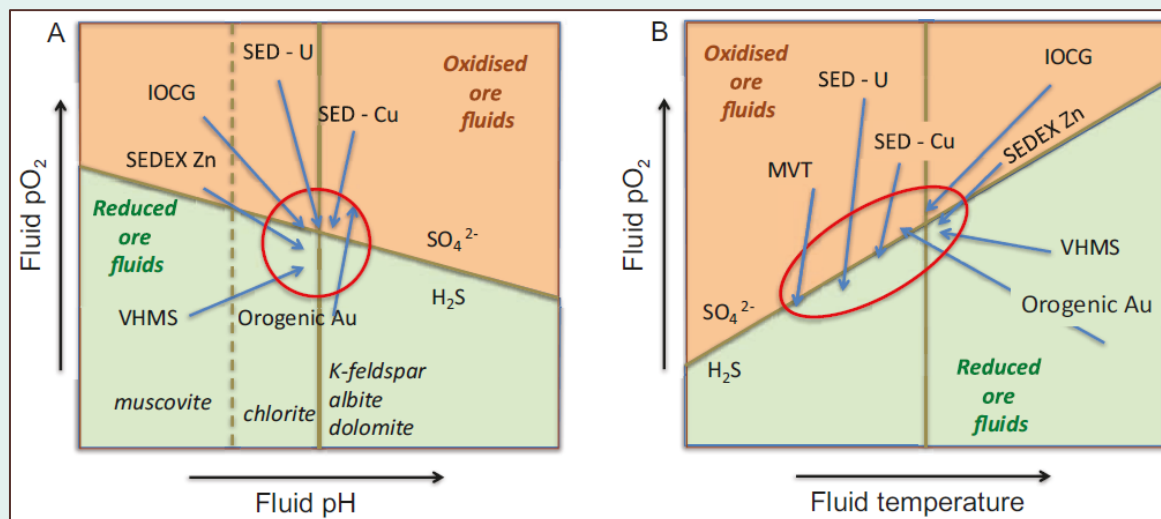
¹¹¹ Columnar that entabular joints form before lavas fully crystallise (386), and as such Greenfields considers that they may have relatively low permeability.

alkali alteration are known to crosscut the younger sediments overlying the basalts (3), which demonstrate that a hydrothermal event occurred well after the emplacement of the lavas¹¹².

Regionally there is a significant change in the oxidation state between J.C. Christensen Land and Mylius-Erichsen Land. Stream sediment analysis shows that titanomagnetite is dominant on Mylius-Erichsen Land (244). In J.C. Christensen Land the stream sediments are dominated by haematite (244). Haematite forms under more oxidative conditions than magnetite, which are typically closer to the surface (245; 246). Haematite also develops as an alteration from magnetite by oxidised fluids (247). Within the Jyske Ås Fm, haematite rims quartz grains, which indicates a secondary origin (3).

Mineral assemblages can be an important indicator in determining the mineral potential of an area (248). The hydrothermal deposition of economically attractive minerals is link to the properties of the fluids from which they form (249). Influencing factors on mineral formation are fluid oxygen concentration (pO_2), acidity (pH), and temperature (249). The pO_2 , pH and temperature transitions shown in Figure 49 define essential conditions associated with hydrothermal deposit formation (249). Common to all deposit types is a trajectory from high temperature to low temperature (249). The zone surrounding the transitions from reduced to oxidised conditions as well as the change from chlorite to K-feldspar and albite is also significant (249). Within J.C. Christensen Land, there is clear evidence of pH-controlled transitions between K-feldspar, albite and chlorite conditions. Additionally, haematite abundance in J.C. Christensen Land and magnetite abundance in Mylius-Erichsen Land indicate an important change in the oxidative state¹¹³ that is associated with copper mineralisation (250; 251; 252; 253).

Figure 49: Mineralisation fluids in pH- pO_2 space



Source: Large et al. (2017) (249). Note: Blue arrows represent ore fluid trajectory. Red circles marks conditions associated with deposit models.

Alteration minerals are present as pseudomorphs after primary phenocryst minerals, in the groundmass, and filling vesicles (225). Of the basalt's primary mineral assemblage clinopyroxene is preserved; olivine is replaced by mafic phyllosilicates; and calcic plagioclase is replaced by albite and K-feldspar (225), such that:

¹¹² The evidence of alkali alteration in the overlying Neoproterozoic-aged sediments indicates that the basalts were subjected to more than spilitic alteration.

¹¹³ Low-temperature, slightly alkaline brines with elevated fugacity can transport copper in solution up to 800ppm (250).



- Albite pseudomorphs after Ca-plagioclase in the altered flows, and is ubiquitous with chlorite, smectite, and celadonite¹¹⁴ (225). Albite also occurs in vesicles and cross-cutting veins (225). In these later features, albite is associated with the metamorphic mineral, pumpellyite (225).
- K-feldspar also pseudomorphs after primary Ca-plagioclase in the altered flows, but additionally occupies the groundmass (225). There is intense potassic alteration in the Brown Marker flow (225). The Brown Marker flow is a particularly prominent flow throughout J.C. Christensen Land and Mylius-Erichsen Land (225).
- Mafic phyllosilicates, usually chlorite and smectite clay minerals completely replace olivine phenocrysts (225). Chlorite and smectite are not exclusively diagnostic of metamorphism but can be a function of low-temperature hydrolysis (245). There are common fine-grained metamorphic intergrowths between chlorite-celadonite, and chlorite-pumpellyite (225). Celadonite is a ferromagnesian mica group mineral that develops under zeolite facies metamorphism (254). In the groundmass of the altered flows, intergrowth occurs between celadonite, chlorite and smectite (225).

Thomsonite¹¹⁵, a white to pink mineral with blade like crystals, is the only exclusively zeolite group mineral identified in the altered flows and is important in classifying the metamorphic facies (225). Thomsonite is found with chlorite in vesicles at the top of lava flow 68 (225). In some vesicles, chlorite appears in pseudomorphs after thomsonite (225). Bevins et al. (1991) state that the absence of epidote indicates that temperatures did not exceed ~200°C, and therefore did not achieve Prehnite-Pumpellyite Facies (225). However, Rehnström (2012) states that epidote is present (3). Pyrobitumen reflectance in the overlying sediments indicates a temperature of ~150°C (3).

Other alteration minerals that are indicative of the metamorphic grade are prehnite¹¹⁶ and pumpellyite¹¹⁷. These two minerals occur in zeolite facies, as well as the higher temperature namesake facies¹¹⁸ (225). Within the basalts, pumpellyite typically occurs in the groundmass of altered flows, as crystal aggregates in albitised plagioclase, and in veins intergrown with albite (225). Prehnite occurs with pumpellyite in vesicles and veins (225). Prehnite occurs in the groundmass of some altered flows, but this is rare (225).

Titanite occurs as small aggregates in chlorite within the most altered flows (225). Titanite only occurs in hydrothermal rocks and is suited to dating the difference between the hydrothermal and metamorphic alteration.

Native copper occurs in the aphyric basalts as part of vein assemblage of prehnite, quartz, and calcite (225). The copper occurs within prehnite minerals, and at the interface between prehnite and quartz (Figure 50) (225). However, large clasts of native copper weighing up to 1kg occur (2). The veining is important as it links a hydrothermal component to the copper mineralisation. While spilitic alteration can produce native copper (255), there is no known

FAVOURABLE
TEMPERATURES
FOR MOBILISING
COPPER

¹¹⁴ Celadonite, a phyllosilicate of potassium, iron, aluminium, and hydroxide, $K(Mg,Fe^{2+})(Fe^{3+},Al)Si_4O_{10}(OH)_2$ (254).

¹¹⁵ Thomsonite is a series of tecto-silicate minerals in the zeolite group. $NaCa_2Al_5Si_5O_{20} \cdot 6H_2O$ (368).

¹¹⁶ Prehnite, an inosilicate of calcium and aluminium, $Ca_2Al_2Si_3O_{10}(OH)_2$ (366).

¹¹⁷ Pumpellyite, a sorosilicate group mineral with related Mg, Fe^{2+} , Fe^{3+} , Mn^{2+} , and Al equivalents. Mg formula: $Ca_2MgAl_2[(OH)_2SiO_4Si_2O_7] \cdot (H_2O)$ (367).

¹¹⁸ As prehnite and pumpellyite being to form in zeolite conditions, by themselves these minerals are not diagnostic of Prehnite-Pumpellyite Facies metamorphism (225).

mechanism for enriching the copper to the observed nugget sizes¹¹⁹. Hydrothermal fluids after lava emplacement is likely to be the most effective¹²⁰ mechanism for liberating copper from basalt. The presence of copper sulphide mineralised faults in the overlying sediment demonstrates that the hydrothermal fluids must have contained sulphur from a distal or unknown source, as the element is not known to be a significant component of the Zig-Zag Fm basalts (128).

**NATIVE COPPER
CLASTS WEIGHING
UP TO 1KG ARE NO
ACCIDENT**



Figure 50: Metamorphic alteration of basalt

Source: Rehnström (2012) Fig 7.2.A (3). Note: Basalt is encrusted with prehnite, calcite, quartz, and native copper (3).

5.2.7 Age determination

The geochronological dating of the rocks in and around J.C. Christensen Land has a colourful history, with multiple, contrasting studies (Table 2). Understanding the evidence and what it means is material to understanding the geological history, and its potential impact on economic mineral distribution.

**DATING THE
OROGENIC EVENTS
WAS THE KEY TO
THE NORTH**

¹¹⁹ Spilitic alteration occurs when basaltic lavas interact with a source of sodium (e.g. seawater), resulting calcic plagioclase and clinopyroxene being converted to sodic plagioclase and chlorite (385).

¹²⁰ Due to prevalence of veins in the subaqueous basalts relative to the overlying subaerial flows, seawater induced alteration cannot be entirely discounted.



Table 2: Geochronological dating summary

Source	Method	Summary	Greenfields' observations and interpretations
Henriksen & Jepsen (1970) (256)	K/Ar Ar/Ar	Dating of two dolerite sills in the Jørgen Brønlund Fjord / Midsommersø area resulted in ages of: 988 ± 20 Ma for a dolerite sill; and 799 ± 68 Ma for a 'badly' altered, porphyritic dolerite.	There are no apparent correlatives for the dates of these intrusions.
Larsen & Graff-Petersen (1980) (257)	Rb-Sr	Dating of the clay minerals from an Independence Fjord Group siltstone on the north side of Hagan Bræ suggest an age of: 1,380 Ma	The intrusive and extrusive activity reset the Rb-Sr of the second oldest member within the formation. The sediments are older than 1,380 Ma.
Kalsbeek & Jepsen (1980) (216)	Rb-Sr	Dating of a xenolith in dolerite indicates a basement metamorphic event at: 1,750 to 1,600 Ma.	c. 1,750 Ma coincides with the start of sedimentation in the Independence Fjord Group.
Kalsbeek & Jepsen (1984) (221)	Rb-Sr	Dating of a red, altered dolerite yielded an age of 1,230 ± 20 Ma ; and 1,220 ± 25 Ma for a rheopsammite.	The Rb-Sr ratio was reset by alteration fluids during the Elzevirian Orogeny.
Kalsbeek et al. (1999) (258)	U-Pb	Dating from the northeastern Greenland Caledonides yielded: 2,000 to 1,730 Ma for granitoids 1,740 ± 6 Ma for Independence Fjord Group hosted meta-rhyolitic ignimbrites associated with basalts.	These dates correlate with the orogenic event identified in Kalsbeek & Jepsen (1980).
Pedersen et al. (2002) (171)	U-Pb	Using the 1,740 Ma date of Kalsbeek et al. (1999), the rhyolitic ignimbrites are attributed to rift-related volcanism and establishes the basalts as being unrelated to the Zig-Zag Fm.	The 1,740 Ma volcanics may occur at the base of Independence Fjord Group which accumulated at the onset of rifting on the east coast. The 1,380 Ma Zig-Zag Basalts Fm erupted onto a sagging, filled basin
Upton et al. (2005) (159)	U-Pb Rb-Sr re-analysis	Dating of 'fresh' dolerite gave an age of: 1,382 ± 2 Ma. Reanalysis of the red dolerite Rb-Sr gave a consistent result of: 1,230 Ma.	The 1,382 Ma age gives the correct date of emplacement given the stratigraphic and global relationships; and the 1,230 Ma reflects the Elzevirian Orogeny.
Kalsbeek & Frei (2006) (228)	Isotope, major and trace element analysis	Various basalt and intrusion results were used to argue for field relationships to debase the reliability of the 1,230 Ma date, and in support of the 1,382 Ma date. Loss of Sr due to weathering is proposed as a cause of the repeatable 1,230 Ma date.	This appears to assume that spilitisation being the only alteration. However, this is inconsistent with Bevins et al. (1991)'s metamorphic description (225); Kirkland et al. (2009)'s identification of orogenesis, and the presence of altered Neoproterozoic-aged sediments (3; 2).
Kirkland et al. (2009) (186)	U-Pb detrital zircon analysis	Dating yielded the youngest age of 1,814 ± 23 Ma for the Inuiteq Sø Fm; 970 Ma minimum age for the Morænesø Fm; and a 1,250 Ma orogenic event in the basement (Elzevirian)	The 1,814 Ma for the youngest zircon grain is consistent with the formation of the Independence Fjord Fm around 1750 Ma. The 970 Ma date may have no relationship with the Ar/Ar, K/Ar dated dolerites; and it confirms the Neoproterozoic-age of the sediments. The 1,250 Ma Elzevirian Orogeny is fundamental to the understanding of North Greenland.

6 EXPLORATION

6.1 PROSPECTING

Prospecting within North Greenland has been restricted to reconnaissance-scale commercial exploration and government/academic work. In 1969, Greenarctic conducted a reconnaissance survey between Danmark Fjord, starting at the head of Danmark fjord, to Kap Harald Moltke and a final campsite at Midsommer Sø (130; 58). The 1969 field program was successful in identifying native copper occurrences at two locations¹²¹ in the 'Hagan Arch'¹²² (Mylius-Erichsen Land) (130), although logistical constraints prevented sampling (130). In 1970, Greenarctic commissioned an airborne photogeological survey and interpretation over the area (58; 128). In 1972, Greenarctic conducted its second field mapping program over a ~5,000 km² exploration licence on Heilprin Land and southern Peary Land (58; 259). The 1972 field campaign identified occurrences of sediment-hosted copper-silver sulphides; a minor barite vein, and investigated the historically reported 'solfataras'¹²³ (58). No visits to J.C. Christensen Land nor Mylius-Erichsen Land occurred in the 1972 field program.

ONLY ONE FOCUSED
COMMERCIAL EXPLORATION
PROGRAMS IN THE 50 YEARS
SINCE COPPER WAS FIRST
DESCRIBED

In 2010, three Avannaa geologists conducted a twenty-day mapping and sampling program focussed in a tiny area at the northern terminus of Neergaard Dal¹²⁴ (2) in the north of ARC. This program was self-supported with only one day of helicopter reconnaissance¹²⁵ (2). The work involved mapping and sampling designed to follow up on sediment-hosted copper sulphides identified by government workers in the 1990s (2). The program was successful in identifying the three brecciated faults that comprise the 'Discovery Zone'. In response to this success, trench sampling was performed.

In 2011, Avannaa greatly increased its exploration by conducting a three-week, nine geologist, heli-supported reconnaissance program. The area of investigation included the original 405 km² licence on J.C. Christensen land, as well as an additional licence covering 4,096 km² over both J.C. Christensen Land and Mylius-Erichsen Land (3). The 2011 program extended the Discovery Zone breccias from 800 to over 2,000 m; and successfully identified copper anomalous horizons over the entire licence area (3).

6.2 GEOCHEMISTRY

There are 549 known geochemical results from within J.C. Christensen Land (Figure 51). These samples comprise a mix of Government and private sector programs:

- **310 rock chip, trench and grab samples** from the year 2010 and 2011 commercial exploration program. These samples cluster in northern ARC;

¹²¹ 1) White Hill located at approximately 81° 03' N and 24° 15' W where a 5 m wide zone of native copper particles, malachite and azurite were identified within basalts (130). A maximum assay grade of 1.4% is reported, although higher grades are possible (130). 2) North Stordalen located at approximately 81° 27' N and 23° 55' W (130). Disseminated native copper, malachite and bornite are reported to occur in basalt geodes, with the mineralised zone being up to 10 m thick and intermittently traceable over at least 8km (130).

¹²² The Hagen Arch is an abandoned term used to describe the Proterozoic-aged rocks of Heilprin Land, J.C. Christensen land, and Mylius-Erichsen Land. The 'Arch' served as inspiration for the ARC acronym.

¹²³ The solfataras are mounds that typically have a gravel collar with a core of gypsum, sulphur, pyrite, and copiatite (58). Despite no volcanic rocks in the area, they were historically thought to be some sort of active volcanic feature (58). However, investigation by Avannaa in 2011 determined that the mounds are the result of exothermic sulphide reactions (3). Avannaa sampled the solfataras and did not identify anomalies of commercial interest (3).

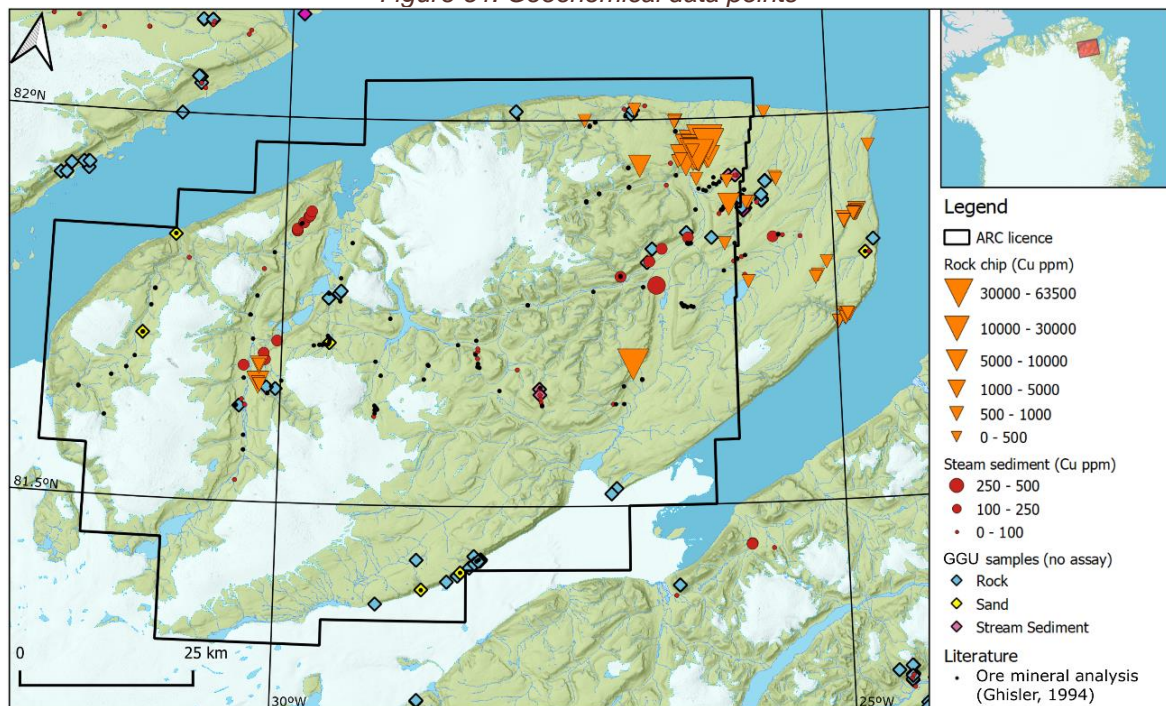
¹²⁴ Dal is valley in Danish and appears in many of the English publications.

¹²⁵ Through a charter of a helicopter working at Citronen



- **227 stream sediment samples** were collected by Avannaq in 2011 and analysed in the field using handheld X-ray fluorescence ('XRF') equipment. No other assay methods were used¹²⁶.
- **145 rock chip samples** from 1978 to 1980. The samples are heterogeneously distributed and comprise 1 litre of unsieved sediment (260). Native copper occurs in 80% of samples from ARC (261). In four instances the native copper occurred with covellite, sometimes with cuprite and in one case with bornite (261). One sample included native iron¹²⁷ (260). The sample duplication was 13% of the total population (including samples from outside of ARC); and
- **94 stream sediment samples** collected by the Greenland Geological Survey between 1993 and 1994.

Figure 51: Geochemical data points



Source: Based on all data identified by Greenfields from GreenMin (2020) (262); Ghisler (1994) (260); Haugaard (2011) (2); Rehnström (2012) (3).

There are an additional 627 samples collected by the Government for which geochemical results are not available. At the time of writing, Greenfields was investigating whether these samples are in storage and whether additional detail is available.

¹²⁶ Rehnström (2011) states "Generally the concentrations are too low for this measuring technique to be totally reliable and no further data analyses have been made, maximum value of Cu is 97 ppm, Pb is 26 ppm and Zn is 344 ppm" (3). It is presently unknown if these samples are in storage, were left in the field, or disposed of.

¹²⁷ The natural source of the native iron was not identified in the literature (260). It is not known if the native iron is pure, or an alloy such as awaruite.

6.3 GEOPHYSICS

There are five identified geophysical surveys within or covering ARC. The most recent survey that focussed on ARC was conducted over twenty years ago.

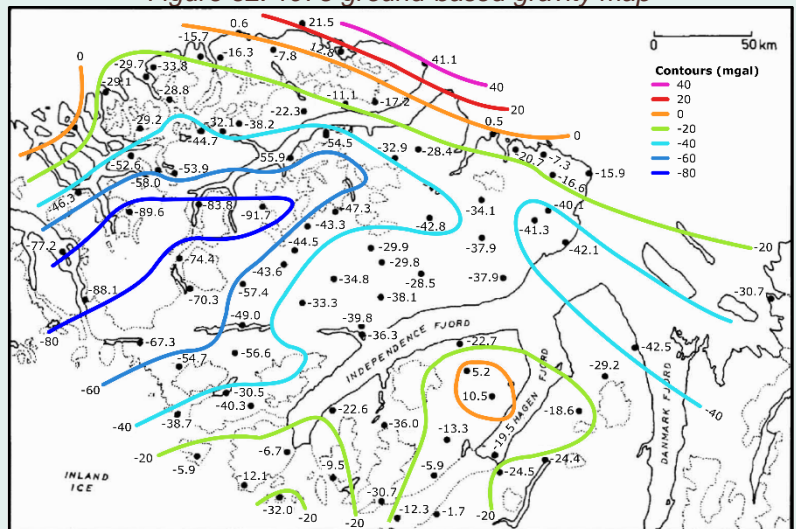
In 1971, the Greenarctic Consortium funded an airborne magnetic survey over much of northern Greenland, from Washington Land to lower Kronprins Christens Land (259; 58). The first-pass, low-resolution survey flew with a grid spacing of 2.5 by 15 km and at an altitude of 1.85 km (259).

In 1978, the Geodetic Institute (Copenhagen) conducted a land-based gravity survey of North Greenland with an irregular grid (263). A gravity map was produced with contours of 20 mgal, although the error margin was 10 mgal (263)(Figure 52). The gravity investigation showed a rapid rise in gravity which is reported to represent crustal thinning towards the continental shelf, which is particularly narrow in the Wandel Sea (263). A gravity high was identified in the north of Hagen Fjord (within northern ARC), which was attributed to Proterozoic-aged Zig-Zag Fm and Midsommersø Intrusions (263).

Between 1993 and 1996, the Alfred Wegener Institute ('AWI') for Polar and Marine Research conducted a high-level aeromagnetic survey of eastern and northeastern Greenland (Figure 53) (264). The survey flew using inline and crossline direction from 10 to 40 km and the altitudes up to 3,700 m above sea level (264).

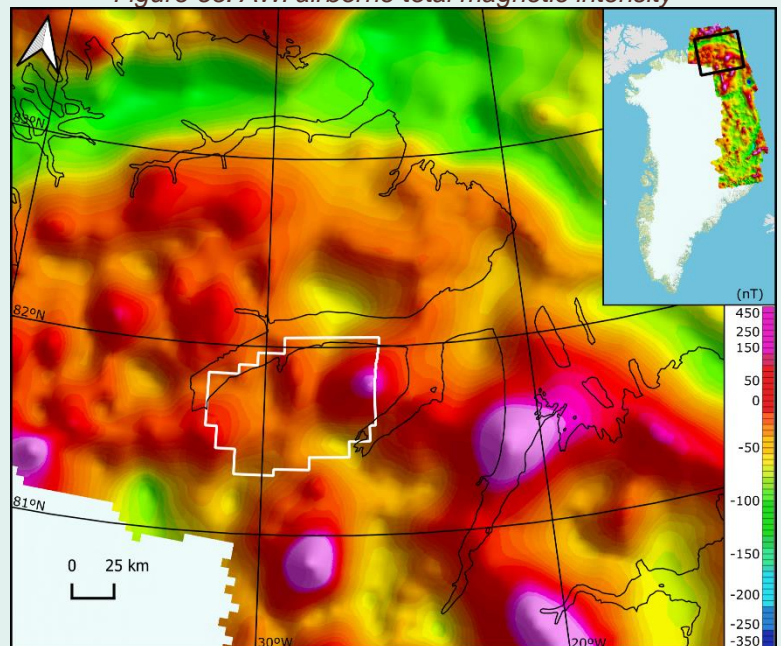
In 1998, the Greenland Government commissioned an airborne electromagnetic-magnetic survey ('AEM1998') which focussed on the northern portion of J.C. Christensen Land (265). The survey had 400 m line spacing with 4,977 line kilometres flown between 81°25'N to 82°10'N, and 28°0'W and 24°8'W (265). The total magnetic intensity ('TMI') was highest in the middle of the survey area (Figure 54). The apparent electromagnetic conductance indicates linear anomalies¹²⁸ that are consistent with the regional mapping of the lithology and faults in the area (Figure 55). The survey

Figure 52: 1978 ground-based gravity map



Source: Forsberg (1979) (263), coloured by Greenfields. Note: No terrain correction is applied in this figure and the anomalies may be understated.

Figure 53: AWI airborne total magnetic intensity



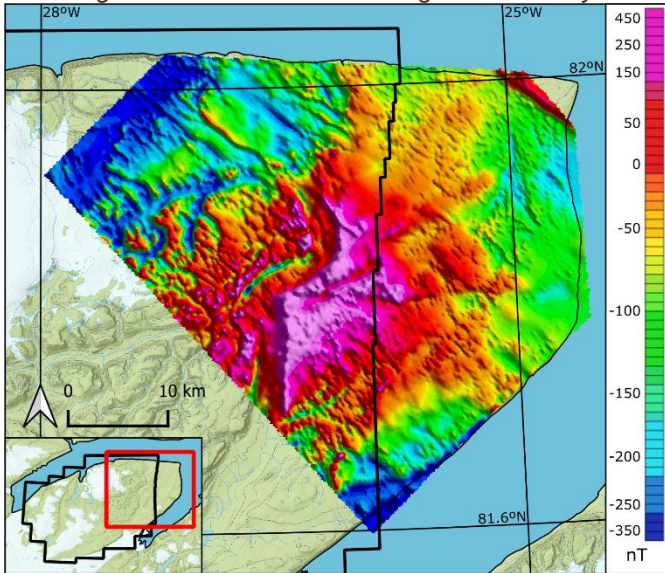
Source: Greenfields using data from GreenMin (2020) (262) and structures from Piepjohn et al. (2016) (204).

¹²⁸ Terrain influence cannot be completely discounted on geophysical responses.



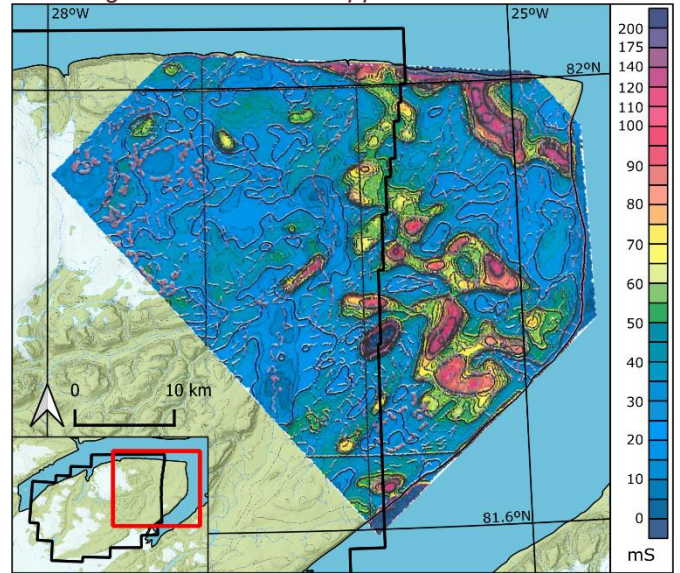
was an attempt to detect copper mineralisation directly, but no clear geochemical-geophysical correlations were reported at the time (128).

Figure 54: AEM1998 total magnetic intensity



Source: Greenfields using GeoTerrex (1998) (265).

Figure 55: AEM1998 apparent conductance

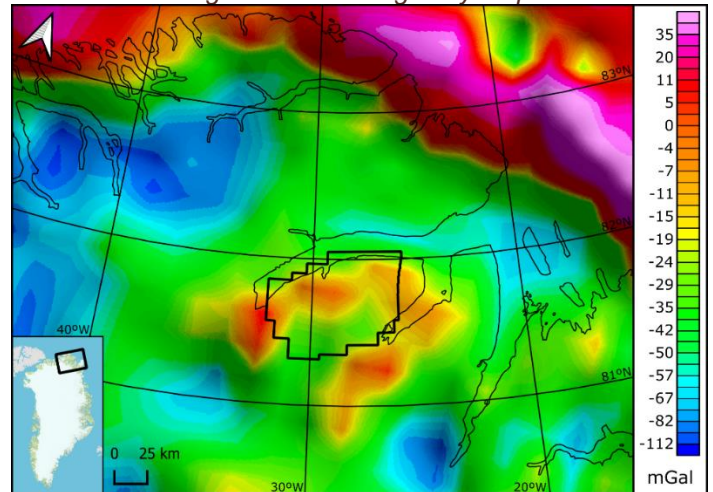


Source: Greenfields using GeoTerrex (1998) (265).

In 2009, a collaborative effort between academics and geological surveys with arctic interests compiled and released new gravity and magnetic anomaly maps under the Circum-Arctic Mapping Project ('CAMP') (266). The project merged potential field data from the collaborating institutes to create seamless gravity and magnetic maps of the Arctic (above 60°N) (266). The magnetic map has a grid resolution of 2 x 2 km and the gravity map has a resolution of 10 x 10 km (266).

In 2011, satellite imagery was processed over J.C. Christensen Land, Mylius-Erichsen Land, Heilprin Land, and Erlandsen Land (3). ASTER multispectral data was used to identify lithologies with some success, but the resolution is too low to detect alteration/mineralisation (3). RadarSat data was processed to produce a digital elevation model (± 10 m vertical within a 15 m radius) (3). The recommendation from this work is to acquire and process higher resolution satellite imagery.

Figure 56: CAMP gravity map



Source: Gaina et al (2011) (266).

6.4 SINGULARITY

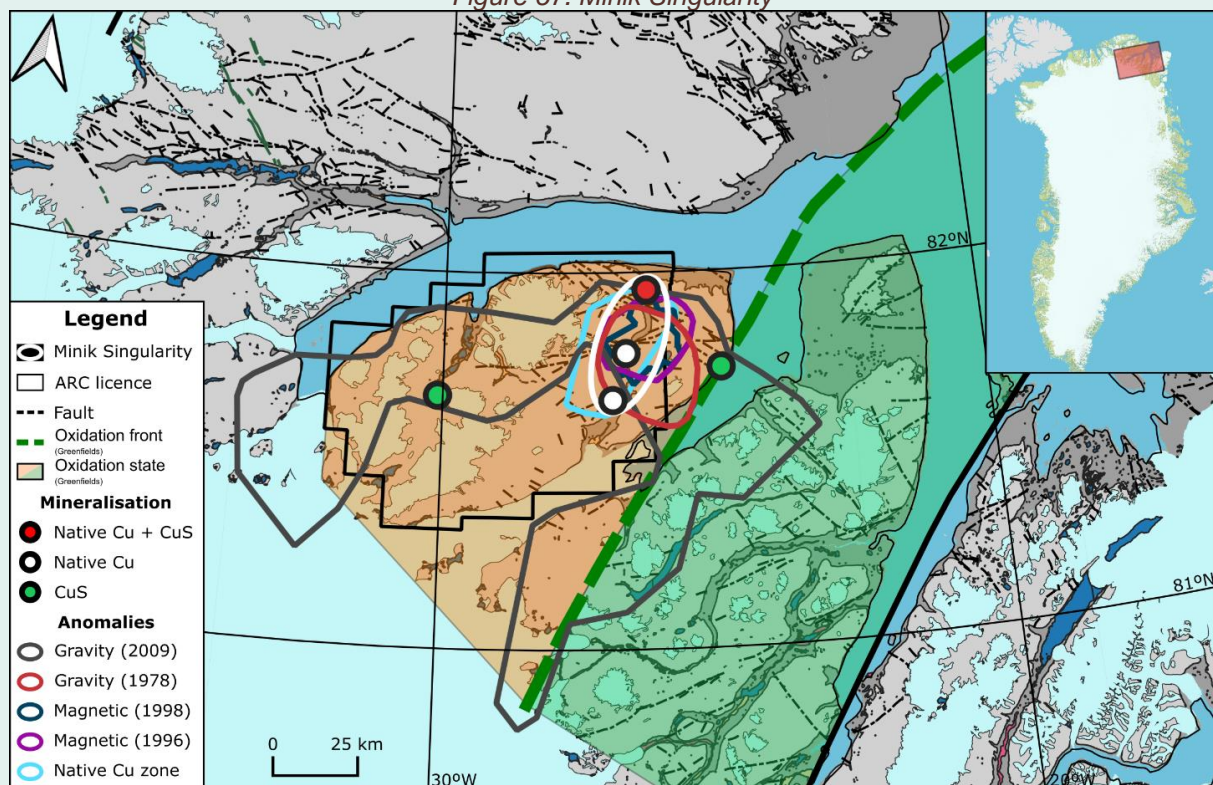
The empirical geophysical and geochemical evidence shows multifaceted anomalism within ARC that is not readily explained by normal geological features. This singularity is designated by:

1. A gravity high in northeastern ARC. In the 1978 land-based survey this appears as a point anomaly, and in the 2009 CAMP collation, this has an arc-like shape. While there are distinct differences between the irregularly distributed land-based and 10 x 10 km resolution CAMP data, both show a high gravity response in northeastern ARC.

2. Coincident magnetic highs in northeastern ARC. Both the AWI and AEM1998 data show a high TMI response in northeastern ARC. The TMI highs occur at approximately the same location as the gravity anomalies. The magnetic response is in an area of sedimentary rocks, not basalts or intrusions, as attributed in the reviewed literature. However, the fault offsets near Kap Bernhard between the Campanuladal Fm and Portfjeld Fm are obvious in TMI and suggests that the response may have a stratabound control at depth. The volcanics are estimated to be around 250 m below surface (4).
3. Native copper anomalism in northeastern ARC. Ghisler & Stendal (1980) (261) show an oval-shaped area of native copper in the stream sediments in an area that overlaps with the gravity and magnetic highs.
4. The electrical conductivity response is erratic bordering in the same area as the AEM1998 TMI high.
5. The geophysical and geochemical copper anomalies are located near a large-scale oxidation boundary. Only magnetite is present within the stream sediments of Mylius-Erichsen Land, whereas haematite is found on J.C. Christensen Land.

The multiple co-incident, and proximal, geophysical and geochemical anomalies are not readily explained by the information reviewed by Greenfields (Figure 57). These deviations from the expected background responses represent important empirical evidence that must be considered in understanding ARC. Consequently, Greenfields uses these features to delineate a ~640 km² singularity which it names 'Minik', in honour of Minik Wallace (1890-1918)¹²⁹.

Figure 57: Minik Singularity



Source: Greenfields

¹²⁹ Minik Wallace was a Greenlandic child brought to New York following one of Robert Peary's first expeditions. Minik and the other Inughuit were subject to abuse, neglect and deception (409). The indigenous peoples impacted by early exploration should be remembered in the same way as the foreign explorers themselves.



6.5 DRILLING

No drilling has ever occurred within ARC or the immediate region. The nearest known site of drilling is at the Citronen zinc deposit owned by Ironbark Zinc Ltd, some 130 km to the north of the ARC centroid.

Mechanically assisted sampling occurred in 1979 as part of a palaeomagnetic survey (267). A hand drill was used to collect core to a diameter of 2.5 cm, and length between 5 to 10 cm (267). With ambient temperatures ranging from +1°C to +10°C¹³⁰, there were no issues associated with freezing drilling fluids (267).

6.6 PROSPECTIVITY AND ENDOWMENT STUDY

As part of a United States Geological Survey Program, the Bureau of Minerals and Petroleum¹³¹ ('BMP') and the Geological Survey of Denmark and Greenland¹³² ('GEUS') commissioned workshops on quantifying the mineral resource potential of Greenland (268). As part of this program, BMP and GEUS held workshops on sedimentary-hosted copper in 2009 (268), and magmatic nickel in 2012 (269). The workshops relied on deposit models and involved:

- i) delineation of tracts of land where the geology is permissive for predefined types of deposits;
- ii) selection of appropriate grade/tonnage models; and
- iii) estimation of the number of undiscovered deposits consistent with the grade and tonnage model. The number of estimated deposits was combined with the grade and tonnage model to assess the total undiscovered endowment (268).

...TWO EXPERTS THINK THERE IS A 50% CHANCE OF THERE BEING A COPPER DEPOSIT IN THE HAGEN FJORD AREA...

The sediment-hosted workshop identified that while a large area in North Greenland is prospective for copper mineralisation, the ARC region has the best prospectivity (268). Greenfields notes that despite the use of a deposit model framework, the workshop correctly included the basaltic copper in its assessment (268).

The workshop participants concluded that for the Hagen Fjord area there is a 10% probability of two¹³³ undiscovered copper deposits, and 1% chance of six¹³⁴ undiscovered deposits (268). Of the eight respondents, two opined that there is a 50% chance of containing a copper deposit in the Hagen Fjord area (268). No estimate was given for the quantity of undiscovered metal, however, the area ranks second in all of Greenland after the Company's Frontier project (147).

The 2012 magmatic nickel workshop considered Zig-Zag Fm (269; 146). The participants accounted for a break in the olivine control on the nickel distribution within the sulphur undersaturated basalt (269). With no commercial field evaluation, and only very sparse Government/academic work on the nickel potential of the region, the workshop ranked the area poorly against other tracts in Greenland that contain unambiguous indications of nickel sulphides¹³⁵. Greenfields believes that the lack of data rather than missing components of a mineral system understated the potential.

¹³⁰ The 1979 geomagnetic field program occurred between 20 June and 16 August (267).

¹³¹ Now called the Mineral Resources Authority

¹³² A combined entity that supersedes the Greenland Geological Survey

¹³³ Within a range of zero to three deposits.

¹³⁴ Within a range of four to eight copper deposits.

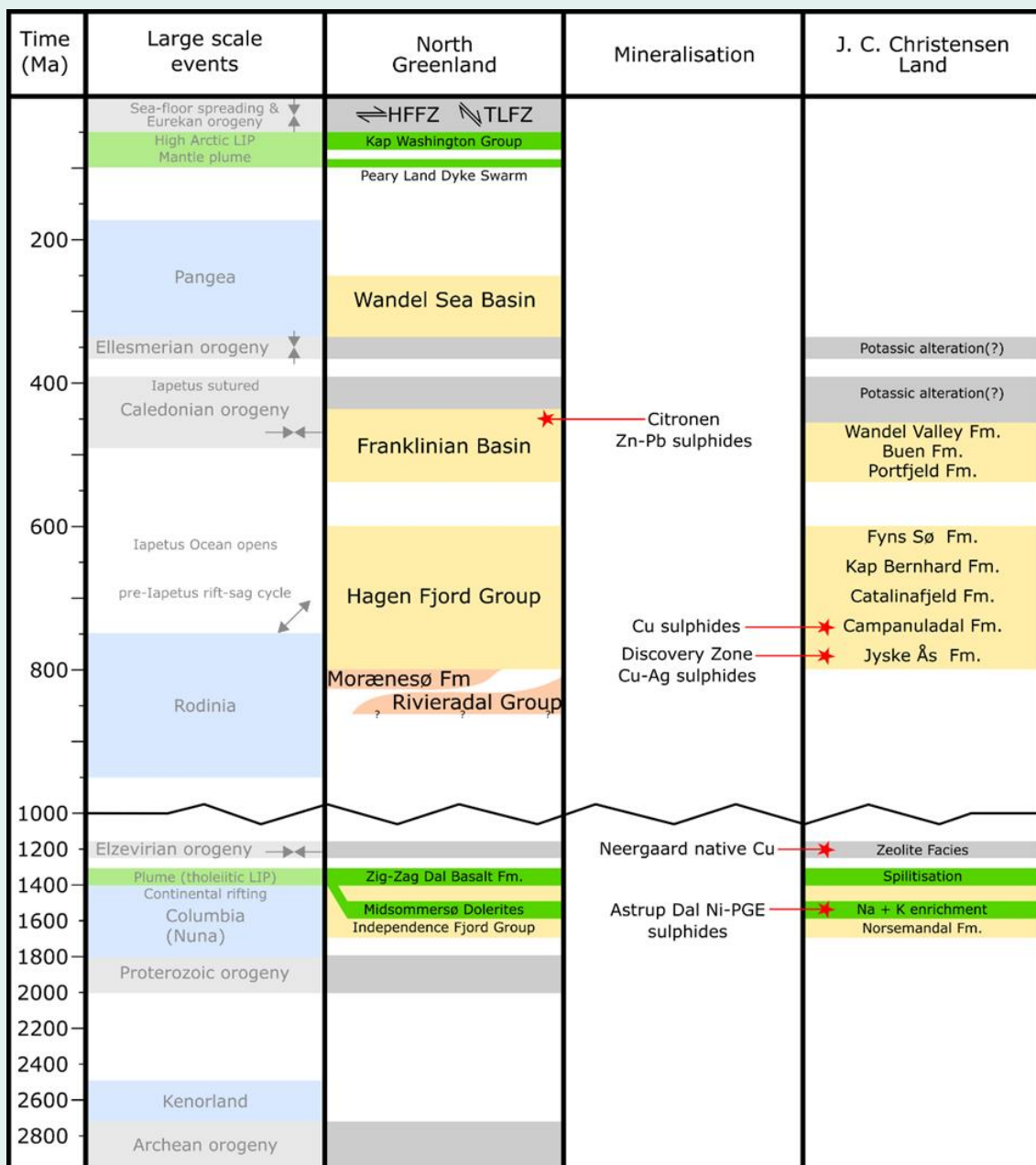
¹³⁵ The highest ranked nickel sulphide tracts are those linked to the passage of the Icelandic hotspot, which is common to ARC.

7 MINERALISATION

North Greenland contains multiple indications of mineralisation. Copper is the primary target commodity in this Report; however, the region includes a large zinc deposit (Citronen) and clues of nickel-platinum group elements within the ARC licence. The known mineralisation occurs across a range of stratigraphic positions (Figure 58) and is the result of more than one mineralising event (summarised in Figure 59).

The following sections cover the known copper and nickel occurrences within ARC and present the analogous 'deposit models'. Following this, the mineral systems approach is used to characterise and understand the interactions between regional- and local-scale features, and how they result in mineralisation. Effectively, the layout presents what ARC is known to contain, its analogies, and Greenfields understanding of the system that formed the mineralisation.

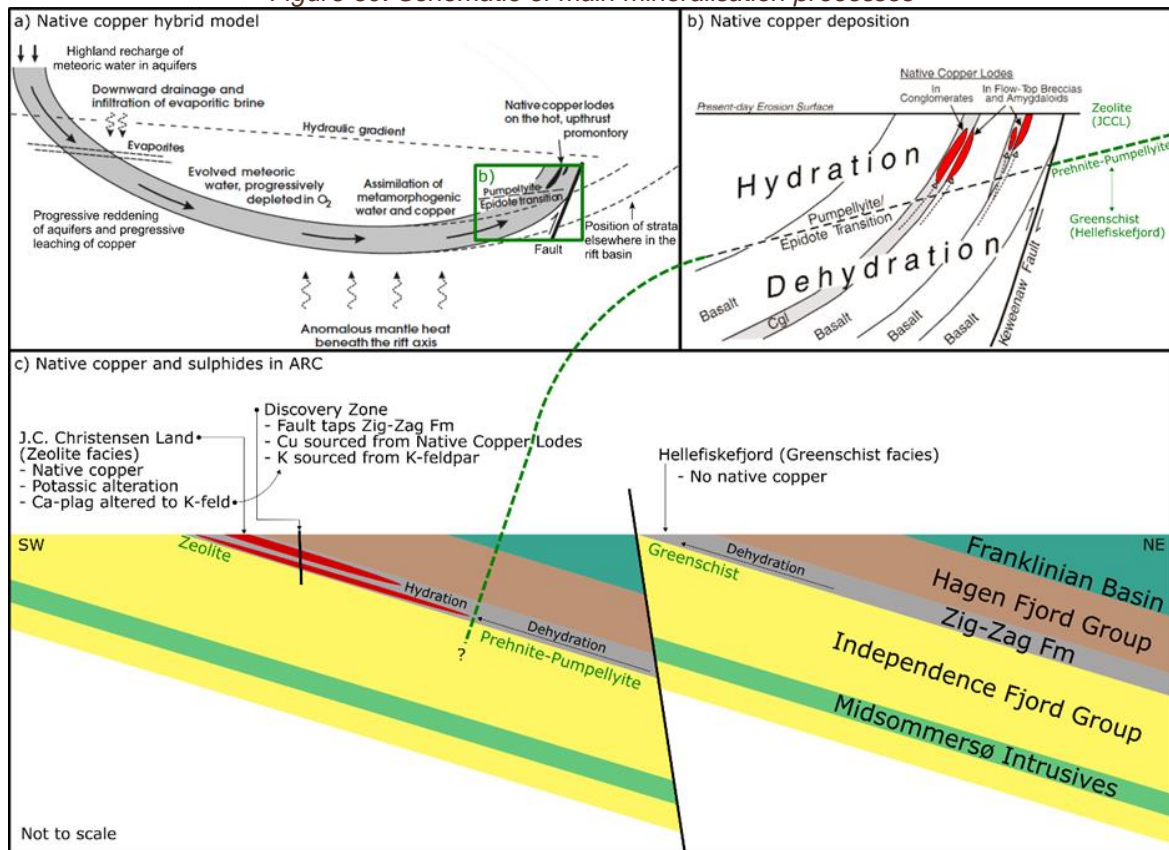
Figure 58: Time-space plot of the known mineralisation in North Greenland



Source: Greenfields.



Figure 59: Schematic of main mineralisation processes



Source: Greenfields based on elements from Brown (2008) (270). Note: a) The Basaltic copper hybrid genetic model by Brown (2006; 2009) (246; 270) with green text added by Greenfields highlighting comparisons to North Greenland, i.e. Zig-Zag Fm basalts metamorphosed to zeolite facies at J.C. Christensen Land and to greenschist facies at Hellefiskefjord. b) A schematic cross-section of gently dipping stratigraphy in North Greenland. The Zeolite to Prehnite-Pumpellyite facies transition in North Greenland is interpreted by Greenfields to be within ARC downdip from the exposed Zig-Zag Fm. Greenfields considers that the Zig-Zag Fm is the significant source of copper and potassium for the mineralised and altered fault-related copper sulphides in the Discovery Zone – a high grade copper sulphide prospect.

There are essentially two approaches to exploration targeting, one based on deposit models, and the other based on a systemic approach (271; 272). Deposit models are highly prescriptive stereotypes that are easy to apply (272). However, it is easy to draw incorrect conclusions from stereotypical shortcuts (272). Conversely, the mineral systems approach is holistic, but many consider it to be challenging to apply in practice (271). Greenfields uses the mineral systems approach in a holistic, commodity agnostic manner¹³⁶. Due to the scale of the area which the Company targets, implementation of the mineral system approach is relatively easy. This approach is important in understanding why the Company selected ARC for its exploration efforts.

¹³⁶ Greenfields considers the removal of commodity targeting as a vital step in the systems approach to targeting, for the moment that a commodity is applied in the targeting process, it invariably invokes the use of deposit model analogues. The Company considers that only once a system has been identified it is appropriate to start considering which metals may be concentrated through empirical evidence. Deposit models are only used by the company for the ease of conveying concepts.

7.1 KNOWN PROSPECTS

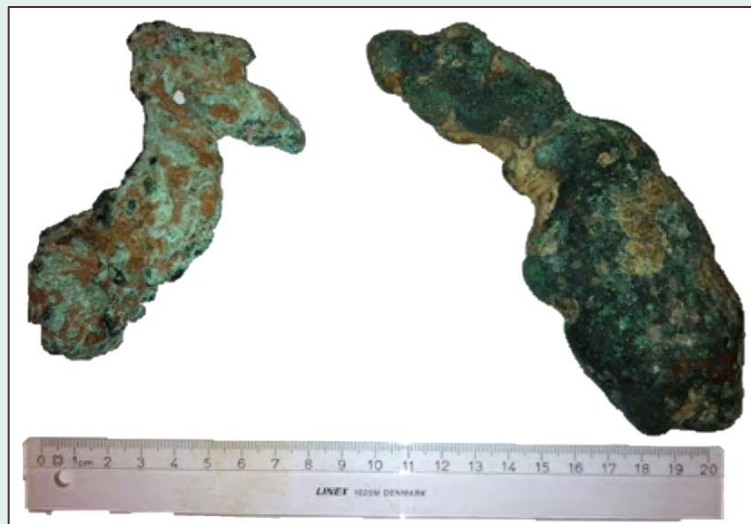
ARC is at an early stage of exploration, and there are only a handful of named prospects. The Discovery Zone delineated in 2010 is the most advanced, although promising areas occur elsewhere within the licence and are only referred to by their geographical location.

7.1.1 Copper

7.1.1.1 Zig-Zag Fm

Native copper float frequently occurs near the Zig-Zag Fm in the area around the Discovery Zone (2). The prior commercially oriented work considered the mineralisation “*not to be of economic importance*”¹³⁷ (3), an opinion not shared by Greenfields. Outside of ARC a 1.5 m long chip sample returned an economically significant grade of 1.97% Cu, and a grab sample returned 3.17% Cu from chalcocite filled vesicles (128). The Company considers the widespread occurrence of low-grade copper mineralisation, the frequent presence of sizeable native copper lumps, and the sampled grades to be very commercially significant.

Figure 60: Large native copper specimens from ARC



Source: Rehnström (2012) (3). Note: the sample on the right weighs around 1 kg.

7.1.1.2 Discovery Zone

The copper-silver bearing Discovery Zone is located at the northern end of Neergaard Dal, at approximately 81.953° N, 26.221° W. (Figure 61) The Discovery Zone was identified in 2010 as a follow up to a geochemical anomaly identified the Greenland Geological Survey in 1994 (3). The Discovery Zone is comprised of at least three parallel breccia faults trending northwest-southeast (2), with the furthest faults being around 2 km apart. The faults are traced for a minimum of 2 km along strike before they disappear underneath moraine (3). The Discovery Zone is open in both directions (3). The width of the fault breccias is variable, ranging from 1 to 25 m thick (2). The host lithology is red sandstones of the lower Jyske Ås Fm (3; 2), and they are proximal to outcrops of Zig-Zag Fm. The breccias contain extensive potassic alteration minerals that indicated mineralising fluids passed through the faults at temperatures around 150 °C¹³⁸ (3). The breccias have copper sulphide and copper oxide mineralisation. The copper-bearing species include chalcocite, brochantite, bornite, chalcopyrite, and malachite (3; 2). The mineralisation is expressed in two main forms, within which there are two sub-forms (Figure 62):

**A HEAVILY
MALACHITE-STAINED
QUARTZITE FLOAT
SAMPLE HAS A GRADE
OF 53.8% CU AND
2,480 G/T AG**

¹³⁷ Much of the commercial focus was on horizons using a sediment-hosted deposit model.

¹³⁸ 150°C in the sediments is estimated from pyrobitumen reflectance (3).



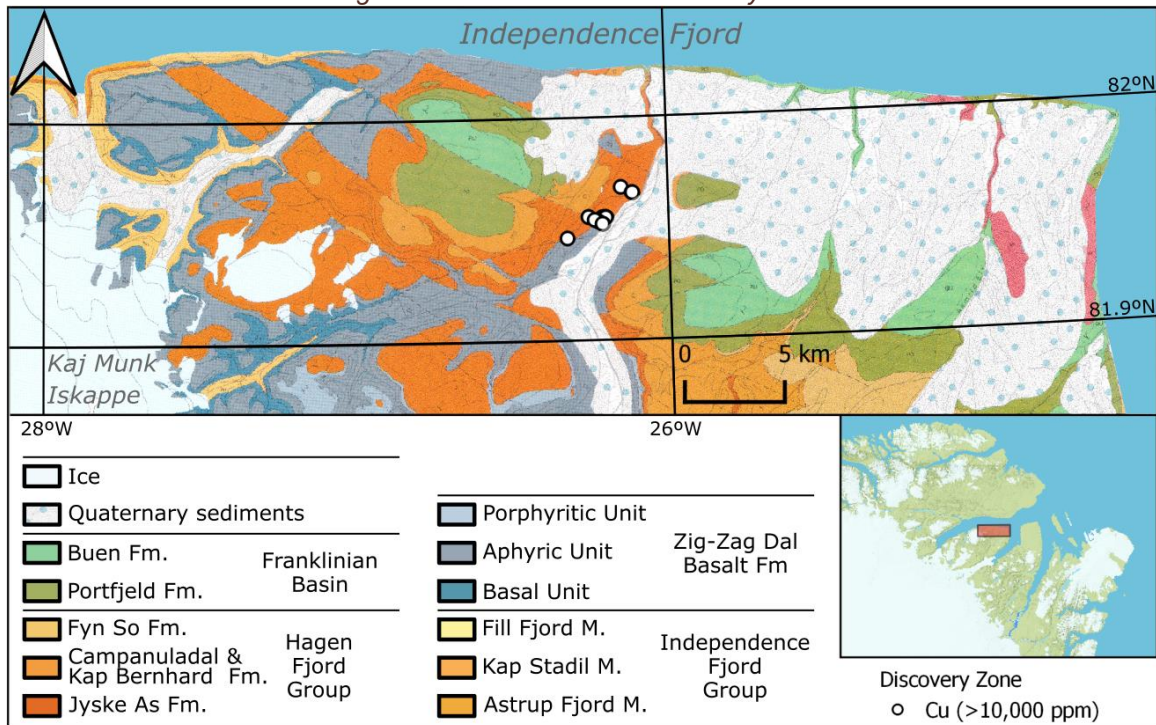
1. **Breccia bound.** Mineralisation occurs in thin quartz-dominated veining within the fault breccia and contains disseminated copper sulphides (Figure 63). Assay from this material grades up to 53.8% Cu and 3,480 g/t Ag (3).

Within the breccia-bound mineralisation are intensely potassic, unconsolidated materials known as 'Black Earth' (Figure 64) (2). The multiple but discontinuous 0.7 to 3 m horizons have lengths between 2 to 50 m (3). The Black Earth material contains remarkably high copper and silver grades, with reported true widths of 4.5 m grading 2.15% Cu and 35.5 g/t Ag (3). XRD analysis of a single Black Earth sample showed that it is highly potassic¹³⁹. The alteration includes microcline, a potassic feldspar that associates with the intense native copper mineralisation in the Michigan basalts¹⁴⁰ (273; 214).

2. **Stratiform.** This mineralisation occurs immediately adjacent to the faults and comprises lenses and blebs of chalcocite and bornite measuring from mm-scale to 15 cm long (Figure 65).

Within the stratiform mineralisation is a poorly consolidated sandstone that is identified as a potentially vast target horizon within the Jyske Ås Fm (2). The outcrop shows pervasive interstitial chalcocite, bornite and chalcopyrite (Figure 66) (3).

Figure 61: Location of the Discovery Zone



Source: Greenfields using public domain data.

¹³⁹ Muscovite and microcline accounting for 39% of the mass (3). The quartz, from the host sandstone, accounts for 40% of the mass (3). The balance comprises chlorite (13%) and brochantite, a mineral containing 56.2% Cu (3; 383).

¹⁴⁰ Abundant microcline is associated with the Keweenaw Peninsula. The smaller Baltic and Isle Royal areas contain little to no microcline, and are instead contain abundant sericite (273). Sericite alteration also negatively correlates with copper mineralisation at the Olympic Dam deposit (318).

Figure 62: Mineralisation types of the Discovery Zone



Source: Haugaard (2011) (2).

Figure 63: Breccia bound copper mineralisation



Source: Haugaard (2011) (2).



Figure 64: 'Black Earth' copper mineralisation



Source: Haugaard (2011) (2).

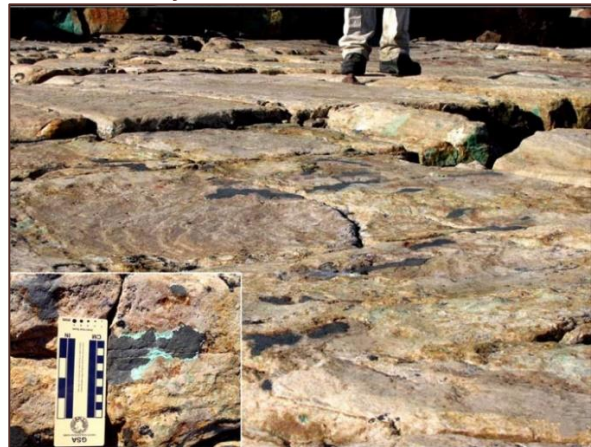


Source: Haugaard (2011) (2).

Figure 65: Stratiform mineralisation in the Jyske Ås Fm



Source: Haugaard (2011) (2). Note: Green minerals are primarily malachite.



Source: Haugaard (2011) (2). Note: Dark minerals are mostly chalcocite, although bornite is present as well.

Figure 66: Stratiform copper mineralisation (pervasive) in the poorly consolidated Jyske Ås layer



Source: Haugaard (2011) (2). Note: The white arrows denote chalcopyrite, and the red arrows show bornite with chalcocite rims. This sample had a grade of 0.74% Cu and 16 g/t Ag, although similar material returned grades of 2.35% Cu and 59 g/t Ag (2).

7.1.1.3 Campanuladal Fm

The Campanuladal Fm also is a theoretical metal deposition site given the reduced nature of the beds and the decreased permeability (2). The Campanuladal Fm was known to contain anomalous copper since the late 1970s (261; 244). Government work in the early 1990s managed to trace chalcopyrite and galena for several kilometres within the central part of the formation (274). The Campanuladal Fm consists of variegated greenish, fine- to medium-grained sandstones and shaley siltstones representing a transition from tidal to offshore conditions (Figure 67) (128). Disseminated copper sulphides (often chalcopyrite) are widespread, and one such location is close to the Discovery Zone in the northeast corner of ARC (3). Outside of the Project area, the Campanuladal Fm is known to contain lead anomalies in the form of galena (Figure 68) (128). However, due to a lack of evidence, Greenfields does not consider the area in the vicinity of ARC to be particularly prospective for lead and instead, notes its presence as support of a broader mineralisation event.

LATERALLY
EXTENSIVE
FLUID FLOW

Figure 67: Reduced and oxidised beds of the Campanuladal Fm



Source: Rehnström (2012) (3).

Figure 68: Galena in a Campanuladal Fm sample



Source: Tukianen (2011) (128). Note: the galena is about 1cm long.

7.1.2 Nickel

7.1.2.1 Midsommersø Intrusions

Greenfields considers the mafic intrusions of the Midsommersø Intrusions to be prospective for magmatic-hosted nickel-copper-platinum group element ('Ni-PGE') mineralisation¹⁴¹. The Company identifies supportive evidence in both the intrusions and their extrusive equivalents in the overlying Zig-Zag Fm.

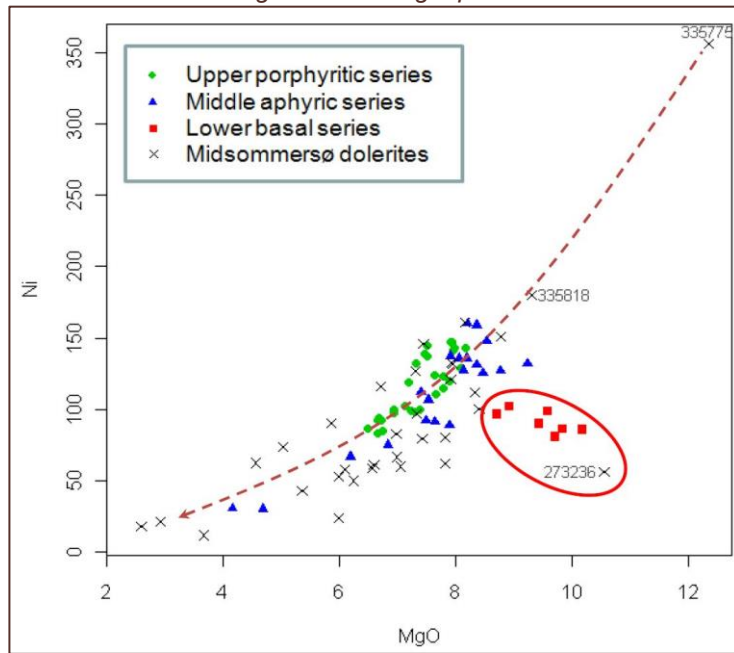
Rift settings are prospective for nickel-sulphide mineralisation, and in particular mantle plumes and LIPs (275). Ni-PGE sulphide mineralisation in proximity to rift-related native iron is known to occur in the Upper Michigan Peninsula (276). Nickel sulphide deposits are associated with primitive mantle plume magmas (275). Greenfields considers Midsommersø Intrusives to be 'upstream' and the Zig-Zag Fm flows to be 'downstream' of a LIP system. The basal flows of the Zig-Zag Fm flood source from a primitive magma, with the overlying flows coming from an increasingly evolved source (221). These basal flows also have a Ni:MgO profile that is inconsistent with a silicate (olivine) line of control (Figure 69) (269). Such depletion is associated with crustal contamination and nickel sulphide formation (275).

¹⁴¹ The main purpose of this document is to demonstrate the copper potential, consequently a mineral system discussion on Ni-PGE is not presented. However, there are key commonalities between the sedimentary-system and magmatic systems, namely: "locating in rifted environments, where voluminous mafic or ultramafic rocks were emplaced into sedimentary basins containing abundant sulphur-bearing rocks" (275).



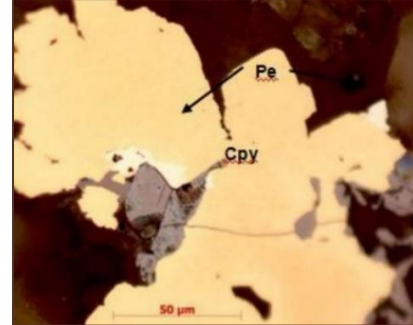
As such, the search space for nickel-sulphide mineralisation is earlier/upstream into the magmatic system¹⁴².

Figure 69: Ni:MgO plot



Source: Rosa et al. (2013) (269). Note: Lower basal series (red points and oval) depart from the silicate (olivine) fractionation curve indicating possible 'upstream' separation of Ni into an immiscible phase.

Figure 70: Astrup Dal pentlandite



Source: Tukianen & Lind (2011) (128).

Note: Pe stands for pentlandite, and Cpy for chalcopyrite.

Dolerite sills in Astrup Valley¹⁴³ contain minor amounts of the nickel-bearing mineral pentlandite (128 p. 17), (Figure 70), and contain PGE anomalies¹⁴⁴ (3). The basal portion of a 60 m sill has metre sized pockets of gabbroic pegmatites¹⁴⁵ (128 p. 16). Taxites¹⁴⁶ at a sill margin demonstrate the solidification of high volatile content from initially dry magmas and associate with Ni- PGE sulphide deposits¹⁴⁷ (275). The taxites at Astrup Valley are visually distinctive as they have copper-oxide¹⁴⁸ coatings (128), which highlights the metal-bearing nature of the volatile fluids. Chalcopyrite frequently occurs in many of the Independence Fjord Group stream sediment-samples (261). Chalcopyrite mineralisation occurs in several places near dolerite intrusions (261)¹⁴⁹.

¹⁴² This could be elsewhere in the extrusive lavas, or within the stratigraphically deeper intrusive dolerites.

¹⁴³ It is located at approximately 81.683°N, 30.146°W. Note that the 2011 Avannaq (3) expedition failed to locate the site that had been sampled in 1978 and 1994 and as such, the location must be interpreted as guidance.

¹⁴⁴ 0.13% Cu, 113 ppb Au, 227 ppb Pt and 40 ppb Pd (128 p. 16).

¹⁴⁵ Such gabbroic pegmatite units are also called taxites or vari-textured rocks (275).

¹⁴⁶ Taxites are distinctive pegmatoidal mafic units within intrusions otherwise dominated by dry cumulus assemblages (275).

¹⁴⁷ According to Barnes & Robertson (2019): "A high proportion of mineralised systems, including those in the super-giant Noril'sk- Talnakh camp, are formed in small conduit intrusions where assimilation of country rock has played a major role. Evidence of this process is reflected in the common association of sulfides with varitextured contaminated host rocks containing xenoliths in varying stages of assimilation" (396).

¹⁴⁸ Malachite and azurite (128).

¹⁴⁹ It appears that prior researchers did not focus on the magmatic mineralisation potential, and instead discuss the potential for sedimentary-hosted copper. There is scant mention in the North Greenland literature on nickel prospectivity.

The presence of native iron within the Zig-Zag Fm¹⁵⁰ supports the intrusion-related nickel potential (260). Terrestrial native iron is unusual because it tends to oxidise (277). The most prominent example of large deposits of native iron is on Disko Island, in West Greenland (278). At Disko Island, the iron is associated with TiO₂-rich basalts (titanomagnetite being present in the North Greenland basalts), magma sediment-contamination, and layering within the sub-volcanic plumbing. Disko Island is known to contain 22 t boulders of native iron, as well as boulders of conduit-related massive nickel-sulphide up to 25 t (146). In the Siberian Traps and near the world-class Noril'sk–Talnakh Nickel-PGE deposits, native iron is associated with high concentrations of Cu, Ni, Co, Pt, Pd, Rh and Ge (277). The Siberian Trap iron formation is similar to the processes of the Skaergaard intrusion in East Greenland (277). Siberian native iron is associated with granophyres (277). While the extent of native iron in North Greenland is virtually unknown, its presence is positively correlated with Ni-PGE sulphide mineralisation.

The 'missing' nickel in the lava combined with the appearance of pentlandite in the underlying dolerites reinforces that ARC is prospective for magmatic nickel. The unusual identification of native iron may also be indicative of nickel mineralisation, although its location within the unintruded flood basalts is perplexing¹⁵¹. While the exposure in Astrup Valley is a known prospect, future fieldwork may yield similar opportunities.

THE 'MISSING'
NICKEL MAY HAVE
CONCENTRATED
INTO A DEPOSIT

7.2 DEPOSIT TYPE

While Greenfields does not use deposit models, the NI43-101 format requires the discussion of deposit model types (10). Within the prescriptive deposits model framework, the known mineralisation within ARC can be ascribed to two distinctly different deposit types:

- **Sediment-hosted stratiform copper** deposit models ('sediment-hosted'). Within this family of deposit types, ARC is analogous to the world-class Katangan Basin ('Copperbelt') (279) and the substantial White Pine-Presque Isle ('White Pine') deposit model (268); and
- **Basaltic native copper**, a comparatively unknown deposit model (268) that is closely associated but segregated from the White Pine model (280).

While ARC contains mineralisation that can be classified into three¹⁵² deposit model types, it concerns a single mineral system. Compared to basaltic copper, sediment-hosted copper deposits are well known. Consequently, this Report does not address the specifics of sediment-hosted copper but does elaborate on the basaltic model in section 5.

¹⁵⁰ Sample GGU270372 is located at 81.90472°N, -27.13139°W (260). This location is close to a plateau showing an anomalously high number of dark circular features. It is plausible that they may reflect escape vents in the underlying basalts. Using the known strata dip of 1-2°, and a lateral distance of 9 km, the depth of a hypothetical vent to the peak geophysical response is around 100m to 200m below surface (it could be less). This depth is consistent with a maximum 500 m thickness of the Jyske Ås Fm. The location of a fluid vent at this locality would explain why native iron appears in an unnamed valley to the northeast of the vent and is not observed elsewhere in North Greenland. Greenfields cautions that geographical features must be treated with caution and that this 'working' theory is contingent on strata concordant fluid flow.

¹⁵¹ Due to the paucity of data on the native iron, it is not possible to ascribe its presence to magmatic or hydrothermal processes, or human error. Given its understanding of the information reviewed, Greenfields prefers a hydrothermal explanation but cannot discount a magmatic Ni-PGE.

¹⁵² Due to geochemical profiles and hydrothermal alteration, it is also possible to include elements of an Iron Oxide Copper Gold ('IOCG') deposit model. However, this deposit model does not appear in the existing literature on North Greenland (west of Victoria Fjord) and is associated with a much hotter system. As inclusion of commentary on IOCGs may lead to confusion with those used to dealing with deposit models rather than mineral systems, it is not presented in the main body of the text to improve clarity of communication.



7.2.1 Sediment-hosted stratiform copper

Commercial targeting within the ARC project has previously been for sediment-hosted copper (279; 3; 2). This family of models typically comprise of relatively thin (3 to 30 m thick) copper-sulphide zones located in a wide variety of rock types of varying ages (268). The shape of sediment-hosted deposits is equally variable, ranging from extreme sheet-like dimensions to more constrained tabular, and roll-front geometries (268). These deposit types display different styles of mineralisation and alteration types (281). Such deposit models account for a large proportion of the world's highest quality mineral deposits (282), due to their potential favourable size and grade combinations. Despite their immense value, sediment-hosted copper deposit models are poorly researched and understood relative to other deposit types (283).

Mention of the sediment-hosted deposit model usually results in comparisons to the 'supergiant' Katangan (Copperbelt) and Zechstein (European Kupferschiefer) deposit models, which are the largest and richest of the known archetypes (284). Of these two type-examples of the 'reduced-facies' deposit model, Greenfields feels that ARC has most in common with the Katangan Basin due to its similarly aged host rocks¹⁵³, tectonic setting, and lithologies¹⁵⁴. These qualities also correlate with the Neoproterozoic-aged component of Greenfields' Frontier project¹⁵⁵ in northeastern Greenland (151). While challenging to demonstrate, the Frontier and ARC projects contain equivalent sediment units (151). Sediment-hosted systems may contain more than one commodity type (e.g. copper deposits, zinc deposits); however, one commodity type usually dominates (282). The Kipushi zinc deposit in the Katangan Basin is an example of an addition, but non-dominant commodity type. Greenfields considers that the ARC project is part of an extensive system similarly that encapsulates the Citronen zinc deposit

The White Pine sediment-hosted deposit¹⁵⁶ model, located in Michigan, USA, is also applicable. This model includes chalcocite as the dominant economic mineral and native copper as a secondary occurrence (285). Similarities between White Pine and ARC are the silver co-commodity; the prevalence of chalcocite; and a close relationship with haematite, and widespread copper in stream sediments (253; 286). The White Pine deposit model also incorporates a similar Mesoproterozoic-aged rift (~1,100 Ma (287)) containing mineralised flood basalts (288).

SEDIMENT-HOSTED AND BASALTIC COPPER MODELS

7.2.2 Basaltic copper

Basaltic native copper¹⁵⁷ deposits occur around the world, however documentation of the American and Canadian deposits is most readily available (e.g. Keweenaw, Michigan; Kennecott, Alaska; Sustut, British Columbia) (286). Of the historical native copper districts, the Keweenaw Peninsula dominates the literature and production statistics are available (288).

The Keweenaw Peninsula had a pre-mining endowment of 8.9 Mt of native copper, of which 6.5 Mt was mined (288; 285). The area was subject to extensive¹⁵⁸ prehistoric mining as early as 7000 BCE¹⁵⁹ but had its heyday between 1845 to 1939¹⁶⁰(Figure 72) (289; 290). A copper-rush started

¹⁵³ It is important to note that while the Katangan Basin in Zambia contains Neoproterozoic-aged sedimentary rocks, both types of known mineralisation are distinctly Cambrian-aged, at c. 540 Ma to 490 Ma (387).

¹⁵⁴ Much emphasis is placed on source rock ages in deposit models, however the age of the mineralisation is different to that of the host rock, making the latter a weak predictor.

¹⁵⁵ For further information, see Bell & Saleem (2018) (376).

¹⁵⁶ The original White Pine mine operated between 1953 and 1966 and produced 180 Mt of material grading 1.14% Cu and 7.7 g/t Ag (253).

¹⁵⁷ Native copper can be formed from primary (magmatic), serpentinisation ultramafic rocks, supergene enrichment, or hydrothermal fluids (381). Serpentinisation is not reported within ARC, and supergene enrichment is not likely

¹⁵⁸ An astounding 680,000 t of copper metal is estimated to have been mined during pre-historic times (290). The ancient miners are estimated to have developed around 5,000 excavations that included up to 5 m deep shafts and minor lateral development (290).

¹⁵⁹ Before the Current Era.

¹⁶⁰ Mining of the spatially related White Pine sediment-hosted deposit occurred between 1953 and 1996 (253).

at Keweenaw Peninsula in the 1840s when prospectors discovered and mined high-grade vertical ‘fissure veins’ that crosscut the stratigraphy. These fissure deposits contained native copper, chalcocite and native silver (285; 288). They are also known for their massive native copper boulders weighing more than 500 t¹⁶¹ (see Figure 73 to Figure 76) (291; 292). Later, commercial-scale operations mined the stratiform deposits below. Despite the early focus on the vertical fissure-hosted deposits, 98% of the district’s copper production came from the stratiform mineralisation (288). The stratiform mineralisation was mined to at least 1.6 km below surface (293).

While the Keweenaw Peninsula is notable for its native copper, the sulphidic sediment-hosted mineralisation is significant. The known endowment of the copper sulphide mineralisation is around 4.5 Mt Cu, contained in two deposits (288). The copper sulphide deposits contain substantial amounts of silver, with the White Pine deposit having yielded 50 million ounces of silver as part of the 2.0 Mt of copper that was mined (288). The White Pine mine was in production between 1953 and 1996 (294). The remaining White Pine mineralisation is subject to current economic evaluation and the Copperwood copper-sulphide deposit is construction ready (295; 296; 297).

A PRE-MINING
ENDOWMENT OF AT
LEAST 8.9 MT OF
COPPER

In the Keweenawan native-copper mines, a positive relationship exists between the presence of the potassic feldspar polymorph microcline and copper grade (273). Secondary microcline originates from a low to moderate temperature fluid (273). During microcline’s formation, it incorporated iron which imparts a ‘brick-red’ colour to the feldspar (273). A microcline and sericite zonation occurs, with increasing sericite correlating with decreasing copper at some mines (273). In the paragenesis of the Keweenaw native copper mineralisation, microcline is an early phase before prehnite and copper precipitation (285).

The stratiform native copper mines are in the Portage Lake Volcanics (‘PLV’), a mid-continental rift tholeiitic lava flow sequence (288). The PLV is a sequence of subaerial basaltic, and intermediate lava flows with intravolcanic sediments (246). The stratiform deposits contain native copper in amygdaloidal basalt, flow top breccias, and intravolcanic conglomerates and dolomites (246; 288). The intravolcanic clastic units make up less than 5% of the volume of the PLV, but account for ~40% of the district’s copper production (288). The sequence records metamorphic grades between zeolite to prehnite-pumpellyite facies (246). Hot fluids preferentially channelled into permeable lava flows, leaving some unaltered (298). The altered flows contain the native copper (298).

The basaltic copper deposit model is similar to the sediment-hosted deposit model in terms of tectonic settings, depositional environment, fluid pressure and temperature, and consequently, the two have a close spatial association (246). However, the models deviate in that the fluid composition before deposition, with basaltic copper involving sulphur poor, reduced fluids whereas sediment-hosted copper draws on oxidised, sulphur bearing fluids. The difference in the fluid is reflected by the deposited mineral species, with basaltic copper dominated native copper or low-sulphur minerals such as chalcocite (246; 298). The incumbent theory is that reduced mineralising fluids originate from burial metamorphism and are mobilised by the compressive forces from a distal orogenic event¹⁶² (298; 299; 300). The more recent hybrid model contends that both meteoric and metamorphic fluids are involved and that copper comes from sedimentary units as well as metamorphosed basalts (Figure 71) (e.g. (246; 298; 301; 288)). The mineralised fluid

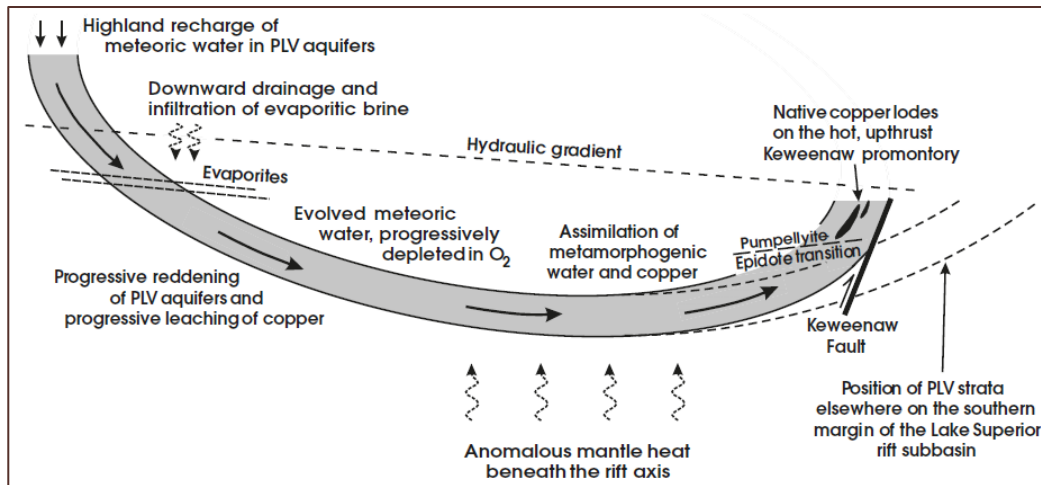
¹⁶¹ For comparison to a large modern mine with a grade of 0.5% Cu, this equates to nearly 100,000 t of mineralised rock which has to undergo processing before reaching a comparable state to the massive copper specimens.

¹⁶² The mobilisation of the fluids is linked to compression created by the Grenville Orogen (246; 300).



focused along flow-top breccias and intravolcanic sediments (299). At the time of mineralisation, the fluid was slightly reduced and precipitated native copper above the epidote-pumpellyite transition, although the meteoric fluids were initially oxidised¹⁶³ (246; 301).

Figure 71: Hybrid metamorphic-meteoric brine model of native copper deposition



Source: Brown (2008) (270).

Greenfields sees comparisons between the Keweenaw Peninsula and the ARC project:

- The PLV and Zig-Zag Fm basalt are metamorphosed to zeolite facies, host native copper in voids; have secondary mineral assemblages of feldspar, calcite, quartz, pumpellyite, prehnite, zeolite, and sericite; and show a positive association with microcline;
- Both contain vertical features hosting high-grade copper mineralisation that crosscut the basalt flows, namely the Keweenaw Peninsula's fissure vein deposits and ARC's Discovery Zone¹⁶⁴;
- The PLV and Zig-Zag Fm have intravolcanic sedimentary rocks. The PLV intravolcanic units are highly-endowed however little is known about ARC's intravolcanic sediments; and
- Both contain sulphidic, sediment-hosted copper mineralisation above the native copper bearing basalts.

¹⁶³ Although two competing 'deposit models' exist for the Keweenaw Peninsula native copper deposits and the White Pine copper-silver deposits, they are part of the same mineral system (246). While they are separated geographically by approximately 100 km, the White Pine deposits sit only 700 to 1,600 m stratigraphically above the mineralised PLV basalts (246). For the White Pine genetic model, the underlying volcanics are a source of copper (406), although they may have formed at the same time (380). The White Pine deposit model also incorporates saline meteoric fluids as a mechanism for transporting metals (246). Greenfields highlights that under a unified mineral system perspective, the meteoric component of White Pine provides empirical support to the 'hybrid' model used to explain the native copper. Age differences between deposits can be explained by a hiatus in the hydrodynamic system.

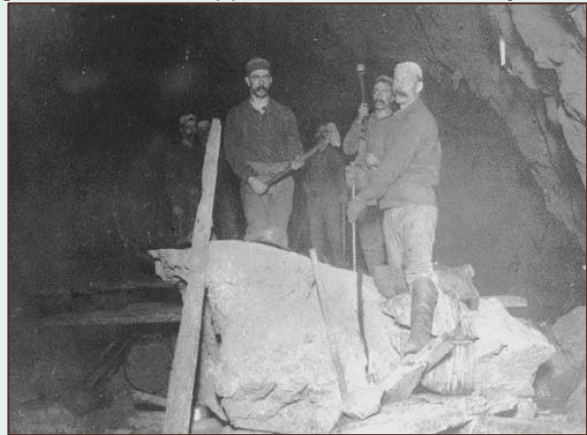
¹⁶⁴ The copper clasts discovered by Avanna were extracted from an in situ position the Jyske Ås sedimentary rocks, but are thought to have come from the basalts (2).

Figure 72: Depiction of ancient mining activity at Lake Superior



Source: Baldwin (2014) (290).

Figure 73: Native copper boulder from Quincy 2 Shaft



Source: MSA (2020) (291). Note: The miners are standing on the remains of a 270 t native copper sample. Due to physical constraints in the mines, the large samples were broken into manageable sized pieces. The photo is from ~1912.

Figure 74: Massive native copper protrusion, Quincy 2 Shaft, Michigan



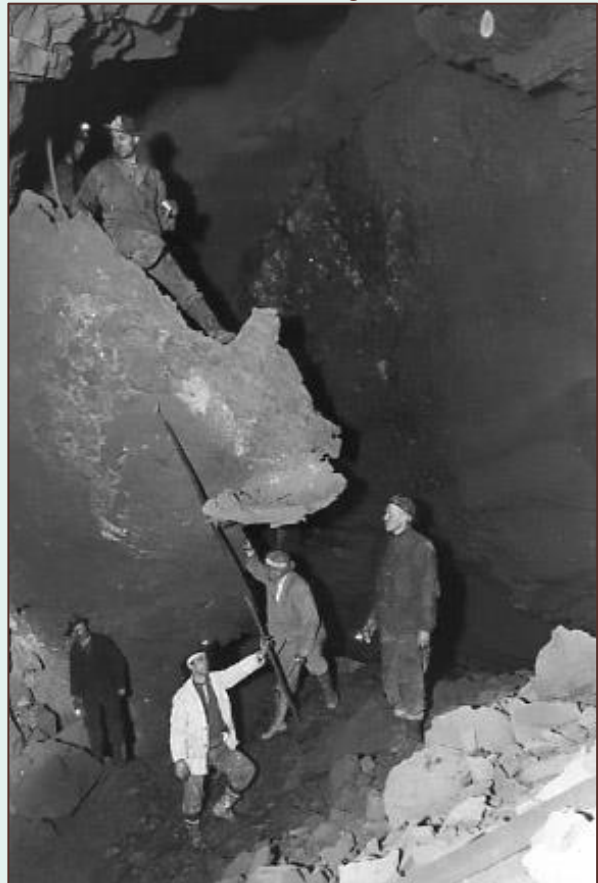
Source: VOP (2020) (302). Note: Native copper is hanging from the wall of the mine. Specimens of this size were the largest that could be handled without being broken into smaller masses. The photo is from 1900.

Figure 75: Massive native copper in the Calumet mine, Michigan



Source: VOP (2020) (302). Note: Native copper is hanging from the wall of the mine. The photo is from 1900.

Figure 76: Massive native copper from an unspecified mine, Michigan



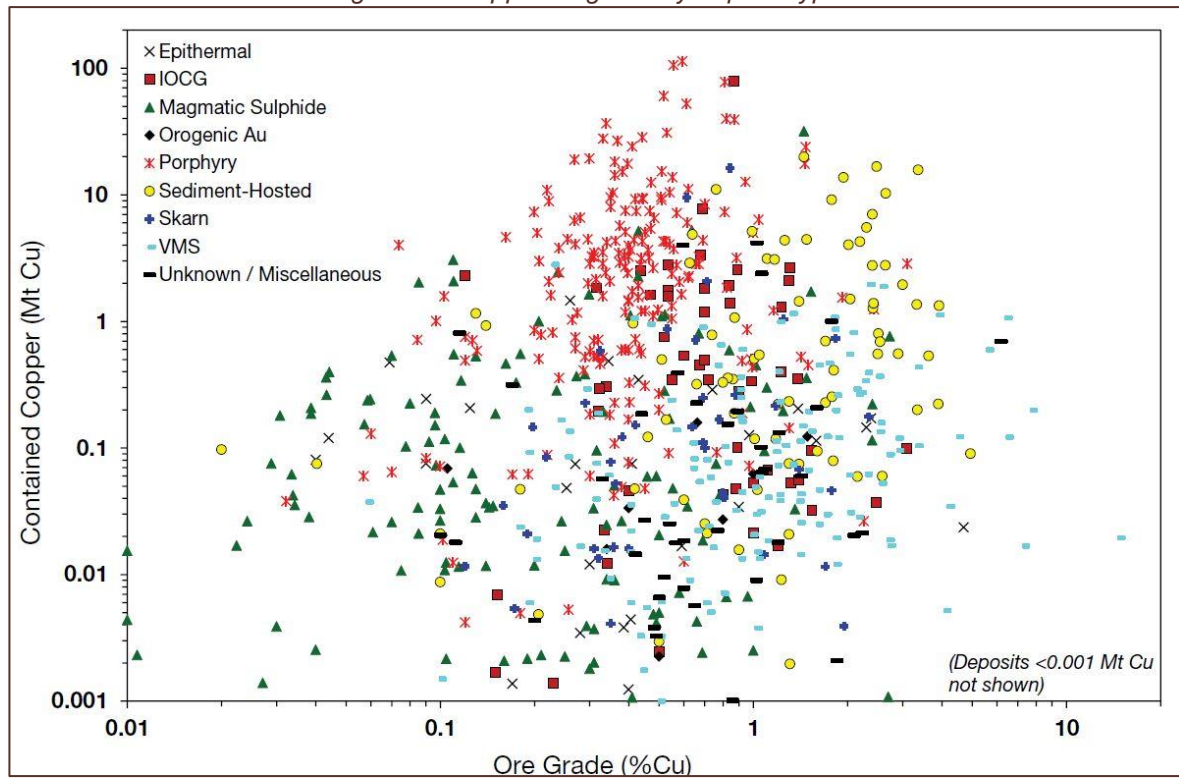
Source: VOP (2020) (302). Note: The source caption is 'largest mass copper', but no further detail is provided.



7.2.3 Endowment proxy

Deposit models are associated with estimates of tonnage and grade. Sediment-hosted deposits have favourable size and quality (Figure 77) (303).

Figure 77: Copper vs grade by deposit types



Source: Mudd et al. (2013) (303).

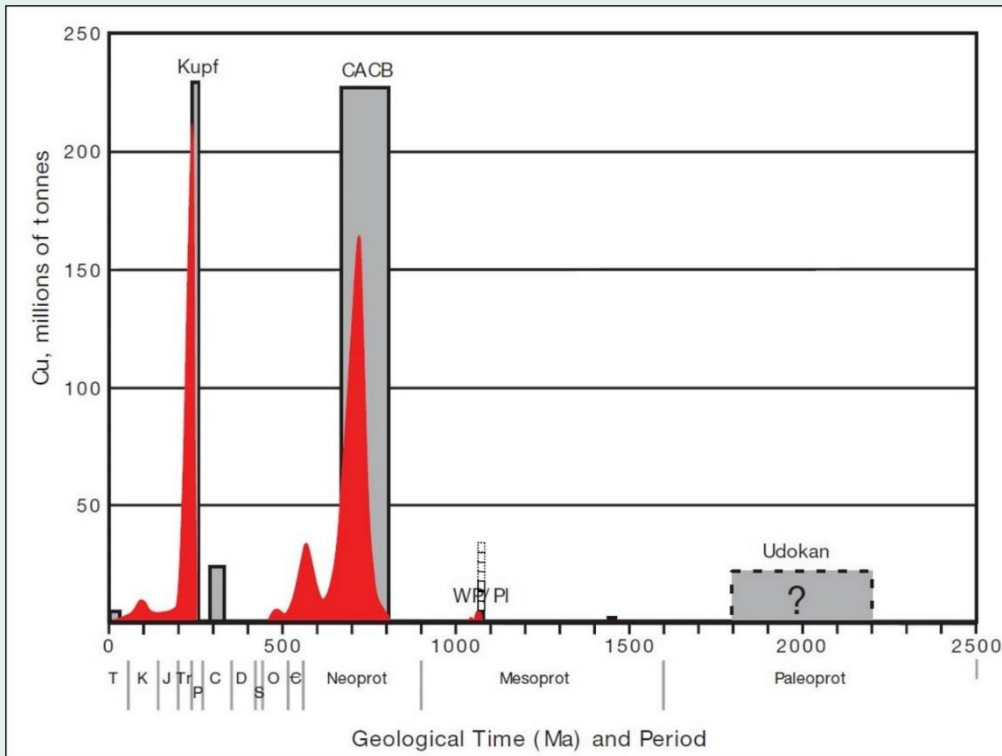
Like all stereotypes, deposit models suffer from classification error. Greenfields highlights that the basaltic native copper and stratiform sediment-hosted deposits of Michigan are the same mineral system. However, based on its host lithology, the basalt-hosted mineralisation is often excluded from the total metal attributed to the White Pine area (Figure 78). This is significant as the sediments only account for 37% of the tonnes and 31% of the metal in the Michigan Upper Peninsula (284; 288). However, using a more realistic approach by combining the sediment- and basalt-hosted mineralisation, the endowment of the Upper Peninsula mineral system comes to 13.4 Mt of contained copper metal¹⁶⁵.

Additionally, the Upper Peninsula itself may only be a small portion of exposure, as similar copper occurs across Lake Superior at Isle Royal 80 km to the northwest (288; 304). This distribution means that the mineral system is located underneath Lake Superior. While estimating endowments is difficult at the best of times, an exercise of including the mineralisation outside of the Keweenaw Peninsula brings the endowment close to 'supergiant'¹⁶⁶ status. However, as under half of this mineralisation associates with sediments, the puritan 'deposit-model' substantially understates the significance of the system. This classification error is why Greenfields discourages deposit models even for analogies.

¹⁶⁵ No estimate was identified for the silver endowment.

¹⁶⁶ According to the metrics published by Hitzman et al (2010) of 24Mt of contained metal (284).

Figure 78: Sediment-hosted copper deposit endowments



Source: Hitzman et al. (2010) (284), modified by Greenfields. The Company expanded the White Pine/Presque Isle (WP/PI) endowment by including the basalt hosted copper (solid borders) and extrapolating the quoted mineralisation for the Keweenaw Peninsula to reflect the presence of native copper on Isle Royale (hatched border). The red curves schematically illustrate the probable ages of sulphide precipitation in the

major districts.

7.3 MINERAL SYSTEM

The mineral systems approach¹⁶⁷ is relatively simple to understand but is difficult in practice due to input uncertainties (271; 305). The mineral system relies on the identification of connectivity and interaction between multiple criteria¹⁶⁸ that focus mass and energy flux at regional and local scales (306; 282; 307). In the simplest terms, mineral systems describe chemical, physical and energy components, which subset into:

1. **Sources** of reagents and un/pre-concentrated metals for mobilising into a transient fluid;
2. **Geodynamic triggers** that mobilise the reagents and metals from their sources;
3. **Permeable architecture** that provides a pathway for energy and mass flow ranging in scale from the entire lithosphere to the local deposition site;
4. **Focus site** where there are means to scrub and concentrate metals from the fluids in a tight area; and
5. **Preservation**, so that geological forces after the concentration of metals into mineral deposit don't destroy it.

¹⁶⁷ For additional Company information on mineral systems, refer to Bell & Saleem (2018) (376).

¹⁶⁸ There is variance in the literature and additional criteria may be included.



What constitutes each of the above criteria will vary with the geological terrane (305). It is also important that there is no dependence or hierarchy between key elements of a mineral framework (308). Non-hierarchical elements are a key measure of a proposed framework's robustness (308).

In assessing the prospectivity of the ARC project, the Company considered criteria from macro-through to project-scale. Identifying such 'mappable' features are important for when all of these 'interest', deposit formation is possible. By using credible sources and a holistic thought process, Greenfields presents in the follow sections how ARC satisfies the mineral system requirements; how the Company defines a previously undescribed metallogenic province; and reduces the search-space so that its current focus is on an area at least three orders of magnitude smaller. This section also contains an estimate on the certainty of the mineral system, the type of disclosure for which the Company has not identified precedents¹⁶⁹.

7.3.1 Evidence

Greenfields identifies that North Greenland contains all of the mineral system components and that these can be identified from regional down to a local scale at ARC (Table 3). Being able to identify each is important as a system is a linkage, where if a component is missing the outcome, every time, is no deposit. While ARC is at an early stage of exploration, there is significant empirical evidence for successful linkages across the system (Table 4). Furthermore, the proposed framework and evidence have non-interdependence and fit into a non-hierarchical framework (Figure 79).

Table 3: North Greenland mineral system hierarchy

	Regional (North Greenland)	→	Local (ARC)
Source of salt	Upland evaporites.	1. Mesoproterozoic, and 2. Neoproterozoic-aged sediments.	
Source of metal	1. Basalts, 2. Mesoproterozoic sediments, and 3. Neoproterozoic sediments.		
Geodynamics	Mantle plume.	1. Elzevirian Orogeny, and 2. Caledonian Orogeny and its fluid front.	1. Rhepsammite and granophyre intrusions 2. Burial metamorphism of basalts, and 3. Topography driven evolved meteoric fluid flow.
Permeable architecture	Lithospheric thickness contrast.	1. Translithospheric faults, and 2. Features associated with igneous intrusion paths.	Fault sets and lineament intersections.
Focus site			1. Basalts; 2. Neoproterozoic-Silurian aged reduced beds; and 3. Coincident haematisation and focussed potassic alteration.
Preservation		Absence of the folding seen further north.	Present level of erosion is favourable.

Source: Greenfields.

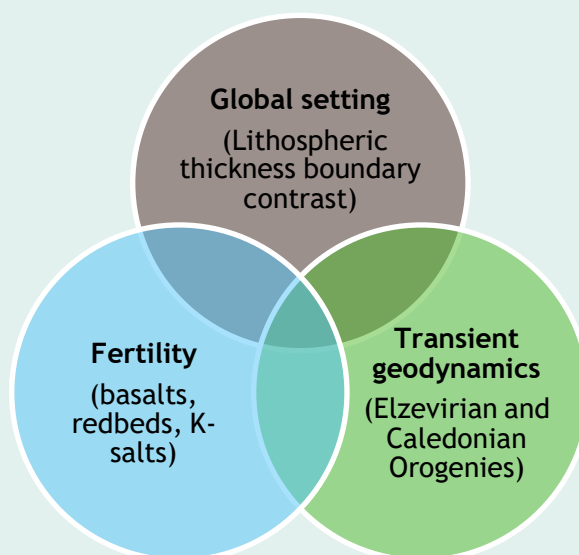
¹⁶⁹ No precedents were identified within the public domain, commercial documents concerning mineral systems (as distinct from petroleum systems for which probabilities are commonly disclosed).

Table 4: Empirical evidence of a mineral system

	Regional (North Greenland)	→	Local (ARC)
Province fertility	Citronen deposit.		
Geochemical indications		Widespread fine-grained native copper.	
		Widespread sulphidic copper.	
		Widespread copper sulphidic beds; and RedOx boundary between J.C. Christensen Land (not Mylius-Erichsen).	
			Focussed potassic alteration zones in basalts and overlying sediments. Microcline is noteworthy.
Empirical evidence			Large clasts of native copper.
			Discovery Zone.

Source: Greenfields.

Figure 79: Non-hierarchical mineral system framework



Source: Greenfields. Note: The geodynamic events are tightly constrained to c. 1,250 Ma for the Elzevirian Orogeny, and c. 385 Ma for the waning phase of the Caledonian Orogeny.

7.3.1.1 Fluid and metal sources

There are multiple reagent and metal sources in the region, in the form of Mesoproterozoic-aged redbed sediments and basalts, to sediments as young as c.385 Ma.

1. Mesoproterozoic-aged Zig-Zag Fm is permeable, and subject to metamorphism ranging from zeolite to greenschist facies (214; 225). The passage of saline fluids may strip copper from the basalts, and the Greenschist metamorphism of the basalts can also release metalliferous, sulphur-poor fluids (301). The temperature of the fluid induced alteration in the Zig-Zag Fm is 125° to 200°C, 150°C in the Discovery Zone, and 80° to 160°C at Citronen. This temperature gradient indicates to Greenfields that the fluid flowed from east to west.



2. The Mesoproterozoic-aged Independence Fjord Group overlies the basement and contains evaporites and redbed siltstones that can be traced for more than 100 km (220; 151). The overlying Zig-Zag Fm in ARC and Mylius-Erichsen Land is both a metal source¹⁷⁰ and a focus site. The presence of extensive fine-grained, and localised coarse, native copper in areas¹⁷¹ at least 160 km apart (128) demonstrates the scale of the source rock productivity.
3. Unconformably overlying the basalts are the redbeds belonging to the Hagen Fjord Fm (Figure 80) (223). The medium- to coarse-grained sandstones may act as a highly permeable and therefore efficient, complementary¹⁷² metal source. Furthermore, evaporites to the east of ARC¹⁷³ likely located at a palaeo-high, could have resulted in evolved highly saline, topographically driven meteoric waters¹⁷⁴. Multiple sources from rocks with substantial separations in time¹⁷⁵ played an essential role in the Katangan Basin (309).
4. The basement- and sediment-derived siliceous component in the subvolcanic plumbing provides a source of highly potassic fluids¹⁷⁶. Volatiles within the siliceous crystal mush were liberated when the rheopsammities and granophyres were emplaced into the overlying sediments (228). These fluids contributed to the widespread potassic alteration.
5. Rehnström (2011) describes epidote near known copper occurrences while Bevins et al (1991) describe epidote as being absent (3; 225). As Rehnström (2011) observed epidote near known copper occurrences, the epidote may reflect more focussed, and higher temperatures fluid flow. Epidote is associated with the native copper on the Keweenaw Peninsula (310).
6. A significant discordance records the removal of evaporites (149). For the most part, the gypsum now is expressed as desiccations and pseudomorphs (3).

Figure 80: Redbeds in Neergaard Valley



Source: Haugaard (2011) (2). Note: Bleached sandstones with copper oxide staining in the foreground, red beds in the background.

7.3.1.2 Permeable Architecture

Northern Greenland is located at an area where there is a significant thickness contrast in the lithosphere-asthenosphere boundary ('LAB') (159). The LAB has a thickness of ~170 km is located

¹⁷⁰ Metamorphic fluid by itself is unlikely to be significantly cupriferous to lead to the formation of large copper deposits, and therefore additional sources of Cu-rich fluid are necessary. At the Upper Michigan Peninsula, the metamorphic fluids mix with saline, cupriferous evolved meteoric waters. The mixing of such fluids explains the presence of native copper and the copper isotopes observed, while honouring the metamorphic alteration in the surrounding rocks (246; 270).

¹⁷¹ From North Neergaard valley (~81° 56.783'N, 26° 15.022'W) to Campanula Dal (~80° 37'N, 24° 430'W).

¹⁷² The historical sediment-hosted copper deposit model was that redbed clastics are the source of copper. However, this is disputed by Koziy et al. (2009) (408). These authors argue that in Zambia, there are volumetrically insufficient redbeds to explain the copper deposits, and present a mechanism by which fluid circulation into the underlying igneous rocks accounts for the missing copper in the source rock model (408).

¹⁷³ In Kronprins Christiansen Land.

¹⁷⁴ The combination of evolved meteoric waters, with metamorphic derived fluids from basalts is used to explain the copper isotopes in the Upper Michigan peninsula, and electrochemical pH-eH conditions needed to explain them (246).

¹⁷⁵ Dating of the Domes region within Copperbelt copper suggests that there may have been a Mesoproterozoic-aged (within 'the boring billion') precursor copper source rock within non-sediment basement (309).

¹⁷⁶ Potassic brines preferentially transport metals relative to sodic fluids, and are associated with a wide range of deposit types (377; 378; 379; 284; 245).

about 25 km to the east of ARC¹⁷⁷. This transition zone is significant as 85% of all the sediment-hosted metal, and all the 'giants' deposits occur within 200 km of the boundary (Figure 81) (311).

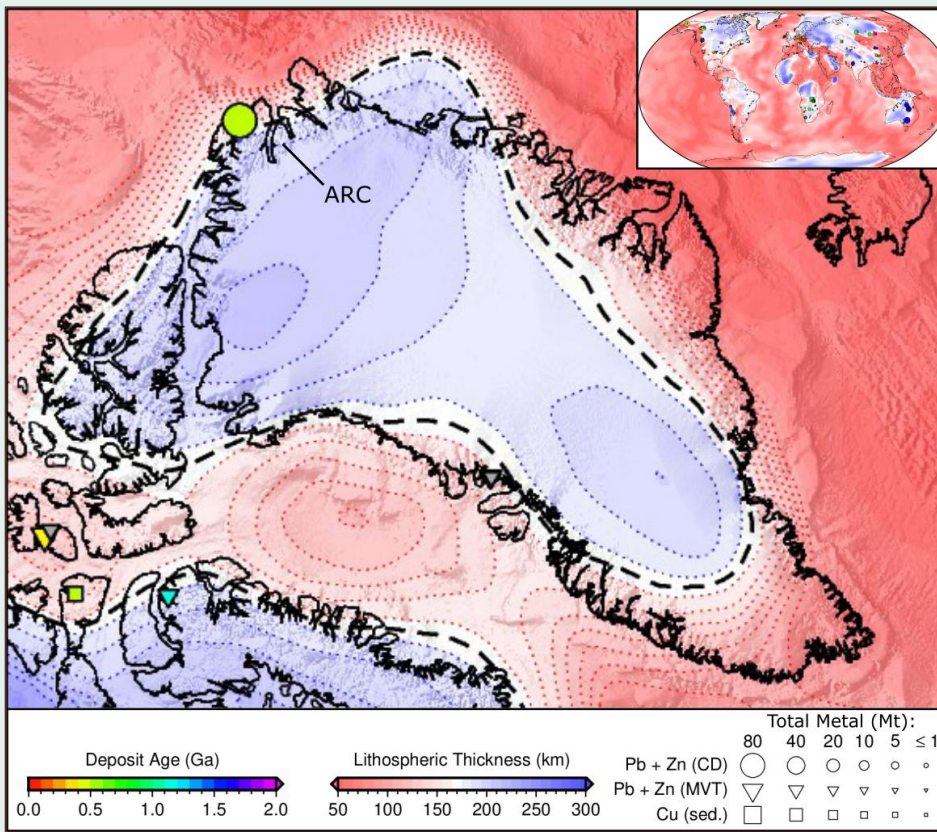


Figure 81: Deposits and lithospheric thickness

Source: Hoggard et al. (2020) (311). Note:

The Citronen zinc (+lead) deposit (yellow circle, North Greenland) has not been drilled out to its full extent, and like ARC, it locates at a favourable location in terms of lithospheric thickness.

North Greenland's permeable architecture comprises both structural, and primary features.

1. The fault and lineament sets¹⁷⁸ identified by Greenfields provide large-scale structures along which fluids may move vertically through the stratigraphic column. These fault zones are known to have been active at least since the Carboniferous (312). Due to the location at the passive margin, reactivation of these structures over time is likely (206). Within ARC, there are parallel faults to these large-scale systems (3).
2. There are permeable layers¹⁷⁹ within the flood basalts and sediments, which provide lateral pathways for fluid flow (214; 225). Thin lava flows display higher degrees of alteration, as do those with vesicular margins; and thicker flows (even those with vertical fractures) show little evidence of alteration. This confinement between flows and layers allows for a large source area from which fluids can strip copper and continue to concentrate as they travel laterally. This mechanism explains the contrasting states of metamorphism and multiple reduced and oxidised horizons within the basalt flow stack (225).

ALL SEDIMENT-HOSTED 'GIANTS' OCCUR IN THIS SETTING.

¹⁷⁷ The boundary used Hoggard et al. (2020) extends from east of the Citronen deposit to northern Mylius-Erichsen Land (311).

¹⁷⁸ Trolle Land Fault Zone and Harder Fjord Fault Zone set, and Navarana Lineament and Peary Land Fault set

¹⁷⁹ Thin vesicular flows, and the intercalations of conglomerate, sandstone, dolomite, and tuff (159).



In addition to the regional permeability within the basalts, permeable tephra occurs within ARC. These 50 m thick tephra¹⁸⁰ are only present within the upper Porphyritic Unit on J.C. Christensen Land. The tephra are known to be subject to potassic alteration and appear to contain salt staining

(Figure 82) (224; 225). Intense potassic alteration is observed in the stratigraphy cutting faults in the sediments overlying the tephra/basalts (the 'Discovery Zone' (3; 2), refer to section 7.1). The potassic alteration common to both links project level conduits with prospect level targeting.

There are many published faults, and Greenfields interpreted lineaments within ARC. Three published sites of in situ native copper occur near the junction of these structures (Figure 48), which suggests to Greenfields that they have been active pathways for metalliferous fluid.

As Greenfields attributes the geophysical component Minik Singularity to fluid induced iron-enrichment, it represents a low-pressure escape path within the hydrodynamic framework. Low-pressure zones result in higher-flow rates that disproportionately account for much of the flow volume.

7.3.1.3 Geodynamic triggers

North Greenland locates in a zone of anomalous energy and dynamics. The high contrasts in lithospheric thicknesses is associated with edge-driven convection and magma (energy) genesis (313; 311). Areas with high lithospheric contrast are also robust (311), and therefore can provide energy over long periods. The sustained supply of energy is important in maintaining fluid flow over a prolonged period, something that is associated with the known 'supergiant' sediment-hosted copper deposits (284).

An ascending mantle plume likely enhanced the energy input into northern Greenland. The lithospheric thinning allowed for a distal mantle plume to ascend to a depth of 35 to 50 km (159). The presence of a plume is crucial as it injects geodynamic energy during a period of reduced tectonic energy (314). The evolving plume is associated with a large igneous province in the form of the Zig-Zag Fm and Midsommersø Intrusions (159). The basaltic flows show a significant range in composition, and the succession reflects an increase in melt fraction in the sub-lithospheric mantle (159). The ascension of the plume is likely to have influenced the overarching stress regime and provided a source of sustained energy inflow with known events around 1,382 Ma (159). Greenfields postulates that mantle plumes may have added heat and pressure to northern Greenland between the known eruptive events by exploiting the LAB contrast.

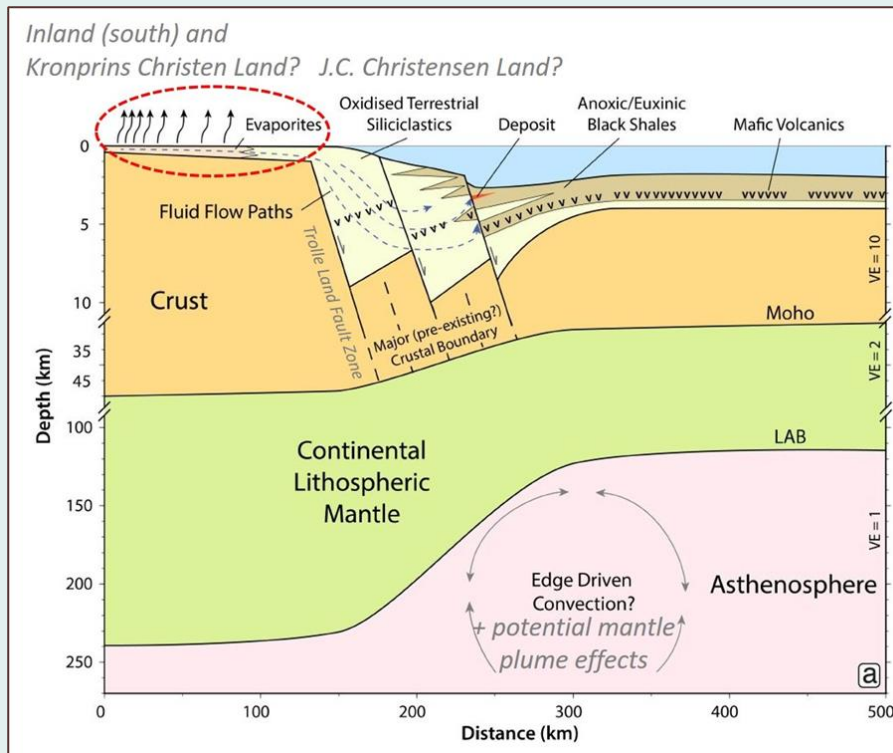
Figure 82: Potassic-altered tuff



Source: Rehnström (2012) (3). Note: The lower right third of the photo appears to show evidence of fluid flow in the form of residual salt. The original author of this photo interprets the rock to be a fine-grained basaltic tephra.

¹⁸⁰ Greenfields did not identify an explicit statement of the mineral composition of the tuffs. Due to the higher volatile content of the magma resulting in more explosive eruption than basaltic equivalents, the tuffs may be rhyolitic (371).

Figure 83: Sediment-hosted mineral system



Source: Hoggard et al. (2020) (311). Note: Greenfields modified the image to highlight the evaporites, an additional geodynamic trigger (plume) and conceptual North Greenland equivalent settings.

Greenfields identifies two transient geodynamic triggers that influenced the formation of copper mineralisation in North Greenland:

1. The 1,250 Ma Elzevirian Orogeny is a mechanism for introducing heat energy into the region. As the basalts south of Independence Fjord are not known to have undergone significant burial, the 200°C peak metamorphism must be explained by other mechanisms (225; 214). The orogenic event is one such mechanism, as it occurred after the ~1,382 Ma intrusions and extrusions. The timing overlaps within confidence interval of the original, well-constrained and repeatable date of c. 1,230 Ma estimated for the alteration of the Midsommersø Intrusions (159). The presence of 1,230 Ma alteration in the Midsommersø Intrusives demonstrates that the Elzevirian Orogeny is a geodynamic trigger, that is possibly accompanied by magmatism¹⁸¹.
2. The Late Caledonian Orogeny (c. 385 Ma, (196)) is Greenfields' preferred¹⁸² timing of the fluid-induced alteration in post-Elzevirian sediments. The Caledonian Orogeny resulted in

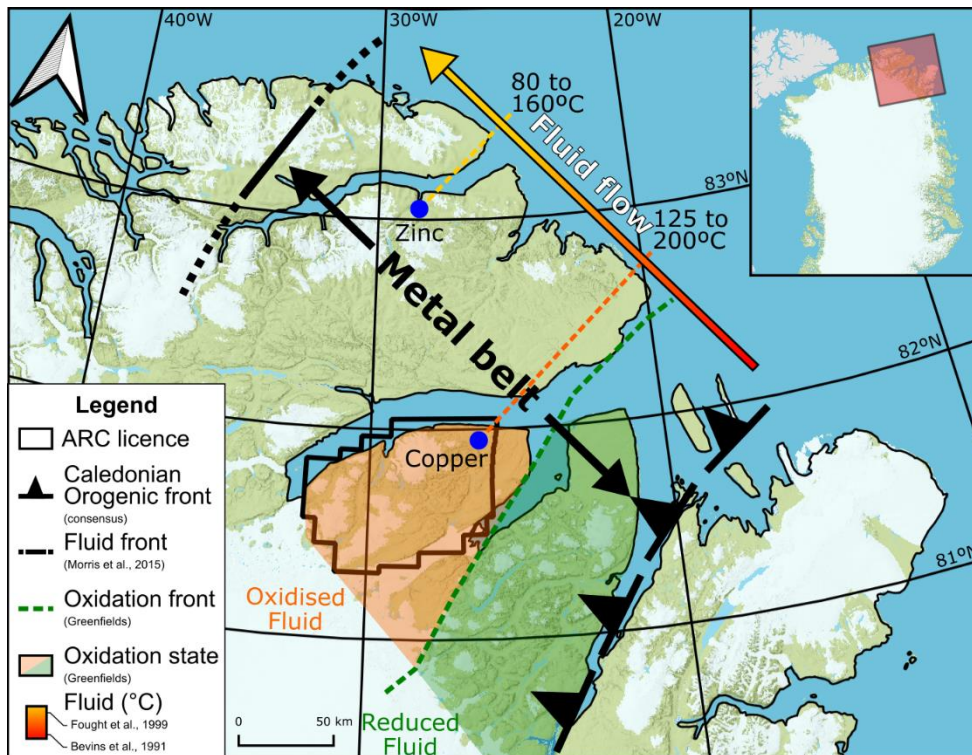
¹⁸¹ The granophyres and rheopsammites result from partial melting in the sub-volcanic plumbing (228). Dating of the fresh dolerites shows an age of 1,382 Ma, but the altered intrusions date at 1,230 Ma (159). It is possible that the 1,230 Ma dates an alteration the age of these Si-rich intrusion instead of alteration or that there are multiple intrusion ages and overprinting alteration events (159).

¹⁸² The late Devonian to early Carboniferous-aged Ellesmerian Orogeny is a potential geodynamic trigger. The orientation of the Discovery Zone faults are similar to the Trolle Land Fault Zone (which exploited an undated 'fossil' structure) and the much older Wandel Dal Lineament. As the Ellesmerian Orogeny has a different orientation to the Elzevirian Orogeny, fluids would have to exploit a different hydraulic architecture. Greenfields has not identified any evidence of mineral emplacement younger than Silurian. Based on the available information, the Company considers the Ellesmerian Orogeny as a plausible geodynamic event but less probable than the Caledonian Orogeny.



preserved mountainous terrain¹⁸³, and compressive forces promoting an east-west fluid flow that extend west of the orogenic front (Figure 84) (196). Due to burial, a Caledonian mineral event could also draw on burial metamorphism of the basalts as a source of copper. Greenfields considers that the c. 385 Ma fluids could have exploited similar permeable architecture as the Elzevirian¹⁸⁴. The Company notes that there is a change in oxidation state near the orogenic front. The Silurian/Ordovician-age of the Citronen deposit, its north-northeast bounding fault orientations (315), north-south 'feeder zone orientation' (87; 315) and approximate north-south orientation of the host fjord correspond well with the Caledonian Orogeny¹⁸⁵. The structural similarity and age indicate to Greenfields that there is a metallogenic province ('metal belt'), which it provisionally names Kiffaangissuseq¹⁸⁶. This West Greenland term means 'independence'.

Figure 84: Kiffaangissuseq metal belt



Source: Bevins et al. (1991) (225); Fought et al. (1999) (215); Morris et al. (2015) (196). Modified by Greenfields to show the known metal occurrences, and interpretation of the Kiffaangissuseq metal belt with an oxidation boundary between J.C. Christensen Land and Mylius-Erichsen Land.

¹⁸³ The c. 385 Ma event is supported by Caledonian-aged exhumation on Svalbard (202), which further indicates major tectonic activity occurred at this time.

¹⁸⁴ In the absence of evidence to the contrary, Greenfields interprets the temperature of both the Elzevirian and Caledonian fluid at ARC to be in the range of 125°to 200°C. This interpretation is based on the overlapping nature of the orogenies, and that this temperature band is often with both native copper and copper sulphide formation in sedimentary systems.

¹⁸⁵ Greenfields did not identify evidence of commercially relevant mineralising events younger than the Silurian (i.e. stratigraphically above/younger than the Citronen deposit). The existence of the Ellesmerian is uncertain (197) and the younger orogenies may have only a secondary impact on the mineralisation.

¹⁸⁶ The word pronunciation is approximately 'kee-faa-gnee-su-sohk', with the k being a soft sound. The pronunciation can be heard at the link: <https://oqaasileriffik.gl/langtech/martha/?st=kiffaangissuseq#result>. The word means independence in West Greenlandic. While using the Independence Fjord is an appropriate choice using a standard naming convention, it has a colonial background that is inconsistent with the Company's views. The Company has not identified other appropriate place names within the relevant area. The Company also notes that the term 'independence' is ascribed to two palaeo-Inuit cultures (Independence I and II) that lived in North Greenland from ~2,400 to ,1000 BCE, and 700 to 80 BCE respectively. Consequently, Greenfields elects to use the Greenlandic equivalent of independence to honour the naming convention while being more culturally appropriate.

7.3.1.4 Focus

Copper is known to occur within the Zig-Zag Fm (268), cross-cutting faults and in stratiform positions within overlying sedimentary rocks. The evidence for focussed metal deposition includes:

1. The stream sediments within ARC are between 146% to 170%¹⁸⁷ richer in copper than the median¹⁸⁸ for elsewhere in the area (316).
2. In J.C. Christensen Land, the stream sediments magnetite is complemented by haematite (261). Haematite is not reported on Mylius-Erichsen Land (261). The transition from magnetite to haematite is associated with copper mineralisation (Figure 49) (249; 250; 251). ARC is also notable for its presence of dolomite; and potassic¹⁸⁹ and sodic alteration minerals, which are features associated with a wide range of sedimentary mineralisation types (249). The multifaceted geochemical contrast with Mylius-Erichsen Land is what makes the area which is now ARC an exploration priority.
3. Mapped sites of in situ native copper surround a coincident magnetic-gravity anomaly that is not explained by the lithologies mapped at surface. The deposition of metals¹⁹⁰ due to oxidation of reduced fluids may explain the geophysical response and the proximity to the known native copper.
4. In North Neergaard Valley, the Discovery Zone displays carbonaceous¹⁹¹ zones of intense copper-silver deposition over a significant area of anomalism (Figure 87) (2). The Discovery Zone is also notable for its intense potassic-alteration of sedimentary rock (3). Microcline occurs in the Discovery Zone, and sericite occurs in the least-altered basalts. The presence of microcline is intimately associated with native copper mineralisation (273; 317), and sericite is negatively correlated mineralisation intensity (214; 318; 3). By mineral assemblage proxy, the Discovery Zone is suggestive of a copper deposit in the near vicinity¹⁹².
5. The observation of potassic alteration in both the Mesoproterozoic-aged lavas and Neoproterozoic-aged sediments provides a chemical link between the native copper and copper sulphide mineralisation. The proximal location of the Discovery Zone and large native copper clasts suggests a spatial link.
6. The reduced beds of the Campanuladal Fm are anomalous in copper (261). The Campanuladal Fm shows signs of lateral saline fluid flow over extensive distances (Figure 86). The overlying strata, including the Portfjeld Fm, contain algal mats (Figure 85) and pyrobitumen (3) which enhance the potential for the reduction of oxidized metal-bearing fluids.

MICROCLINE IS
ASSOCIATED WITH
OPTIMAL NATIVE
COPPER
DEPOSITION

¹⁸⁷ 98 to 114 ppm Cu (316).

¹⁸⁸ 67 ppm Cu (316).

¹⁸⁹ Potassic alteration occurs as K-feldspar in the ARC basalts (222). In the Discovery Zone of the Neoproterozoic sediments, the potassic alteration is known to occur as muscovite-microcline (3).

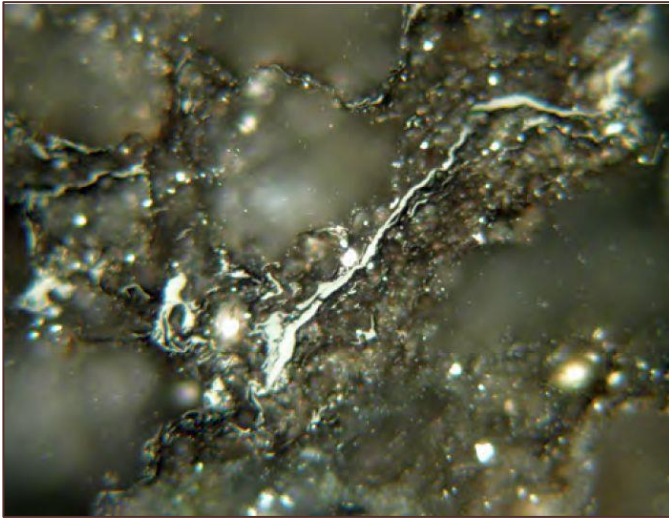
¹⁹⁰ Greenfields thinks that iron deposition results in the geophysical response, although it is possible that copper co-precipitated at the same site.

¹⁹¹ 0.24-0.49wt.% total organic carbon, with an average of 0.35% (3), and for example "3 m thick bed of dark grey limestone with abundant lenses of black, shiny lithology. The lenses are possibly clay with high organic content – almost like lignite. It smells funny, a bit like methane." (Rehnström, 2012, (3)).

¹⁹² Copper mineralisation may be 'upstream' or 'downstream' of the Discovery Zone. Given the proximity to the basalts, and the observation that vertical cross-cutting 'fissures' link to larger deposits in the Keweenaw Peninsula (273), Greenfields considers a nearby native copper deposit in the basalts most probable.



Figure 85: Portfeld Fm hydrocarbons



Source: Rehnström (2012) Fig 7.2.C (3). Note: 300 micrometre view of pyrobitumen.

Figure 86: Fluid flow staining within the Campanuladal Fm



Source: Rehnström (2012) (3). Note: this laterally persistent horizon extends at for at least 50 km. The staining is manganese and iron-rich, but also note the white salt at the bottom of the horizon.

Figure 87: Malachite breccia within redbeds



Source: Haugaard (2011) (2). Note: The potassic breccia within redbeds of the Jyske Ås Fm in Neergaard Valley.

7.3.1.5 Preservation

Despite the long geological history, the ARC rocks are only weakly metamorphosed (zeolite facies) and no destructive structures are apparent. To the immediate north of Independence Fjord, the basalts and stratigraphy of interest (e.g. Campanuladal Fm) dip underneath cover stratigraphy making targeting difficult. Further north on the coast of Peary Land, uplift exposes basalts which display a higher metamorphic grade (Greenschist Facies) which may be less suited to preservation but are instead potential source rocks. Mechanical erosion is the only identified mechanism that may affect preservation.

7.3.2 Interpretation

In this Report, 'hydrodynamics' is used to encompass the interplay between the sources of fluids, salts, and metals; permeable architecture; and geodynamic triggers. Greenfields notes the evidence in the preceding and presents in this section its interpretation.

7.3.2.1 Elzevirian fluid flow

The compressive forces associated with the 1,250 Ma Elzevirian Orogeny provides a mechanism¹⁹³ for driving fluids, potentially from east to west¹⁹⁴. This orogenic event also provides significant volumes of hot potassic fluids (228). As basalt may not liberate enough copper by itself¹⁹⁵, a secondary source is beneficial (246). Elsewhere, meteoric waters, driven by topographic changes and passing through evaporite sequences can provide the additional copper from the enclosing sediments (301). The progressive haematisation of the aquifers by evolved saline meteoric waters, combined with fluid mixing with low-salinity metamorphic fluids satisfies the eH-pH conditions necessary to precipitate native copper (Figure 88) (246; 301). Based on the dating of the dolerite metamorphism¹⁹⁶ and the intergrowth of basaltic native copper and prehnite (159), this scenario explains a mineralisation event during the Mesoproterozoic. However, in isolation, the Elzevirian cannot account for the difference in age with the Neoproterozoic hosted copper-silver or the distal Ordovician-Silurian hosted Citronen deposit; or the different eH-pH fluids required to precipitate sulphide minerals.

Figure 88: Native copper from the Zig-Zag Fm



Source: Haugaard (2011) (2).

THE ELZEVIRIAN IS
TIED TO THE
INTRUSIONS,
ALTERATION, AND
NATIVE COPPER
MINERALISATION

¹⁹³ Orogenesis is associated with both the Kupferschiefer, and Copperbelt (284).

¹⁹⁴ The current evidence suggests that the Elzevirian and Caledonian Orogenies have similar spatial distribution. Compressive forces of such mountain building events could have driven fluids to lower-pressures in the west in combination with topographical changes.

¹⁹⁵ As suggested by Brown (2006) (246) for the formation of the native copper on the Upper Michigan Peninsula.

¹⁹⁶ Attempts to determine the age of the basalt were unsuccessful as they did not yield isochrons (227). Consequently, the successful dating of the dolerites was assumed to reflect the age of the basalts due to their stratigraphic relationships. The Company does not question the age of emplacement but does caution that the assumption that the basalts were metamorphosed shortly after emplacement is not known to be supported by any field evidence. It is therefore possible that the metamorphism of the basalts occurred later than assumed in the literature.

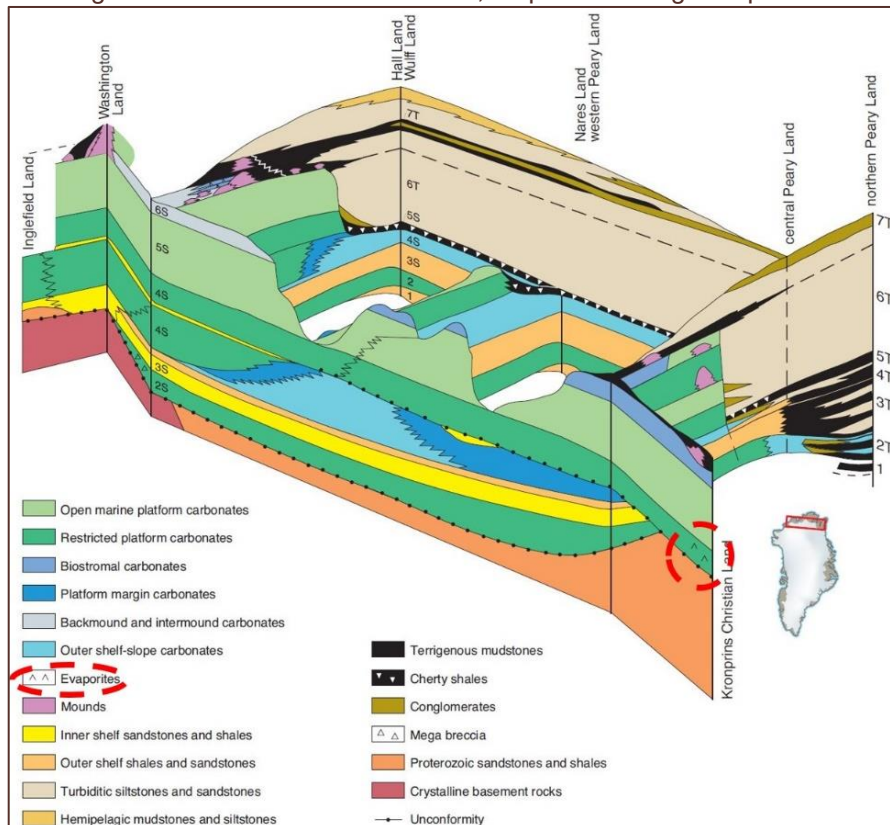


7.3.2.2 Caledonian fluid flow

The 490 to 390 Ma Caledonian Orogeny provides a second compressive and topography changing event that yielded fluid flows¹⁹⁷ through evaporitic rocks¹⁹⁸ (Figure 89). The extent of the fluid flow is far to the west of ARC (196) and defines the boundaries of the Kiffaangngissuseq metal belt. The waning phase of this orogeny at c.385Ma could have mobilised salts and metals from sediments deposited during the subsequent Neoproterozoic through to Silurian (Figure 89). These fluids need to mix to explain the presence of sulphidic minerals at the Discovery Zone. Due to a similar orientation between the Elzevirian and Caledonian orogenies, the second fluid migration could have followed similar or the same permeable architecture. It is plausible that in the absence of metamorphic waters, these potassic brines could have remained oxidised¹⁹⁹ until the site of focussed metal deposition. The occasional presence of chalcocite filled amygdales in the primarily native copper carrying basalts supports an interpretation that saline fluids exploited similar architecture. This additional event²⁰⁰ accounts for the copper sulphides hosted in the Neoproterozoic-aged sediments and basalts; and it implies that that the mineralisation is Silurian and potentially contemporaneous with Citronen.

LATE CALEDONIAN SULPHIDE MINERALISATION EVENT

Figure 89: Schematic of the shelf, slope and trough sequences



Source: Henriksen et al (2009) (148). Note: Modified by Greenfields to highlight the evaporites. ARC locates between Kronprins Christian Land (lower right of the figure), and central Peary Land (upper right of the figure). S: shelf, T: trench, 1: Neoproterozoic-Early Cambrian, 2 & 3: Early Cambrian, 4: Late/early Cambrian-Middle Ordovician, 5: Middle Ordovician-Early Silurian, 6: Early Silurian, and 7: younger than Silurian.

¹⁹⁷ A dense saline fluid would preferentially flow down slope. In Zambia, it is shown that dense saline fluids can drive fluid flow deep into basement rocks (even mid-crustal level) even in the absence of a permeable network (408). This deep basement interaction is supported by dating from the Domes region in the Zambian Copperbelt (309).

¹⁹⁸ The Early Cambrian to Middle Ordovician-aged Ryder Gletscher Group contains multiple evaporite horizons, including the early to middle Ordovician-aged Wandel Valley Fm (243; 238).

¹⁹⁹ Salt staining within the Campanuladal Fm is evidence of saline solutions having migrated along the strata.

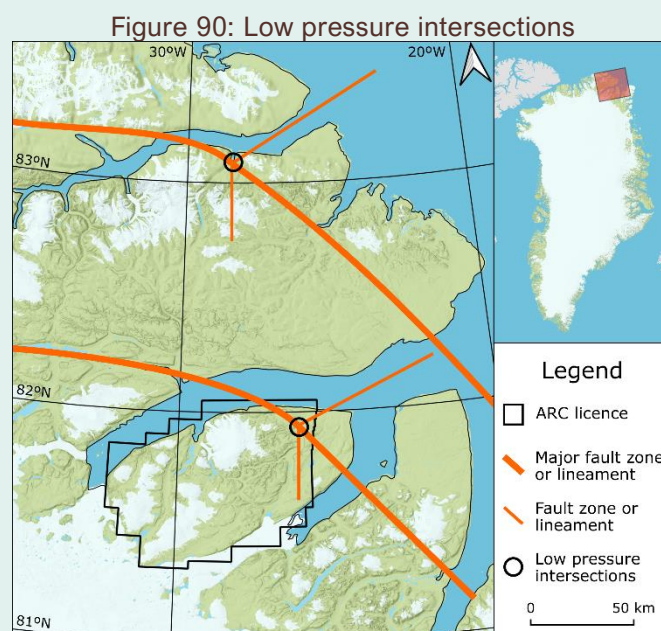
²⁰⁰ Two orogenic events are associated with the Copperbelt mineralisation, the Irumide (1084-1059 Ma) and Lufilian (539.9-497.1 Ma) orogenies (309). Composite metallogenic provinces involving multiple orogenesis and mantle plumes are also reported in China (384).

7.3.2.3 Metamorphic dehydration

Burial related metamorphism may also have been an additional source of metal during the Caledonian event. The deep burial of the basalts at Hellefiskefjord to the north of ARC results in Greenschist Facies metamorphism (214). This process is a potential copper source and could have induced complementary convection in connecting aquifers at both ARC and Citronen. The source of deep, hot fluids derived from older rocks is consistent with the isotopes and chemical compositions observed at Citronen.

7.3.2.4 Preferential flow

The overpressure created by hot fluids deep below the surface would result in exploiting the paths of least resistance to the surface²⁰¹. While there are several faults system in North Greenland, a focus mechanism is needed to provide rapid ascent of fluids to ensure copper concentration (270). Greenfields notes that the Citronen deposit occurs at the junction of the present-day Tolle Land and Harder Fjord Fault Zones (and close to the Navarana Fjord Lineament (12)), the intersection of which can create a low-pressure conduit. The overall shape of the Proterozoic-aged lithologies ('historically known as the Hagen Arch') places ARC at a similar hinge-like location (Figure 90). Furthermore, the orientation of Citronen Fjord is north-south. Within ARC, the in situ occurrences of native copper locate close to fault intersections within the north-south oriented Neergaard Valley. Such extensional structures at hinge-like locations promote rapid fluid depressurisation and change in oxidation state. The rapid changes in thermal and chemical qualities due to depressurisation and fluid mixing and can be expected to be sites of focussed metal deposition.



Source: Greenfields.

7.3.2.5 Oxidation and pressure change

The presence of haematite in stream sediment samples from J.C. Christensen Land and its absence in Mylius-Erichsen Land (316) is considered by Greenfields to be a key indicator²⁰². The area of haematisation also shows significant copper enrichment in the stream sediment. The progressive haematisation of magnetite is an essential factor in obtaining the requisite eH-pH for the cupriferous fluid so that it deposits native copper rather than a copper sulphide (246). For fluid focus²⁰³, a mechanism is needed to produce a 'plume'. The presence of a coincident magnetic-gravity anomaly may, conceptually, reflect the effect of an iron-rich fluid flow^{204,205}. Notably, only a small percentage of metal, such as iron²⁰⁶ or copper, needs to be scavenged from a source to generate significant metal accumulations

OXIDATION
AND
PRESSURE
FLUX

²⁰¹ In the Upper Michigan Peninsula, the Keweenaw thrust is thought to provide the depressurisation architecture (270).

²⁰² The alteration of magnetite to haematite is associated with native copper deposits (251; 252).

²⁰³ Minor amounts of native copper are widespread in the Lake Superior region which contains the Upper Michigan Peninsula copper deposits (246).

²⁰⁴ The combination of moving from magnetite to haematite, mixing of fluids, and rapid ascent results in IOCG-like mechanisms.

²⁰⁵ Sediment-hosted copper is not usually detectable by geophysical methods. However, the expression left by iron-rich waters may result in detectable qualities.

²⁰⁶ In the case of the El Laco IOCG magnetite deposit, the source magma is shown to be depleted by only 0.5% iron through a process akin to metallurgical flotation (319; 407).



(319), and thus produce a geophysical signature. The Minik Singularity corresponds with the proposed low-pressure outlet presented in section 7.3.2.4.

7.3.2.6 Search space

The search space is defined by the extent of the fluid flow. The fluid flow underpinning the Kiffaangissuseq metal belt is volumetrically significant. Using the western boundary published by Morris et al. (2015) (196), and the eastern boundary using Danmark Fjord, the Kiffaangissuseq search space is in the order of 50,000 km². The extent of this search space is supported by multiple other observations. The geochemistry of the circulating palaeowater near the Ordovician-Silurian aged Citronen deposit has similar characteristics to those of the Proterozoic-aged sediments (261; 320; 12). Isotope studies show that the Citronen lead is distinct from the lead in the surrounding area and is sourced from much deeper, older rocks (320). The oldest mapped rocks in the Citronen area belong to the Buen Fm, which is the stratigraphically highest lithological unit in ARC. With the Caledonian fluid flow known to extend 150 to 300 km²⁰⁷ west of the orogenic front, there is a mechanism for linking the known mineralisation. The lower temperatures of the Citronen mineralising fluids (80° to 160°C) compared to that of ARC's (125° to 200°C) is consistent with Citronen having a more distal position relative to the Caledonian Orogeny. The area between ARC and Citronen is known to contain multiple Mississippi Valley 'deposit model type' ('MVT') zinc anomalies²⁰⁸ (321), which is consistent with the setting expected between clastic-dominated zinc-lead and sediment-hosted copper (322). Greenfields considers there to be ample evidence to support the position that Kiffaangissuseq is a singular mineral system with a mappable search space that has a north-south orientation.

KIFFAANGISSUSEQ
HAS SUBSTANTIAL
FLUID FLOW

Within the 50,000 km² Kiffaangissuseq search space, Greenfields identified heightened copper prospectivity within the ~6,000 km² that is ARC. In turn, the Minik Singularity covers around 640 km². Greenfields achieved this spatial reduction through a combination of system modelling, geophysical interpretation, oxidation boundary analysis, and geochemical evidence. The Company has areas of interest within the Minik Singularity that are an order of magnitude smaller again, however additional data is needed before a more definitive reduction in search space is made as part of the current targeting process. While Greenfields believes it has identified the most commercially interesting area within the search-space, the remaining area of the Kiffaangissuseq search space is still prospective for mineralisation.

7.3.2.7 Mass balance

North Greenland has both voluminous sources and means of triggering focussed metal deposition. It is important that the sources and triggers have enough energy and mass to result in the formation of a mineral deposit.

Both the basalt lavas and rebedded sediments are potential metal sources. Greenfields calculates that the volume of this copper source rock^{209,210} is at least 8,100 km³ to 13,500 km³ based on the

²⁰⁷ Morris et al. (2015) (196) place the Caledonian Orogenic front through J.C. Christensen Land, in an area where there is a change in oxidation state. However, most of the research places the front in Danmark Fjord.

²⁰⁸ Rosa et al. (2014) attribute the zinc anomalies between ARC and Citronen to the Ellesmerian-aged Mississippi Valley Type deposit model, as opposed to the Clastic Dominated deposit model for Citronen (321).

²⁰⁹ Based on Jepsen's (1984) minimum of 6,000 km² x 1.35 km thickness based on the minimum dimensions published (224). Bevins et al (1991) published an area of 10,000 km² which gives a volume of 13,500 km³ (225). No area has been published that links the Hellefiskefjord basalts, and those on J.C. Christensen Land and Mylius-Erichsen Land. There is potential for a significantly larger volume of source rocks than what is formally published.

²¹⁰ The 1,382 ± 2 Ma falls within the 'boring billion' age range that is associated with few sedimentary derived deposits (249). The paucity of sediment derived deposits during this time is ascribed to a lack of reducing fluids and oxygen rich oceans (249). However, the 'boring billion' also correlates with a period when there was a hiatus in plate subduction

dimensions published by a number of different researchers. This source rock volume is larger than what is required to form the Kupferschiefer and Central African Copper Belt (1,154 and 2,337 km³ respectively) (323; 282). Due to the lack of information, no volume estimates for the sediment sources were attempted.

While mobilising metal from the source is important, it must be balanced with mechanism for causing focussed deposition. The surface expression of the geophysical anomaly that is interpreted by Greenfields to be a hydrothermal footprint covers approximately 640 km². The area of the anomaly is less than 2% of the basalt surface expression. However, if conduit and strata thickness differences and additional sediment sources are considered, the concentration factor is likely to be at least an order of magnitude higher. As the source rock surface area (not volume) is multiple orders of magnitude larger than the hydrothermal choke point, a strong and voluminous chemical trigger is required to precipitate the copper into deposits. As the native copper was transported by a reduced fluid, a suitably large oxidation source is the Earth's atmosphere. As the co-incident geophysical and geochemical Minik Singularity is suggestive of a fluid plume (a term used by Brown, 2008 (270)), depressurisation is another mechanism that is essentially unlimited and capable of triggering a suitably focussed mineralisation event. Greenfields considers it likely that the externally buffered oxidation and depressurisation are related and represent mechanisms capable of precipitating metal from large volumes of metalliferous fluids without being exhausted.

UNLIMITED
PRECIPITATION
PHYSICS

7.3.2.8 Certainty

To quantify the certainty of the ARC mineral system, Greenfields undertook a subjective probability analysis of each of the crucial components of the mineral system. This analysis involves a survey using descriptive words which have assigned multiplicative²¹¹ probabilities²¹² giving rise to system certainty. This approach is used as it is easier for people to describe certainty using vague words rather than precise numbers.

While certainty analysis relates to the process of finding a deposit, it is not interchangeable with the probability of a finding a deposit. For example, an accidentally found deposit is a known result, however how it was formed may be poorly understood (i.e. the presence of a deposit is 100% certain but the systemic certainty is less than 100%).

The Greenfields certainty estimates are presented in Table 5 and Table 6. The certainty of the native copper component of the system ranges from 47% to 49%, and for the younger sulphide component the certainty is 64% to 83%. The responses show that good probabilities are assigned in most cases, but cumulatively the small uncertainties have a significant compounding effect. These probabilities are much lower when erosion is considered because while neither respondent considers it excessive, there is no conclusive evidence upon which definitive responses can be made²¹³. To the surprise of the respondents, the copper sulphide mineralisation is assigned a higher certainty than the native copper system. As both respondents intuitively have a stronger

(314). As atmospheric chemistry is unlikely to drive the physics of slab subduction, it is more important that during the Boring Billion, a local enhancement of energy should be identified. At ARC, the mantle plume may have injected energy at a time when passive margin energy may have otherwise been in an ebb.

²¹¹ A multiplicative process is then used for if any element of a system is missing (0% certainty) then a deposit cannot exist.

²¹² Proven, definitely true: 100%; Virtually certain, convinced: 94%; Highly probable, strongly believed; highly likely: 83%; Likely, probably true, chances are good: 68%; Chances are about even or slightly better or slightly less than even: 50%; Could be true but more probably not, unlikely, chances are fairly poor, two or three times more likely to be untrue than true: 30%; Possible but very doubtful, only a slight chance, very unlikely indeed, very improbable: 11%; Proven untrue; impossible: 0%.

²¹³ For comparison, the impact of an erosional level may be more easily to gauge in some well understood magmatic systems.



preference for the likelihood of a native copper deposit, the disparity in the available information for each event is highlighted. As the overwhelming amount of prior exploration focussed on the sulphide targets, this relatively improved the certainty estimates. Greenfields expects that the certainty of the native copper system will change substantially and rapidly, with a dedicated exploration program. Overall, the authors consider there is a high degree of certainty, which they feel is remarkable given how little exploration has occurred in the region. The reader is encouraged to undertake a similar exercise and the Company is interested in receiving the results as feedback.

STRENGTH COMES
FROM KNOWING THE
WEAKNESSES

Table 5: Mineral system certainty estimates c. 1,250 Ma

NATIVE CU		BELL			BURKIN		
		Confidence	Reason	Probability	Confidence	Reason	Probability
GEODYNAMIC	Mass/energy flow	Proven; definitely true.	Certain c.1,250Ma orogenic event, rheopsammites.	100%	Proven; definitely true.	Multiple events. Tectonics and plume.	100%
	Salt	Virtually certain; convinced.	Extensive K-alteration.	94%	Virtually certain; convinced.	Evidence in rock record. And belief that salt exists in a system/environment if it is preserved or not.	94%
SOURCE	Metal	Proven; definitely true.	1 kg native copper clasts.	100%	Proven; definitely true.	Direct evidence and large source volume.	100%
	Structural permeability	Likely; probably true; about twice as likely as untrue; chances are good.	Lineament and fault correlation with native Cu occurrences.	68%	Chances are about even or slightly better or slightly less than even.	May have been present at the time, might not have been. Might be important or might not have been.	50%
PERMEABL ARCHITECTURE	Lithological permeability	Virtually certain; convinced.	Flowtops, intrabasaltic sediments, tephra.	94%	Proven; definitely true.	Permeable basalt flows and sediments present.	100%
	Trigger/precipitation	Highly probable; strongly believed; highly likely.	While favourable, the size of the Minik Singularity is still large.	83%	Proven; definitely true.	Metamorphism/alteration channelled into permeable paths.	100%
PRESERVATION	Unweathered	Proven; definitely true.	High Arctic. Even malachite staining of copper sulphides is rare.	100%	Virtually certain; convinced.	Not concerned about it.	94%
	No excessive alteration	Highly probable; strongly believed; highly likely.	Unclear if c. 385 Ma event depleted an existing deposit or enriched it.	83%	Proven; definitely true.	Zeolite to greenschist metamorphism confirmed.	100%
	Not eroded	Likely; probably true; chances are good.	Extensive exposure of potential deposit horizon.	68%	Virtually certain; convinced.	Just enough erosion to expose the stratigraphy. Glacier-transported clasts imply that an accumulation of copper is at the surface somewhere.	94%
System certainty				27%			42%
Certainty excluding preservation				49%	Certainty excluding preservation		47%



Table 6: Mineral system certainty estimates c. 385 Ma

SULPHIDE CU-AG		BELL			BURKIN		
		Confidence	Reason	Probability	Confidence	Reason	Probability
GEODYNAMIC	Mass/energy flow	Proven; definitely true.	Certain c.385 Ma orogenic event, Citronen, copper sulphides.	100%	Proven; definitely true.	Multiple events. Tectonics and plume.	100%
	Salt	Virtually certain; convinced.	Extensive K-alteration (remobilised?).	94%	Virtually certain; convinced.	Evidence in rock record. And belief that salt exists in a system if it is preserved or not.	94%
SOURCE	Metal	Proven; definitely true.	Sediments and native Cu basalts.	100%	Proven; definitely true.	Direct evidence and large source volume.	100%
	Structural permeability	Proven; definitely true.	Discovery Zone.	100%	Proven; definitely true.	More important here than the native copper.	100%
PERMEABL ARCHITECTURE	Lithological permeability	Highly probable; strongly believed; highly likely.	Faults, coarse permeable sandstone.	83%	Virtually certain; convinced.	Faults, yes. Lithology, maybe.	94%
	Trigger/precipitation	Likely; probably true; about twice as likely as untrue; chances are good.	Very high grades, unusual mineral species.	83%	Proven; definitely true.	Throttled into faults, yes. Into sediments, maybe.	94%
PRESERVATION	Unweathered	Proven; definitely true.	High Arctic. Even malachite staining of copper sulphides is rare.	100%	Highly probable; strongly believed; highly likely.	Not concerned.	83%
	No excessive alteration	Proven; definitely true.	Zeolite facies?	100%	Virtually certain; convinced.	Not concerned.	94%
	Not eroded	Likely; probably true; chances are good.	Younger than basalts so more likely to be mechanically eroded.	68%	Chances are about even or slightly better or slightly less than even.	Less preservation above basalts for vertical flowing conduits.	50%
System certainty				43%			32%
Certainty excluding preservation				64%	Certainty excluding preservation		83%

8 DATA INTEGRITY

8.1 SAMPLE PREPARATION, ANALYSES AND SECURITY

For the Government-funded exploration, no sample preparation, analysis and security documents were identified by the Company. However, given the non-commercial and often academic nature of this work, Greenfields has no concerns.

The 2010 Avannaa geochemical sampling appears to have been done using acceptable procedures, handling and submission to Actlabs Laboratories Ltd, Ontario, Canada, an appropriately certified laboratory (2). The 2011 Avannaa samples were submitted to ALS Laboratories, Öjebyn, Sweden, another appropriately certified laboratory (3). The Company has sighted the laboratory certificates and does not have concerns about the historical sample preparation, analysis or security.

8.2 DATA VERIFICATION

Greenfields relied upon public domain information and conversations with people and organisations that are familiar with the history of central North Greenland. The Company performed a detailed review of historical documentation so that where possible, facts are validated. However, given when the ARC licence was granted, Greenfields has not had an opportunity to conduct a field-check sampling program.

9 MINERAL RESOURCE ESTIMATES

There are no ARC mineral estimates, informal, historical or present.

10 MODIFYING FACTORS

10.1 ENVIRONMENTAL STUDIES PERMITTING, AND SOCIAL/COMMUNITY IMPACT

Greenfields reviewed the Greenland Government's portals and did not identify any designated cultural or environmentally sensitive areas that could impede the permitting of a future mining licence application (Figure 91).

While there are no designated zones within ARC, the Company notes that there are areas of archaeological interest in the broader regions, primarily in Jørgen Brøndlund Fjord outside of the licence area (61). Two sites are located within ARC²¹⁴. The area around Krognæs (61 pp. 191-194) is a low exploration priority to Greenfields, and the artefacts are not considered by the Company to be material to the Project's economic potential. There are also archaeological sites at the mouth of Neergaard Elv (61 pp. 194-196) into Independence Fjord, but again the location does not have an apparent impact on ARC's economic potential. Additional sites are located between Mylius-Erichsen Land and Station Nord, however, these have no foreseeable impact on ARC's potential. Overall, according to Grønnow and Jensen (2008) (61 p. 191):

²¹⁴ The Company will not disturb the known archaeological sites and will voluntarily restrict activities in these areas consistent with the requirements of the Park and good practice.



“even though Independence Fjord is less well surveyed than Jørgen Brønlund Fjord, with its scientific stations, it must be considered reasonably well known. During his sledge journeys Knuth often camped on the fjord ice far from the shores. Much of the travelling may have been conducted in seasons when large tracts were still covered by snow. Sites may thus easily have been overlooked during Knuth’s extensive survey work but it is unlikely that major concentrations of prehistoric settlement would have been missed. Not only did Knuth have a keen interest in elucidating the prehistoric settlement of the area, he also had a very well developed sense for locating ancient settlements. Furthermore, one can argue that since dog sledge and hiking were the main means of transportation during most of Knuth’s surveys, it is likely that the topography and local geography lead him to many of the same places that would have been used as camping grounds by ancient hunters” (61 p. 190); and

“Knuth did not find a single locality with prehistoric settlement to the east of Jørgen Brønlund Fjord. He also noted that driftwood was virtually absent on the ancient shorelines in the inner part of Independence Fjord, defined by a line from Kap Knud Rasmussen to Astrup Fjord. He believed that there may be a relationship between the absence of driftwood and of prehistoric settlements. Knuth thus suggests that the inner part of Independence Fjord could have been filled up with a glacier tongue protruding from Academy Glacier or it could have been so filled with calf ice that neither driftwood nor humans could enter the area. Knuth’s observations and interpretation may be correct. Studies of the mass balance and physiognomy of North Greenlandic glacier outlets have shown that open water conditions severely increase the calf ice production of floating glaciers (Weidick 2001)”.

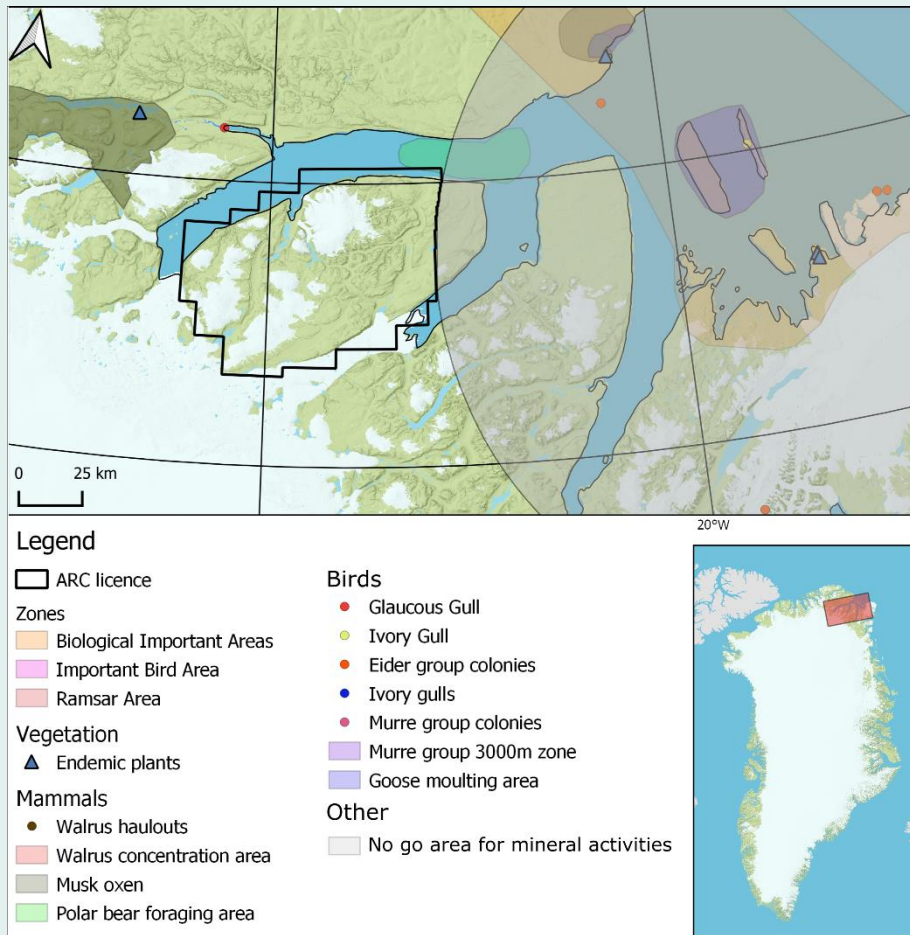
There are no designated environmentally sensitive areas within ARC. Musk ox are in the region, and polar bears may inhabit Independence Fjord (324). In 2011, no bears were sighted but Arctic Fox, seals, lemmings and Arctic Hare were observed (3).

A no-go area for mineral exploration activity is located immediately to the east of the licence (324). Air quality monitoring is carried out at the Villum Research Station (at Station Nord), and to aid with this activity restrictions are placed on nearby activity (13). If drilling, blasting or similarly disruptive exploration activities occur, it may be necessary to undertake environmental measurements and share the results of such with the public or relevant public institutions (325).

Greenfields is unaware of any prior environmental, social or community impact studies within ARC. As the Citronen deposit to the north was subject to a full Feasibility Study and Mining Licence review and documentation (326; 327; 328), guidance can be gained from these documents.

THERE ARE NO
DESIGNATED
ENVIRONMENTALLY
SENSITIVE AREAS
WITHIN ARC

Figure 91: Designated sites from the Government portal



Source: Greenfields using data from the NunaGIS.gl portal.

10.2 PROJECT INFRASTRUCTURE

There is no infrastructure within ARC. Rudimentary buildings (Kap Harald Moltke Station and Brønlundhus) are in Jørgen Brønlund Fjord, along with an airstrip capable of handling C130 aeroplanes. However, as deep-water fjords bound J.C. Christensen Land, minimal infrastructure is required to gain access to international markets. For base-metal projects, access to global export markets is economically essential (329). For example, the inland Kabanga nickel deposit in western Tanzania has a substantial size and grade combination but has remained undeveloped for more than two decades (330; 331; 332). Greenfields notes that the fjords around ARC provide seasonal²¹⁵ access to the market. However, the most recent research suggests that summer sea ice may disappear entirely by 2035²¹⁶ (49), which would have a material impact on ocean access well before this date. As the trend towards substantially improved sea-ice conditions across the Arctic is occurring in North Greenland, multiple new shipping options are increasingly available (333). Furthermore, the current surplus of Polar-class ships gives

DEEP WATER
FJORDS PROVIDE
MARKET ACCESS

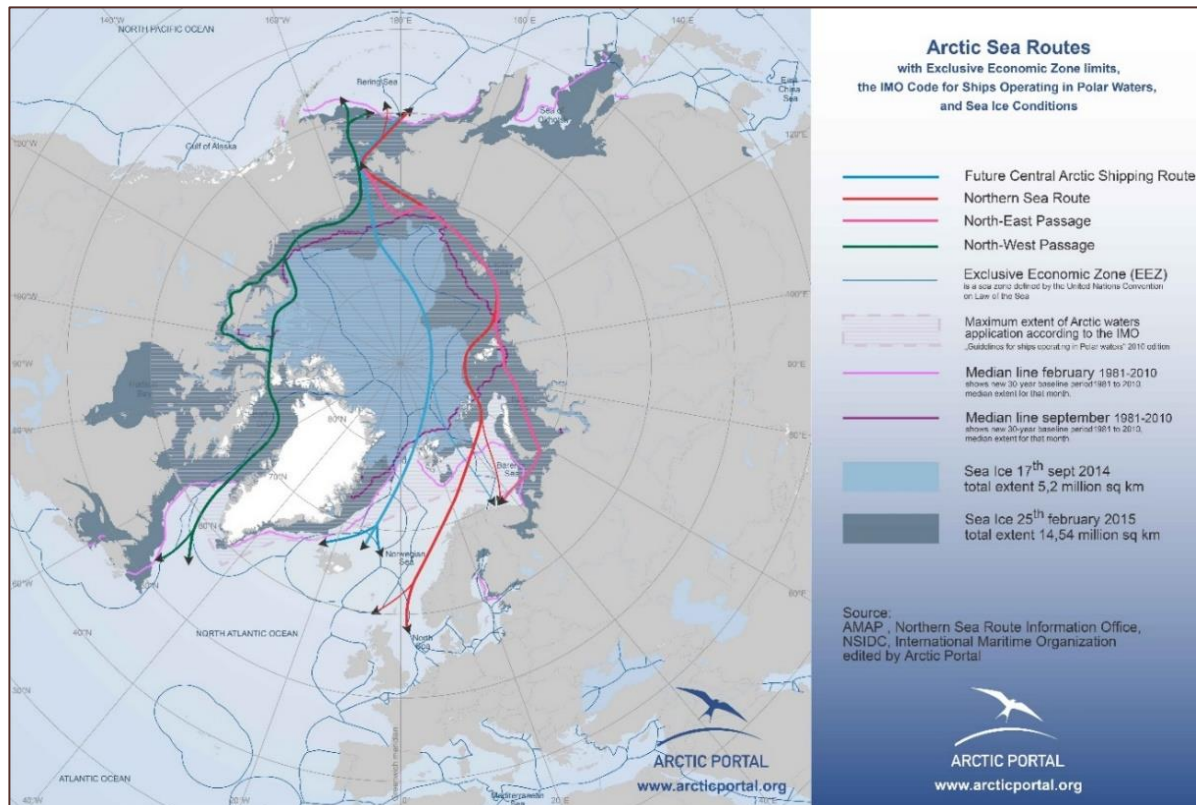
²¹⁵ Shipping windows will be constrained to when the fjords are ice-free. This will be contingent on which fjord, or subsidiary fjord is used.

²¹⁶ The Company notes these projections with extreme concern and takes this as a motivation to rapidly and responsibly develop high-quality, efficient mineral projects to supply the growing renewable economy.



additional logistical options during the exploration and evaluation phases (333). Once in production, ARC is well located for the European and North American markets, and potentially the Asian market through the Northern Sea Route (Figure 92). Greenfields notes that the presence of the sizeable Citronen deposit bodes well for a potential co-development with an ARC discovery, as both projects could significantly benefit from logistical co-operation. Furthermore, ARC's isolation from the general population allows for greater control over risks such as infectious diseases such as COVID-19. The benefits of being able to effectively isolate a work site is demonstrated by the production disparity between Australian and Latin American mines during 2020 (334).

Figure 92: Arctic sea routes



Source: Arctic Portal (2018) (335).

10.3 MINING METHODS

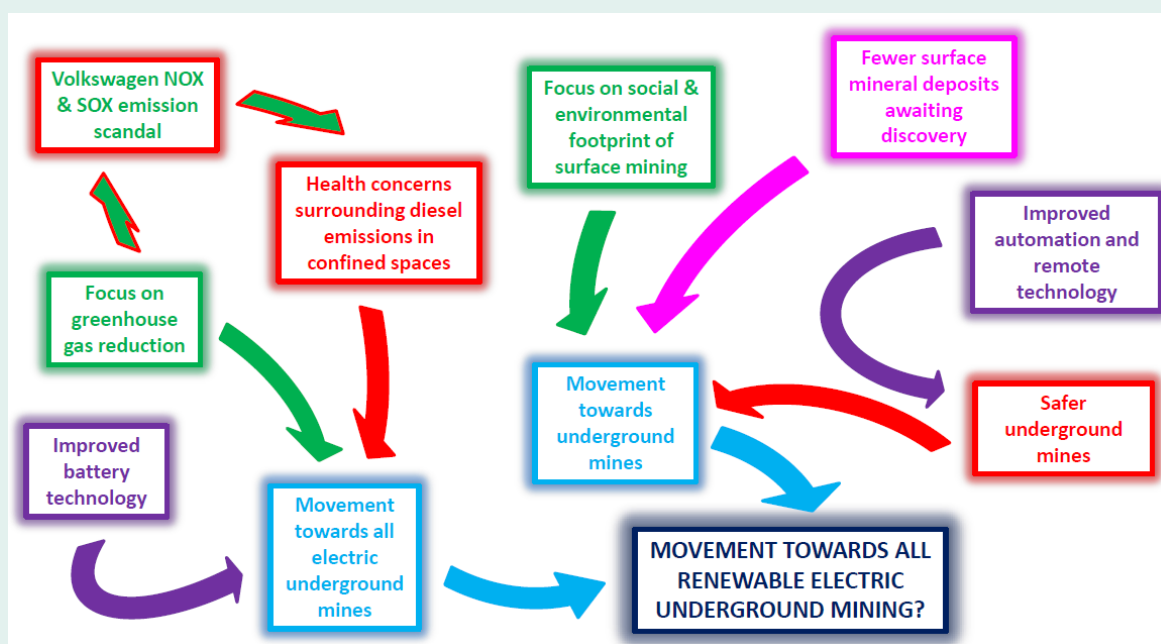
Many factors influence mining methods, including the shape, quantity, quality and location of the mineralisation. In the case of ARC, Greenfields highlights that the Project is located in an Arctic desert climate that experiences highly variable temperatures, and seasonal daylight (48; 36; 52). These factors may influence a mining method. Greenfields thinks that relative to more temperate climates, underground mining in the Arctic may be more favourable than open-pit equivalents as:

- severe temperature can negatively impact the performance of mobile and fixed equipment (336). Excess heat management is a consideration in most underground mines (337; 338), but in an Arctic environment such heat may represent an advantage over open-pit equivalents;
- visibility may be minimal during the winter months and snowstorms (whiteouts) which may negatively impact safety (339) and productivity;

- underground operations are at less risk from potentially destructive and life-threatening (340) katabatic winds²¹⁷;
- while mining is permitted in the area, the societal expectation is that the footprint of a mining operation is as small as reasonably possible. Given underground mines often use waste rock and tailing for filling voids, they may have lower permitting and environmental risk associated with them as compared to open-pit waste dumps and tailings dams²¹⁸ (341).

Furthermore, research by Sykes (2018) suggests that future mines are likely to increasingly trend towards underground mining methods due to an energy transition away from fossil fuels and steadily increasing health and environmental standards (Figure 93) (342). Greenfields considers that with the climatic considerations, it may also be economically favourable to have a dynamic mining plan that changes tempo with the season, or even switch to seasonal mining. Such dynamism, which conceptually could include seasonal operations, could be further encouraged using green energy that is most effective during the warmer half of the year.

Figure 93: Macro trends withing the mining industry



Source: Sykes (2018) (342).

10.4 MINERAL PROCESSING AND METALLURGICAL TESTING

No mineral processing or metallurgical test work has occurred on samples within ARC.

10.5 RECOVERY METHODS

A conceptual copper deposit in ARC is likely to comprise of native copper, or copper sulphides (e.g. chalcocite, chalcopyrite). The recovery of sulphide mineral species is reasonably well established through flotation. For chalcocite, there are precedents for producing direct shipping products (343; 344). For native copper, flotation was historically used although recovery using

²¹⁷ The Company is unaware of Piteraqa (katabatic) winds in the ARC region. However, it cannot discount their potential occurrence and until better information becomes available, the Company treats ARC as though it is subject to katabatic winds.

²¹⁸ Assuming tailings material can be incorporated into a paste suitable for back filling underground voids



gravity circuits may be preferential (345; 346; 347). However, modern sensor-based sorting²¹⁹ may be preferable for processing native copper (348; 349). A simple crush-screen-sort native copper flowsheet (350) may keep capital and operating costs lower than sulphide equivalents. Furthermore, native copper can require little to no chemical reagents which can have a significant positive impact on costs, logistics and environmental impacts. If native copper is processed, it also has the potential to produce a relatively environmentally benign product due to the low sulphur content (351).

**SIMPLE
BENEFICIATION,
DIRECT-
SHIPPING
POTENTIAL**

The ability to produce high-grade concentrates, either sulphide or native metal, reduces the volume of export material. Fewer ships and lower freight costs results from producing a highly concentrated product. Higher smelter payabilities can be expected for both copper and silver for high-grade concentrates (352). Furthermore, such high-grade material, especially if in the form of native copper, has the potential to have an inherently low level of carbon intensity. Conceptually, the carbon intensity can be further reduced by using green energy. Wind turbines are demonstrated to be effective for supplying mining operations in the Arctic (353; 354; 355; 356), and solar energy is a viable and simple²²⁰ means of supplying power (357). Furthermore, there is a nascent renewably sourced hydrogen industry in Iceland that may add another option for low-carbon recovery of metals (358; 359).

**LOW-CARBON
OPTIONS**

10.6 CAPITAL AND OPERATING COSTS

There are no material capital and operating costs for ARC. The Citronen zinc deposit was subject to multiple Feasibility Studies and may provide benchmarks to support first-principle estimates. In 2017, Ironbark estimated that for a 3.3 Mt per annum processing operation, the Citronen capital cost would be US\$514 M²²¹ (63). Citronen's estimated capital cost has no bearing on ARC, however useful data may be gleaned from that study.

10.7 MARKET STUDIES AND CONTRACTS

There are four market variables relevant to ARC, the copper and silver prices, and the US Dollar and Danish Krone currency exchange rates (Figure 94 to Figure 97). The Coronavirus pandemic of 2020 makes quantitative speculation on future metal prices fraught with risk. However, as copper is a mainstay commodity, there is always strong demand compared to other metal commodity types.

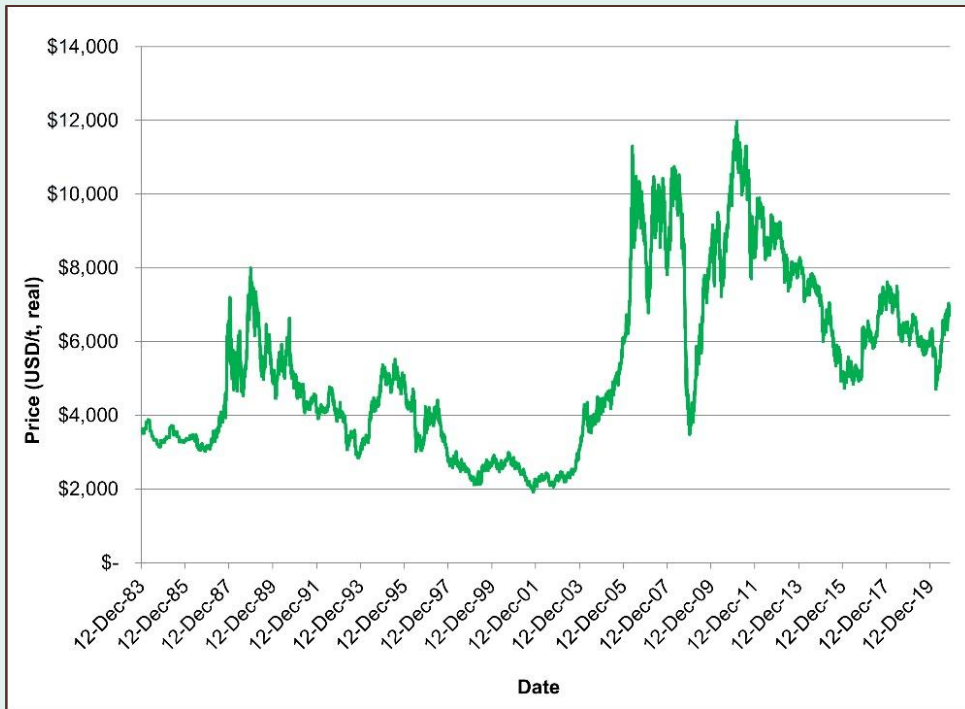
There are no third-party contracts that relate to ARC.

²¹⁹ 'ore' sorters such as optical, XRT, XRF, near infrared, radiometry, electromagnetic, colour (347). Note the term 'ore' is in the common language and must not be confused with the JORC term 'Ore'.

²²⁰ Solar power is significantly easier than wind power to permit, transport and assemble.

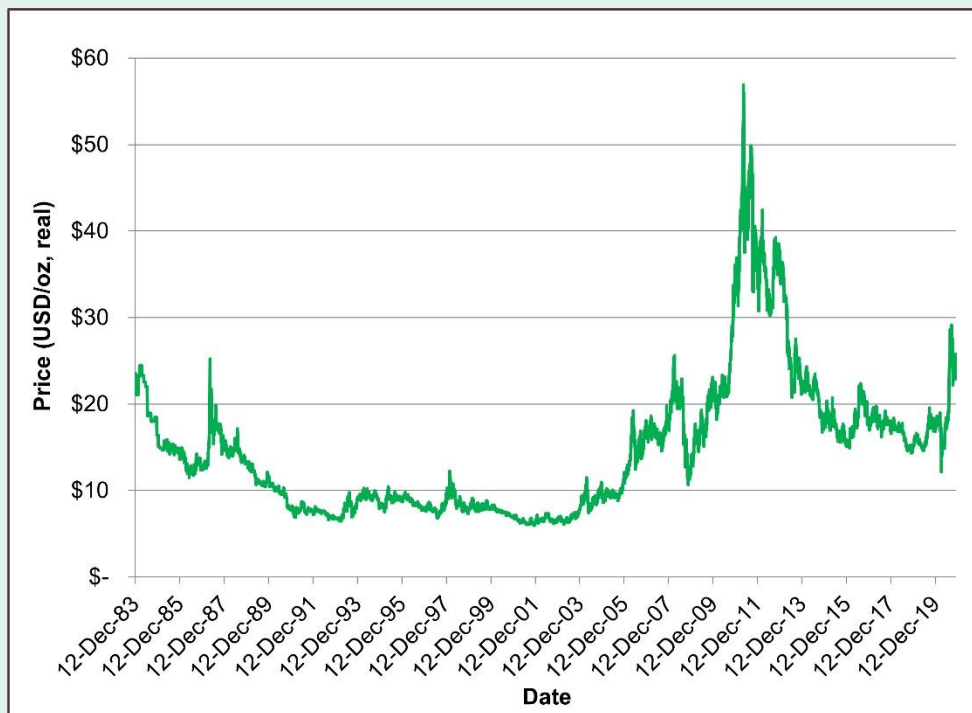
²²¹ On 7 September 2020, Ironbark announced that it had updated its capital cost estimate. However, the new monetary figure was not disclosed in that announcement (88).

Figure 94: Copper prices



Source: Collated by Greenfields using public domain data from the float of the AUD to 10 November 2020. Note: The prices adjusted for inflation.

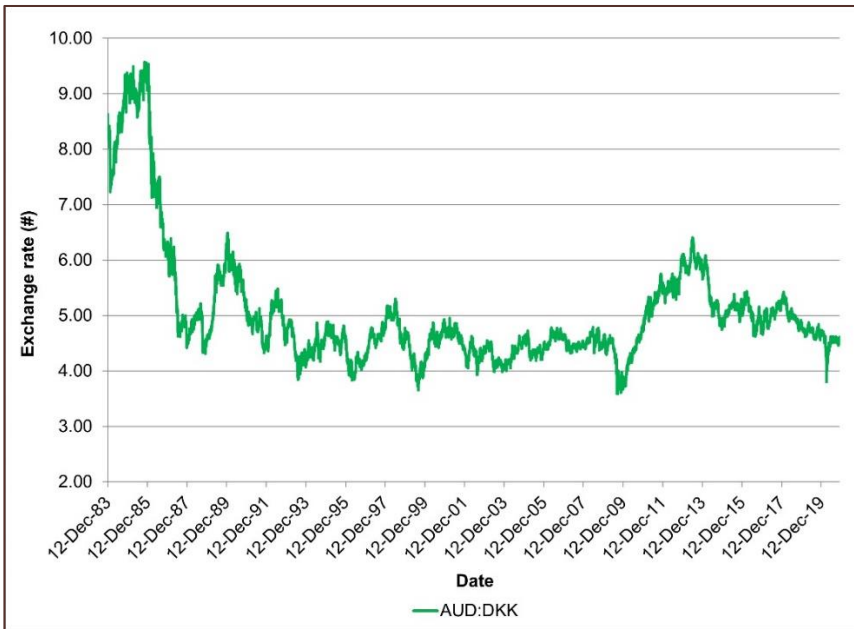
Figure 95: Silver prices



Source: Collated by Greenfields using public domain data from the float of the AUD to 10 November 2020. Note: The prices adjusted for inflation.



Figure 96: AUD-DKK exchange rate



Source: Collated by Greenfields using public domain data from the float of the AUD to 10 November 2020.

Figure 97: AUD-USD exchange rate



Source: Collated by Greenfields using public domain data from the float of the AUD to 10 November 2020.

10.8 ECONOMIC EVALUATIONS

No economic evaluations have ever been conducted within ARC.

11 ORE RESERVE ESTIMATES

ARC is at an early stage of exploration and there are no Ore Reserve estimates.

12 OTHER RELEVANT DATA AND INFORMATION

All relevant data and information are in the preceding sections.

13 INTERPRETATIONS AND CONCLUSIONS

13.1 NEW INSIGHTS

This Report presents the most holistic review of the ARC area to date. It brings together various facets and synthesises a new perspective using the mineral system approach. Based on the reviewed data and knowledge, the Report makes original contributions to the geological understanding of North Greenland. The main²²² contributions are that this Report:

1. explicitly states that much of North Greenland is part of a north-south trending mineral system that encapsulates the Citronen deposit²²³. Defining the Kiffaanngissuseq metal belt has a fundamental implication for regional exploration as the belt's orientation is sub-perpendicular²²⁴ to previous interpretations;
2. recognises that the c. 1,250 Ma Elzevirian Orogeny is fundamental as it provides a new thermodynamic event for explaining the copper enrichment in the basalt. The rhepsammites and granophyres being evidence of its intensity;
3. identifies the waning Caledonian Orogeny, at c. 385 Ma, as the geodynamic trigger that explains the presence of the high-grade copper sulphides in the post-Elzevirian sediments (Figure 98);
4. highlights a regional change in oxidation state as a fundamental feature in the mineral system;
5. links the alteration within the volcanics with the overlying sedimentary formations. This observation shows there is significant and widespread mineral system linkage between the sedimentary-rocks and the basalts;
6. identifies a singularity (multiple coincident anomalies) and postulates that it is the site of a hydrothermal outflow; and

Cumulatively, these new insights create a **significantly new, integrated understanding of North Greenland's geology**. Importantly, these insights significantly change the 'prospectivity map' and reduce the primary search space for copper to a well-constrained area within ARC.

NEW PARADIGM
THINKING, BIG
VALUE
REVELATION

²²² New findings considered by Greenfields to have less direct commercial relevance include: 1) correlating the palaeomagnetic flow direction of the Zig-Zag Fm a mantle plume located to Greenland's northeast; 2) noting that a previously disregarded sample of native iron may be evidence of proximal fluid activity; and 3) notes that microcline is associated with the most significant native copper deposits in the Keweenaw Peninsula, and that microcline is abundant within ARC's Discovery Zone. Similarly, it suggests that sericite and microcline might form a zonation around a conceptual deposit in ARC.

²²³ Clastic-dominated deposit type (formerly called Sedimentary Exhalative or 'SEDEX' (389)).

²²⁴ The prospectivity of the clastic-dominated deposit model was previously interpreted to have an ~east-west orientation that matched the Franklinian Basin and Ellesmerian Orogeny.



13.2 SIGNIFICANCE

By performing a holistic mineral system analysis, Greenfields has identified a **high-value copper target within the previously undescribed Kiffaangissuseq metallogenic province**. The approach produced a step-change in the understanding of a mineral system in one of the least explored portions of the world. The result is a near 90° rotation in the orientation of the prospective corridor, which substantially affects the search space. This dramatic revision of the understanding of an entire metal belt happens extremely rarely. Furthermore, this rotation has significant economic importance as it links the known copper mineralisation with a large zinc deposit. This linkage attests the intensity of the mineralising process in the world's newest²²⁵ metal belt. Importantly, due to the large scale and intensity of the well-constrained Kiffaangissuseq metallogenic province, ARC has world-class deposit potential.

The Company identifies that ARC's very high-grade copper is associated with the Minik Singularity, a coincident magnetic-electromagnetic-gravity feature in an area where there is a change in oxidation state and widespread native copper in stream sediments. These features are presented as the footprint of a large-scale hydrothermal system that is tightly constrained to being active c.1,250 Ma and again at c.385 Ma. The frequency and size of the native copper clasts, and the high grade of the copper-silver sulphides that are exposed at the surface, bode well for the probability of discovery. The size, grade, and probability of discovery make ARC an attractive economic proposition to the largest of mining companies.

Within the ARC portion of the mineral system, there are multiple sites of economic potential that can be tested. The highly anomalous basalt is a high-priority target that, remarkably, was never the focus of commercial exploration. The sulphide mineralised faults passing through these basalts into the overlying sediments have been subject to first-pass exploration and shown to be rich in copper and silver. The high-grades sulphides in these faults justify further exploration²²⁶. The permeable coarse-grained sandstone within the Jyske As Fm has high-grade stratiform copper that is effectively unexplored. This stratiform mineralisation adds the potential for significant lateral extension of the known mineralisation exposed in the faults of the Discovery Zone. As such, ARC mineral system is known to be prospective for basalt, fault, and stratiform-hosted mineralisation that despite the attractive grades, is virtually unexplored.

Being able to identify all the components of a large-scale mineral system, at the surface, with scant prior exploration²²⁷, within a single exploration licence, is unusual anywhere in the world. Furthermore, the weight of evidence is such that not only is a copper discovery relatively probable, but it could be extensive and high-quality. As Greenland is pro-mining, low-taxing and corruption-free, the Company believes there is an excellent framework to turn a discovery into a mine. While the main challenge will be shipborne transport in a small seasonal window, the sailing of a cargo ship to Citronen by Ironbark demonstrates that bulk logistics are possible. The development of a mine at Citronen significantly improves the logistics for ARC and vice versa. Furthermore, the logistics are improving each year with the inexorable and unfortunate, decline in sea ice. As such, **North Greenland has the potential not only to host a copper deposit but to be a substantial mining province** in the world's newest metal belt, Kiffaangissuseq.

**THE WEIGHT OF EVIDENCE IS THAT A COPPER DISCOVERY IS
RELATIVELY PROBABLE**

²²⁵ While Citronen was discovered in 1993 its presence was interpreted to be due to roughly east-west oriented metal belt.

²²⁶ By analogy to the 'fissures' on the Keweenaw Peninsula in Michigan, such cross-cutting features have the potential to contain extreme copper enrichment that leads to massive native copper accumulations.

²²⁷ Three years of commercial exploration work in the fifty years since copper was first described in the area.

13.3 KNOWLEDGE GAPS

Greenfields has holistically reviewed the available information on northern Greenland. The Company interprets there to be a compelling case for the presence and preservation of an extensive mineral system. Despite the weight of evidence, much of the information is old and of regional context. Consequently, knowledge gaps remain in the understanding of the Arctic rift in northern Greenland:

- **The cause of the geophysical component of the Minik Singularity.** Published lithological maps show no obvious reason for the geophysical responses. While sediment-hosted copper sulphides are not generally considered to be detectable in gravity or magnetic data, other types of sediment-hosted 'deposit types' do have such responses. The presence of high-grade native and copper sulphides close to the anomaly warrants a better understanding of the cause of the geophysical response²²⁸.
- **Source of the copper.** Greenfields puts forth its interpretation of the mineralisation history, although it is possible to create alternative hydrodynamic scenarios. It is uncertain if burial metamorphism of the basalts provided additional low-sulphur copper-bearing fluid. It is also unknown if there are basalts atop the basement²²⁹ which could act as a source of copper. Confirming the sedimentary and basaltic copper sources affects the fluid flow modelling used in future targeting work.
- **Structural relationships.** There are multiple faults and lineaments that appear to have reactivated. It is currently uncertain which structures are the most important in terms of a hydrodynamic model. Remote mapping and field mapping will help understand the structural component of the hydrodynamic framework.
- **Lithological relationships.** The reason for the stratigraphic offset difference between the Norsemandal Fm and Inuiteq SØ Fm on either side of Independence Fjord is not well described. This potentially large-scale feature can materially affect the understanding of the hydrodynamic framework and the prospective areas. Understanding the cause of the difference on either side of the Independence Fjord will help constrain the regional search space.
- **Magmatic Ni-PGE potential.** There is little knowledge or understanding of the Ni-PGE potential. Relatively easy fieldwork could drastically change ARC's economic potential for additional elements.

Gaining better insight into the above knowledge gaps will significantly improve the ability to model the mineral system through time. Such time dynamic models are valuable when targeting below the surface, or beneath cover. Addressing these knowledge gaps also helps to ensure that information turns into understanding. Fortunately, the knowledge gaps can be easily and rapidly addressed.

**BIG INCREASE IN
CERTAINTY FROM A
SINGLE FIELD
PROGRAM**

²²⁸ Site investigation of the geophysical response is warranted. However, Greenfields suspects that the source may be at depth and surface exposure above the area of interest may not provide any evidence.

²²⁹ Basalts are known to locate at the basement contact to the east of ARC, at Hekla Sund.



14 RECOMMENDATIONS

Greenfields recommends the use of a systemic approach to exploring ARC. The Company reasons that the most cost-effective and impactful approach is to:

1. **Conduct high-resolution satellite mapping.** Since the last exploration activity, commercial products available have become available at a 30 cm pixel resolution. These products include multispectral bands at coarser resolutions that can aid in identifying different types of alteration type and intensity, lithologies, and structures. Such information will help to refine geological maps. Improving the mapping is important as historically it was difficult to differentiate basalts and redbeds in airborne photos. The value of this work is in identifying permeability, alteration (e.g. Discovery Zone), oxidation state, and potentially fluid flow as evidenced through alteration. Any activity that increases the efficiency of the time-limited field campaigns is of high value.
2. **Re-analyse historical samples.** The assay suite used in the government-funded work is very restricted²³⁰. Greenfields has located the storage locations of 311²³¹ unique samples that are suited to comprehensive, modern analysis methods. The higher precision and additional element information, along with mineral species identification, can provide new insights that can help refine the exploration search space.
3. **Reprocess airborne magnetic data.** While the age of the data means that it is significantly below current standards, the cost of reprocessing and reinterpreting existing data is relatively low. It is unlikely that 'sediment-hosted copper' mineralisation is directly detected, however, indirect vectoring plays an important role in the discovery process.
4. **Create a three-dimensional model.** The available geological maps, reprocessed geophysics and satellite imagery can be incorporated into a low cost three-dimensional ('3D') model. The purpose of this model is to provide an initial framework design that can be easily validated by field inspection.
5. **Perform a passive seismic survey.** Understanding the subsurface distribution of the lithologies and sub-surface structure is fundamental to improving a 3D model which would initially be built using two-dimensional data. Seismic data will also provide more context to the gravity-magnetic anomaly. Passive seismic tomography does not require explosives or vibration equipment to collect data. Instead, the method relies on natural ambient sounds and spikes. As calving glaciers and movements within the inland ice sheet produce distinct and high-contrast sound events, ARC should be well suited to this method. The trade-off is that the measuring instruments need to be in position for periods of at least 30 days for a reliable and good resolution profile to be established. Passive seismic is low-cost, low environmental impact, and a highly portable 3D survey technique (360).
6. **Undertake a widespread geochemical sampling campaign.** There is useful first-pass geochemical data available for stream sediments. However, the data is clustered, and the southern portion of ARC is mostly

A DAY SAVED IN
THE FIELD HAS A
BIG MONETARY
PAYOFF

PASSIVE SEISMIC IS LOW-
COST, LOW IMPACT,
PORTABLE, AND YIELDS
3D INFORMATION

²³⁰ Of note is the lack of data on silver. This element occurs in both the native copper and copper sulphides and may improve direct detection potential of the existing stream sediment samples.

²³¹ A total of 405 samples are identified, of which 311 are unique, and 40 have been subject to more recent analysis.

unsampled. The stream sediment samples overall have a low density of ~1 sample per 80 km² within ARC²³². Historical rock chip samples appear to incorporate a lithological bias towards the sedimentary units. There is an opportunity to conduct widespread stream sediment and rock chip sampling. Ideally, rock samples are collected with a handheld drill to produce core that can be subject to non-destructive analysis²³³. Much of the infill sampling should focus on the permeable portions of the Zig-Zag Fm. This work can be done while the passive seismic nodes are collecting data (typically 30 days) and has the benefit of adding additional noise sources to the seismic data.

7. **Constrain the mineralising events.** By analysing the copper isotopes²³⁴, a better constraint on the timing of the multiple mineralising events can be gained. Copper dating is important in the understanding of the timing (single or two stages). Similarly, geochemical analysis of magnetite can uncover the formative fluids. The mineral system within ARC contains multiple sources of potential fluids (metamorphic, magmatic-hydrothermal, evaporitic brines, seawater, and meteoric waters). Confirming the timing and origin of the fluids and metals is key to recreating the mineral system through time, and modelling targets accordingly.
8. **Create a system model.** A spatial and temporal ('4D') model for the Kiffaangissuseq metal belt should be created once more, and better data is obtained. It is important to emphasise that a 4D model requires field data on where non-copper bearing fluids have flown. The intent is for the 4D model to aid in generating more advanced exploration targets undercover²³⁵ within ARC and its immediate surrounds.

The proposed exploration above could be completed within eighteen months and creates the potential for discovery from the outset. This approach has low cost²³⁶ per unit of information gained and permits a significant increase in the targeting accuracy. Based on Greenfields' in-country experience and indicative quotes, the proposed work program may cost in the order of \$4.5 M (Table 7). After creating a 4D simulation, a new work plan will be required to be tailored to the results. The company envisages that the proposed work program will yield relatively high-certainty, drill-ready targets.

DESIGNED FOR
CERTAINTY

²³² This simple calculation of sample density includes inaccessible areas within the boundary of ARC including glaciers and fjords.

²³³ Modern non-destructive methods can provide information on three-dimensional elemental concentrations, rock density, particle size and distribution, and structural information. Such additional information can provide a greater understanding of the relationships between the mineral phases, allowing for better exploration targeting. The additional information is also of great value in understanding metal distribution, metallurgical qualities, and impacts on mining. Use of non-destructive methods is preferential to destructive methods as a first pass as more diverse information is gleaned from the sample (more than just an assay result) and the sample can be reanalysed when better technologies arise, or if high-resolution destructive methods are warranted. Given the cost of securing samples, their destruction should be avoided wherever possible.

²³⁴ ⁶³Cu and ⁶⁵Cu (298).

²³⁵ While exposure is spectacular in the fjords and steep mountains, much of the accessible areas are under cover.

²³⁶ It is also noteworthy that the combination of a dry Arctic desert and passive-seismic surveying means that the field season can begin early relative to most other field programs in Greenland. This allows for a trade between movement speed with program duration without potentially distorting costs, making alternative transport methods, such as all-terrain vehicles ('ATV'), a potential alternative to extensive helicopter use. However, special dispensation will need to be obtained from the government before ATVs can be used in the Park. Until such permission is granted by the Government, Greenfields assumes a 100% helicopter supported program.



Table 7: Proposed budget

Component	Cost (AUD)
Field work	\$3,060,000
Passive seismic	\$150,000
Satellite data	\$200,000
Sample re-analysis	\$120,000
Consultants	\$130,000
Overheads	\$490,000
Contingency	\$350,000
TOTAL	\$4,500,000

Source: Greenfields.

For safety and cost-effectiveness, Greenfields recommends the coordination of logistics with Ironbark's activities at Citronen and the Korea Polar Research Institute²³⁷. The Company also recommends that other groups, such as government, and academic institutions, be invited to join the field programs. Both Government and academic institutions will require significant lead-up times to commit a collaborative work program, however, the potential cost-saving and knowledge-generating synergies justify the effort.

Figure 98: Chalcocite filled vesicles of the Zig-Zag Fm



Source: Tukiainen & Lind (2011) (128). Note: The chalcocite appears light grey in colour due to metallic reflections. The sample is approximately 4cm in width. Small hydrothermal veins connecting the vesicles demonstrate permeability. The approximate sample location is 80.64°N, 24.59°W.

THE GOAL IS TO BE
DRILL-READY BY THE
END OF THIS
PROGRAM

²³⁷ Greenfields understands that the Korea Polar Research Institute is planning to work in Peary Land in 2021, and that there is potential to share logistics and facilities at Kap Harald Moltke station.

15 REFERENCES

1. **GEUS.** GEUS Web Shop. *Greenland Portal*. [Online] [Cited: 1 March 2020.] <https://frisbee.geus.dk/webshop/index.jsp>.
2. **Haugaard, R.** *Technical Report on the 2010 Exploration Program: Geological work carried out under exploration license 2010/ 32 and prospecting license 2010/ 35: Sediment-hosted copper and silver mineralisation in J.C. Christensen Land, North Greenland*. London : Avannaa Resources Ltd, 2011. GEUS Report file no: 22542.
3. **Rehnström, E. F.** *Geological Report from the 2011 Field Program: Work Carried Out Under Licenses 2010/32, 2010/35 and 2011/30: Sediment Hosted Copper Mineralisation in Eastern North Greenland*. London : Avannaa Exploration Ltd, 2012. GEUS Report file no. 22606.
4. **Rasmussen, T. M.** *Airborne Electromagnetic and Magnetic Survey of North-Eastern J.C. Christensen Land, Eastern North Greenland*. Copenhagen : Grønlands Geologiske Undersøgelse, 1999. GEUS Report file no. 16108.
5. **JORC.** *Australasian Code For Reporting of Exploration Results, Mineral Resources and Ore Reserves - the JORC Code*. s.l. : The Joint Ore Reserves Committee of The Australasian Institute of Mining and Metallurgy, Australian Institute of Geoscientists and Minerals Council of Australia, 2012.
6. **VALMIN.** *Australasian Code For Reporting for Public Reporting of technical Assessments and Valuations of Mineral Assets - The VALMIN Code*. s.l. : The VALMIN Committee of the Australasian Institute of Mining and Metallurgy and the Australian Institute of Geoscientists, 2015.
7. **ASIC.** Regulatory Guide 111: Content of Expert Reports. *Australian Securities & Investments Commission*. [Online] March 2011a. [Cited: 22 July 2020.] <http://download.asic.gov.au/media/1240152/rg111-30032011.pdf>.
8. —. RG 112 Independence of Experts. *Australian Securities and Investments Commission*. [Online] 30 March 2011b. [Cited: 22 July 2020.] <http://asic.gov.au/regulatory-resources/find-a-document/regulatory-guides/rg-112-independence-of-experts/>.
9. —. Regulatory Guide 170: Prospective Financial Information. *Australian Securities & Investments Commission*. [Online] April 2011c. [Cited: 22 July 2020.] <http://download.asic.gov.au/media/1240943/rg170-010411.pdf>.
10. **NI43-101.** Standards & Guidelines for Resources & Reserves. *Canadian Institute of Mining, Metallurgy and Petroleum*. [Online] 24 June 2011. [Cited: 22 July 2020.] http://web.cim.org/standards/documents/Block484_Doc111.pdf.
11. **ASX.** Listing Rules Chapter 5. *Australian Securities Exchange*. [Online] 1 July 2014. [Cited: 22 July 2020.] <http://www.asx.com.au/documents/rules/Chapter05.pdf>.
12. **van der Stijl, Frank W and Mosher, Greg Z.** *The Citronen Fjord Massive Sulphide Deposit, Peary Land, North Greenland: Discovery, Stratigraphy, Mineralization and Structural Setting*. Copenhagen : Geological Survey of Denmark and Greenland, 1998. Bulletin 179.
13. **Villum Research.** [Online] Aarhus University, 2020. [Cited: 22 July 2020.] <https://villumresearchstation.dk/>.
14. *To See What State We Are In: First Years of the Greenland Self-Government Act and the Pursuit of Inuit Sovereignty*. **Kuokkanen, R.** 2, s.l. : Taylor & Francis, 2017, *Ethnopolitics*, Vol. 16, pp. 179-195. <https://doi.org/10.1080/17449057.2015.1074393>.
15. **CIA.** Greenland. *The World Factbook*. [Online] Central Intelligence Agency, 9 June 2020. [Cited: 14 July 2020.] <https://www.cia.gov/library/publications/the-world-factbook/geos/gl.html>.



16. **ABS.** Australian Bureau of Statistics - Australian Demographic Statistics. [Online] 19 December 2019. [Cited: 14 July 2020.] [https://www.abs.gov.au/ausstats/abs@.nsf/0/1CD2B1952AFC5E7ACA257298000F2E76?OpenDocument#:~:text=The%20median%20age%20\(the%20age,remained%20steady%20at%2037%20years..](https://www.abs.gov.au/ausstats/abs@.nsf/0/1CD2B1952AFC5E7ACA257298000F2E76?OpenDocument#:~:text=The%20median%20age%20(the%20age,remained%20steady%20at%2037%20years..)
17. *Mineral Riches, A Route to Greenland's Independence?* **Taagholt, J., Brooks, K.** 3, Copenhagen : Cambridge Core, 2016, Polar Record, Vol. 52, pp. 360-371. <https://doi.org/10.1017/S0032247415000935>.
18. *Chinese Investment in Greenland's Mining Industry. Toward a New Framework for Foreign Direct Investment.* **Têtu, P., Lasserre, F.** 3, s.l. : Elsevier, July 2017, The Extractive Industries and Society, Vol. 4, pp. 661-671. <https://doi.org/10.1016/j.exis.2017.05.008>.
19. *Contemplating Governance for Social Sustainability in Mining in Greenland.* **Tiainen, H.** 282-289, s.l. : Elsevier, September 2016, Resources Policy, Vol. 49, pp. 282-289. <https://doi.org/10.1016/j.resourpol.2016.06.009>.
20. **TI.** Corruption Around the World in 2019. [Online] 2019. [Cited: 22 July 2020.] <https://www.transparency.org/research/cpi/overview>.
21. **UN.** International Human Development Indicators. [Online] 2019. [Cited: 22 July 2020.] <http://hdr.undp.org/en/countries>.
22. **CATO.** Human Freedom Index. [Online] 2019. [Cited: 22 July 2020.] <https://www.cato.org/human-freedom-index>.
23. **Naalakkersuisut.** *Unofficial consolidation of the Mineral Resources Act.* s.l. : Government of Greenland, 28 November 2016.
24. —. *Standard Terms for Exploration Licences for Minerals (Excluding Hydrocarbons) in Greenland.* [Legislation] 25 June 2013.
25. —. Organisational Structure. *GovMin.* [Online] Government of Greenland, 2020. [Cited: 22 July 2020.] <https://govmin.gl/about-us/organizational-structure/>.
26. —. Online Applications Portal. *Govmin.* [Online] 2018. [Cited: 13 July 2020.] <https://portal.govmin.gl/dashboard>.
27. —. Guidelines. *Mineral Resources Authority.* [Online] 2019. <https://govmin.gl/local-mining/small-scale-mining/guidelines/>.
28. —. How to get a Licence. *Mineral Resources Authority.* [Online] 2020. [Cited: 26 October 2020.]
29. **Bjørnshauge, Samuel í Geil .** *Subject: Sv: Clarification (Nanoq - ID nr.: 7524094).* [email to J.A. Bell 19 March 2018] Nuuk : Government of Greenland, 2018. Nanoq - ID nr.: 7524094).
30. **DMP.** Fees and Charges 2020-21. *Government of Western Australia Department of Mines, Industry Regulation and Safety.* [Online] 1 July 2020. [Cited: 14 July 2020.] https://www.dmp.wa.gov.au/Documents/Minerals/Minerals-Feesandcharges_2020-21.pdf.
31. **Bjørnshauge, Samuel í Geil .** *Subject: Follow-up on the question related to additional environmental permits (Nanoq - ID nr.: 7558209).* [email to J.A. Bell 23 March 2018] Nuuk : Government of Greenland, 2018. Nanoq - ID nr.: 7558209.
32. **Lexology.** Getting the Deal Through, Mining Greenland (2020). [Online] <https://www.lexology.com/gtdt/tool/workareas/report/mining/chapter/greenland>, 2020. [Cited: 27 July 2020.] <https://www.lexology.com/gtdt/tool/workareas/report/mining/chapter/greenland>.
33. **Naalakkersuisut.** Amendment to the Mineral Resources Act . *Mineral Resources Authority.* [Online] 28 January 2020. [Cited: 27 July 2020.] <https://govmin.gl/2020/01/amendment-to-the-mineral-resources-act/>.

34. —. How to get an Exploitation Licence. *GovMin*. [Online] Government of Greenland, 2020. [Cited: 27 July 2020.] <https://govmin.gl/exploitation/get-an-exploitation-licence/how-to-get-an-exploitation-licence/>.
35. —. Exploitation Permit (§16). *GovMin*. [Online] Greenland Government, 2020. [Cited: 27 July 2020.] <https://govmin.gl/exploitation/get-an-exploitation-licence/exploitation-permit-%c2%a716/>.
36. *Ittoqqortoormiit and the National Park of Greenland. A Community's Option for Tourism Development*. **Tommasini, D.** 3, Roskilde : Cambridge University Press, 2013, *The Polar Record*, Vol. 49, pp. 237-239. <https://doi.org/10.1017/S0032247412000691>.
37. **UNESCO**. Biosphere Reserves in Europe & North America. [Online] United Nations Educational, Scientific and Cultural Organization, 2019. [Cited: 26 October 2020.] <https://en.unesco.org/biosphere/eu-na>.
38. **Ironbark**. ASX Announcements >>2016. *Ironbark Zinc Ltd*. [Online] 19 December 2016. [Cited: 24 February 2018.] ASX Announcements >>2016. <https://ironbark.gl/investor-centre/asx-announcements/2016-2/>.
39. **Hollis, J.** *Re: your enquiry (Nanoq - ID nr.: 5290851)*. [email] Nuuk : Ministry of Mineral Resources, 29 April 2017.
40. **Statistics Denmark**. Consumer Price Index. *Statistics Denmark*. [Online] 2020. [Cited: 14 July 2020.] <https://www.dst.dk/en/Statistik/emner/priser-og-forbrug/forbrugerpriser/forbrugerprisindeks>.
41. **Naalakkersuisut**. Adjustment of exploration obligations for 2020 to zero. *Mineral Resources Authority*. [Online] 2 April 2020. <https://govmin.gl/2020/04/adjustment-of-exploration-obligations-for-2020-to-zero/>.
42. —. Government of Greenland provides additional help to mineral licensees. *Mineral Resources Authority*. [Online] 26 May 2020. <https://govmin.gl/2020/05/government-of-greenland-provides-additional-help-to-mineral-licensees/>.
43. **Government of Greenland**. Additional adjustments of the exploration obligations and a one-year extension of the licence period. [Online] 28 August 2020. [Cited: 29 September 2020.] <https://govmin.gl/2020/08/additionally-adjustments-of-the-exploration-obligations-and-a-one-year-extension-of-the-licence-period/>.
44. **Bloomberg**. Bloomberg Markets. [Online] 14 July 2020. [Cited: 14 July 2020.] <https://www.bloomberg.com/quote/AUDDKK:CUR>.
45. **Naalakkersuisut**. Greenland Parliament Act No. 39 of 28 November 2019 concerning the amendment of [...]. [Online] 28 November 2019. <https://govmin.gl/wp-content/uploads/2020/01/Greenland-Parliament-Act-No.-39-of-28-November-2019-1.pdf>.
46. —. *Explanatory Notes to the Bill (Act No 39 of 28 November 2019)*. [Explanatory Memorandum] 2019.
47. —. New Mineral Acts Postponed. *Mineral Resources Authority*. [Online] 15 April 2020. <https://govmin.gl/2020/04/new-mineral-acts-postponed/>.
48. **TimeAndDate**. Station Nord, Greenland — Sunrise, Sunset, and Daylength, July 2020. *tineanddate.com*. [Online] Time and Date AS, 2020. [Cited: 22 July 2020.] <https://www.timeanddate.com/sun/greenland/station-nord>.
49. *Sea-ice-free Arctic during the Last Interglacial supports fast future loss*. **Guarino, M., Sime, L. C., Schröder, D., Malmierca-Vallet, I., Rosenblum, E., Ringer, M., Ridley, J., Feltham, D., Bitz, C., Steig, E. J., Wolff, E., Stroeve, J., Sellar, A.** s.l. : Nature Research, 2020, *Nature Climate Change*, Vol. 10, pp. 928-932. <https://doi.org/10.1038/s41558-020-0865-2>.
50. *Past Perspectives on the Present Era of Abrupt Arctic Climate Change*. **Jansen, E., Christensen, J. H., Dokken, T., Nisancioglu, K. H., Vinther, B. M., Capron, E., Guo, C., Jensen, M. F., Langen,**



P. L., Pedersen, R. A., Yang, S., Bentsen, M., Kjaer, H. A., Sadatzki, H., Sessford, E., Stendel, M. s.l. : Nature Research, 2020, Nature Climate Change, Vol. 10, pp. 714-721. <https://doi.org/10.1038/s41558-020-0860-7>.

51. **Schultz-Nielsen, J.** Study: Temperature Rises Faster Than Expected in the Arctic. [Online] Sermitsiaq, 29 July 2020. [Cited: 30 July 2020.] <https://sermitsiaq.ag/studietemperatur-stiger-hurtigere-ventet-i-arktis>.

52. **TimeAndDate.** Climate & Weather Averages in Station Nord, Greenland. [Online] Time and Date AS, 2020. [Cited: 21 July 2020.] <https://www.timeanddate.com/weather/greenland/station-nord/climate>.

53. **NASA.** C-130 Hercules #439 03/24/15. [Online] National Aeronautical and Space Agency, 2015. [Cited: 1 August 2020.] https://espo.nasa.gov/flight_reports/C-130_Hercules_439_03_24_15.

54. **Blog Before Flight.** Canadian C17 Lands for First time on Frozen Runway. *Blog Before Flight*. [Online] 17 February 2017. [Cited: 22 July 2020.] <https://www.blogbeforeflight.net/2017/02/canadian-c17-lands-for-fist-time-on-frozen-runway.html>.

55. **Villum Research.** SITE MANUAL Villum Research Station, Station Nord, 2015. [Online] Villum Research Station, 2015. [Cited: 22 July 2020.] https://asp-net.org/sites/default/files/website_files/Station%20Nord%20-%20Site%20Manual%202015-01-20.pdf.

56. **Norlandair.** Greenland. [Online] 2020. [Cited: 22 July 2020.] <https://www.norlandair.is/en/pictures/greenland?page=2>.

57. **Peel, J. S., Sonderholm, M.** *Sedimentary Basins of North Greenland*. Copenhagen : Grønlands Geologiske Undersøgelse, 1991. GEUS Report file no. 22312.

58. **Patterson, J. M., Campbell, D. L.** *Geology and Mineral Potential of the Independence Fjord Concession*. Alberta : J.C. Sproule and Associates Ltd, 1973. GEUS report file: 20809.

59. **NANOK.** *Field Report from the Journey to Northeast Greenland in the Summer 2001*. Copenhagen : North East Greenland Company, 2001.

60. **ISAFFIK.** Kap Harald Moltke Station. [Online] ISAFFIK - the arctic gateway, 2020. [Cited: 23 July 2020.] <https://www.isaaffik.org/kap-harald-moltke-station>.

61. **Grønnow, B., Jensen, J. F.** *The Northernmost Ruins of the Globe*. Copenhagen : Museum Tusulanum Press, 2003. Vol. 329. ISBN 87-90369-65-3.

62. **Arktisk Kommando.** Joint Arctic Command. [Online] Danish Defence, 13 April 2020. [Cited: 22 July 2020.] <https://www.facebook.com/JointArcticCommand>.

63. **Ironbark.** *Feasibility Study*. Perth : Ironbark Zinc Ltd, 2017.

64. —. Milestone Achievement - Ship Route Proven. [Online] Ironbark Zinc Ltd, 30 August 2018. [Cited: 22 July 2020.] <https://ironbark.gl/investor-centre/asx-announcements/2018-2/>.

65. —. *Shipping and Site Preparation Update at the Citronen Project*. Perth : Ironbark Zinc Ltd, 2018.

66. *Trend and Interannual Variability in Southeast Greenland Sea Ice: Impacts on Coastal Greenland Climate Variability*. **Moore, G. W. K., Straneo, F., Oltmanns, M.** 23, s.l. : AGU, December 2014, Geophysical Research Letter, Vol. 41, pp. 8619-8626. <https://doi.org/10.1002/2014GL062107>.

67. **NSIDC.** Arctic Sea Ice News & Analysis. [Online] National Snow & Ice Data Centre, 2020. [Cited: 11 November 2020.] <http://nsidc.org/arcticseaicenews/>.

68. *Dynamic ice loss from the Greenland Ice Sheet driven by sustained glacier retreat*. **King, M. D., Howat, I. M., Candela, S. G., Noh, M. J., Jeong, S., Noël, B. P. Y., van den Broek, M. R., Wouters, B., Negrete, A.** 1, s.l. : Nature Research, 2020, Nature Communications Earth & Environment, Vol. 1. <https://doi.org/10.1038/s43247-020-0001-2>.

69. **SentinelHub**. Sentinel Playground. [Online] Sinergise, 12 July 2020. [Cited: 14 July 2020.] <https://www.sentinel-hub.com/explore/sentinelplayground/>.
70. **Naalakkersuisut**. Mining History. *Govmin*. [Online] Government of Greenland, 2018. [Cited: 20 February 2018.] <https://www.govmin.gl/minerals/mining-history>.
71. *Importance of Geochemistry: The Black Angel Lead-zinc Mine, Greenland*. **Poling, G. W., Ellis, D. V.** 1-2, s.l. : Taylor & Francis, 1995, Marine Georesources & Geotechnology, Vol. 13, pp. 101-118. <https://doi.org/10.1080/10641199509388280>.
72. *Exploitation of Lead and Zinc Deposits at Mesters Vig*. **Polar Record**. 58, s.l. : Cambridge University Press, 1958, Polar Record, Vol. 9, pp. 50-51. <https://doi.org/10.1017/S0032247400048907>.
73. *A Palaeoproterozoic Multi-stage Hydrothermal Alteration System at Nalunaq Gold Deposit, South Greenland*. **Bell, R., Kolb, J., Waight, T. E., Bagas, L., Thomsen, T. B.** s.l. : Springer, 2017, Mineralium Deposita, Vol. 52, pp. 383-404. <https://doi.org/10.1007/s00126-016-0667-7>.
74. **Kolb, J.** History of Mining. [book auth.] R., Bjerkgård, T., Nordahl, B., Schiellerup, H. Boyd. *Mineral Resource in the Arctic*. Trondheim : Geological Survey of Norway, 2016.
75. *Ivigut Cryolite and Modern Greenland*. **Lloyd, T.** 3, s.l. : Wiley, 1953, Canadian Geographer, Vol. 1, pp. 39-52. <https://doi.org/10.1111/j.1541-0064.1953.tb01724.x>.
76. **Alba**. Amitsoq Graphite, Greenland. *Alba Mineral Resources*. [Online] Alba Mineral Resources Plc, 2018. [Cited: 20 February 2018.] <http://www.albamineralresources.com/page.php?PID=13>.
77. **GEUS**. The Black Angel Lead-zinc Mine at Maarmorilik. *Geology and Ore: Exploration and Mining in Greenland*. 2, 2003, Vol. 2.
78. **ARC**. Mining Operation. [Online] Arctic Resources Capital, 2020. [Cited: 24 July 2020.] <http://arctic-resources.com/services/>.
79. **Nordisk**. *Copper/lead/silver project, Devondal, Preliminary study*. Copenhagen : Nordisk Mineselskab A/A, 1983. GEUS report file: 21049.
80. —. *Scheelite Project, Ymers Ø Pre Feasibility Study*. Copenhagen : Nordisk Mineselskab, 1982.
81. **Fouche, G.** Chinese Firm Unlikely to Develop \$2 Billion Greenland Iron Ore Mine Soon: Minister. *Reuters*. [Online] 27 January 2016. [Cited: 14 March 2018.] <https://www.reuters.com/article/us-greenland-mining-china/chinese-firm-unlikely-to-develop-2-billion-greenland-iron-ore-mine-soon-minister-idUSKCN0V425D>.
82. **TetraTech**. Feasibility Study for Malmbjerg Project Molybdenum Mine Development. *TetraTech Inc.* [Online] 2010. [Cited: 2 February 2018.] <http://www.tetrattech.com/pdf/download?url=http://localhost%252fen%252fdocs%252fdp14%252d023%252den%252dmalmbjerg%252dproject%252epdf>.
83. **Greenland Rubies**. News and Events. *Greenland Rubies A/A*. [Online] 11 May 17. [Cited: 22 February 2018.] http://greenlandruby.gl/pr_170511.html.
84. **HUD**. Presentations. [Online] 2 January 2018. [Cited: 2 March 2018.] https://hudsonresourcesinc.com/wp-content/uploads/2018/02/Hudson_January_2018.pdf.
85. **Ironbark**. ASX announcements. [Online] 15 January 2018. [Cited: 22 February 2018.] <https://ironbark.gl/investor-centre/asx-announcements/2018-2/>.
86. —. Ironbark Receives LOI from US Export-Import Bank. *ASX Announcements*. [Online] 2 November 2020. [Cited: 2 November 2020.] <https://ironbark.gl/investor-centre/asx-announcements/2020-2/>.
87. —. Feasibility Study. [Online] 12 September 2017. [Cited: 27 July 2020.] <https://ironbark.gl/investor-centre/asx-announcements/2017-2/>.



88. —. Citronen Mine Plan Optimisation. [Online] 9 September 2020. [Cited: 10 September 2020.] <https://www.asx.com.au/asxpdf/20200907/pdf/44mcsqcf1bh2rr.pdf>.
89. **GGG**. ASX announcements. [Online] 11 October 2017. [Cited: 22 February 2018.] <http://www.ggg.gl/docs/ASX-announcements/Maritime%20Safety%20Study.pdf>.
90. —. ASX announcements. [Online] 6 April 2016. [Cited: 2 March 2018.] <http://www.ggg.gl/docs/ASX-announcements/Feasibility-Study-Update-April-2016.pdf>.
91. **Bluejay**. Dundas Ilmenite Project. [Online] Bluejay Mining Plc, 2018. [Cited: 2 March 2018.] <https://www.titanium.gl/projects/dundas-ilmenite-project/>.
92. —. Summary of Pre-Feasibility Study for the Dundas Ilmenite Project. [Online] 27 June 2019. [Cited: 24 July 2020.] https://polaris.brighterir.com/public/bluejay_mining/news/rns/story/wk5z7yw.
93. **Greenland Anorthosite Mining**. Greenland Anorthosite Resources A/S and Greenland Anorthosite Mining ApS. *LinkedIn*. [Online] Microsoft Corporation, 2020. [Cited: 27 July 2020.] <https://www.linkedin.com/company/greenland-anorthosite-resources-a-s/about/>.
94. **Thaarup, Simon M, et al.** *Study on Arctic Mining in Greenland*. Helsinki : Ministry of Economic Affairs and Employment, 2020. ISBN PDF: 978-952-327-567-6.
95. **PGM**. Skaergaard. [Online] Platina Resources Ltd, 2017. [Cited: 4 March 2018.] <https://www.platinaresources.com.au/projects/skaergaard/>.
96. **Naalakkersuisut**. Anglo American is Now a Licensee. [Online] Government of Greenland, 31 July 2019. [Cited: 27 July 2020.] https://naalakkersuisut.gl/en/Naalakkersuisut/News/2019/07/3107_AngloAmerican.
97. **BlueJay**. Agreement with Rio Tinto Iron and Titanium Canada Inc. [Online] Bluejay Mining Plc, 28 May 2019. [Cited: 24 July 2020.] https://polaris.brighterir.com/public/bluejay_mining/news/rns/story/rdp233r.
98. **Sermitsiaq**. Renewed Uranium Interest Worries Environmental Organization [translated from Danish]. [Online] Sermitsiaq AG, 3 May 2020. [Cited: 24 July 2020.] <https://sermitsiaq.ag/node/221310>.
99. **IGO**. Macquarie Australia Conference. [Online] 7 May 2020. [Cited: 27 July 2020.] <https://www.igo.com.au/site/PDF/116207e2-65d5-489f-8142-1bf63da39029/MacquarieAustraliaConference>.
100. **GEUS**. The Blyklippen lead-zinc Mine at Mesters Vig, East Greenland. *Geology and Ore: Exploration and mining in Greenland*. 5, December 2005.
101. **MLSA**. Online Applications Portal. [Online] Government of Greenland, 27 July 2020. [Cited: 27 July 2020.] <https://portal.govmin.gl/dashboard>.
102. **Alien Metals**. <https://www.alienmetals.uk/news>. *Alien Metals*. [Online] 26 October 2020. [Cited: 27 October 2020.] <https://www.alienmetals.uk/news/m-and-a-update-on-mexico-silver-projects-and-award-of-new-licence-adjacent-to-world-class-citronen-zinc-lead-deposit>.
103. **Conley, H. A., Rahbek-Clemmensen, J.** Arctic Temperatures and Greenland Politics Heat Up. *CSIS*. [Online] 9 March 2018. [Cited: 14 March 2018.] <https://www.csis.org/analysis/arctic-temperatures-and-greenland-politics-heat>.
104. **Naalakkersuisut**. Events. *Govmin*. [Online] 2018. [Cited: 23 February 2018.] <https://www.govmin.gl/events>.
105. **Deloitte**. Information Guide How to Set Up a Company in Greenland. *Deloitte*. [Online] October 2015. [Cited: 25 February 2018.] <https://www2.deloitte.com/content/dam/Deloitte/dk/Documents/audit/2015Set-up-business-Greenland.pdf>.

106. **Government.** Rules for Fieldwork and Reporting in Greenland. *Govmin.* [Online] 2000. [Cited: 23 February 2018.] https://www.govmin.gl/images/stories/minerals/rules_for_fieldwork.pdf.
107. **Naalakkersuisut.** Government of Greenland provides additional help to mineral licensees. [Online] 26 May 2020. [Cited: 24 July 2020.] <https://govmin.gl/2020/05/government-of-greenland-provides-additional-help-to-mineral-licensees/>.
108. **FinnAust.** Positive Changes to Greenland Mining Obligations. *BlueJay Mining Plc.* [Online] 17 February 2017. [Cited: 24 February 2018.] <http://www.titanium.gl/announcements/positive-changes-greenland-licence-obligations/>.
109. **Hollis, J.** *Re: your enquiry (Nanoq - ID nr.: 5290851).* [email] Nuuk : Ministry of Mineral Resources, 26 April 2017.
110. **GGG.** Greenland and Denmark Pass Uranium Export Legislation, Solid Foundation Set for Kvanefjeld Project. *Greenland Minerals and Energy Ltd.* [Online] 2018 June 2016. [Cited: 24 February 2018.] <http://www.ggg.gl/docs/ASX-announcements/Denmark-Passes-Export-Legislation.pdf>.
111. **VisitGreenland.** The National Park. *Visit Greenland.* [Online] 2018. [Cited: 24 February 2018.] <https://visitgreenland.com/about-greenland/national-park/>.
112. **Naalakkersuisut.** About. *Ujarassiorit.* [Online] Government of Greenland, 2018. [Cited: 24 February 2018.] http://www.ujarassiorit.gl/index.php?option=com_content&view=article&id=57&Itemid=129&lang=en.
113. **MMR.** Greenland Day in Perth. *Govmin.* [Online] 11 December 2016. [Cited: 25 February 2018.] https://www.govmin.gl/images/stories/minerals/events/Greenland_Day_in_Perth_2016_-_December_9th/GreenlandDay2016_19_Hollis_Strategy_Geoscience.pdf.
114. **Saqqaqaa.** Råstofskolen - Greenland School of Minerals & Petroleum. *KTI.* [Online] 2018. [Cited: 24 February 2018.] <https://www.kti.gl/kl/>.
115. **PWC.** Greenland: Corporate - Taxes on Corporate Income. [Online] 2 June 2020. [Cited: 24 July 2020.] <https://taxsummaries.pwc.com/greenland/corporate/taxes-on-corporate-income>.
116. **Naalakkersuisut.** Greenland Fact Sheet: Tax, Duty and Royalty. [Online] 10 February 2020. [Cited: 12 October 2020.] <https://govmin.gl/publications/tax-and-royalties/>.
117. **ATO.** Company Tax Rates. *Australian Tax Office.* [Online] 12 December 2017. [Cited: 24 February 2018.] <https://www.ato.gov.au/Rates/Company-tax/>.
118. **Naalakkersuisut.** Knowledge. *Arctic Cluster of Raw Materials.* [Online] March 2017. [Cited: 25 February 2018.] Tax losses incurred by exploration companies can be carried forward indefinitely..
119. **Akilerartarnermut Aqutsisoqarfik.** Home. *Tax Greenland.* [Online] Government of Greenland, 2018. [Cited: 24 February 2018.] <http://int.aka.gl/en/Tax-Greenland>.
120. **Tax Greenland.** Tax Rates 2016/2017. *Akilerartarnermut Aqutsisoqarfik.* [Online] 2018. [Cited: 24 February 2018.] <http://int.aka.gl/en/Tax-Greenland/Tax-rates-2017>.
121. **Naalakkersuisut.** Appendix 1 to addendum no. 3 to Standard Terms for Exploration Licences. *Govmin.* [Online] 1 July 2014. [Cited: 24 February 2018.] https://www.govmin.gl/images/stories/faelles/Standard_terms_for_Exploration_Licences_for_Minerals_-_Addendum_no_3_-_Appendix_1.pdf.
122. **DMP.** Mineral Royalties. *Department of Mines, Industry Regulation and Safety.* [Online] Government of Western Australia, 2018. [Cited: 24 February 2018.] <http://www.dmp.wa.gov.au/Minerals/Royalties-1544.aspx>.



123. **Stedman, A., Yunis, J., Aliakbari, E.** Annual Survey of Mining Companies, 2019. [Online] 25 February 2020. [Cited: 24 July 2020.] <https://www.fraserinstitute.org/studies/annual-survey-of-mining-companies-2019>.
124. **Wikipedia.** Peary Expedition to Greenland of 1891–1892. *Wikipedia the Free Encyclopedia*. [Online] Wikimedia Foundation LLC, 30 April 2019. [Cited: 27 July 2020.] https://en.wikipedia.org/wiki/Peary_expedition_to_Greenland_of_1891%E2%80%931892.
125. **Muenchow, A.** Independence Fjord, Peary, and the First Thule Expedition. *Ice Seas*. [Online] Public Blog, 4 July 2012. [Cited: 27 July 2020.] <https://icyseas.org/2012/07/04/independence-fjord-peary-and-first-thule-expedition/>.
126. **ArchivesHub.** Robert Peary Collection. [Online] Archives Hub. [Cited: 27 July 2020.] <https://archiveshub.jisc.ac.uk/search/archives/9fa7f4f0-5d9d-341c-b097-b926307fa9ee>.
127. *Lauge Koch. Pioneer Geo-Explorer of Greenland's Far North.* **Dawes, P. R.** 2, s.l. : History of Earth Sciences Society, 1991, Earth Sciences History, Vol. 10, pp. 130-153. <https://www.jstor.org/stable/24137832>.
128. **Tukiainen, T., Lind, M.** *Economic Geological Reconnaissance between Lambert Land and J.C. Christensen Land (North and North-East Greenland 79N to 82N)*. Copenhagen : Geological Survey of Denmark and Greenland, 2011. Report 129.
129. **Jepsen, H. F.** *Preliminary Report on the Stratigraphy of the Precambrian and Eocambrian Sediments in the Jørgen Brønlands Fjord - Midsommersø Area, Southern Peary Land*. Copenhagen : Grønlands Geologiske Undersøgelse, 1969. GEU report file: 22341.
130. **Stewart-Smith, J. H., Campbell, D. L.** *The Geology of Greenland North of Latitude 74° 30' N, Report No.2, Volume 2: Mineral Prospects of Northern Greenland*. Alberta : J.C. Sproule and Associates Ltd, 1971. GEUS report file: 20811.
131. **GGU.** *Report on the 1978 Geological Expedition to the Peary Land Region, North Greenland*. Copenhagen : Grønland Geologiske Undersøgelse, 1979. GEUS report file: 22410.
132. **Ghisler, M.** *Report of Activities 1994: New Perspective for Greenland Geological Research*. Copenhagen : Grønlands Geologiske Undersøgelse, 1994. GEUS report file: 22502.
133. **NSIDC.** Quick Facts on Ice Sheets. *NSIDC*. [Online] National Snow & Ice Data Center, 2018. [Cited: 25 February 2018.] <https://nsidc.org/cryosphere/quickfacts/icesheets.html>.
134. *Changes in Greenland Ice Bed Conditions Inferred from Seismology.* **Toyokuni, G., Takenaka, H., Takagia, R., Kanao, M., Tsuboi, S., Tono, Y., Childs, D., Zhao, D.** s.l. : Elsevier, 2018, Physics of the Earth and Planetary Interiors, Vol. 277, pp. 81-98. <https://doi.org/10.1016/j.pepi.2017.10.010>.
135. *Evidence for ephemeral middle Eocene to early Oligocene Greenland glacial ice and pan-Arctic sea ice.* **Tripati, A., Darby, D.** 1038, s.l. : Nature Research, 2018, Nature Communications, Vol. 9. <https://doi.org/10.1038/s41467-018-03180-5>.
136. *Metallogeny of Greenland.* **Kolb, J., Keiding, J. K., Steinfeldt, A., Secher, K., Keulen, N., Rosa, D., Stensgaard, B. M.** s.l. : Elsevier, 2016, Ore Geology Reviews, Vol. 78, pp. 493-555. <https://doi.org/10.1016/j.oregeorev.2016.03.006>.
137. **CIA.** Sweden. *World Factbook*. [Online] Central Intelligence Agency, 2018. [Cited: 24 February 2018.] <https://www.cia.gov/library/publications/the-world-factbook/geos/sw.html>.
138. **Dawes, P. R.** The bedrock geology under the Inland Ice: the next major challenge for Greenland mapping. *GEUS Bulletin*. 17, 2009, <https://doi.org/10.34194/geusb.v17.5014>, pp. 55-70.
139. **GEUS.** Airborne geophysical data from Greenland. *Geology and Ore: Exploration and Mining in Greenland*. February, 2013, Vol. 22.

140. **Nutman, A.** Greenland's Precambrian Crustal Architecture: Four Decades of Geochronology Goes Online. *Govmin.* [Online] 9 December 2015. [Cited: 2 March 2018.] https://www.govmin.gl/images/stories/minerals/events/Greenland_Day_in_Perth_2016_-_December_9th/GreenlandDay2016_07_Nutman_Geochronology-1.pdf.
141. *Earth's Oldest Mantle Fabrics Indicate Eoarchean Subduction.* **Kacsmarek, M., Reddy, S. M., Nutman, A. P., Friend, C. R. L., Bennett, V. C.** 10665, s.l. : Nature Research, 2016, Nature Communications, Vol. 7. <https://doi.org/10.1038/ncomms10665>.
142. *Constraining the Process of Eoarchean TTG Formation in the Itsaq Gneiss Complex, Southern West Greenland.* **Hoffman, J. E., Nagle, T. J., Münker, C., Næraa, T., Rosing, M. T.** s.l. : Elsevier, 2014, Earth and Planetary Science Letters, Vol. 388, pp. 374-386. <https://doi.org/10.1016/j.epsl.2013.11.050>.
143. *Evidence for Early Life in Earth's Oldest Hydrothermal Vent Precipitates.* **Dodd, M. S., Papineau, D., Grenne, T., Slack, J. F., Rittner, M., Pirajno, F., O'Neil, J., Little, C. T. S.** s.l. : Springer, 2017, Nature, Vol. 543, pp. 60-64. <https://doi.org/10.1038/nature21377>.
144. *Metallogeny of the North Atlantic Craton in Greenland.* **Kolb, J., Bagas, L., Fiorentini, M. L.** 4, London : Cambridge University Press, 2015, Mineralogical Magazine, Vol. 79, pp. 815-855. <https://doi.org/10.1180/minmag.2015.079.4.01>.
145. *Structure of the Palaeoproterozoic Nagssugtoqidian Orogen, South-East Greenland: Model for the tectonic evolution.* **Kolb, J.** Part 3, s.l. : Elsevier, December 2014, Precambrian Research, Vol. 255, pp. 809-822. <https://doi.org/10.1016/j.precamres.2013.12.015>.
146. **Stensgaard B. M., Sørensen, L. L., Bernstein, S., Rosa, D.** Magmatic Nickel Potential in Greenland. *Geology and Ore: Exploration and Mining in Greenland.* 31, October 2018, p. 12.
147. **Stensgaard, B. M.** Sediment-hosted copper in Greenland. *Geology and Ore: Exploration and Mining in Greenland.* 18, January 2011, p. 12.
148. **Henriksen, N., Higgins, A. K., Kalsbeek, F., Pulvertaft, T. C. R.** *Greenland from Archaean to Quaternary: Descriptive Text to the 1995 Geological Map of Greenland, 1:2 500 000. 2nd edition.* Copenhagen : GEUS Bulletin, 18, 2009. pp. 1-126. <https://doi.org/10.34194/geusb.v18.4993>.
149. **Surlyk, F.** Tectonostratigraphy of North Greenland. [book auth.] J. S., Sønderholm, M. Peel. *Sedimentary basins of North Greenland.* s.l. : GEUS, 1991, Vol. Report 22312, pp. 25-47.
150. *Assembly and Breakup of Rodinia (Some results of IGCP project 440).* **Bogdanova, S. V., Pisarevsky, S. A., Li, Z. X.** 3, s.l. : Pleiades Publishing, 2009, Stratigraphy and Geological Correlation, Vol. 17, pp. 259-274. <https://doi.org/10.1134/S0869593809030022>.
151. *Precambrian Evolution of North and North-East Greenland. Crystalline Basement and Sedimentary Basins.* **Jepsen, H. F., Kalsbeek, F.** Bremerhaven : Alfred Wegener Institute for Polar and Marine Research & German Society of Polar Research, 2000, Polarforschung, Vol. 68, pp. 153-160. <https://doi.org/10.2312/polarforschung.68.153>.
152. *A Giant Circumferential Dyke Swarm Associated with the High Arctic Large Igneous Province.* **Buchan, K. L., Ernst, R. E.** s.l. : Elsevier, 2018, Gondwana Research, Vol. 58, pp. 39-57. <https://doi.org/10.1016/j.gr.2018.02.006>.
153. *Exhuming the Top End of North America: Episodic Evolution of the Eureka Belt and Its Potential Relationships to North Atlantic Plate Tectonics and Arctic Climate Change.* **Vamvaka, A., Pross, J., Monien, P., Piepjohn, K., Estrada, S., Lisker, F., Spiegel, C.** 12, s.l. : AGU, 2019, Tectonics, Vol. 38, pp. 4207-4228. <https://doi.org/10.1029/2019TC005621>.
154. *What's in a name? The Columbia (Paleopangaea/Nuna) Supercontinent.* **Meert, G. R.** 4, s.l. : Elsevier, 2012, Gondwana Research, Vol. 21, pp. 987-993. <https://doi.org/10.1016/j.gr.2011.12.002>.



155. *Configuration of Columbia. A Mesoproterozoic Supercontinent*. **Rogers, J. J. W., Santosh, M.** 1, s.l.: Elsevier, 2002, Gondwana Research, Vol. 5, pp. 5-22. [https://doi.org/10.1016/S1342-937X\(05\)70883-2](https://doi.org/10.1016/S1342-937X(05)70883-2).
156. *Paleoproterozoic High-pressure Metamorphism in the Northern North China Craton and Implications for the Nuna Supercontinent*. **Wan, B., Windley, B. F., Xiao, W., Feng, J., Zhang, J.** 8344, s.l.: Nature Research, 2015, Nature Communications, Vol. 6, p. 10. <https://doi.org/10.1038/ncomms9344>.
157. **Sønderholm, M., Frederiksen, K. S., Smith, M. P., Tirsgaard, H.** Neoproterozoic Sedimentary Basins with Glacigenic Deposit of the East Greenland Caledonides. [book auth.] A. K., Gilotti, J. A., Smith, P. M. Higgins. *The Greenland Caledonides: Evolution of the Northeast Margin of Laurentia*. s.l.: Geological Society of America, 2008.
158. *The Midsommersø Dolerites and Associated Intrusions in the Proterozoic Platform of Eastern North Greenland— A Study of the Interaction Between Intrusive Basic Magma and Sialic Crust*. **Kalsbeek, F., Jepsen, H. F.** 4, s.l.: Oxford Academic Journals, 1983, Journal of Petrology, Vol. 24, pp. 605-634. <https://doi.org/10.1093/petrology/24.4.605>.
159. *The Mesoproterozoic Zig-Zag Dal Basalts and Associated Intrusions of Eastern North Greenland. Mantle Plume-Lithosphere Interaction*. **Upton, B. G. J., Rämö, O. T., Heaman, L. M., Blichert-Toft, J., Kalsbeek, F., Barry, T.L., Jepsen, H. F.** 149, s.l.: Springer-Verlag, 2005, Contributions to Mineral Petrology, pp. 40-56. <https://doi.org/10.1007/s00410-004-0634-7>.
160. **Pehrsson, S. J., Eglinton, B. M., Evans, D. A. D., Huston, D., Reddy, S. M.** Metallogeny and its link to orogenic style during the Nuna supercontinent cycle. [book auth.] Z. X., Evans, D. A. D., Murphy, J. B. (eds) Li. *Supercontinent Cycles Through Earth History*. London: The Geological Society of London, 2016, Vol. 424.
161. *Tectonic map of the Ellesmerian and Eureka Deformation Belts on Svalbard, North Greenland, and the Queen Elizabeth Islands (Canadian Arctic)*. **Piepjohn, K., van Gosen, W., Tessensohn, F., Reinhardt, L., McClelland, W. C., Dallmann, W., Gaedicke, C., Harrison, J. C.** 12, s.l.: Springer, 2015, Arktos, Vol. 1. <https://doi.org/10.1007/s41063-015-0015-7>.
162. *Towards a Nares Strait Solution. Structural Studies on Southeastern Ellesmere Island and Northwestern Greenland*. **Okulitch, A. V., Dawes, P. R., Higgins, A. K., Soper, N. J., Christie, R. L.** s.l.: Elsevier, 1990, Marine Geology, Vol. 90, pp. 369-384. [https://doi.org/10.1016/0025-3227\(90\)90093-Y](https://doi.org/10.1016/0025-3227(90)90093-Y).
163. *Explosive volcanism on the ultraslow-spreading Gakkel ridge, Arctic Ocean*. **Sohn, R. A., Willis, C., Humphris, S., Shank, T. M., Singh, H., Edmonds, H. N., Kunz, C., Hedman, U., Helmke, E., Jakuba, M., Liljebadh, B., Linder, J., Murphy, C., Nakamura, K., Sato, T., Schlindwein, V., Stranne, C., Tausenfreund, M., et al.** s.l.: Nature Research, 26 June 2008, Nature Letters, Vol. 453, pp. 1236-1238. <https://doi.org/10.1038/nature07075>.
164. *Seismicity, Structure and Tectonics in the Arctic Region*. **Kanao, M., Surorov, V. D., Toda, S., Tsuboi, S.** 5, s.l.: Elsevier, 2015, Geoscience Frontiers, Vol. 6, pp. 665-677. <https://doi.org/10.1016/j.gsf.2014.11.002>.
165. *A New Model for the Paleogene Motion of Greenland Relative to North America: Plate Reconstructions of the Davis Strait and Nares Strait Regions Between Canada and Greenland*. **Oakey, G. N., Chalmers, J. A.** B10, s.l.: AGU, 2012, Journal of Geophysical Research, Vol. 117. <https://doi.org/10.1029/2011JB008942>.
166. *4D Arctic: A Glimpse into the Structure and Evolution of the Arctic in the Light of New Geophysical Maps, Plate Tectonics and Tomographic Models*. **Gaina, C., Medvedev, S., Torsvik, T. H., Koulakov, I., Werner, S. C.** 5, s.l.: Springer, 2014, Surveys in Geophysics, Vol. 35, pp. 1095-1122. <https://doi.org/10.1007/s10712-013-9254-y>.

167. **Marcussen, C.** *Continuation of the Palaeomagnetic Field Work in Eastern North Greenland*. Copenhagen : Grønlands Geologiske Undersøgelse, 1981. GEUS report file #22443.
168. *Precambrian Evolution of North and North-East Greenland. Crystalline Basement and Sedimentary Basins*. **Jepssen, H. F., Kalsbeek, F.** 143-168, s.l. : Alfred Wegener Institute for Polar and Marine Research & German Society of Polar Research, 2000, Polarforschung, Vol. 68, pp. 153-160. <https://epic.awi.de/id/eprint/28428/>.
169. *Palaeoproterozoic and Archaean gneiss complexes in northern Greenland. Palaeoproterozoic terrane assembly in the High Arctic*. **Nutman, A. P., Dawes, P. R., Kalsbeek, F., Hamilton, M. A.** 3-4, s.l. : Elsevier, 2008, Precambrian Research, Vol. 161, pp. 419-451. <https://doi.org/10.1016/j.precamres.2007.09.006>.
170. **Collinson, J. D.** Stratigraphy of the Independence Fjord Group (Proterozoic) of Eastern North Greenland. *Report on the 1979 geological expedition to the Peary Land region, North Greenland*. 1980, Vol. GEUS Report file no. 22436, Rapport Nr. 99, pp. 7-24.
171. *Palaeoproterozoic (1740 Ma) rift-related volcanism in the Hekla Sund region, eastern North Greenland: field occurrence, geochemistry and tectonic setting*. **Pedersen, S. A. S., Graig, L. E., Upton, B. G. J., Rämö, O. T., Jepsen, H. F., Kalsbeek, F.** 3-4, Copenhagen : Elsevier, 2002, Precambrian Research, Vol. 114, pp. 327-346. [https://doi.org/10.1016/S0301-9268\(01\)00234-0](https://doi.org/10.1016/S0301-9268(01)00234-0).
172. *Supercontinent–superplume Coupling, True Polar Wander and Plume Mobility: Plate Dominance in Whole-mantle Tectonics*. **Li, Z., Zhong, S.** 3-4, s.l. : Elsevier, 2009, Physics of the Earth and Planetary Interiors, Vol. 176, pp. 143-156. <https://doi.org/10.1016/j.pepi.2009.05.004>.
173. *A New Plumbing System Framework for Mantle Plume-related Continental Large Igneous Provinces and their Mafic-Ultramafic Intrusions*. **Ernst, R. E., Liikane, D. A., Jowitt, S. M., Buchan, K. L., Blachard, J. A.** s.l. : Elsevier, 2019, Journal of Volcanology and Geothermal Research, Vol. 384, pp. 75-84. <https://doi.org/10.1016/j.jvolgeores.2019.07.007>.
174. *Fragments of 1.79-1.75 Ga Large Igneous Provinces in reconstructing Columbia (Nuna): A Statherian supercontinent-superplume coupling?* **Chaves, A. de O. C., de Rezende, C. R.** 1, s.l. : Episodes, 2019, Journal of International Geoscience, Vol. 42, pp. 55-67. <https://doi.org/10.18814/epiiugs/2019/019006>.
175. *U–Pb baddeleyite Ages and Geochemistry of Dolerite Dykes in the Bas Drâa Inlier of the Anti-Atlas of Morocco: Newly identified 1380 Ma event in the West African Craton*. **Bahat, A., Ikenne, M., Söderlund, U., Cousens, B., Youbi, N., Ernst, R., Abderrahmane, S., El Janati, M., Hafid, A.** s.l. : Elsevier, 2013, Lithos, Vol. 174, pp. 85-98. <https://doi.org/10.1016/j.lithos.2012.07.022>.
176. *The ca. 1380 Ma Mashak Igneous Event of the Southern Urals*. **Puchkov, V. N., Bogdanova, S. V., Ernst, R. E., Vjacheslav, V. I., Krasnobaev, A. A., Söderlund, U., Wingate, M. T. D., Postnikov, A. V., Sergeeva, N. D.** s.l. : Elsevier, 2012, Lithos, Vol. 174, pp. 109-124. <https://doi.org/10.1016/j.lithos.2012.08.021>.
177. *Palaeomagnetism of the Proterozoic Zig-Zag Dal Basalt and the Midsommersø Dolerites, Eastern North Greenland*. **Marcussen, C., Abrahamsen, N.** 2, s.l. : Oxford University Press, May 1983, Geophysical Journal International, Vol. 73, pp. 367-387. <https://doi.org/10.1111/j.1365-246X.1983.tb03321.x>.
178. **Ernst, R. E., Buchan, K. L.** The Use of Mafic Dike Swarms in Identifying and Locating Mantle Plumes. *Mantle plumes: their identification through time*. s.l. : Geological Society of America Special Papers, 2001, Vol. 352, pp. 247-265.
179. *The Age of the Kap Washington Group Volcanics, North Greenland*. **Larsen, O.** Copenhagen : Bulletin of the Geological Society of Denmark, 1982, Vol. 31, pp. 49-55.
180. *Cretaceous/Tertiary Volcanism in North Greenland: the Kap Washington Group*. **Estrada, S., Hohndorf, A., Henjes-Kunst, F.** 1, 2001, Polarforschung, Vol. 2, pp. 17-23.



181. *Volcanism in the Canadian High Arctic Related to the Opening of the Arctic Ocean*. **Estrada, S., Henjes-Kunst, F.** 4, 2004, *Zeitschrift der Deutschen Gesellschaft für Geowissenschaften*, Vol. 154, pp. 579-603. <https://doi.org/10.1127/zdgg/154/2004/579>.
182. *Geothermal Heat Flux Reveals the Iceland Hotspot Track Underneath Greenland*. **Martos, Y. M., Jordan, T. A., Catalan, M., Jordan, T. M., Bamber, J. L., Vaughan, D. G.** 16, s.l. : AGU, 2018, *Geophysical Research Letters*, Vol. 45, pp. 8214-8222. <https://doi.org/10.1029/2018GL078289>.
183. *Three Distinct Types of Hotspots in the Earth's Mantle*. **Coutillot, V., Davaille, A., Besse, J., Stock, J.** 3-4, s.l. : *Earth and Planetary Science Letters*, January 2003, Vol. 205, pp. 295-308. [https://doi.org/10.1016/S0012-821X\(02\)01048-8](https://doi.org/10.1016/S0012-821X(02)01048-8).
184. *The Flinton Group: a late Precambrian metasedimentary succession in the Grenville Province of eastern Ontario*. **Moore Jr., J. M., Thompson, P. H.** 12, s.l. : *Canadian Journal of Earth Science*, 1980, Vol. 17, pp. 1685-1707. <https://doi.org/10.1139/e80-178>.
185. *Tectonic model for the Proterozoic growth of North America*. **Whitmeyer, S. J., Karlstrom, K. E.** 4, s.l. : GSA, 2007, *Geosphere*, Vol. 3, pp. 220-259. <https://doi.org/10.1130/GES00055.1>.
186. *Provenance Record from Mesoproterozoic-Cambrian Sediments of Peary Land, North Greenland: Implications for the Ice-covered Greenland Shield and Laurentian Palaeogeography*. **Kirkland, C. L., Pease, V., Ineson, J. R.** 1-2, s.l. : Elsevier, 2009, *Precambrian Research*, Vol. 170, pp. 43-60. <https://doi.org/10.1016/j.precamres.2008.11.006>.
187. *Zircon fingerprint of the Neoproterozoic North Atlantic: Perspectives from East Greenland*. **Olierook, H. K. H., Barham, M., Kirkland, C. L., Hollis, J., Vass, A.** s.l. : Elsevier, June 2020, *Precambrian Research*, Vol. 342, p. 105653. <https://doi.org/10.1016/j.precamres.2020.105653>.
188. *Breaking the Grenville–Sveconorwegian link in Rodinia reconstructions*. **Slagstad, T., Kulakov, E., Kirkland, C. L., Roberts, N. M. W., Ganerød, M.** 5, s.l. : John Wiley & Sons Ltd, 2019, *Terra Nova*, Vol. 31, pp. 430-437. <https://doi.org/10.1111/ter.12406>.
189. *Palaeomagnetism of Igneous Rocks of the Lake District (Caledonian) Terrane, Northern England: Palaeozoic Motions and Deformation at a Leading Edge of Avalonia*. **Piper, J. D. A.** 3, s.l. : Wiley, 1997, *Geological Journal*, Vol. 32, pp. 211-246. [https://doi.org/10.1002/\(SICI\)1099-1034\(199709\)32:3<211::AID-GJ740>3.0.CO;2-O](https://doi.org/10.1002/(SICI)1099-1034(199709)32:3<211::AID-GJ740>3.0.CO;2-O).
190. *The Caledonian Orogeny redefined*. **McKerrow, W. S., Niocaill, C. M., Dewey, J. F.** 6, s.l. : Geological Society of London, 2000, *Journal of the Geological Society*, Vol. 157, pp. 1149-1159. <https://doi.org/10.1144/jgs.157.6.1149>.
191. *New Perspectives on the Caledonides of Scandinavia and Related Areas: Introduction*. **Corfu, F., Gasser, D., Chew, D. M.** s.l. : GSL, February 2014, *Special Publications*, Vol. 390, pp. 1-8. <https://doi.org/10.1144/SP390.28>.
192. *⁴⁰Ar/³⁹Ar Mineral Age Constraints on the Timing of Deformation and Metamorphism, North-East Greenland Caledonides*. **Dallmeyer, R. D., Strachan, R. A.** 153-165, Copenhagen : Grønlands Geologiske Undersøgelse, 1994, Vol. 162. GEUS report field #22499.
193. **Tollo, R. P.** Grenvillian Orogeny. [book auth.] R. C., Cocks, L. R. M., Plimer, I. R. Selley. *Encyclopedia of Geology*. s.l. : Elsevier, 2005, pp. 155-165.
194. *Lithospheric Structure of Greenland From Ambient Noise and Earthquake Surface Wave Tomography*. **Pourpont, M., Anandakrishnan, S., Ammon, C. J., Alley, R. B.** 9, s.l. : AGU, 2018, *Journal of Geophysical Research*, Vol. 123, pp. 7850-7876. <https://doi.org/10.1029/2018JB015490>.
195. *Large-scale Gravity Anomaly in Northern Norway: Tectonic Implications of Shallow or Deep Source Depth and a Possible Conjugate in Northeast Greenland*. **Gradmann, S., Ebbing, J.** 3, s.l. : Royal Astronomical Society, 2015, *Geophysics Journal International*, Vol. 203, pp. 2070-2088. doi: 10.1093/gji/ggv426.

196. *Orogenic Paleofluid Flow Recorded by Discordant Detrital Zircons in the Caledonian Foreland Basin of Northern Greenland*. **Morris, G. A., Kirkland, C L., Pease, V.** 2, s.l. : GeoScienceWorld, April 2015, Lithosphere, Vol. 7, pp. 138-143. <https://doi.org/10.1130/L420.1>.
197. *The Ellesmerian Orogeny: Fact or Fiction?* **Ripington, S., Scott, R. A., Smyth, H., Bogolepova, O., Gubanov, A.** s.l. : Conference Paper: GeoCanada, 2010.
198. *Models for the Ellesmerian Mountain Front in North Greenland: A basin margin inverted by basement uplift*. **Soper, N. J., Higgins, A. K.** 1, s.l. : Elsevier, 1990, Journal of Structural Geology, Vol. 12, pp. 83-97. [https://doi.org/10.1016/0191-8141\(90\)90050-9](https://doi.org/10.1016/0191-8141(90)90050-9).
199. *Devonian-Carboniferous paleogeography and orogenesis, northern Yukon and adjacent Arctic Alaska*. **Lane, L. S.** 5, s.l. : Canadian Science Publishing, 2007, Canadian Journal of Earth Science, Vol. 44, pp. 679-694. <https://doi.org/10.1139/e06-131>.
200. *Ellesmerian Fold-and-thrust Belt (Northeast Ellesmere Island, Nunavut) and its Eureka Overprint*. **Piepjohn, K., von Gosen, W., Tessensohn, F., Saalman, K.** s.l. : Geological Survey of Canada, 2008, Geological Survey of Canada Bulletin, Vol. 592, pp. 285-303. <https://doi.org/10.4095/226148>.
201. *The Svalbardian-Ellesmerian Deformation of the Old Red Sandstone and the Pre-Devonian basement in NW Spitsbergen (Svalbard)*. **Piepjohn, K.** London : Geological Society of London, January 2000, Special Publications, Vol. 180, pp. 585-601. <https://doi.org/10.1144/GSL.SP.2000.180.01.31>.
202. *Timing of Paleozoic Exhumation and Deformation of the High-Pressure Vestgötabreen Complex at the Motalafjella Nunatak, Svalbard*. **Barnes, C. J., Walczak, K., Janots, E., Schneider, D., Majka, J.** 125, s.l. : MDPI, 2020, Minerals, Vol. 10(2). <https://doi.org/10.3390/min10020125>.
203. *Polyphase Deformation at the Harder Fjord Fault Zone (North Greenland)*. **Piepjohn, K., van Gosen, W.** 04, London : GSA, 01 July 2001, Geological Magazine, Vol. 138, pp. 407-434.
204. *The Eureka Deformation in the Arctic: An outline*. **Piepjohn, K., von Gosen, W., Tessensohn, F.** 6, s.l. : GSL, 22 September 2016, Journal of the Geological Society, Vol. 173, pp. 1007-1024. <https://doi.org/10.1144/jgs2016-081>.
205. **Soper, N. J., Higgins, A. K.** Late Cretaceous–Early Tertiary Deformation, North Greenland. [book auth.] H.P. (ed.) Trettin. *Geology of the Inuitian Orogen and Arctic Platform of Canada and Greenland*. s.l. : Geological Survey of Canada, 1991, pp. 461-465.
206. *The Wandel Hav Strike-Slip Mobile Belt – A Mesozoic Plate Boundary in North Greenland*. **Håkansson, E., Pedersen, S.A.S.** 2, Copenhagen : Bulletin of the Geological Society of Denmark, 2001, Vol. 48, pp. 148-158.
207. *Opening of the Fram Strait gateway: A review of plate tectonic constraints*. **Engen, O., Faleide, J. I., Dyreng, T. K.** 1-4, s.l. : Elsevier, 2008, Tectonophysics, Vol. 450, pp. 51-69. <https://doi.org/10.1016/j.tecto.2008.01.002>.
208. **Stijl, F. W. van der., Mosher, G. Z.** *The Citronen Fjord massive sulphide deposit, Peary Land, North Greenland: discovery, stratigraphy, mineralization and structural setting*. s.l. : GEUS, 1998. p. 40 pp.
209. **Sørensen, L. L., Kalvig, P., Thrane, K., Rosa, D.** *The zinc potential in Greenland - Assessment of undiscovered sediment-hosted zinc deposits*. s.l. : GEUS, 2018. p. 12 pp.
210. *Geological map of Greenland, 1:500 000, Nyeboe Land, Sheet 7, Peary Land, Sheet 8. Descriptive Text*. **Henriksen, N.** s.l. : GEUS, 1992.
211. *Structural, tectonic and glaciological controls on the evolution of fjord landscapes*. **Glasser, N. F., Ghiglione, M. C.** 3-4, s.l. : Elsevier, April 2009, Geomorphology, Vol. 105, pp. 291-302. <https://doi.org/10.1016/j.geomorph.2008.10.007>.



212. **GEUS.** Geological Map of Greenland 1:2,500,000. *GEUS*. [Online] Geological Survey of Denmark and Greenland, 20 June 2003. [Cited: 24 February 2018.] <http://www.geus.dk/program-areas/raw-materials-greenl-map/greenland/gr-map/anhstart-uk.htm>.
213. *Sr-isotopic studies and mineral composition of the Hagen Brae Member in the Proterozoic clastic sediments at Hagen Brae, eastern North Greenland.* **Larsen, O., Graff-Petersen, P.** [ed.] GEUS Report 22436. Rapport Nr. 99, Nuuk : Grønlands Geologiske Undersøgelse, 1980, Vol. GEUS Report file no. 22436, pp. 111-118.
214. **Bevins, R. E., Rowbotham, G.** *Greenschist Facies Metabasites from the Hellefiskefjord - G.B. Schley Fjord Area, Eastern Peary Land, North Greenland.* Copenhagen : Grønlands Geologiske Undersøgelse, 1984. GEUS Report file no. 22455.
215. **Fought, H., Jensen, S. M., Kragh, K., Langdahl, B. R., Pedersen, M.** *Mineral Resources of the Sedimentary Basin of the North and East Greenland - final report.* Copenhagen : Danmarks og Grønlands Geologiske Undersøgelse, 1999. GEUS Report File #16101.
216. **Kalsbeek, F., Jepsen, H. F.** Preliminary Rb-Sr isotope evidence on the age and metamorphic history of the North Greenland crystalline basement. *Report on the 1979 geological expedition to the Peary Land region, North Greenland.* GEUS Report no. 22436, 1980, Vol. Rapport Nr. 99, pp. 106-110.
217. **GEUS.** *J.C. Christensen Land 1:100 000 Geological Map.* [Digital Map] Copenhagen : Geological Survey of Denmark and Greenland, 1985. Geological map of Greenland 1:100 000 .
218. *Proterozoic Basins of North Greenland.* **Sønderholm, M., Jepsen, H. F.** GEUS report 22312, s.l. : GEUS, 1991, Vol. Bull. Grønlands geol. Unders. 160.
219. **Collinson, J. D., Kalsbeek, F., Jepsen, H. F., Pedersen, S. A. S.** Paleoproterozoic and Mesoproterozoic Sedimentary and Volcanic Successions in the Northern Parts of the East Greenland Caledonian Orogen and its Foreland. [book auth.] A. K., Gilotti, J. A., Smith, M. P. Higgins. *The Greenland Caledonides: Evolution of the Northeast Margin of Laurentia.* s.l. : The Geological Society of America, 2008, Vol. GSA Memoirs, pp. 73-98.
220. **Collinson, J. D.** The Proterozoic Sandstones Between Heilprin Land and Mylius-Erichsen Land, Eastern North Greenland. *Report on the 1978 Geological Expedition to the Peary Land Region, North Greenland.* 88, 1979, Vols. 5-10, GEUS Report File Number 22410.
221. *The Late Proterozoic Zig-Zag Dal Basalt Formation of Eastern North Greenland.* **Kalsbeek, F., Jepsen, H. F.** 3, s.l. : Oxford Academic, August 1984, Journal of Petrology, Vol. 25, pp. 644-664. <https://doi.org/10.1093/petrology/25.3.644>.
222. **Jepsen, H. F., Kalsbeek, F., Suthren, R. J.** The Zig-Zag Dal Basalt Formation, North Greenland. [book auth.] GEUS. *Report on the 1979 geological expedition to the Peary Land region, North Greenland.* s.l. : GEUS, 1980, Vol. Report file no. 22436, pp. 25-32.
223. **Clemmensen, L. B., Jepsen, H. F.** *Lithostratigraphy and Geological Setting of Upper Proterozoic Shoreline-shelf Deposits, Hagen Fjord Group, Eastern North Greenland.* s.l. : GEUS, 1992. pp. 1-27. Grønlands Geologiske Undersøgelse, no. Rapport 157. Report file no. 22494.
224. **Jepsen, H. F., Kalsbeek, F., Suthren, R. J.** *The Zig Zag Dal Basalt Formation, North Greenland.* Copenhagen : Geological Survey of Greenland, 1980. Report file number 22436.
225. *Zeolite to Prehnite-pumpellyite Facies Metamorphism of the Late Proterozoic Zig-Zag Dal Basalt Formation, Eastern North Greenland.* **Bevins, R. E., Rowbotham, G., Robinson, D.** 3, Cardiff : Elsevier, 1991, Lithos, Vol. 27, pp. 155-165. [https://doi.org/10.1016/0024-4937\(91\)90010-I](https://doi.org/10.1016/0024-4937(91)90010-I).
226. **Abrahamsen, N., Marcussen, C.** Preliminary Results of Rock- and Palaeomagnetic Field Work in Peary Land, North Greenland. *Report on the 1979 geological expedition to the Peary Land region, North Greenland.* 1980, Vol. 99, Report file no. 22436, pp. 137-145.

227. **Jepsen, H. F., Kalsbeek, F.** Igneous Rocks in the Proterozoic Platform of Eastern North Greenland. *Report on the 1978 geological expedition to the Peary Land region, North Greenland*. 1979, Vol. 88, Report file no. 22410, pp. 11-14.
228. *The Mesoproterozoic Midsommersø Dolerites and Associated High-silica Intrusions, North Greenland: Crustal melting, contamination and hydrothermal alteration.* **Kalsbeek, F., Frei, R.** Copenhagen : Springer, 2006, Contributions to Mineral and Petrology, Vol. 152, pp. 89-110. <https://doi.org/10.1007/s00410-006-0096-1>.
229. **Sønderholm, M., Tirsgaard, H.** *Lithostratigraphic framework of the Upper Proterozoic Eleonore Bay Supergroup of east and north-east Greenland.* s.l. : Grønlands Geologiske Undersøgelse, 1993. p. 38 pp. GEUS Report file no. 22319.
230. **Dawes, P. R.** *The Proterozoic Thule Supergroup, Greenland and Canada: History, lithostratigraphy and development.* s.l. : GEUS, 1997. pp. 1-150. Vol. Bulletin 174. <https://doi.org/10.34194/ggub.v174.5025>.
231. **Clemmensen, L. B.** Notes on the Palaeogeographical Setting of the Eocambrian Tillite-bearing Sequence of Southern Peary Land, North Greenland. *Report on the 1978 geological expedition to the Peary Land region, North Greenland*. Rapp. Grønlands geol. Unders, 88, 1979, Vol. GEUS Report file no. 22410, pp. 15-22.
232. **Tucker, M. E.** *Sedimentary Rocks in the Field: A practical Guide (fourth edition).* 4th. s.l. : Wiley-Blackwell, 2011. p. 288. Vol. The Geological Field Guide Series. ISBN: 978-0-470-68916-5.
233. **Adams, P. J., Cowie, J. W.** *A Geological Reconnaissance of the Region Around the Inner Part of Danmarks Fjord, Northeast Greenland.* s.l. : C.A. Reitzels Forlag, 1953. p. 24 pp. Vol. 111. ASIN : B0026CFF2I.
234. *The Precambrian, Eocambrian and Lower Palaeozoic Stratigraphy of the Jørgen Brønlund Fjord Area, Peary Land, North Greenland.* **Jepsen, H. F.** 2, 1971, Meddr Grønland, Vol. 192, p. 42 pp.
235. *Contributions to the Geology of North Greenland.* **Cowie, J. W.** 3, Copenhagen : C. A. Reitzel, 1961, Meddr Grønland, Vol. 164, p. 47 pp.
236. **Trettin, H. P.** The Arctic Islands. [book auth.] A. W., Palmer, A. R. Bally. *The Geology of North America - An Overview.* Boulder, Colorado : Geological Society of America, 1989.
237. **Higgins, A. K., Ineson, J. R., Peel, J. S., Surlyk, F., Sønderholm, M.** Lower Palaeozoic Franklinian Basin of North Greenland. [book auth.] J. S., Sønderholm, M. Peel. *Sedimentary basins of North Greenland.* Copenhagen : GEUS, 1991, Vol. Report 22312, pp. 71-139.
238. **Ineson, J. R., Peel, J. S.** *Cambrian Shelf Stratigraphy of North Greenland.* s.l. : GEUS, 1997. p. 120 pp., Geology of Greenland Survey Bulletin. Bulletin 173.
239. *The Sirius Passet Lagerstätte of North Greenland: A Remote Window on the Cambrian Explosion.* **Harper, D. A. T., Hammarlund, E. U., Topper, T. P., Nielsen, A. T., Rasmussen, J. A., Park, T. S., Smith, M. P.** 6, London : Geological Society of London, 2019, Journal of the Geological Society, Vol. 176, pp. 1023-1037. <https://doi.org/10.1144/jgs2019-043>.
240. *Ediacaran Doushantuo-type Biota Discovered in Laurentia.* **Villman, Sebastian, et al.** 3, s.l. : Communications Biology, 2020, Vol. 647. doi.org/10.1038/s42003-020-01381-7.
241. **O'Connor, B.** The Portfjeld Formation (? Early Cambrian) of Eastern North Greenland. *Report on the 1978 geological expedition to the Peary Land region, North Greenland*. 1979, Vol. 88, pp. 23-28.
242. **Bryant, I. D., Pickerill, R. K.** Lower Cambrian Trace Fossils from the Buen Formation of Central North Greenland: Preliminary Observations. 1990, Vol. Rapport 147, pp. 44-62.
243. **Peel, J. S., Smith, P.** The Wandel Valley Formation (Early - Middle Ordovician) of North Greenland and its Correlatives. 1988, Vol. 13, 137, pp. 61-92.



244. **Ghisler, M., Henriksen, N., Steenfelt, A., Stendal, H.** A Reconnaissance Geochemical Survey in the Proterozoic-Phanerozoic Platform Succession of the Peary Land Region, North Greenland. *Report on the 1978 geological expedition to the Peary Land region, North Greenland*. 1979, Vol. 88, pp. 85-91.
245. *Mapping iron oxide Cu-Au (IOCG) mineral potential in Australia using a knowledge-driven mineral systems-based approach*. **Skirrow, R. G., Murr, J., Schofield, A., Huston, D. L., Wielen, S. V. D., Czarnota, K., Coghlan, R., Highet, L. M., Connolly, D., Doublier, M., Duan, J.** 103001, s.l. : Elsevier, 2019, Ore Geology Reviews, Vol. 113. <https://doi.org/10.1016/j.oregeorev.2019.103011>.
246. *Genesis of Native Copper Lodes in the Keweenaw District, Northern Michigan: A hybrid evolved meteoric and metamorphogenic model*. **Brown, A. C.** 7, s.l. : Economic Geology, 2006, Economic Geology, Vol. 10, pp. 1437-1444. <http://doi.org/10.2113/gsecongeo.101.7.1437>.
247. *Transformation of Magnetite to Hematite and its Influence on the Dissolution of Iron Oxide Minerals*. **Lagoeiro, L. E.** 3, s.l. : Wiley, 1998, Journal of Metamorphic Geology, Vol. 16, pp. 415-423. <https://doi.org/10.1111/j.1525-1314.1998.00144.x>.
248. *The Nature of Metamorphic Fluids and Significance for Metal Exploration*. **Phillips, G. N., Williams, P. J., De Jong, G.** London : Geological Society of London, January 1994, Special Publications, Vol. 78, pp. 55-68. <https://doi.org/10.1144/GSL.SP.1994.078.01.06>.
249. *Ocean and Atmosphere Geochemical Proxies Derived from Trace Elements in Marine Pyrite: Implications for Ore Genesis in Sedimentary Basins*. **Large, R. R., Mukherjee, I., Gregory, D. D., Steadman, J. A., Maslennikov, V. V., Meffre, S.** 2, s.l. : GeoScienceWorld, June 2017, Economic Geology, Vol. 112, pp. 423-450. <https://doi.org/10.2113/econgeo.112.2.423>.
250. *Atmosphere Oxygen Cycling Through the Proterozoic and Phanerozoic*. **Large, R. R., Mukherjee, I., Gregory, D., Steadman, J., Corkrey, R., Danyushevsky, L. V.** 485-506, s.l. : Springer, 2019, Mineralium Deposita, Vol. 54, pp. 485-506. <https://doi.org/10.1007/s00126-019-00873-9>.
251. *Copper mineralization in the Permian basalts of the Hronicum Unit, Slovakia*. **Ferenc, Š., Rojkovič, I.** G13-03, 2001, GeoLines, Vol. 13, pp. 22-27. <http://geolines.gli.cas.cz/>.
252. *Epigenetic Hydrothermal Origin of Native Copper and Supergene Enrichment in the Vista Alegre District, Paraná Basaltic Province, Southernmost Brazil*. **Pinto, V. M., Hartmann, L. A., Wildner, W.** 10, s.l. : International Geology Reviews, 2011, International Geology Review, Vol. 53, pp. 1163-1179. <https://doi.org/10.1080/00206810903464547>.
253. *Age and Genesis of the White Pine Stratiform Copper Mineralization, Northern Michigan, USA, from Paleomagnetism*. **Symons, D. T. A., Kawasaki, K., Diehl, J. F.** 2, s.l. : Wiley, 2013, Geofluids, Vol. 13, pp. 112-126. <https://doi.org/10.1111/gfl.12024>.
254. **Anthony, J. W., Bideaux, R. A., Bladh, K. W., Nichols, M. C.** Celadonite. *Handbook of Mineralogy*. Chantilly : s.n., 2001.
255. *Volcanic Red-bed Copper Mineralisation Related to Submarine Basalt Alteration, Mont Alexandre, Quebec Appalachians Canada*. **Cabral, A. R., Beaudoin, G.** s.l. : Springer, 2007, Mineralium Deposita, Vol. 42, pp. 901-912. <https://doi.org/10.1007/s00126-007-0141-7>.
256. **Henriksen, N., Jepsen, H. F.** *K/A Age Determinations on Dolerites from Southern Peary Land*. Copenhagen : Grønlands Geologiske Undersøgelse, 1970. GEUS Report file no. 22350.
257. **Larsen, O., Graff-Petersen, P.** *Si-Isotopic Studies and Mineral Composition of the Hagen Bræ Member in the Proterozoic Clastic Sediments at Hagen Bræ, Eastern North Greenland*. Copenhagen : Grønlands Geologiske Undersøgelse, 1980. GEUS Report file: no. 22436.
258. *Geochronology of Granitic and Supracrustal Rocks from the Northern Part of the East Greenland Caledonides: Ion Microprobe U-Pb zircon Ages*. **Kalsbeek, F., Nutman, A. P., Escher, J. C.,**

- Friderichsen, J. D., Hull, J. M., Jones, K. A., Pedersen, S. A. S.** 31-48, Copenhagen : Geological Survey of Denmark and Greenland, 1999, Vol. 184. <https://doi.org/10.34194/ggub.v184.5228>.
259. **Keller, F.** *Preliminary Interpretation - Aeromagnetic Survey of Northern Greenland*. New York : Grumman Ecosystems Corporation, 1972. GEUS report file # 20668.
260. **Ghisler, M.** *Ore Minerals in Stream Sediments from North Greenland*. Copenhagen : Grønlands Geologiske Undersøgelse, 1994.
261. **Ghisler, M., Stendal, H.** Geochemical and Ore Microscopic Investigations on Drainage Sands from the Peary Land Region, North Greenland. *Report on the 1979 geological expedition to the Peary Land region, North Greenland*. Rapport Nr. 99, 1980, Vol. GEUS Report file no. 22436, pp. 121-128.
262. **Naalakkersuisut.** GreenMin. *Greenland Portal*. [Online] Government of Greenland, 2020. [Cited: 11 September 2020.] <http://www.greenmin.gl/>.
263. **Fosberg, R.** A Gravity Map of Peary Land, North Greenland. *Report on the 1978 geological expedition to the Peary Land region, North Greenland*. Rapport Nr. 88, 1979, Vol. GEUS Report file no. 22410.
264. *Aeromagnetic Study of the Continental Crust of Northeast Greenland*. **Schlundwein, V., Meyer, U.** B4, Bremerhaven : AGU, 1999, Journal of Geophysical Research, Vol. 104, pp. 7527-7537. <https://doi.org/10.1029/1998JB900114>.
265. **Geoterrex-Dighem.** *Project AEM Greenland 1994-1998 Ariborne GEOTEM/Magnetic Survey over J.C. Christensen Land in central North Greenland*. GEUS. Ottawa : CGG Canada Ltd, 1998. Logistics and Processing Report. GEUS report file no. 21907.
266. **Gaina, C., Werner, S. C., Saltus, R., Maus, S., CAMP-GM GROUP.** Chapter 3 Circum-Arctic mapping project: new magnetic and gravity anomaly maps of the Arctic. [book auth.] A, M., Embry, A. F., Gautier, D. L., Stoupakova, A. V., Sørensen, K. (eds) Spencer. *Arctic Petroleum Geology*. s.l. : Geological Society of London, 2011, Vol. Memoirs v. 35, pp. 39-48.
267. **Abrahamsen, N., Marcussen, C.** *Preliminary Results of Rock- and Palaeomagnetic Field Work in Peary land, North Greenland*. Copenhagen : Grønlands Geologiske Undersøgelse, 1980. GEUS Report file no. 22436.
268. **Stensgaard, B. M., Kalvig, P., Stendal, H.** *Quantitative Mineral Resource Assessment: Sedimentary-hosted copper in Greenland, Reporting the Copper Assessment Workshop, March 2009*. Copenhagen : GEUS, 2011. p. 169 pp. Rapport 2011/104.
269. **Rosa, D., Stensgaard, B. M., Sørensen, L. L.** *Magmatic Nickel Potential in Greenland: Reporting the mineral resource assessment workshop 27-29 November 2012*. Copenhagen : GEUS, 2012. Rapport 2013/57.
270. *District-scale Concentration of Native Copper Lodes from a Tectonically Induced Thermal Plume of Ore Fluids on the Keweenaw Peninsula, Northern Michigan*. **Brown, A. C.** 8, s.l. : Society of Economic Geologists, 2008, Economic Geology, Vol. 103, pp. 1691-1694. <https://doi.org/10.2113/gsecongeo.103.8.1691>.
271. *Translating the Mineral Systems Approach into an Effective Exploration Targeting System*. **McCuaig, T. C., Beresford, S., Hronsky, J.** 3, s.l. : Ore Geology Reviews, 2010, Vol. 38, pp. 128-138. <https://doi.org/10.1016/j.oregeorev.2010.05.008>.
272. *Fooling Ourselves – Dealing with Model Uncertainty in a Mineral Systems Approach to Exploration*. **McCuaig, C. T., Kreuzer, O. P., Brown, W. M.** [ed.] C.J. et al. (eds.) Andrew. Dublin, Ireland : Society for Geology Applied to Mineral Deposits, 2007. Proceedings of the 9th Biennial Meeting of the Society for Geology Applied to Mineral Deposits. pp. 1435-1438.
273. *Microcline in the Native Copper Deposits of Michigan*. **Klein, I.** 10, s.l. : American Mineralogist, 1939, Vol. 24, pp. 643-650.



274. **Della, V. G.** *Geological Report on the 1994 Exploration Programme in Kronprins Christian Land North-East Greenland*. Copenhagen : Plainova A/S, 1995. GEU Report file no. 21415.
275. *The Mineral System Approach Applied to Magmatic Ni-Cu-PGE Sulphide Deposits*. **Barnes, S. J., Cruden, A. R., Arndt, N., Saumur, B. M.** s.l. : Elsevier, 2016, Ore Geology Reviews, Vol. 76, pp. 296-316. <https://doi.org/10.1016/j.oregeorev.2015.06.012>.
276. **Bitterroot**. Bitterroot Resources Intersects Magmatic Ni/Cu/Pgm Mineralization At The LM Property In Michigan. <https://bitterrootresources.com/>. [Online] 24 August 2020. [Cited: 8 September 2020.] <http://www.bitterrootresources.com/s/newsreleases.asp?ReportID=880581>.
277. *Native Iron (–platinum) Ores from the Siberian Platform Trap Intrusions*. **Ryabov, V. V., Lapkovsky, A. A.** 6, s.l. : Taylor & Francis, 2010, Australian Journal of Earth Sciences, Vol. 57, pp. 707-736. <https://doi.org/10.1080/08120091003739056>.
278. *Formation of Native Iron in Sediment-contaminated Magma: A Case Study of the Hanekammen Complex on Disko Island, West Greenland*. **Ulf-Møller, F.** 1, s.l. : Elsevier, 1989, Geochimica et Cosmochimica Acta, Vol. 54, pp. 57-70. [https://doi.org/10.1016/0016-7037\(90\)90195-Q](https://doi.org/10.1016/0016-7037(90)90195-Q).
279. **Bernstein, S.** Minex39. *Greenland Mineral Exploration Newsletter*. [Online] March 2011. [Cited: 14 July 2020.] <https://www.geus.dk/media/17896/minex39.pdf>.
280. **Cox, D. P.** *Mineral Deposit Models: Descriptive model of basaltic Cu*. Denver : United States Geological Survey, 1992. Bulletin 1693.
281. **Hitzman, M. W., Broughton, D., Selley, D., Woodhead, J., Wood, D., Bull, S.** The Central African Copperbelt: Diverse Stratigraphic, Structural, and Temporal Settings in the World's Largest Sedimentary Copper District. [book auth.] J. W., Harris, M., Camus, F. Hedenquist. *Geology and Genesis of Major Copper Deposits and Districts of the World: A Tribute to Richard H. Sillitoe*. s.l. : Society of Economic Geologists, 2012, Vol. Special Publication 16, pp. 487-514.
282. **McCuaig, C. T., Sonia, S., O'Connor, T., Busuttill, S., McCormack, N.** The Power of a Systems Approach to Mineral and Petroleum Exploration in Sedimentary Basins. [book auth.] A. M. R., Mauk, J. L. Arribas. [ed.] R. A. M., Mauk, J. L. Arribas. *Metals, Minerals, and Society*. s.l. : Society of Economic Geologists, 2018, Vol. 21.
283. *Research Trends in Economic Geology....and do we use our knowledge to maximum benefit?* **Robb, L. J.** 110, s.l. : Society of Economic Geologists Newsletter, 2017, p. 5 pp.
284. *Formation of Sedimentary Rock-Hosted Stratiform Copper Deposits Through Earth History*. **Hitzman, M. W., Selley, D., Bull, S.** 3, s.l. : Society of Economic Geologists, 2010, Economic Geology, Vol. 105, pp. 627-639. <https://doi.org/10.2113/gsecongeo.105.3.627>.
285. **Bornhorst, T. J., Barron, R. J.** Proceedings Volume 59: Part 2 - Field Trip Guidebook. [Online] 8-11 May 2013. [Cited: 23 September 2020.] http://flash.lakeheadu.ca/~pnhollin/ILSGVolumes/ILSG_59_2013_pt2_Houghton.pdf.
286. **Cox, D. P.** *Descriptive model of basaltic Cu*. s.l. : USGS, 1984.
287. *Constraining the Thermal History of the North American Midcontinent Rift System Using Carbonate Clumped Isotopes and Organic Thermal Maturity Indices*. **Gallagher, T. M., Sheldon, N. D., Mauk, J. L., Petersen, S. V., Gueneli, N., Brocks, J. J.** s.l. : Elsevier, 2017, Precambrian Research, Vol. 294, pp. 53-66. <https://doi.org/10.1016/j.precamres.2017.03.022>.
288. **Bornhorst, T. J., Barron, R. J.** Copper deposits of the Western Upper Peninsula of Michigan. [book auth.] J. D., Hudak, G. J., Wittkop, C., McLaughlin, P. I. Miller. *Geological Society of America Field Guide*. Houghton : The Geological Society of America, 2011, Vol. Field Guide, pp. 83-99.
289. **Bornhorst, T. J.** *Float Copper, Keweenaw Peninsula, Michigan*. s.l. : A. E. Seaman Mineral Museum, 2016. Web Publication 3.

290. **Baldwin, C.** Who is Responsible for a Massive and Mysterious Copper Operation that Historians Believe Predates the Bronze Age? *CIM Magazine*. [Online] Canadian Institute of Mining, Metallurgy and Petroleum, 1 February 2014. [Cited: 16 September 2020.] <https://magazine.cim.org/en/in-search/lake-superiors-ancient-copper-mining-mystery-en/#:~:text=the%20Bronze%20Age%3F-,Who%20is%20responsible%20for%20a%20massive%20and%20mysterious%20copper%20operation,believe%20predates%20the%20Bronze%20Age%3F&text=In%20t>.
291. **MSA.** Virtual Field Trip to the Keweenaw Peninsula, Michigan - Mining History (1840-1880). *Collector's Corner*. [Online] Mineralogical Society of America, 2020. [Cited: 16 September 2020.] http://www.minsocam.org/msa/collectors_corner/vft/mi3b.htm.
292. **Wikipedia.** Minesota Mine. *Wikipedia the Free Encyclopedia*. [Online] Wikimedia Foundation LLC, 5 November 2019. [Cited: 16 September 2020.] https://en.wikipedia.org/wiki/Minesota_Mine.
293. **ASME.** *Quincy No. 2 Mine Hoist (1920)*. Hancock : The American Society of Mechanical Engineers, 1984.
294. *The History, Geology, and Mineralogy of the White Pine Mine, Ontonagon County, Michigan*. **Rosemeyer, T.** 3, s.l. : Taylor & Francis, 2010, Journal of Rocks & Minerals, Vol. 74, pp. 160-176. <https://doi.org/10.1080/00357529909602535>.
295. **Highland.** Highland Copper Announces Positive PEA results and Mineral Resource Estimate for the White Pine North Copper Project in Michigan. [Online] 23 September 2019. [Cited: 27 October 2020.] <https://www.highlandcopper.com/19-09-23-news>.
296. **Gignac, L.** Feasibility Study – Copperwood Project. *Copperwood Project*. [Online] 31 July 2018. [Cited: 27 October 2020.] https://19e6d0b6-e4ff-4e43-83c8-ce0713db29bd.filesusr.com/ugd/62921a_41a8193d4db1498e8a2d5b1d1391308f.pdf.
297. —. Preliminary Economic Assessment – White Pine North. *White Pine project*. [Online] 6 November 2019. [Cited: 27 October 2020.] https://19e6d0b6-e4ff-4e43-83c8-ce0713db29bd.filesusr.com/ugd/62921a_e7ef326d82c34a02b50d5989931f6fb7.pdf.
298. *Copper Isotope Constraints on the Genesis of the Keweenaw Peninsula Native Copper District, Michigan, USA*. **Bornhorst, T. J., Mathur, R.** 185, s.l. : MDPI, 2017, minerals, Vol. 7, p. 20 pp. <https://doi.org/10.3390/min7100185>.
299. *Differentiation in lavas of the Keweenawan series and the origin of the copper deposits of Michigan*. **Cornwall, H. R.** 2, s.l. : Geological Society of America, February 1951, GSA Bulletin, Vol. 62, pp. 159-202. [https://doi.org/10.1130/0016-7606\(1951\)62\[159:DILOTK\]2.0.CO;2](https://doi.org/10.1130/0016-7606(1951)62[159:DILOTK]2.0.CO;2).
300. **Bornhorst, T. J.** Tectonic context of native copper deposits of the North American Midcontinent Rift System. [book auth.] R. W., Dickas, A. B., Green, J. C. Ojakangas. *Middle Proterozoic to Cambrian rifting, central North America*. s.l. : Geological Society of America, 1997, Vol. 312, pp. 127-139.
301. **Brown, A. C.** Copper Isotope Constraints on the Genesis of the Keweenaw Peninsula Native Copper District, Michigan, USA: A Comment. *minerals*. 2018, Vol. 8, 11.
302. **VOP.** Occupations: Copper Mining. *Superior View*. [Online] Views of the Past, 2020. [Cited: 16 September 2020.] <http://www.viewsofthepast.com/topics/fr-coppermining.htm>. CM-QUIN-10.jpg, M-MISC-08.jpg, CM-QUIN-08.jpg, CM-QUIN-10.jpg, CM-QUIN-21.jpg.
303. *A Detailed Assessment of Global Cu Resource Trends and Endowments*. **Mudd, G. M., Weng, Z., Jowitt, S. M.** 5, s.l. : Society of Economic Geologists, 2013, Economic Geology, Vol. 108, pp. 1163-1183. <https://doi.org/10.2113/econgeo.108.5.1163>.
304. *Aboriginal Copper Mines of Isle Royale, Lake Superior*. **Holmes, W. H.** 4, s.l. : American Anthropological Association, 1901, American Anthropologist, Vol. 3, pp. 684-696.



305. *Mineral System Analysis: Quo Vadis*. **Hagemann, S. G., Lisitsin, V. A., Huston, D. L.** s.l. : Elsevier, 2016, Ore Geology Reviews, Vol. 76, pp. 504-522. <https://doi.org/10.1016/j.oregeorev.2015.12.012>.
306. **Wyborn, L. A. I., Heintich, C. A., Jaques, A. L.** Australian Proterozoic Mineral Systems: Essential Ingredients and Mappable Criteria. [book auth.] P. C. Hallenstein. *Australian Mining Looks North – The Challenges and Choices*. Melbourne : Australasian Institute of Mining and Metallurgy, 1994.
307. **McCuaig, C. T., Hronsky, J. M. A.** The Mineral System Concept: The Key to Exploration Targeting. [book auth.] K. D., Golden, H. C. Kelly. *Building Exploration Capability for the 21st Century*. s.l. : Applied Earth Science, 2014, Vol. 18, pp. 153-175.
308. —. The Mineral System Concept: The Key to Exploration Targeting. [book auth.] K. D., Golden, H. C. Kelly. *Building Exploration Capability for the 21st Century*. s.l. : Society of Economic Geologists, 2014.
309. *Two Stages of Copper Mineralization in the Mwombezhi Dome in Northwestern Zambia: Metallogenic Implications for the Central African Copperbelt*. **Sillitoe, R. H., Perelló, J., Creaser, R. A., Wilton, J., Dawborn, T.** 8, s.l. : Economic Geology, 2015, Vol. 110, pp. 1917-1923. <https://doi.org/10.2113/ECONGEO.110.8.1917>.
310. *Age of Native Copper Mineralisation, Keweenaw Peninsula, Michigan*. **Bornhorst, Theodore J, et al.** 619-625, s.l. : Economic geology, 1988, Vol. 83. <https://doi.org/10.2113/gsecongeo.83.3.619>.
311. *Global Distribution of Sediment-hosted Metals Controlled by Craton Edge Stability*. **Hoggard, M. J., Czarnota, K., Richards, F. D., Huston, D. L., Jaques, A. L., Ghelichkhan, S.** s.l. : Nature Research, 2020, nature geoscience, Vol. 7, pp. 504-510. <https://doi.org/10.1038/s41561-020-0593-2>.
312. *Eurekan Transpressive Deformation in the Wandel Hav Mobile Belt (Northeast Greenland)*. **von Gosen, W., Piepjohn, K.** 4, s.l. : AGU, 2003, Tectonics, Vol. 22. <https://doi.org/10.1029/2001TC901040>.
313. *Timing and Origin of Magmatism in the Sverdrup Basin, Northern Canada—Implications for lithospheric evolution in the High Arctic Large Igneous Province (HALIP)*. **Dockman, D. M., Pearson, D. G., Heaman, L. M., Gibson, S. A., Sarkar, C.** s.l. : Elsevier, September 2018, Tectonophysics, Vols. 742-743, pp. 50-65. <https://doi.org/10.1016/j.tecto.2018.05.010>.
314. *Surface Erosion Events Controlled the Evolution of Plate Tectonics on Earth*. **Sobolev, S. V., Brown, M.** s.l. : Nature Research, 2019, Nature, Vol. 570, pp. 52-57. <https://doi.org/10.1038/s41586-019-1258-4>.
315. **Gibbon, E.** *Citronen Fjord Annual Exploration Report 2012 Field Season*. Perth : Ironbark Zinc Ltd, 2013. GEUS Report file no. 23661.
316. **Steenfelt, A.** The Geochemistry of Stream Silt, North Greenland. *Report on the 1979 geological expedition to the Peary Land region, North Greenland*. 1980, Vol. GEUS file no. 22436, Rapport Nr. 99, pp. 129-135.
317. *Hydrothermal Character of the Shaba Cu-Co-U Mineralization. Symposium on sediment-hosted copper deposits*. **Cluzel, D., Guilloux, L.** Ottawa : Canadian Mineralogist, 1986. Vol. 24.
318. **Schlegel, T.** *Ingredients for high-grade IOCG mineralization, Gawler craton, Australia*. [YouTube] s.l. : Ore Deposits Hub, 2020. <https://www.youtube.com/watch?v=Lv2VaFwzNos>.
319. *Formation of Massive Iron Deposits Linked to Explosive Volcanic Eruptions*. **Ovalle, J. T., La Cruz, N. L., Barra, F., Simon, A. C., Konecke, B. A., Rodriguez-Mustafa, M. A., Deditius, A. P., Childress, T. M., Morata, D.** 14855, s.l. : Scientific Reports, 2018, Nature Research, Vol. 8. <https://doi.org/10.1038/s41598-018-33206-3>.

320. **Kragh, K., Jensen, S. M., Fought, H.** *Ore Geological Studies of the Citronen Fjord Zinc Deposit, North Greenland: Resources of the Sedimentary Basins of North and East Greenland*. Copenhagen : Geological Survey of Denmark and Greenland, 1997. *Geology of Greenland Survey Bulletin* 176.
321. **Rosa, D., Rasmussen, J. A., Sørensen, E. V., Kalvig, P.** *Reconnaissance for Mississippi Valley-type and SEDEX Zn-Pb Deposits in the Franklinian Basin, Eastern North Greenland*. Copenhagen : Geological Survey of Denmark and Greenland, 2014. Report 2014/6.
322. **Lydon, J W, et al.** *A Preliminary Overview of Canada's Mineral Resources*,. Ottawa : Geological Survey of Canada, 2004. Open file 4668, DOI: 10.4095/215621.
323. **Dicken, C. L., Dunlap, P., Parks, H. L., Hammarstrom, J. M., Zientek, M. L.** *Spatial Database for a Global Assessment of Undiscovered Copper Resources*. Reston : United States Geological Survey, 2016. *Scientific Investigations Report* 2010–5090–Z.
324. **ASIAQ.** NunaGIS. *NunaGIS*. [Online] Greenland Survey, 2020. [Cited: 27 July 2020.] <http://en.nunagis.gl/>.
325. **Naalakkersuisut.** *Exploration licence with exclusive exploration rights for Greenfields Exploration for the area Misissuiffik J. C. Christensen Land in North Greenland*. Nuuk : Government of Greenland, 2020. Licence No. 2021-07.
326. **Golder.** *Air Quality Modelling Report for the Proposed Citronen Mining Operations*. Stockholm : Golder Associates AB, 2011. Report number: 0512450343.
327. **Tertra Tech.** *Citronen Project Screening-Level Ecological Risk Assessment - Final Report*. Golden : s.n., 2012. Project No. 10533201.00/114-311255.
328. **TetraTech.** *Final Stream Discharge and Water Supply Estimates, Citronen Fjord Development Project*. Golden : Tetra tech, 2010.
329. *From Mine to Coast: Transport infrastructure and the direction of trade in developing countries.* **Bonfatti, R and Poelhekke, S.** : 91-108, s.l. : *Journal of Development Economics*, 2017, Vol. 127. 0304-3878.
330. *Chromite Compositions in Nickel Sulphide Mineralized Intrusions of the Kabanga-Musongati-Kapalagulu Alignment, East Africa: Petrologic and exploration significance.* **Evans, D. M.** s.l. : Elsevier, November 2017, *Ore Geology Reviews*, Vol. 90, pp. 307-321. <https://doi.org/10.1016/j.oregeorev.2017.03.012>.
331. **Wilburn, D. R., Porter, K. E.** *Exploration. Mining Engineering*. 1999, Vol. 51, 5, pp. 39-49.
332. *Main Characteristics and Review of Mineral Resources of the Kabanga-Musongati Mafic-ultramafic Alignment in Burundi.* **Deblond, A., Tack, L.** 2, s.l. : Elsevier, 1999, *Journal of African Earth Sciences*, Vol. 29, pp. 313-328. [https://doi.org/10.1016/S0899-5362\(99\)00100-1](https://doi.org/10.1016/S0899-5362(99)00100-1).
333. **Ironbark.** *Shipping Conditions, Citronen Project, Greenland. Ironbark Zinc Limited*. [Online] 21 October 2010. [Cited: 26 October 2020.] <https://ironbark.gl/investor-centre/asx-announcements/2020-2/>.
334. **Chau, David.** Australian economy and miners to profit from Brazil's coronavirus outbreak. *ABC news*. [Online] 8 June 2020. [Cited: 10 November 2020.] <https://www.abc.net.au/news/2020-06-08/economy-miners-benefit-vale-coronavirus-iron-ore/12332164>.
335. **ArcticPortal.** Downloads. *ArcticPortal*. [Online] 2018. [Cited: 3 March 2018.] <https://arcticportal.org/maps/download>.
336. *An Investigation on a Diesel Jet's Ignition Characteristics Under Cold-start Conditions.* **Liu, F., Zhang, Z., Wu, H., Li, Y., Ma, Y., Li, X., Du, W.** s.l. : Elsevier, 2017, *Applied Thermal Engineering*, Vol. 121, pp. 511-519. <https://doi.org/10.1016/j.applthermaleng.2017.04.133>.



337. *Computational Evaluation of Thermal Management Strategies in an Underground Mine*. **Sasmito, A. P., Kurnia, J. C., Birgersson, E., Mujumdar, A. S.** s.l. : Elsevier, November 2015, Applied Thermal Engineering, Vol. 90, pp. 1144-1150. <https://doi.org/10.1016/j.applthermaleng.2015.01.062>.
338. *Internal Combustion Engine Cold-start Efficiency: A review of the problem, causes and potential solutions*. **Roberts, A, Brooks, R and Shipway, P.** : 327-350, s.l. : Energy Conversion and Management, 2014, Vol. 82. 0196-8904.
339. *Quantifying Safety Benefit of Winter Road Maintenance: Accident frequency modelling*. **Usman, T., Fu, L., Miranda-Moreno, L. F.** 6, s.l. : Elsevier, 2010, Accident Analysis & Prevention, Vol. 42, pp. 1878-1887. <https://doi.org/10.1016/j.aap.2010.05.008>.
340. *Interaction of Katabatic Winds and Mesocyclones Near the Eastern Coast of Greenland*. **Klein, T., Heinemann, G.** 4, s.l. : Royal Meteorological Society, December 2002, Meteorological Applications, Vol. 9, pp. 407-422. <https://doi.org/10.1017/S1350482702004036>.
341. *Laboratory Characterization of Cemented Tailings Paste Containing Crushed Waste Rocks for Improved Compressive Strength Development*. **Hane, I., Belem, T., Benzaazoua, M., Maqsoud, A.** 2, s.l. : Springer, 2017, Geotechnical and Geological Engineering, Vol. 35, pp. 645-662. <https://doi.org/10.1007/s10706-016-0131-6>.
342. *The Current Investment Landscape for Mining, Exploration & Mineral Sands*. **Sykes, J. P.** Perth : 19th Australian Mineral Sands Conference, 22 March, 2018. <http://doi.org/10.13140/RG.2.2.20382.02883>.
343. *The Separation of Chalcopyrite and Chalcocite from Pyrite in Cleaner Flotation After Re grinding*. **Chen, X., Peng, Y., Bradshaw, D.** s.l. : Elsevier, 2014, Minerals Engineering, Vol. 58, pp. 64-72. <https://doi.org/10.1016/j.mineng.2014.01.010>.
344. *Process Mineralogy of Copper-nickel Sulphide Flotation by a Cyclonic-static Micro-bubble Flotation Column*. **Cao, Y., Gui, X., Ma, Z., Yu, X., Chen, X., Zhang, X.** 6, s.l. : Elsevier, 2009, Mining Science and Technology (China), Vol. 19, pp. 784-787. [https://doi.org/10.1016/S1674-5264\(09\)60143-5](https://doi.org/10.1016/S1674-5264(09)60143-5).
345. **Bendict, C. H.** *Lake Superior Milling Practice: A Technical History of a Century of Copper Milling*. s.l. : Michigan College of Mining and Technology Press, 1955. ASIN B0007FI4X8.
346. **AustMine**. Gekko supplies technology for Native Copper Gravity Circuit. [Online] AustMine Ltd, 12 March 2018. [Cited: 15 October 2020.] <http://www.austmine.com.au/News/category/articles-editorials/gekko-supplies-technology-for-native-copper-gravity-circuit>.
347. **Wikipedia**. Copper Extraction. [Online] Wikimedia Foundation LLC, 26 August 2020. [Cited: 15 October 2020.] https://en.wikipedia.org/wiki/Copper_extraction.
348. **Ahlness, J. K., Kirchner, J. C.** *Electronic Ore-sorting Tests on Native Copper Ore*. Washington DC : United States Bureau of Mines, 1980. RI 8490.
349. **Rohner, P.** Innovations in Copper Mineral Processing Technology. [Online] 17 June 2014. [Cited: 15 October 2020.] <https://www.coreresources.com.au/wp-content/uploads/2014/05/Core-Presentation-Copper-Conference-June-2014.pdf>.
350. **ASIA Miner**. Native Copper signalled way to modern metallurgy. *The ASIA Miner*. [Online] SEMCO Publishing, 22 May 2014. [Cited: 15 October 2020.] <http://asiaminer.com/features/5654-native-copper-signalled-way-to-modern-metallurgy.html#.X4feztAzaUk>.
351. *It's Not Time to Be Wasted: Identifying, Evaluating, and Appreciating Mine Wastes in Michigan's Copper Country*. **Gohman, S. M.** 1-2, s.l. : Society for Industrial Archeology, 2013, The Journal of the Society For Industrial Archeology, Vol. 39, pp. 5-22. <https://www.jstor.org/stable/43958424>.
352. **Teck**. Modelling Workshop. *Teck*. [Online] 2 April 2020. [Cited: 15 October 2020.] <https://www.teck.com/media/Teck-2020-Modelling-Workshop-April-2.pdf>.

353. **Glencore.** Raglan Mine Operates its Second Wind Turbine. *Glencore Canada*. [Online] Glencore Canada Corporation, 09 October 2018. [Cited: 12 November 2020.] <https://www.glencore.ca/en/Media-and-insights/Insights/Raglan-Mine-Operates-its-Second-Wind-Turbine>.
354. —. Green Energy Sources. *Glencore Mine Raglan*. [Online] Glencore Canada Corporation, 2020. [Cited: 11 November 2020.] <https://www.mineraglan.ca/en/our-commitments/sustainability/environment/Pages/green-energies.aspx>.
355. **TUGLIQ.** Energy Storage Optimizes Wind Power for Remote Arctic Mine. [Online] May 2020. [Cited: 11 November 2020.] <https://www.saftbatteries.com/case-studies/energy-storage-optimizes-wind-power-remote-arctic-mine>.
356. **RioTinto.** Diavik Diamon Mine 2019 Sustainable Development Report. *Dominion Diamond Mines LLC*. [Online] 31 March 2020. [Cited: 12 November 2020.] <https://www.riotinto.com/-/media/Content/Documents/Operations/Diavik/RT-Diavik-Sustainability-report.pdf>.
357. **Carreau, Michael.** Solar Power in the Arctic. *CIM Magazine*. [Online] 26 September 2019. [Cited: 12 November 2020.] <https://magazine.cim.org/en/voices/solar-powering-the-arctic-en/>.
358. <https://fuelcellworks.com/news/icelandic-new-energy-has-launched-2030-vision-for-hydrogen-in-iceland/>. Icelandic New Energy has Launched 2030 Vision for Hydrogen in Icelena. *News*. [Online] Fullcellworks, 26 June 2020. [Cited: 12 November 2020.] <https://fuelcellworks.com/news/icelandic-new-energy-has-launched-2030-vision-for-hydrogen-in-iceland/>.
359. **Burgess, Molly.** New agreement looks at exporting hydrogen from Iceland to Rotterdam. [Online] H2 View, 26 October 2020. [Cited: 12 November 2020.] <https://www.h2-view.com/story/new-agreement-looks-at-exporting-hydrogen-from-iceland-to-rotterdam/>.
360. *Virtual Sources of Body Waves from Noise Correlations in a Mineral Exploration Context*. **Dales, P., Pinzon-Ricon, L., Brenguier, F., Boué, P., Arndt, N., McBride, J., Lavoué, F., Bean, C. J., Beaupretre, S., Fayjalou, R., Olivier, G.** 4, s.l. : GeoScienceWorld, 2020, Seismological Research Letters, Vol. 91, pp. 2278-2286. <https://doi.org/10.1785/0220200023>.
361. **Meteoblue.** History & Climate. *Meteoblue.com*. [Online] 2020. [Cited: 17 August 2020.] <https://www.meteoblue.com/>.
362. **GGG.** *Kvanefjeld Optimised Feasibility Study: Substantial 40% Capital Cost Reduction*. Perth : Greenland Minerals Ltd, 2019. 9 July 2019.
363. **Wikipedia.** Station Nord Greenland. *Wikipedia the Free Encyclopedia*. [Online] Wikimedia Foundation, 2020. [Cited: 22 July 2020.] https://en.wikipedia.org/wiki/Station_Nord_Greenland.
364. **Berkeley.** Temperature Monitoring Station: Cape Harald Moltke. [Online] Berkeley Earth, 2020. [Cited: 22 July 2020.] <http://berkeleyearth.lbl.gov/stations/14850>.
365. **Wikipedia.** List of Northernmost Settlements. *Wikipedia the Free Encyclopedia*. [Online] Wikimedia LLC, 18 July 2020. [Cited: 22 July 2020.] https://en.wikipedia.org/wiki/List_of_northernmost_settlements.
366. *From Kenorland to Modern Continents: Tectonics and Metallogeny*. **Yakubchuk, A. S.** 2, s.l. : Pleiades Publishing, Inc, 2019, Geotectonics, Vol. 53, pp. 169-192.
367. **Wikipedia.** Fjord. *Wikipedia The Free Encyclopedia*. [Online] Wikimedia Foundation LLC, 21 July 2020. [Cited: 24 August 2020.] <https://en.wikipedia.org/wiki/Fjord>.
368. **Anthony, J. W., Bideaux, R. A., Bladh, K. W., Nichols, M. C.** Prehnite. *Handbook of Mineralogy*. Chantilly : Mineralogical Society of America, 2003.



369. —. Pumpellyite-(Mg). *Handbook of Mineralogy*. Chantilly : Mineralogical Society of America, 2005.
370. —. Thomsonite. *Handbook of Mineralogy*. Chantilly : Mineralogical Society of America, 2003.
371. **The World Bank**. GDP (current US\$) - Greenland. *The World Bank*. [Online] 2020. [Cited: 30 September 2020.] https://data.worldbank.org/indicator/NY.GDP.MKTP.CD?locations=GL&name_desc=true.
372. *Sediment-hosted Stratiform Copper Deposits in the Adelaide Geosyncline, South Australia; Geophysical Responses of Minerals and the Mineralised Environment*. **Dentith, M., Stuart, R.** s.l. : ASEG Extended Abstracts, 2003. https://doi.org/10.1071/ASEGSpec12_14.
373. *The Volcanic Explosivity Index (VEI): An Estimate of Explosive Magnitude for Historical Volcanism*. **Newhall, C. G., Self, S.** C2, s.l. : AGU, 1982, Oceans, Vol. 87. <https://doi.org/10.1029/JC087iC02p01231>.
374. **Henderson, B.** Who Discovered the North Pole? *Smithsonian Magazine*. [Online] Smithsonian Institute, April 2009. [Cited: 28 July 2020.] <https://www.smithsonianmag.com/history/who-discovered-the-north-pole-116633746/>.
375. **Hitzman, M., Kirkham, R., Broughton, D., Thorson, J., Selley, D.** The sediment-hosted stratiform copper ore system. [book auth.] J. W., Thompson, J. F. H., Goldfarb, R. J., Richards, J. P. Hendenquist. *Economic Geology 100th Anniversary Volume*. s.l. : Society of Economic Geologists, 2005, pp. 609-642.
376. **Self, S., Coffin, M. F., Rampino, M. R., Wolff, J. A.** Chapter 24. Large Igneous Provinces and Flood Basalt Volcanism. [book auth.] H., Boughton, B., Rymer, H., Stix, J., McNutt, S., (eds) Sigurdsson. *The Encyclopedia of Volcanoes (Second Edition)*. s.l. : Academic Press Ltd Elsevier Science Ltd, 2015, pp. 441-455.
377. **Pinti, D.** Red Beds. [book auth.] M., Amils, R., Quintanilla, J. C., CleavesII, J., Irvine, W. M., Pinti, D. L., Viso, M. Garaud. *Encyclopedia of Astrobiology*. Berlin : Springer, 2015.
378. **Bell, J. A., Saleem, A.** *Frontier Project - Technical Assessment*. Perth : Greenfields Exploration Ltd, 2018. <https://doi.org/10.13140/rg.2.2.11673.24165>.
379. *Rare Earth Element Mobility in and Around Carbonatites Controlled by Sodium, Potassium, and Silica*. **Anenburg, M., Mavrogenese, J. A., Frigo, C., Wall, F.** 41, s.l. : American Association for the Advancement of Science, 2020, Science Advances, Vol. 6, p. 10 pp. <https://doi.org/10.1126/sciadv.abb6570>.
380. **Müller, D., Groves, D. I.** *Potassic Igneous Rocks and Associated Gold-Copper Mineralization*. s.l. : Springer, 2019. <https://doi.org/10.1007/978-3-319-92979-8>.
381. *Potassic alteration and veining and the age of copper emplacement at Mount Isa, Australia*. **Gregory, M. J., Wilde, A. R., Schaefer, B. F., Keays, R. R.** Beijing : Springer Nature, 2005. https://doi.org/10.1007/3-540-27946-6_192.
382. *Paleomagnetism of the Native Copper Mineralization, Keweenaw Peninsula, Michigan*. **Symons, D. T.A., Kawasaki, K.** 9, s.l. : Canadian Science Publishing, 2019, Canadian Journal of Earth Sciences, Vol. 56, pp. 932-947.
383. *Hydrothermal Native Copper in Ocean Island Alkali Basalt from the Mineoka Belt, Boso Peninsula, Central Japan*. **Ikehata, K., Chida, K., Tunogae, T., Bornhorst, T. J.** 3, s.l. : Society of Economic Geologists, 2016, Economic Geology, Vol. 111, pp. 783-794. <https://doi.org/10.2113/econgeo.111.3.783>.
384. *Magma chambers versus mush zones: constraining the architecture of sub-volcanic plumbing systems from microstructural analysis of crystalline enclaves*. **Holness, M., Stock, M., Geist, D.** 2139,

s.l. : The Royal Society Publishing, 2019, *Philosophical Transactions*, Vol. 377, p. 22 pp. <https://doi.org/10.1098/rsta.2018.0006>.

385. **Barthelmy, D.** Brochantite Mineral Data. *Mineralogy Database*. [Online] 2020. [Cited: 11 September 2020.] <http://webmineral.com/data/Brochantite.shtml#.X1rgzXkzaUk>.

386. *Tectonic Evolution, Superimposed Orogeny, and Composite Metallogenic System in China*. **Deng, J., Wang, Q., Li, G.** s.l. : Elsevier, 2017, *Gondwana Research*, Vol. 50, pp. 216-266. <https://doi.org/10.1016/j.gr.2017.02.005>.

387. *Some Observations on Spilitized Basalts of the Western Deccan Traps, India*. **Naik, A., Sheth, H., Samant, H., D'Souza, S.** Moscow : XXIX International Mineral Processing Congress, 2018.

388. *Entablature: Fracture Types and Mechanisms*. **Forbes, A. E. S., Blake, S., Tuffen, H.** 820, s.l. : Bulletin of Volcanology, 2014, Vol. 76. <https://doi.org/10.1007/s00445-014-0820-z>.

389. *Age of the Zambian Copperbelt*. **Sillitoe, R. H., Perelló, J., Creaser, R. A., Wilton, J., Wilson, A. J., Dawborn, T.** s.l. : Springer, 2017, *Mineralium Deposita*, Vol. 52, pp. 1245-1268. <https://doi.org/10.1007/s00126-017-0726-8>.

390. *Reconciliation of Experiments and Theory on Transport Properties of Iron and the Geodynamo*. **Zhang, Y., Hou, M., Liu, G., Zhang, C., Prakapenka, V. B., Greeberg, E., Fei, Y., Cohen, R. E., Lin, J.** 7, s.l. : American Physical Society, 2020, *Physical Review Letters*, Vol. 125, p. 7 pp. <https://doi.org/10.1103/PhysRevLett.125.078501>.

391. *Sediment-hosted Lead-zinc Deposit in Earth History*. **Leach, D. L., Bradley, D. C., Huston, D., Pisarevsky, S. A., Taylor, R. D., Gardoll, S. J.** 3, s.l. : Society of Economic Geologists, May 2010, *Economic Geology*, Vol. 105, pp. 593-625. <https://doi.org/10.2113/gsecongeo.105.3.593>.

392. **The Editors of Encyclopaedia Britannica.** Devitrification. *Encyclopædia Britannica*. [Online] Encyclopædia Britannica, inc., 27 November 2014. [Cited: 16 August 2020.] <https://www.britannica.com/science/devitrification>.

393. **Anthony, J. W., Bideaux, R. A., Bladh, K. W., Nichols, M. C.** Tridymite. [book auth.] Mineral Data Publishing. *Handbook of Mineralogy*. s.l. : Mineral Data Publishing, 2001.

394. **Haldar, S. K., Tišljarić, J.** Basic Mineralogy. *Introduction to Mineralogy and Petrology*. s.l. : Elsevier, 2014, pp. 39-79.

395. *Nickel: Application of Geophysics to Nickel Sulphide Exploration in the Kambalda District, Western Australia*. **Trench, A., Williams, P. K.** s.l. : Taylor & Francis, 1994, *ASEG Extended Abstracts*, Vol. 1, pp. 169-180. https://doi.org/10.1071/ASEGSpec07_10.

396. *Reconstruction of the Kenorland Supercontinent in the Neoproterozoic Based on Paleomagnetic and Geological Data*. **Lubnina, N. V., Slabunov, A. I.** 4, s.l. : Allerton Press, Inc, 2011, *Moscow University Geology Bulletin*, Vol. 66, pp. 242-249. <https://doi.org/10.3103/S0145875211040077>.

397. **Naalakkarsuisut.** Executive Order no. 7 of 17 June 1992 from the Greenland Home Rule Authority concerning the National Park in North and East Greenland, as amended by Executive Order no. 16 of 5 October 1999. Nuuk : Government of Greenland, 1999.

398. *Time Scales and Length Scales in Magma Flow Pathways and the Origin of Magmatic Ni-Cu-PGE Ore Deposits*. **Barnes, S. J., Robertson, J. C.** 1, s.l. : Elsevier, 2019, *Geoscience Frontiers*, Vol. 10, pp. 77-87. <https://doi.org/10.1016/j.gsf.2018.02.006>.

399. *Assembly, configuration, and break-up history of Rodinia: A synthesis*. **Li, Z. X., Bogdanova, S. V., Collins, A. S., Davidson, A., De Waele, B., Ernst, R. E., Fitzsimons, I. C. W., Fuck, R. A., Gladkochub, D. P., Jacobs, J., Karlstrom, K. E., Lu, S., Natapov, L. M., Pease, V., Pisarevsky, S. A., Thrane, K., Vernikovskiy, V.** 1-2, s.l. : Elsevier, 2008, *Precambrian Research*, Vol. 160, pp. 179-210. <https://doi.org/10.1016/j.precamres.2007.04.021>.



400. *The Lomonosov Ridge as a natural extension of the Eurasian continental margin into the Arctic Basin.* **Poselov, V. A., Avetisov, G. P., Butsenko, V. V., Zholondz, S. M., Kaminsky, V. D., Pavlov, S. P.** 12, s.l. : Elsevier, 2012, Russian Geology and Geophysics, Vol. 53, pp. 1276-1290. <https://doi.org/10.1016/j.rgg.2012.10.002>.
401. *Lomonosov Ridge—A double-sided continental margin.* **Jokat, W., Uenzelmann-Neben, G., Kristoffersen, Y., Rasmussen, T. M.** 10, s.l. : The Geological Society of America, 1992, Geology, Vol. 20, pp. 887-890. [https://doi.org/10.1130/0091-7613\(1992\)020<0887:LRADSC>2.3.CO;2](https://doi.org/10.1130/0091-7613(1992)020<0887:LRADSC>2.3.CO;2).
402. *Signatures of Key Petroleum System Elements: Outcrop examples from the Anambra Basin, Southeastern Nigeria.* **Dim, C. I. P., Mode, A. W., Okware, I. C.** s.l. : Springer, 2019, Journal of Petroleum Exploration and Production Technology, Vol. 9, pp. 1615-1631.
403. *The Nature of Mineralizing Fluids of the Kipushi Zn-Cu deposit, Katanga, Democratic Republic of Congo: Quantitative fluid inclusion analysis using laser ablation ICP-MS and bulk crush-leach method.* **Heijlen, W., Banks, D. A., Muchez, P., Stensgard, B. M., Yardley, B. W. D.** 7, s.l. : Society of Economic Geologists, 2008, Economic Geology, Vol. 103, pp. 1459-1482. <https://doi.org/10.2113/gsecongeo.103.7.1459>.
404. *Textural and Geochemical Analysis of Chalcopyrite, Galena and Sphalerite.* **Cave, B., Lilly, R., Barovich, K.** s.l. : Elsevier, 2020, Ore Geology Reviews, Vol. 124, p. 103647. <https://doi.org/10.1016/j.oregeorev.2020.103647>.
405. **Latitude.** Nord, Greenland. *Find GPS coordinates for any address or location.* [Online] Latitude, 2020. [Cited: 22 July 2020.] <https://latitude.to/articles-by-country/gl/greenland/13101/nord-greenland>.
406. *Tectonically Driven Fluid Flow and Gold Mineralisation in Active Collisional Orogenic Belts: Comparison between New Zealand and western Himalaya.* **Craw, D., Koons, P. O., Horton, T., Chamberlain, C. P.** 1-3, s.l. : Elsevier, 2002, Tectonophysics, Vol. 348, pp. 135-153. [https://doi.org/10.1016/S0040-1951\(01\)00253-0](https://doi.org/10.1016/S0040-1951(01)00253-0).
407. *The Onset of Widespread Marine Red Beds and the Evolution of Ferruginous Oceans.* **Song, H., Jiang, G., Poulton, S. W., Wignall, P. B., Tong, J., Song, H., An, Z., Chu, D., Tian, Li., She, Z., Wang, C.** 399, s.l. : Nature Research, 2017, Nature Communications, Vol. 8, p. 7 pp. <https://doi.org/10.1038/s41467-017-00502-x>.
408. *Zoning in the White Pine Copper Deposit, Ontonagon County, Michigan.* **Brown, A. C.** 4, s.l. : Society of Economic Geologists, 1971, Economic Geology, Vol. 66, pp. 543-573. <https://doi.org/10.2113/gsecongeo.66.4.543>.
409. **Simon, A.** *The Formation of IOCG and IOA Mineral Systems: A case Study of El Laco, Chile – Adam Simon.* [YouTube] s.l. : Ore Deposits Hub, 2020. ODH017.
410. *Salt as a Fluid Driver, and Basement as a Metal Source, for Stratiform Sediment-hosted Copper Deposits.* **Koziy, L., Bull, S., Large, R., Selley, D.** 12, s.l. : The Geological Society of America, 2009, Geology, Vol. 37, pp. 1107-1110. <https://doi.org/10.1130/G30380A.1>.
411. **Wikipedia.** Minik Wallace. *Wikipedia the Free Encyclopedia.* [Online] Wikimedia Foundation LLC, 19 September 2020. [Cited: 9 November 2020.] https://en.wikipedia.org/wiki/Minik_Wallace#In_popular_culture.
412. **Geoscience Australia.** Mineral Deposits Mineral Systems and Mineralising Events. *Geoscience Australia.* [Online] 2020. [Cited: 16 November 2020.] <http://www.ga.gov.au/scientific-topics/minerals/mineral-exploration/deposits-events>.

16 CONSENT AND COMPLIANCE STATEMENT: DR BELL

The information in this Report that relates to Technical Assessment and Valuation of Mineral Assets reflects information compiled and conclusions derived by Dr Jonathan Bell, who is a Member of The Australian Institute of Geoscientists. Dr Bell has sufficient experience relevant to the Technical Assessment and Valuation of the Mineral Assets under consideration and to the activity which he is undertaking to qualify as a Specialist as defined in the 2015 edition of the 'Australasian Code for the Public Reporting of Technical Assessments and Valuations of Mineral Assets'. Dr Bell consents to the inclusion in the report of the matters based on his information in the form and context in which it appears.

I, Jonathan Bell, do hereby certify that:

- a) I am the Managing Director of Greenfields Exploration Ltd, of Level 14, 197 St Georges Terrace, Perth Western Australia, 6000;
- b) This certificate applies to the Arctic Rift Copper Project Technical Assessment Report which has an Effective Date of 17 November 2020;
- c) I am a Member of the Australian Institute of Geoscientist (No. 3116), Graduate of the Australian Institute of Company Directors (No. 0038531), Member of the Resources and Energy Association, and Associate of the Stockbrokers Association of Australia. I have twenty years mining industry experience as a geologist, within which I have a decade of experience as a consulting mineral economist;
- d) I have not visited ARC but have worked in eastern Greenland. I have relied on public domain information, government data and interviews with prior explorers in the region;
- e) I am the responsible person for the entirety of this Report;
- f) I am the founder, major shareholder, and Managing Director of Greenfields;
- g) I am not financially independent of the Company and do not meet tests of Independence as set out in ASIC Regulatory Guide 112 (8). However, I have exercised objective thinking and presented a balanced and referenced Report;
- h) I have read the definition of a Specialist set out in VALMIN (2015) and a Competent Person as set out in JORC (2012), and certify that by reason of my education, affiliation with a professional association and past relevant work experience, I fulfil the requirements to be a Specialist for the purpose of VALMIN Reporting; and
- i) as of the date of this certificate, to the best of my knowledge, information and belief, those portions of the Report for which I am responsible contain all scientific and technical information required to be disclosed to make the report not misleading.
- j) I have read VALMIN (2015) and JORC (2012) and have prepared this Report per the minimum reporting criteria set out in those Codes;
- k) I confirm that I have read the Report and that it fairly and accurately represents the information for which I am responsible; and
- l) I consent to the inclusion of this Report in an offer document.



18 November 2020

Signature of Competent Person

Date



17 APPENDIX 1: JORC TABLE 1

JORC Table 1, section 2

<i>Criteria</i>	Arctic Rift Copper project
<i>Mineral tenement and land tenure status</i>	<p>The Arctic Rift Copper project ('ARC') comprises a single Special Exploration Licence ('SEL') application (identifier: M-MLSA-279). The spatial area of the application is 5,774km², the boundary of which is defined by the points:</p> <p style="text-align: center;"> 82°3'N, 29°18'W 81°35'N, 26°8'W 82°3'N, 25°41'W 81°30'N, 26°8'W 82°0'N, 25°41'W 81°30'N, 26°54'W 82°0'N, 25°43'W 81°25'N, 26°54'W 81°59'N, 25°43'W 81°25'N, 28°20'W 81°59'N, 25°44'W 81°21'N, 28°20'W 81°58'N, 25°44'W 81°21'N, 29°35'W 81°58'N, 25°46'W 81°19'N, 29°35'W 81°56'N, 25°46'W 81°19'N, 31°0'W 81°56'N, 25°48'W 81°27'N, 31°0'W 81°55'N, 25°48'W 81°27'N, 31°42'W 81°55'N, 25°50'W 81°34'N, 31°42'W 81°53'N, 25°50'W 81°34'N, 32°7'W 81°53'N, 25°52'W 81°51'N, 32°7'W 81°50'N, 25°52'W 81°51'N, 31°0'W 81°50'N, 25°54'W 81°54'N, 31°0'W 81°46'N, 25°54'W 81°54'N, 30°18'W 81°46'N, 25°55'W 81°58'N, 30°18'W 81°35'N, 25°55'W 81°58'N, 29°18'W </p> <p>An SEL confers an exclusive right to explore for mineral for three years at a reduced holding cost, provided each licence covers more than 1,000km². After three years, the holder of Special Exploration Licence has the right to convert the area, whole or in part, to conventional Exploration Licences. The fee for licence application was AUD1,092, and upon granting of the licence, a further ~AUD6,730 is payable. The minimum expenditure obligation for an SEL is DKK500/km² indexed to Danish CPI as at January 1992. The Company estimates that upon granting of the licence, the expenditure requirement will be approximately AUD1,080,000 per annum. However, the Government has waived all expenditure obligations for 2020, and as such, no holding cost of the licence will crystallise until 31 December 2021. The obligation for 2021 will be calculated on 1 January 2022 based on the area under licence on a preceding day. Furthermore, Greenfields expects to reduce the licence area before this time. Expenditure above the minimum regulatory requirement is carried forward for a maximum of three years.</p>
<i>Exploration done by other parties</i>	<p>ARC was subject to commercial exploration by Avannaa Resources Limited ('Avannaa') in 2010 and 2011. In its first year, Avannaa focussed its work in a small area in the northern part of the licence area known as Neergaard North. This work focussed on historical government and academic work that had identified highly anomalous copper mineralisation. In 2010, the work included geochemical soil sampling, rock chipping and trenching of high-grade material associated with a NW-SE trending fault breccias. Based on the success of the 2010 program, Avannaa undertook a much larger regional reconnaissance program in 2011. This program involved a heli-supported geochemical sampling program over a large area designed to test the copper prospectivity of various stratigraphic positions, as well as extending the length of the 'Discovery Zone' identified in 2010. Both aspects of this program were successful in that the Discovery Zone was shown to have a minimum strike length of 2km before disappearing undercover; and that certain stratigraphic horizons show copper anomalism over a significant lateral extent. However, much of the extended area explored by Avannaa was located to the southeast of the ARC and is now located in a Government-mandated no-go zone for mineral exploration.</p>

Geology | ARC is located near a triple junction demarcated by three rifts. ARC is in the passive margin of one of these rifts. The triple junction is associated with an ascending mantle plume in Mesoproterozoic (1,600M to 1,000M years ago) times. In more recent times, a mantle plume traversed underneath Greenland and is currently identifiable as the deep mantle-tapping Icelandic mantle plume.

ARC contains a sequence of Mesoproterozoic-aged sediments sandstones belonging to the Independence Fjord Basin that have been intruded by highly-altered dolerites, and overlain by 1.2km of Mesoproterozoic-aged flood basalts ('Zig-Zag Fm' basalts). In turn, the basalts are overlain by 1.1km of Neoproterozoic-aged (1,000M to 541M years ago) clastic and carbonate sediments belonging to the Hagen Fjord Group. The lower portion of the Hagen Fjord Group is dominated by sandstones and siltstones, and the upper part by limestone and dolomites. Based on stream sediment samples, the iron oxide minerals switch from magnetite to the east of ARC, to haematite within ARC, which reflects a change in fluid oxidation state (from reduced to oxidised). Fluid flow is from east to west which implies that oxidation is a component of the copper dropping out of solution. The oxidation of a reduced fluid is consistent with the chemistry required to form native copper such as that observed in ARC. The metamorphic grade of the Zig-Zag Fm basalts is of the zeolite facies, and the Hagen Fjord Group sediments show lower grade metamorphism. Due to the location within a passive margin, there is adequate preservation aside from mechanical erosion.

Commercially interesting copper mineralisation occurs in both the basalts and Hagen Fjord Group sediments. The basalts are known to contain in situ native copper, and native copper is found extensively in the surrounding drainage systems. Significantly, the native copper specimens recovered by Avannaa in 2010 weigh up to 1kg. Greenfields considers that the age, setting and mineral composition makes the Zig-Zag Fm copper analogous to the copper deposits of the Michigan Upper (Keweenaw) Peninsula, and a primary source of copper for the anomalies reported in the overlying sediments. The fault breccias that transect the basalts and Neoproterozoic sediments are interpreted by the Company to represent fluid pathways as there are zones of intense potassium alteration within the surrounding quartz dominated sedimentary rocks. These breccias, which are up to 25m wide show copper mineralisation. The chalcocite and chalcopyrite copper-bearing minerals are significant as they demonstrate that sulphur has been added into the fluids derived from the sulphur-undersaturated system. A source of sulphur is generally considered an important factor in the sediment-hosted copper deposit model. Other important components of the deposit model are also reported, including pseudomorphed gypsum (a source of sulphur, and copper mobilising salts), hydrogeologic seals, and contrasting oxidation states. Copper sulphides occur in the predicted geological lithological settings. The highest copper grades are close to geophysical gravity, magnetic and electromagnetic anomalies. The ~640 km² area of geophysical and geochemical anomalism is dubbed the Minik Singularity. As the fluid flowed from east to west and underwent oxidation, this may have occurred near surface and have been accompanied by depressurisation. As depressurisation and oxidation near surface are near limitless relative to the scale of a mineral system, there is improved potential for substantial copper mineralisation compared to a finite lithological control.

The age of the known mineralisation concerns at least two episodes. The Company identifies the Elzevirian Orogeny (c. 1,250Ma) as the likely event associated with the native copper mineralisation in the basalts. However, the Neoproterozoic-aged sediment-hosted copper sulphides demonstrate that there was a second mineralising event associated with the waning Caledonian Orogeny (c. 390 to 380 Ma) The Elzevirian and Caledonian orogenies have a similar orientation. The c. 385 maximum age is supported by the absence of mineralisation known to younger than the Silurian. Additionally, the Company notes that Government researchers identify that the chemistry of the fluids associated with the world-class Citronen deposit 130km to the north, are the same as those observed within the ARC once the background lithologies are removed as a variable. As Citronen sits higher in the stratigraphic sequence (Ordovician aged host rocks, 485.4 to 443.8M years ago), this may make substantial portions of the ARC sequence above the Zig-Zag Fm prospective for sediment-hosted copper. The fluid temperatures also show a cooling from east to west. Greenfields proposed hydrodynamic framework, combined with dating of the orogenic events and



	fluid temperature gradients are used to define, for the first time, the Kiffaanggissuseq metallogenic province.
	The basal flows of the Zig-Zag Fm basalts show a marked depletion in nickel. Such a depletion suggests that the nickel may have been deposited into sulphides and conceptually, as nickel sulphide deposit. There has been no effective commercial work on testing the nickel sulphide potential.
	An interactive Government portal that contains the geology, and supporting reports can be accessed via: http://www.greenmin.gl/home.seam .
<i>Drill hole information</i>	No drilling has ever occurred within the ARC or in the surrounding area.
<i>Data aggregation methods</i>	All historical results presented in this release are based on those published by third parties. Greenfields has made a point of reporting the weighted-averages and has avoided individual high-grade results that may not be representative of the mineral system (e.g. a 53.8% Cu and 2,480 g/t Ag sample derived from a single float sample near the 'Black Earth' within the Discovery Zone).
<i>Relationship between mineralisation width and intercept lengths.</i>	The reported historical trenching results are presented on a true-width basis.
<i>Diagrams</i>	All relevant maps are presented in the main body of this document.
<i>Balanced reporting</i>	Greenfields has sourced and reasonably presented the relevant results, where available. The reader is cautioned that geochemical rock chip samples, by their nature, are not representative samples. Geochemical rock chip samples are erratically collected, lack scale and design. Geochemical results must be viewed as empirical evidence of anomalism, and not as a representative indication of mineralisation. Furthermore, due to the historical nature of the samples, it is not possible at the time of publication, to perform checks and balances on the numbers quoted in the literature. The planned Technical Assessment report will contain all available data.
<i>Other substantive exploration data</i>	In 1998, the Government conducted an airborne electromagnetic survey in the north of the ARC. The flight lines were carried out at an altitude of 120m above ground on a 400m line spacing. The geophysical data is freely available on the Government portal. Sediment-hosted copper typically does not respond to any geophysical method and as such, the data is not suited to direct-detection. However, Greenfields identifies that the magnetic anomaly is coincident with a gravity anomaly and interprets this signature to represent an iron-enriched hydrothermal footprint. Native copper and copper sulphides occur in the marginal areas of the anomaly.
<i>Further work</i>	Despite the highly encouraging results and strong indications of a large mineral system, the ARC is at an early stage of exploration. To understand the system, it is important to create a 4D model of the region. Greenfields has tightly constrained the main mineralising events, but currently only 2D data are available. Obtaining 3D data down to the basement of the basins will help in modelling the movement of metal rich fluids. Passive seismic is identified as a low-cost method for acquiring 3D data. This method required around 30 days of collection, during which geochemical sampling and site visits can occur. Before a field program satellite data and historical sample analysis should be conducted.

JORC Table 1, section 1

Criteria	Arctic Rift Copper project
<i>Sampling techniques</i>	Assay data presented in this document largely relate to the historical geochemical sampling of trench samples, rock chips, grab samples, and stream sediments. For the 2010 work by Avannaq: "A total of 202 samples were collected during the field program. Of these, 199 samples were bagged and sent to Actlabs, Ancaster Canada for chemical analyses. Some 182 of these samples represent mineralisations, whereas the rest were taken as reference samples. To access the grade of copper and silver mineralisation at J.C. Christensen Land [GEX: effectively the entire ARC licence], semicontinuous chip lines were undertaken through the most pronounced mineralised rocks. The length of individually chip line samples varies but the standard length is 0.5 m or 1.0 m. The entire chip line lengths presented in this report are all estimated as true stratigraphic thickness across the samples structure. Ten chip lines were laid out, resulting in a total of 117 chip samples. A representative hand sample of each chip line section was collected for reference". The weight of the samples sent for chemical analyses were usually in the 1.5 to 2.4kg range, and chip lines were typically taken over 0.5m to 1.0 m

	lengths. In 2011, Avannaa collected 249 rock samples and 227 stream sediment samples across a 4,051 km ² licence package. The rock samples were submitted to ALS laboratories for wet-assay analyses, however the stream sediment samples were only subject to hand-held XRF analysis. The weight of the 2011 samples is typically in the 200g to 300g range. Standards and duplicates were used in both the 2010 and 2011 programs.
<i>Drill techniques</i>	No drilling has ever occurred within the ARC.
<i>Logging</i>	No drilling has ever occurred within the ARC, and as such no logging records exist.
<i>Sub-sampling techniques and sample preparation</i>	The Company is unaware of any sub-sampling techniques or sample preparation.
<i>Quality of assay data and laboratory tests</i>	Avannaa used commercial assay-labs that supply quality certificates as part of the deliverable. Greenfields has no concern about the wet assays. However, XRF information should be treated with caution due to the small sample window available to hand-held devices and the need for in-field calibrations depending on the order of magnitude of the element quanta. Furthermore, as stream sediments may be highly variable and elements of interest having very low levels of detection, the company is wary of the 2011 stream sediment XRF readings.
<i>Verification of sampling and assaying</i>	No third-party verification of the historical assay results has been undertaken.
<i>Location of data points</i>	The data locations and topographic control are based on information that is publicly disclosed by the Government. Grids are based on UTM Zones 26 and 27N using the WGS84 Datum.
<i>Data spacing and distribution</i>	The geochemical sampling is erratically distributed and based visual anomalism or physical/topographical availability. Much of the licence area is undercover which often prevents a grid approach.
<i>Orientation of data in relation to geological structure</i>	Historical assays appear to have been collected across geological features as opposed to lengthwise. The Company considers this to be an appropriate practice.
<i>Sample security</i>	Greenfields has no information on the measures taken to ensure sample security. Given the age of the sampling and the low-probability of sample tampering, the Company has no cause for concern.
<i>Audits or reviews</i>	Greenfields is unaware of any audits or reviews within ARC.



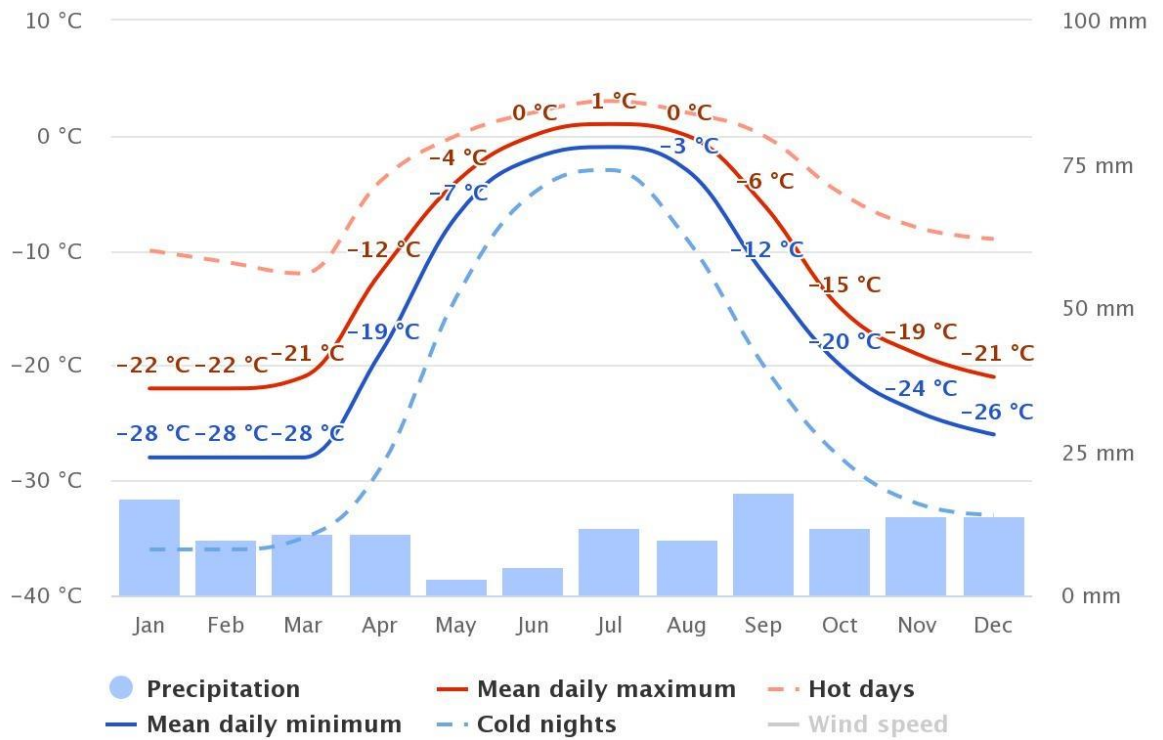
18 APPENDIX 2: LICENSE DETAILS

Table 8: ARC licence co-ordinates

Point	Latitude	Longitude
1	82°3'N	29°18'W
2	82°3'N	25°41'W
3	82°0'N	25°41'W
4	82°0'N	25°43'W
5	81°59'N	25°43'W
6	81°59'N	25°44'W
7	81°58'N	25°44'W
8	81°58'N	25°46'W
9	81°56'N	25°46'W
10	81°56'N	25°48'W
11	81°55'N	25°48'W
12	81°55'N	25°50'W
13	81°53'N	25°50'W
14	81°53'N	25°52'W
15	81°50'N	25°52'W
16	81°50'N	25°54'W
17	81°46'N	25°54'W
18	81°46'N	25°55'W
19	81°35'N	25°55'W
20	81°35'N	26°8'W
21	81°30'N	26°8'W
22	81°30'N	26°54'W
23	81°25'N	26°54'W
24	81°25'N	28°20'W
25	81°21'N	28°20'W
26	81°21'N	29°35'W
27	81°19'N	29°35'W
28	81°19'N	31°0'W
29	81°27'N	31°0'W
30	81°27'N	31°42'W
31	81°34'N	31°42'W
32	81°34'N	32°7'W
33	81°51'N	32°7'W
34	81°51'N	31°0'W
35	81°54'N	31°0'W
36	81°54'N	30°18'W
37	81°58'N	30°18'W
38	81°58'N	29°18'W

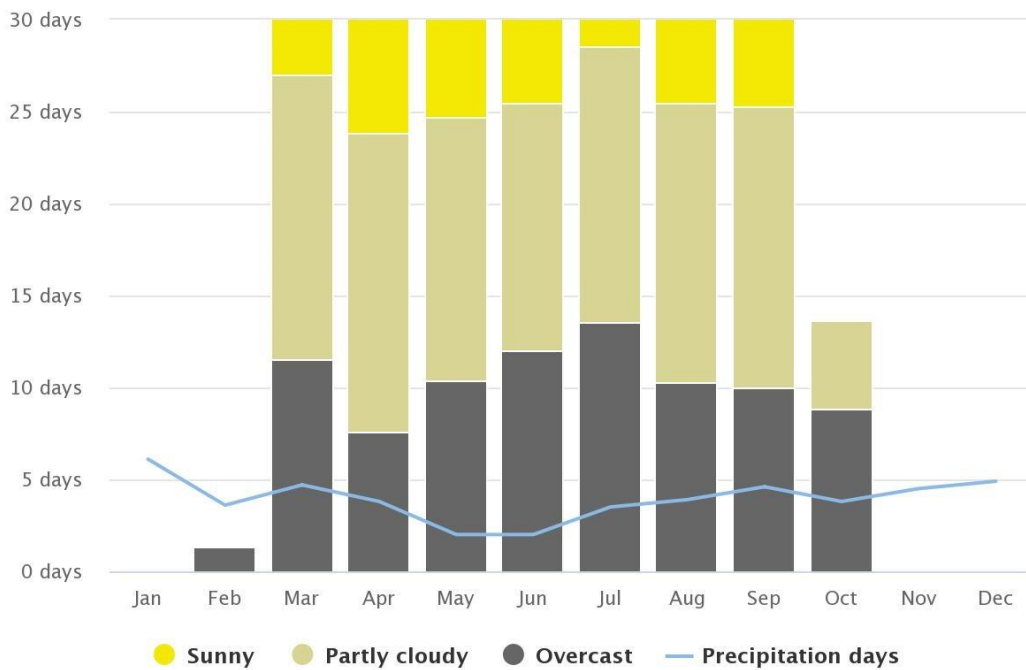
19 APPENDIX 3: SUPPORTING FIGURES

Figure 99: Neergaard average temperatures and precipitation



Source: MeteoBlue (2020) (361) using modelled conditions for 81.96°N 26.21°W, in ARC's north.

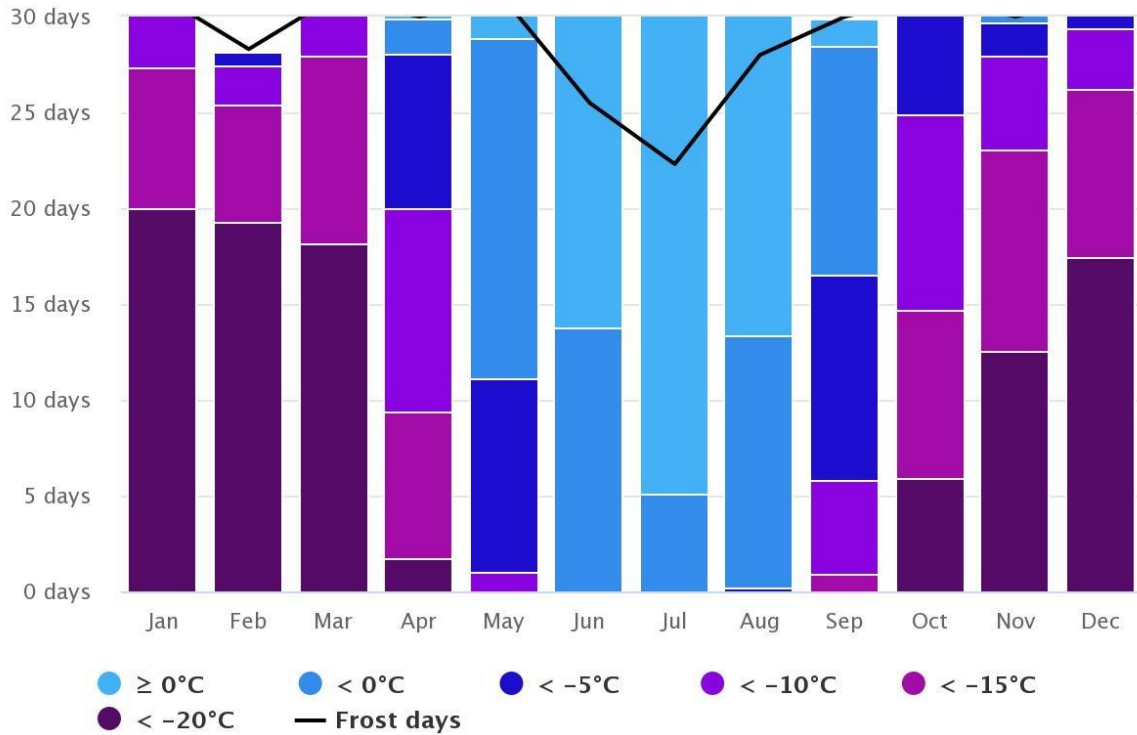
Figure 100: Neergaard cloudy, sunny and precipitation days



Source: MeteoBlue (2020) (361) using modelled conditions for 81.96°N 26.21°W, in ARC's north.

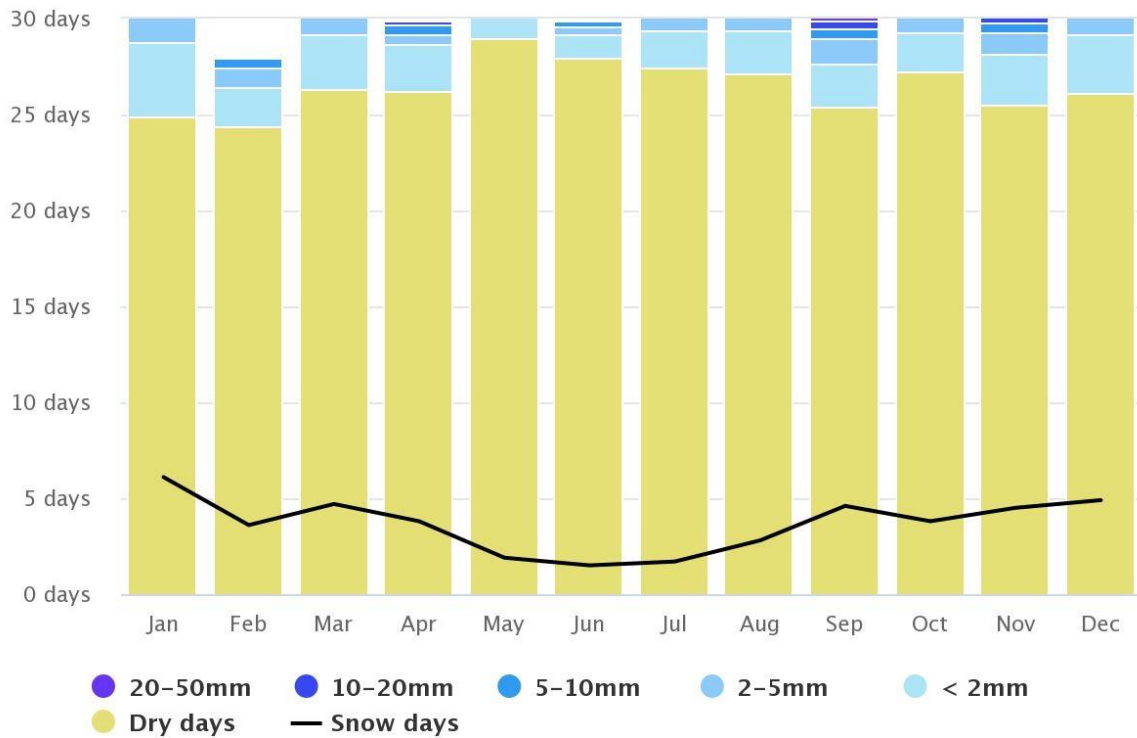


Figure 101: Neergaard maximum temperatures



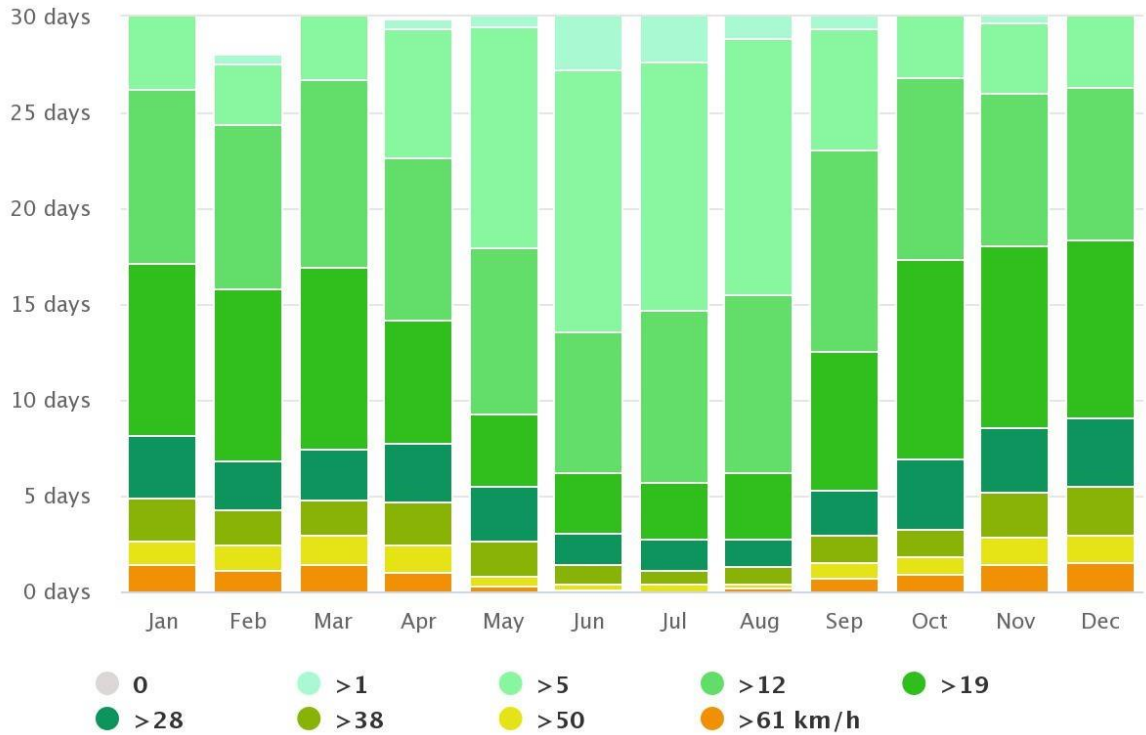
Source: MeteoBlue (2020) (361) using modelled conditions for 81.96°N 26.21°W, in ARC's north.

Figure 102: Neergaard average temperatures and precipitation



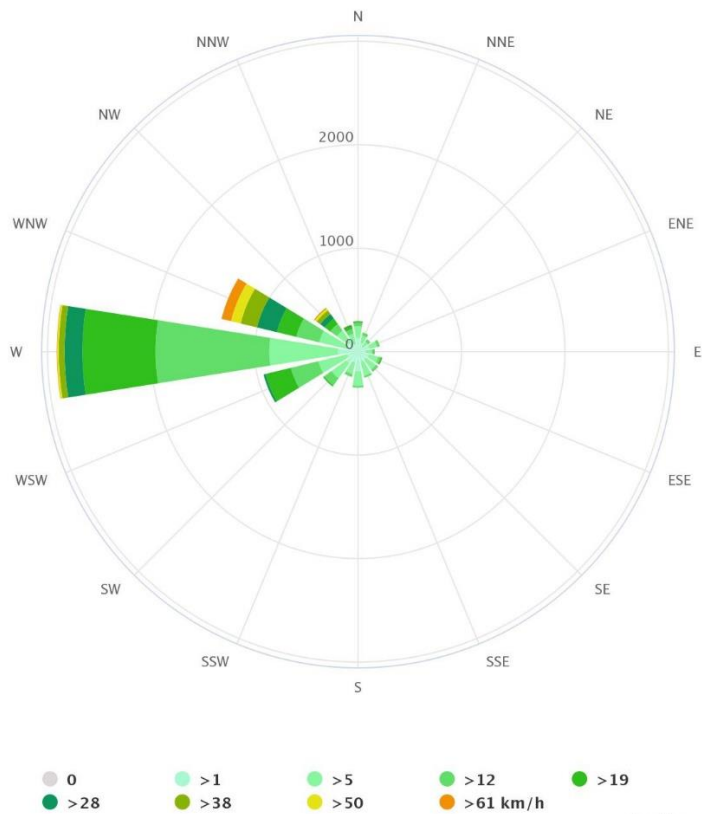
Source: MeteoBlue (2020) (361) using modelled conditions for 81.96°N 26.21°W, in ARC's north.

Figure 103: Neergaard wind speed



Source: MeteoBlue (2020) (361) using modelled conditions for 81.96°N 26.21°W, in ARC's north.

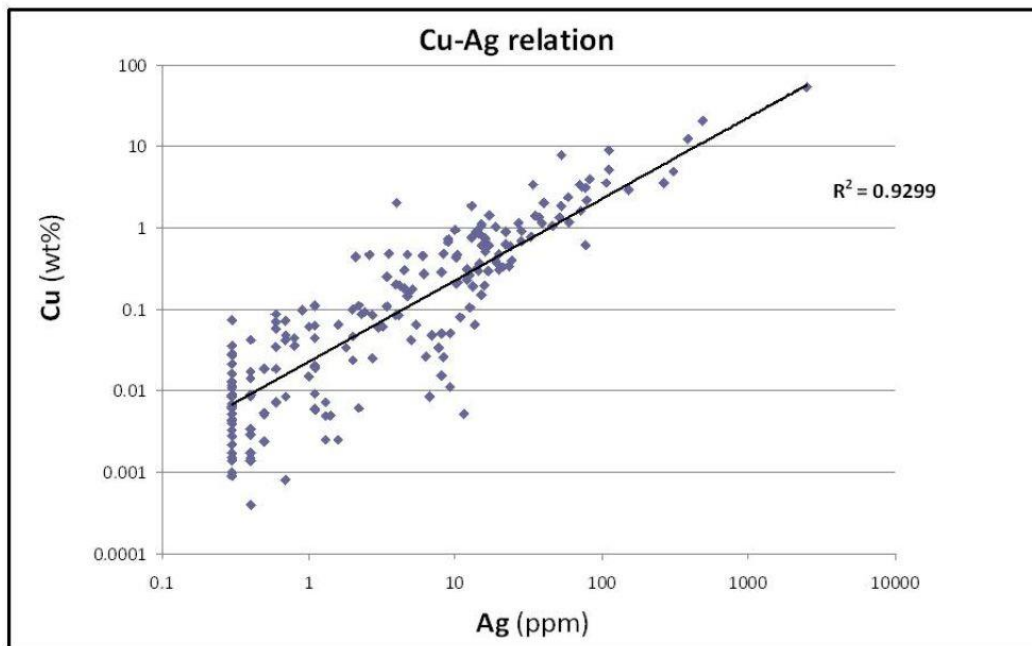
Figure 104: Neergaard wind direction



Source: MeteoBlue (2020) (361) using modelled conditions for 81.96°N 26.21°W, in ARC's north.



Figure 105: Copper-silver correlation from the Discovery Zone



Source: Haugaard (2011) (2).